Molecular insight into the pathogenetic synergy between E. coli and B. fragilis in secondary peritonitis

Sijbrandi, R.

2006

document version
Publisher's PDF, also known as Version of record

MOLECULAR INSIGHT INTO THE PATHOGENIC SYNERGY BETWEEN E. COLI AND B. FRAGILIS IN SECONDARY PERITONITIS

This thesis has been reviewed by:
dr. W. Bitter, VU medisch centrum, Amsterdam
dr. K. Bosscha, Jeroen Bosch Ziekenhuis, 's Hertogenbosch
dr. E.N.G. Houben, University of Basel, Basel, Switzerland
dr. L. Rutten, Universiteit Utrecht, Utrecht
prof.dr. J.R.H. Tame, Yokohama City University, Yokohama, Japan
dr. J.P. van Ulsen, Universiteit Utrecht, Utrecht

Printed by Wöhrmann Print Service, Zutphen

The studies presented in this thesis were carried out at the Department of Molecular Microbiology at the Vrije Universiteit Amsterdam in cooperation with the Genetics and Biochemistry Branch at the National Institutes of Health (Bethesda, MD, USA), the Protein Design Laboratory at the Yokohama City University (Yokohama, Japan), the Department of Crystal and Structural Chemistry and the Department of Molecular Microbiology at the Universiteit Utrecht, and the Department of Molecular Cytology at the Universiteit van Amsterdam.

VRIJE UNIVERSITEIT

Molecular insight into the pathogenic synergy between *E. coli* and *B. fragilis* in secondary peritonitis

ACADEMISCH PROEFSCHRIFT

ter verkrijging van de graad Doctor aan
de Vrije Universiteit Amsterdam,
op gezag van de rector magnificus
prof.dr. T. Sminia,
in het openbaar te verdedigen
ten overstaan van de promotiecommissie
van de faculteit der Aard- en Levenswetenschappen
op maandag 27 maart 2006 om 13.45 uur
in de aula van de universiteit,
De Boelelaan 1105

door

Robert Sijbrandi

geboren te Ermelo

promotor:	prof.dr. B. Oudega
copromotoren:	dr. B.R. Otto
	dr. J. Luirink

Contents

Chapter 1

General introduction

Introduction

The discovery of antibiotics was an enormous advance in medicine, which enabled mankind to fight bacterial diseases that could not be eradicated before. Nevertheless, with the ongoing process of bacterial resistance against (new) antibiotics, bacterial infections still pose a significant threat to human and animal health. Bacterial infections in humans can be categorized in multiple ways. A very easy way is the distinction between mono-infections, where only one bacterial species is the causative agent, and polymicrobial infections, where multiple bacterial species can be isolated from the site of infection. Mono-infections are well known to the general public because of news reports about *Salmonella* in chicken meat, methicillin resistant *Staphylococcus aureus* (MRSA) in hospitals and childhood immunization programs. Although less known to the public, community acquired as well as hospital acquired polymicrobial infections occur very frequently and can pose serious threats to human health.

This thesis is focused on polymicrobial infections in the human intra-abdominal cavity. The abdomen is located between the thorax and the pelvis. The abdominal cavity is lined by the peritoneum: a serous sac, consisting of mesothelium and a thin layer of irregular connective tissue, that covers most of the viscera (internal organs) contained therein. Some abdominal organs, like the kidneys, are located retroperitoneally, but retroperitoneal infections are not considered here.

Intra-abdominal infections and peritonitis

In clinical practice, the term intra-abdominal infection (IAI) is often used as a synonym for peritonitis. However, these two are not the same (Fig. 1). Peritonitis is defined as an inflammation of the peritoneum, but this is not necessarily caused by bacteria (Farthmann and Schöffel, 1998). IAIs comprise a heterogeneous group of conditions encompassing bacterial peritonitis, intra-abdominal abscesses and infections of intra-abdominal organs like appendicitis and pancreatitis (Farthmann and Schöffel, 1998). IAIs are a common cause of hospitalization with approximately two million intra-abdominal procedures carried out annually in the USA (Onderdonk *et al.*, 1990). These infections can be community acquired (e.g. appendicitis, stab wounds or traffic accidents) or hospital acquired, often as a complication of intra-abdominal surgery where the contents of the gut came into contact with the peritoneal cavity.

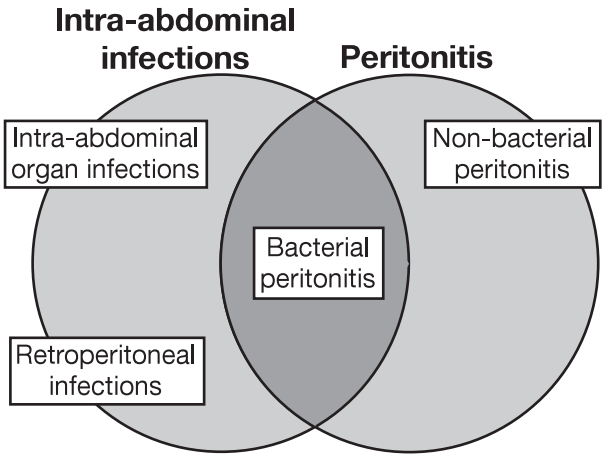

Fig. 1. Bacterial peritonitis in relation to intra-abdominal infections and peritonitis.

The morbidity and mortality of IAI is significant. Data from hospitals in The Netherlands show that there are over 5300 new patients with serious forms of peritonitis each year (Bosscha *et al.*, 1999). Extrapolated to the western world, this means that there must be more than half a million cases per year. Intra-abdominal abscesses occur in approximately 25% of patients treated for generalized peritonitis (Reijnen *et al.*, 2003). Depending on the anatomic origin of the bacterial contamination, mortality ranges from 5 tot 50% (Brook, 1989; Farthmann and Schöffel, 1998). Complications like bacteremia and multiple-organ failure (MOF) frequently occur, increasing mortality rates up to 80% (Anaya and Nathens, 2003). IAIs have been found in 25% of the patients with MOF on a surgical intensive care unit (ICU) (Darling *et al.*, 1988). The high morbidity of peritonitis indicates that the annual cost of treatment of these infections is significant.

Bacterial peritonitis can be divided into three classes (Farthmann and Schöffel, 1998; Marshall, 2004). Primary peritonitis refers to spontaneous bacterial invasion of the peritoneal cavity. This mainly occurs in cirrhotic and immuno-compromised patients and the infections are characteristically aerobic and monomicrobial (Wittmann *et al.*, 1996). Secondary peritonitis refers to peritoneal infections secondary to intra-abdominal lesions like perforation of the hollow viscus, bowel necrosis or penetrating infectious processes. Tertiary peritonitis is defined as peritonitis arising at least 48 hours after the apparently successful treatment of primary or secondary peritonitis. It is characterized by persistent or recurrent

infections with organisms of low intrinsic virulence that are different from the organisms involved in primary or secondary peritonitis and it has a significant mortality.

Host defense systems

Once peritoneal contamination occurs, the body attempts to defend against this invasion with powerful mechanisms devised to deal with breaches in the integrity of the gut (Table 1) (reviewed by Hall *et al.*, 1998). The first mechanism involves physical clearance of the infectious agent using the circa 100 ml of serous peritoneal fluid (Robinson, 1962). Bacteria are removed through gaps (stomata) in the mesothelial lining of the diaphragm into the lymph system (Tsilibary and Wissig, 1983; Nakatani *et al.*, 1996). The second mechanism is destruction of the bacteria using the innate immune system. Complement activation is involved in the opsonization of microorganisms, enhancement of inflammatory responses, clearance of immune complexes and cell lysis (Pascual and French, 1995). The migration of polymorphonuclear neutrophils (PMNs) into the peritoneum is enhanced and also other cells of the innate immune system like macrophages and mast cells are involved (Caldwell and Watson, 1994).

Table 1. Host defense systems in peritoneal infections

System	Mechanism
1. Clearance	Serous peritoneal fluid
	Stomata
2. Innate immune system	Polymorphonuclear neutrophyls
	Macrophages and mast cells
3. Abscess formation	Coagulation favored over fibrinolysis
	Fibrin clot formation

The third defense mechanism of the peritoneal cavity is containment of the infection as an abscess. This is the result of a shift in the balance between the coagulation and fibrinolysis systems in favor of coagulation (van Goor *et al.*, 1994; Vipond *et al.*, 1994). Tissue thromboplastin converts prothrombin to thrombin, which polymerizes fibrinogen in the peritoneal fluid to form fibrin networks. Bacteria become physically trapped in these fibrin clots, by which bacterial spread is prevented and the

formation of abscesses is promoted (Zinsser and Pryde, 1952). In healthy individuals, enzymes of the fibrinolytic system readily dissolve fibrin, but inflammation inactivates this system. This mechanism of bacterial localization in abscesses decreases the early rapid mortality that would otherwise be associated with bacterial peritonitis (Rotstein, 1992). However, as bacteria within fibrin deposits are protected from host clearance mechanisms and phagocytosis, bacterial proliferation can occur rather unopposed and a persistent infection can be established (Rotstein, 1992). As will be discussed below, several bacterial species can produce specific virulence factors that actively interfere with the host fibrinolytic system, thereby promoting either the formation or dissolution of fibrin clots.

Microbiology of peritonitis

Normal intestinal flora consists of many bacterial species, e.g. in the colon alone more than 400 species of anaerobic bacteria can be found (Savage, 1977). Therefore, the initial microflora entering the peritoneal cavity upon a breech in the integrity of the gut is always polymicrobial. Nevertheless, only a very limited number of different bacterial species is recovered from intra-abdominal abscesses (Hau *et al.*, 1979; Wittmann *et al.*, 1996; Farthmann and Schöffel, 1998). *Escherichia coli* is the aerobic Gram-negative species most often isolated from IAI (32-61%) and *Bacteroides fragilis* is the most frequently isolated anaerobic bacterium (circa 46%) (Hau *et al.*, 1979; Brook, 1988; Goldstein and Citron, 1988; Aldridge, 1995; Farthmann and Schöffel, 1998). Precise numbers are difficult to obtain from the literature, because of differences in the inclusion of groups of species or isolation sites in the calculation. Enterococci and streptococci are the most frequently isolated gram-positive species from IAI (Hau *et al.*, 1979; Farthmann and Schöffel, 1998).

The frequent isolation of both *E. coli* and *B. fragilis* from bacterial peritonitis has led to the concept of bacterial synergy between these species (Fig. 2) (Meleney *et al.*, 1932; Altemeier, 1942). This concept has been worked out in studies with experimentally induced infections in mice (Brook *et al.*, 1984; MacLaren *et al.*, 1984) and in rats (Onderdonk *et al.*, 1974; Onderdonk *et al.*, 1976; Dunn *et al.*, 1984; Rotstein *et al.*, 1985a). Synergism was assayed as the induction of sepsis or abscesses or as an increase in death count. In 1985, Brook demonstrated in mice mutual enhancement of growth between *E. coli* and *B. fragilis* in induced subcutaneous abscesses (Brook, 1985). In 1991, Verweij *et al.* developed a model for experimental peritonitis in rats using a fibrin clot model (Verweij *et al.*, 1991) that

was modified by Bosscha *et al.* to create a standardized and reproducible model of IAI (Bosscha *et al.*, 2000). In the later studies, bacterial counts were measured of both *E. coli* and *B. fragilis* in mixed infections and compared to the cell counts from the same organisms in mono infections. The synergistic effect between both species was demonstrated by the increased numbers of viable cells isolated from the site of infection and the ability to induce persistent infection only in the presence of both species.

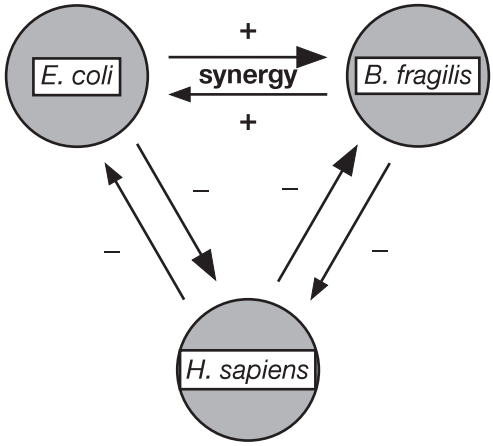

Fig. 2. Interactions between *E. coli*, *B. fragilis* and the human host in bacterial peritonitis. The positive interactions between *E. coli* and *B. fragilis* indicate the microbial synergy between the two species.

Virulence factors in bacterial synergy

The molecular basis of the synergy between *E. coli* and *B. fragilis* in bacterial peritonitis is only partially understood. At least two classes of virulence mechanisms can be identified in this context: the inhibition of phagocytosis by polymorphonuclear neutrophyls (PMNs) and the provision of essential growth factors (Table 2). It has been observed that obligate anaerobes, including *B. fragilis*, can inhibit phagocytosis of various aerobic species (Ingham *et al.*, 1977; MacLaren *et al.*, 1984). The inhibitory effect of *B. fragilis* on PMN function is caused by the secretion of short-chain fatty acids (Rotstein *et al.*, 1989b) and succinic acid (Hart *et al.*, 1986). Also the polysaccharide capsule of *B. fragilis* appears to play an important role in this phenomenon (Rotstein *et al.*, 1985b). In this respect it is noteworthy that most *B. fragilis* strains isolated from abscesses or blood infections are encapsulated, whereas only 10% of the strains isolated from faeces of healthy individuals is

encapsulated (Brook *et al.*, 1992). Besides inhibition of phagocytosis, the encapsulation of *B. fragilis* has been reported to promote adhesion to the peritoneal wall (Rotstein *et al.*, 1985b), improve resistance to oxygen exposure (Patrick *et al.*, 1984) and increase resistance to penetration of antibiotics (Brook and Gillmore, 1994). Encapsulated strains of *B. fragilis* and even purified capsule alone can induce abscess formation (Zaleznik and Kasper, 1982; Tzianabos *et al.*, 1993).

Table 2. Virulence factors in the synergy between *E. coli* and *B. fragilis*

1. Inhibition of phagocytosis by polymorphonuclear neutrophyls
- Secretion of short-chain fatty acids
- Secretion of succinic acid
- Encapsulation
+ Promotes cell adhesion
+ Increases oxygen resistance
+ Increases antibiotic resistance
+ Induces abscess formation
2. Provision of essential growth factors
- Iron and heme acquisition
3. Production of β-lactamases
4. Secretion of tissue-destructing proteases
5. Provision of an anaerobic environment

Proteins secreted by *E. coli* or *B. fragilis* can aid in the provision of essential growth factors and nutrients to either or both species. For instance, the human body keeps the concentration of free iron extremely low (circa 10^{-18} to 10^{-24} M (Braun, 2001; Bullen *et al.*, 2005)) by keeping iron in a protein-bound form in the circulation (e.g. in transferrin, lactoferrin, hemoglobin and albumin). Bacteria need much higher concentrations of iron to maintain growth (circa 1 μM) (Weinberg, 1974) and have developed highly specialized mechanisms to acquire iron or heme (recently reviewed by Wandersman and Delepelaire, 2004). Otto *et al.* identified a hemoglobin protease (Hbp) secreted by *E. coli* that contributes to the synergistic abscess formation and heme-dependent growth of *B. fragilis* in a mouse infection model (Otto *et al.*, 1998; Otto *et al.*, 2002). Hbp degrades hemoglobin *in vitro* and binds the released heme group. It has been proposed that heme-bound Hbp provides the heme as an iron or heme source to the bacteria in peritoneal infections. This would match the observation that the presence of hemoglobin within the peritoneal cavity enhances mortality rates in peritonitis (Yull *et al.*, 1962). Otto has found that *B. fragilis* possesses hemolysin activity, especially upon conditions of iron-starvation (B.R.

Otto, unpublished observations). In fact, as many as nine functional hemolysin proteins have been characterized in *B. fragilis* (E.R. Rocha and coworkers, unpublished observations). These findings underline the importance of iron provision during infections.

Other factors that have been implicated in the synergy between *E. coli* and *B. fragilis* are the production of β-lactamases by *B. fragilis*, greatly increasing the tolerance of *E. coli* to β-lactam antibiotics (Bryant *et al.*, 1980; Cuchural and Tally, 1986; Aldridge *et al.*, 1994), the secretion of proteases that cause tissue destruction (collagenases and hyaluronases) and the provision by *E. coli* of an anaerobic environment for *B. fragilis*, and also inhibiting neutrophyl killing (Aldridge, 1995). In our lab, several proteins have been found in *B. fragilis* that could potentially function as virulence factors in pathogenic synergy. These include a putative extracellular protease of circa 30 kDa, a putative mucin-binding protein of 44 kDa, an adhesion protein of circa 40 kDa, the α-enolase (46 kDa) that is an iron-regulated heme-binding protein, as well as a 60 kDa putative plasminogen-binding protein (Pbp). The first three proteins await further characterization. The characterization of the two latter proteins is described in two chapters of this thesis. The potential role of the α-enolase and of the Pbp in virulence still has to be investigated. For *E. coli*, the results from the murine infection model (Otto *et al.*, 2002) indicate that Hbp very likely acts as a virulence factor *in vivo*.

Bacterial iron and heme uptake systems

Iron in biological systems

Iron is an essential compound for most living organisms, including bacteria and man. It serves as a catalytic center of enzymes for redox reactions, either alone or incorporated into heme or iron-sulfur clusters. However, free iron ions cannot be used by living organisms, because under aerobic conditions oxidized iron (FeIII) in solution forms insoluble complexes and ferrous iron (FeII) is readily converted into FeIII in the presence of oxygen with concomitant production of free radicals that can damage biological macromolecules (Ratledge and Dover, 2000; Braun and Braun, 2002b). Iron in biological systems is therefore almost exclusively liganded to carrier proteins and the concentrations of free iron are kept very low (circa 10^{-18} to 10^{-24} M) (Bullen, 2005; Braun, 2001). Pathogenic bacteria in the human host are confronted with a serious problem, because they need micromolar concentrations of iron for their survival and growth (Braun, 2001). Therefore, bacteria have evolved several

mechanisms to acquire iron from the various sources in the human body (recently reviewed by Wandersman and Delepelaire, 2004). In Gram-negative bacteria, like *E. coli* and *B. fragilis*, these mechanisms rely on specific outer membrane receptors that recognize the various iron and heme-containing molecules (Fig. 3) (Braun and Braun, 2002a). Two classes are distinguished. The first class involves a direct recognition between the receptor and the iron- or hemesource from the host, the second class involves the secretion of scavenger molecules that sequester iron or heme from these sources and deliver it to the bacterium. The various uptake systems more or less converge once the iron or heme is transported into the cell through the outer membrane receptors.

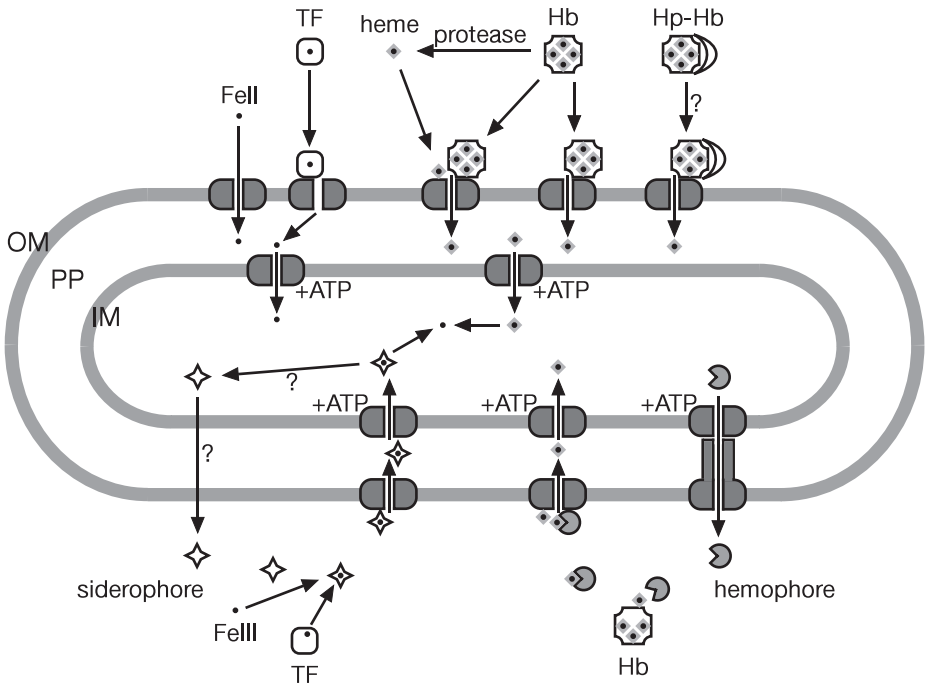

Fig. 3. Iron and heme uptake systems in Gram-negative bacteria. On the upper half of the schematic cell, direct binding of the iron or heme compound to an outer membrane receptor is depicted. On the lower half, iron or heme is sequestered by actively secreted siderophores or hemophores, respectively. All known outer membrane receptors are TonB-ExbB-ExbD dependent (omitted for clarity). Import into the cytoplasm involves an ATP-binding cassette (ABC) protein dependent inner membrane protein. Question marks indicate uncertain pathways. TF = transferrin of lactoferrin, Hb = hemoglobin, Hp-Hb = haptoglobin-hemoglobin, FeII = ferrous iron, FeIII = ferric iron, OM = outer membrane, PP = periplasm, IM = inner membrane.

Iron sources in the human body

Potential iron sources in the human host are FeII, transferrin and lactoferrin and ferritins. FeII is the major form of free iron under anaerobic or reducing conditions (Wandersman, 2004), which is supposed to be the situation in peritoneal infections. Although available in only very low concentrations, the ion is highly soluble and freely diffuses through bacterial outer membrane porins. Transport across the inner membrane is carried out by an ATP binding cassette (ABC)-type ferrous ion transporter conserved in many bacteria (Kammler *et al.*, 1993). Transferrin (Tf) is found in serum, whereas lactoferrin is found in lymph and mucosal secretions. Both proteins are glycoproteins of circa 80 kDa with a very high affinity for FeIII (K_a ~10^{20} M^{-1}). They function as iron chelators protecting the body against iron toxicity. Tf has an iron transport function. Many bacterial species have Tf and/or lactoferrin uptake systems, of which the Neisserial Tbp system is the best characterized (Cornelissen, 2003). Transferrin can be bound by two outer membrane proteins, TbpA and TbpB. TbpA is a classical receptor molecule that is essential for the receptor function and TbpB is a surface localized lipoprotein that is not necessarily required (Boulton *et al.*, 1999). The mechanism of iron transfer from Tf to TbpA is unknown. However, once the iron molecule is translocated to the periplasm, it is bound by the periplasmic protein FbpA (Gomez *et al.*, 1998). Similar receptors exist in *Neisseria* for lactoferrin (LbpAB) (Pettersson *et al.*, 1998; Schryvers *et al.*, 1998). Ferritins are intracellular iron storage proteins (Carrondo, 2003). Although ferritins can be found in plasma as a consequence of cell lysis, there is no evidence that they are used as iron sources by bacteria.

Heme sources in the human body

Potential heme sources in humans are free heme, hemoglobin (Hb), haptoglobin-hemoglobin, hemopexin, albumin and other hemoproteins. Heme (iron protoporphyrin IX) is a constituent of many enzymes, but because of its high toxicity it is hardly freely available. Nevertheless, a heme receptor (HemR) has been described in *Yersinia enterocolitica* (Bracken *et al.*, 1999). This receptor can actually bind both heme and hemoglobin. The bacterial requirements for heme are a factor 10^3 lower than that for iron. Hemoglobin is the oxygen transporter molecule in red blood cells. It is an α_2-β_2 tetramer with each subunit binding one heme molecule (Perutz *et al.*, 1960). Upon lysis of red blood cells, possibly by the action of bacterial hemolysins in an infection, hemoglobin becomes available as a heme source to bacteria. Hemoglobin receptors have been found, for instance in *Neisseria meningitides* (HmbR) (Richardson and Stojiljkovic, 1999). Once released from red blood cells,

hemoglobin rapidly oxidizes to methemoglobin, which quickly dissociates into α-β dimers. These dimers bind heme with a lower affinity, and therefore it can be difficult to make a clear distinction between heme and hemoglobin utilization by bacteria. Hemoglobin from lysed red blood cells is normally bound with a high affinity by haptoglobin (Evans *et al.*, 1999). The haptoglobin-hemoglobin complex is cleared from the circulation in the liver and then degraded. Heme that is released from hemoglobin subunits in the body is quickly bound by hemopexin (Paoli *et al.*, 1999). Heme-hemopexin is also transported to the liver, where heme is taken off and hemopexin is recycled. No direct bacterial binding of heme-hemopexin has been demonstrated so far, but a putative haptoglobin-hemoglobin receptor (HpuAB) from *N. meningitidis* has been described (Lewis *et al.*, 1997). Specialized receptors for hemo-albumin or other hemoproteins (e.g. myoglobin or cytochrome b) have not been found so far. Upon comparison of the known heme, hemoglobin and hemoglobin-haptoglobin receptors, it was found that they all contain several highly conserved histidine residues as well as two conserved motifs: the FRAP and NPNL boxes (Bracken *et al.*, 1999). It is expected that these conserved residues and motifs are directly involved in the recognition and internalization of the heme molecules.

Bacterial iron- and heme-scavenging systems

Besides the ability to bind iron or heme sources directly, many microorganisms can excrete siderophores and/or hemophores to capture iron or heme and shuttle it back into the cell. Siderophores are small iron-chelating molecules with a very high affinity for FeIII (the calculated affinity constant being above 10^{30} M^{-1}). In the more than 500 different siderophores, three chemical types of iron ligation groups are distinguished (Drechsel and Jung, 1998): hydroxamates (e.g. aerobactin and ferrichrome), catechol rings (e.g. enterobactin) and hydroxyacids (e.g. pyochelin). Little is known about the excretion of siderophores. One report describes that EntS, a proton-motive force dependent membrane efflux pump, is directly involved in enterobactin export (Furrer *et al.*, 2002). In the extracellular environment, the high affinity of siderophores for iron is expected to extract iron from the host iron sources. Ferrisiderophores are recognized at the cell surface of Gram-negative bacteria by outer membrane receptors like FhuA (for enterobactin) and FepA (for ferrichrome) of *E. coli*. The crystal structures of both proteins reveal that they are very similar, with a 22-stranded β-barrel spanning the outer membrane and a central channel that contains a molecular plug or “cork” (Fig. 4) (Ferguson *et al.*, 1998; Locher *et al.*, 1998; Buchanan *et al.*, 1999). The ferrisiderophores are internalized

through the channel upon structural rearrangement of the barrel and dislocation of the plug (Ferguson and Deisenhofer, 2004).

Hemophores, that are yet only found in Gram-negative bacteria, are defined as specialized extracellular proteins that acquire heme from diverse sources and bring it to a specific outer membrane receptor (Wandersman and Delepelaire, 2004). These molecules capture free heme or extract heme from hemoglobin in the extracellular environment. A family of hemophore systems called HasA (heme acquisition system) has been described in *Serratia*, *Pseudomonas* and *Yersinia* species. In most species, the secretion apparatus, the hemophore and the outer

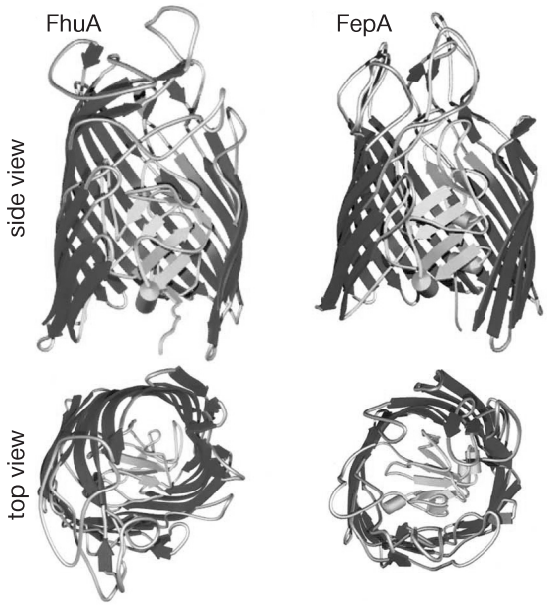

Fig. 4. Comparison of the FhuA and FepA crystal structures (PDB indentifiers 1QJQ and 1FEP). Side and top views are shown. In the side views, part of the β-strands was deleted to visualize the central globular domain (cork structure). Figure adapted from (Braun and Braun, 2002b).

membrane receptor are encoded by genes located in one operon (Ghigo *et al.*, 1997). The hemophore is secreted by ABC transporters consisting of an inner membrane ATPase, a membrane fusion protein and an outer membrane protein belonging to the TolC family (Létoffé *et al.*, 1994). TolC forms a β-barrel in the outer membrane and has a large periplasmic domain that forms a tunnel between the inner and outer membranes (Koronakis *et al.*, 2000). The secretion of HasA is also dependent on the cytosolic SecB chaperone (Delepelaire and Wandersman, 1998).

Heme is extracted from heme carriers like hemoglobin, hemopexin or hemo-albumin due to the high affinity of HasA for heme (a K_d of 10^{-11} M) and it binds to HasA in a 1:1 stoichiometry (Izadi *et al.*, 1997). The hemophore is recognized at the cell surface by the outer membrane receptor HasR, which can also bind heme and hemoglobin directly (Létoffé *et al.*, 1999). A second hemophore system is the HxuA system of *Haemophilus influenzae*. This system is required for heme and heme-hemopexin utilization by this species (Cope *et al.*, 1995). HxuA is a 100 kDa hemophore, that is dependent for its secretion on HxuB that forms a β-barrel in the outer membrane (Cope *et al.*, 1994). This type of secretion pathway is designated the two-partner secretion pathway and is related to the autotransporter pathway that is described below. After binding of heme-loaded hemopexin, the complex is recognized by the outer membrane receptor HxuC (Cope *et al.*, 1995). This receptor can also bind heme and hemoglobin directly.

Internalization of captured heme and iron molecules

Once the iron, the iron-loaded siderophore or heme is bound by the outer membrane receptor, the molecules are generally internalized by a conserved mechanism that involves the TonB complex (Frost and Rosenberg, 1975). This cytoplasmic membrane complex, consisting of TonB, ExbB and ExbD in the ratio 1:7:2 (Higgs *et al.*, 2002), transduces energy from the proton motive force to allow substrate internalization into the periplasmic space. The involved outer membrane receptors contain a stretch of five conserved residues, the TonB box, close to their N-termini (reviewed in Braun, 2003 and Faraldo-Gomez and Sansom, 2003). Although many details about the events in this process are still unknown, it is assumed that substrate binding to the receptor triggers conformational changes of the plug and induces closure of the outside loops of the barrel around the substrate (reviewed in Ferguson and Deisenhofer, 2004). The action of the TonB complex, contacting the TonB box, is proposed to displace the plug from the β-barrel and allow transfer of the substrate into the periplasm (Fig. 5). In the periplasmic space, a periplasmic binding protein immediately picks up the substrate. Periplasmic FeIII binding proteins (FbpA) with an extremely high affinity for iron (K_d 10^{-18} M) have been found and were crystallized from *Haemophilus* and *Neisseria* species (Adhikari *et al.*, 1995; Dhungana *et al.*, 2003). Periplasmic siderophore binding proteins have been characterized in *E. coli* (e.g. FhuD and FebB) (Sprencel *et al.*, 2000; Clarke *et al.*, 2002) and homologues of FhuD are present in *Staphylococcus aureus* (Sebulsky *et al.*, 2003). Their affinities for siderophores are in the micromolar or nanomolar range. Subsequent transport of the substrate across the cytoplasmic membrane is carried

out by an inner membrane ATPase complex (ABC permeases) (Koster, 2001). These are found in both gram-positive and Gram-negative bacteria.

Not much is known about the intracellular fate of iron and heme. Two processes have been proposed for the release of iron from siderophores. Either the iron is released from the siderophore upon reduction by electron donors and the siderophore is recycled (Müller *et al.*, 1998), or the siderophore is degraded intracellularly, releasing the iron molecule (Brickman and McIntosh, 1992). Iron is stored intracellularly in ferritins, found in most living organisms, or bacterioferritins, only found in bacteria. Both types are composed of 24 identical subunits forming a spherical structure with the capacity to store about 5000 iron ions (Carrondo, 2003). Besides, bacterioferritins contain up to twelve heme groups of unknown function. Acquired heme molecules are either degraded by heme oxygenases to be used as an iron source (Zhu *et al.*, 2000), or stored. Heme storage proteins are not known so far, but several proteins first considered to be heme oxygenases (e.g. HemS and ShuS) are now suspected to be heme storage proteins (Wilks, 2001).

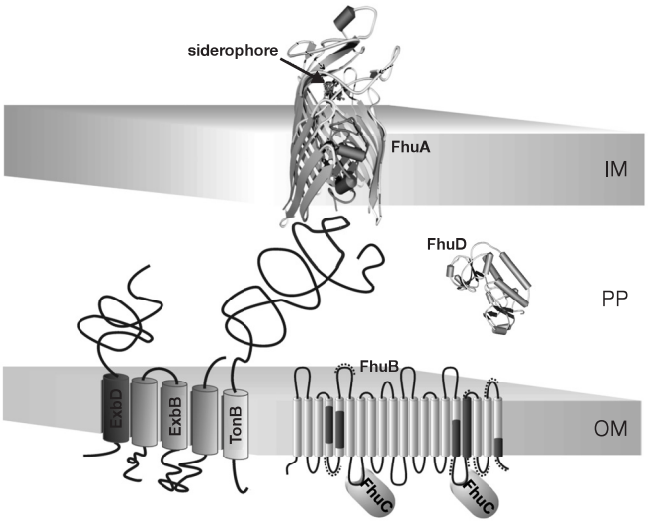

Fig. 5. Iron-loaded siderophore import. Ferrichrome is recognized by the outer membrane (OM) receptor FhuA. The β-strands in the front were deleted to visualize the cork structure. Ferrichrome binding induces conformational changes of the receptor, resulting in TonB-ExbB-ExbD mediated displacement of the cork. Ferrichrome transport through the periplasm (PP) involves the periplasmic chaperone FhuD. A structural change of FhuD is predicted when it binds to the inner membrane (IM) permease FhuB. FhuC is an ATPase that provides the energy for transport of the siderophore across the inner membrane. Figure adapted from (Braun, 2001).

Regulation of the iron- and heme-uptake systems

Most iron and heme uptake genes are negatively regulated by FeII-binding metalloproteins. The prototype of these molecules is the *E. coli* protein Fur (ferric uptake regulator) (Hantke, 1981). Iron-loaded Fur binds as a dimer to a 19-bp consensus sequence located near or within iron-regulated promoters (Baichoo and Helmann, 2002). Fur regulation also exists in *B. fragilis*, but the consensus sequence of the Fur-box differs from that in *E. coli* and remains to be elucidated (E.R. Rocha, personal communication). Fur-like repressors are characterized by a low affinity for FeII (K_d 10^{-5} M) (Wee *et al.*, 1988). Because of this, a small change in the intracellular iron concentration may induce large changes in Fur iron load and therefore in the transcriptional level of Fur-regulated genes. Depending on the bacterial species, 50 to 100 genes are negatively regulated by Fur, including genes for iron and heme acquisition, acid resistance and virulence factors (McHugh *et al.*, 2003). All these types of genes can play important roles in an infection situation.

Otto *et al.* have characterized a novel *E. coli* protein called Hemoglobin protease (Hbp). It belongs to the autotransporter type of proteins described below and is a 111 kDa secreted serine protease (Otto *et al.*, 1998). In the extracellular environment, it can degrade hemoglobin by a so far unknown mechanism. Subsequently, it binds the released heme from that molecule and delivers it to a putative outer membrane receptor of *E. coli* and/or *B. fragilis* that still has to be identified. Based on what is described above, Hbp can be considered a hemophore, somewhat resembling the HxuA system.

Coagulation and fibrinolysis

Pathogenic bacteria often possess virulence factors that influence the balance between coagulation and fibrinolysis in the host organism. In the normal situation in the human body, there is a well-regulated balance between these two mechanisms responsible for the maintenance of the endothelial cell lining (reviewed by Norris, 2003). Upon minor or more extensive damage to the endothelium, platelets adhere to the subendothelium and activate the coagulation cascade (Stassen *et al.*, 2004). This cascade involves the activation of a range of inactive zymogens and cofactors by proteolytic cleavage (Fig. 6). Two main pathways are traditionally distinguished: the intrinsic or contact pathway and the extrinsic or tissue factor pathway. However, more recent evidence shows that these two pathways are not so

independent and that the main function of the intrinsic pathway may be to amplify the coagulation activation triggered by the extrinsic pathway (Hoffman, 2003; Norris, 2003). Tissue factor is the only cofactor that is always present in an active form. Upon vascular injury, membrane bound tissue factor is exposed to plasma and can bind factor VII (Morrisey, 2001). This complex activates the cascade of blood clotting factors, starting with factor IX and X. These factors are activated to form

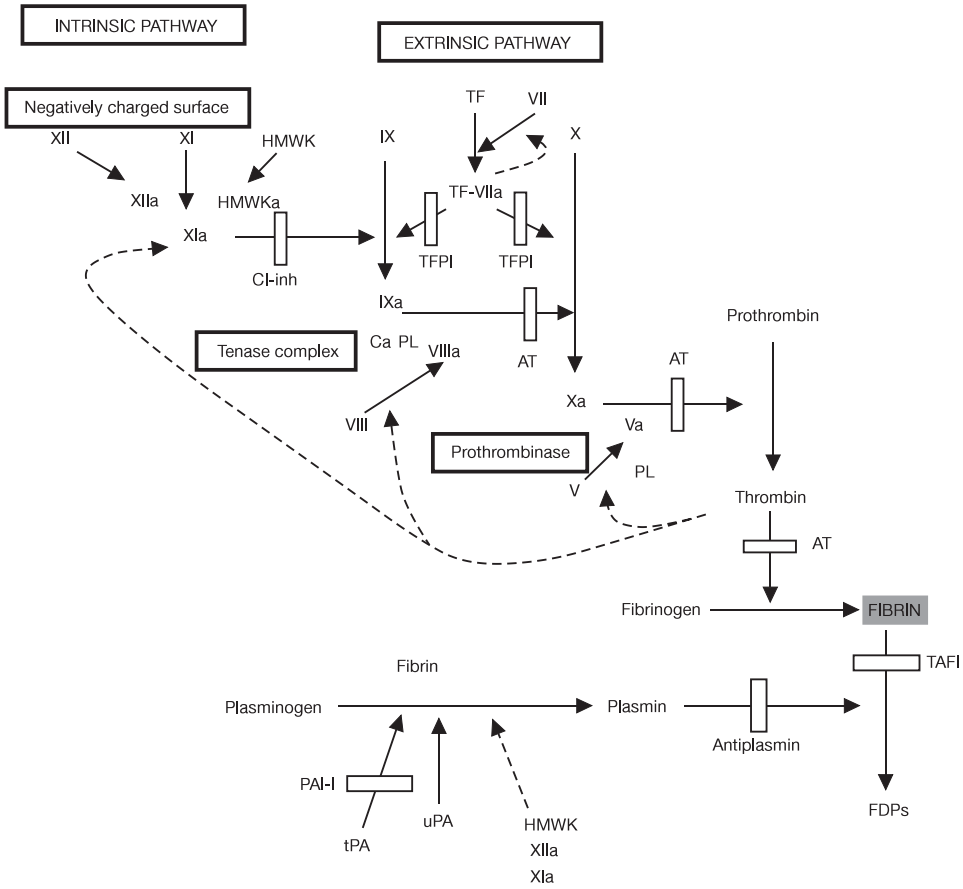

Fig. 6. The coagulation cascade and the fibrinolytic pathway. The coagulation cascade shows both intrinsic and extrinsic activation, inhibitors (blocks) and feedback activation (dashed lines). Fibrin (gray box) is the endproduct of the coagulation cascade. ?a = activated form of factor ?, HMWK = high molecular-weight kininogen, CI-inh = CI-inhibitor, TF = tissue factor, TFPI = tissue factor pathway inhibitor, PL = phospholipids, Ca = calcium, AT = antithrombin, tPA = tissue plasminogen activator, uPA = urokinase plasminogen activator, PAI-I = plasminogen activator inhibitor I, TAFI = thrombin activatable fibrinolysis inhibitor, FDPs = fibrin degradation products. Figure adapted from (Norris, 2003).

factor IXa and Xa, respectively. The intrinsic pathway through factors XII and XI can also activate factor IX. Activated factor IX forms a complex with factor VIIIa, calcium and phospholipids and activates factor X to Xa. When factor Xa is bound to factor Va and a phospholipid membrane surface, inactive prothrombin is converted to α-thrombin, a serine protease (Nesheim *et al.*, 1979). Thrombin has multiple functions in haemostasis: the conversion of fibrinogen to fibrin, the activation of platelets, factors V, VIII and IX, and the activation of coagulation inhibitors (Brummel *et al.*, 2002). These multiple functions are possible because of the multiple binding sites on α-thrombin. Fibrin formation is a multistep process, starting with the cleavage of dimeric fibrinogen by thrombin to form soluble fibrin monomers. Non-covalent interactions result in the formation of fibres that aggregate to form a mesh. Finally, this network is stabilized by cross-linking induced by activated factor XIIIa (Weisel, 1986). The coagulation pathways are tightly controlled with respect to place and time to avoid massive fibrin deposition. A series of anticoagulant proteins and cofactors bind to activated coagulation factors, limiting their period of activity. These include tissue factor pathway inhibitor (TFPI), antithrombin, CI inhibitor and the protein C anticoagulant pathway (Kisiel, 1979; Fuchs *et al.*, 1982; Pixley *et al.*, 1985; Broze, 1995).

Besides this negative regulation of coagulation, the fibrinolytic system acts to limit fibrin clot formation and dissolve fibrin clots (Fig. 6, lower part). Fibrin is degraded by the serine protease plasmin into fibrin degradation products (FDPs). Plasmin is formed by activation of plasminogen, a zymogen circulating in the bloodstream (Castellino, 1984). The major activator of plasminogen is tissue plasminogen activator (tPA), a serine protease produced by endothelial cells (Camiolo *et al.*, 1971; Lijnen and Collen, 1995). Urinary type plasminogen activator (uPA) or urokinase can also activate plasminogen. This is important in tissues where plasmin degrades extracellular matrix proteins, facilitating migration of cells important for wound healing (Plow *et al.*, 1999). The fibrinolytic system is negatively regulated by inhibition of plasmin function and inhibition of plasminogen activation. In plasma, plasmin is rapidly bound by α_2-antiplasmin in an irreversible fashion (Wiman and Collen, 1978). Plasmin attached to fibrin is less rapidly bound by antiplasmin because fibrin already occupies the lysine binding sites of plasmin that are also used by antiplasmin. Plasminogen activation is inhibited by plasminogen activator inhibitor I (PAI-I) and others (Chandler *et al.*, 1990).

Bacterial pathogenesis and haemostasis

The finely tuned system of coagulation and fibrinolysis also plays an important role in the host defense against intra-abdominal infections. As described earlier, upon an infection, the balance between the two systems shifts in favor of coagulation. This results in the formation of peritoneal fibrin clots into which bacteria become trapped, which eventually results in abscess formation. Conversely, bacteria have been shown to actively interfere with the fibrinolytic system for their pathogenesis in several ways (Lähteenmäki *et al.*, 2005). Several pathogenic species produce plasminogen activators (PAs), enhance plasminogen activation by host PAs, influence the production of host PAs or PA inhibitors (PAIs) or inhibit host antiplasmins (reviewed in Lähteenmäki *et al.*, 2001). Also, various bacteria can immobilize plasminogen or plasmin on their cell surface, converting the cell into a proteolytic organism. This gives the bacteria the capability to dissolve fibrin clots in which they have become trapped and/or degrade basal membranes and extracellular matrix proteins to be able to cross tissue barriers and become invasive. When immobilized on the cell surface, host or bacterial plasminogen activators more easily activate plasminogen and bound plasmin is protected against rapid inactivation by α_2-antiplasmin.

Various candidate receptors on the bacterial cell surface have been described in the last decade (those up to 2001 are listed in Lähteenmäki *et al.*, 2001). Importantly, most bacterial plasminogen receptors have other, in many cases essential, functions such as adhesion, movement or metabolism. This complicates the research into these molecules, because specific mutations or deletions can often not be made. Well-characterized types of plasminogen receptors are the α-enolases. These proteins have an essential function in glycolysis or gluconeogenesis, catalyzing the interconversion between 2-phosphoglycerate and phosphoenol-pyruvate. Recently it was discovered that α-enolase is also present on the cell surface of mammalian, fungal, nematode and bacterial cells, functioning as a plasminogen receptor (Redlitz *et al.*, 1995; Pancholi and Fischetti, 1998; Bergmann *et al.*, 2001; Jolodar *et al.*, 2003; Jong *et al.*, 2003). The plasminogen-binding site to α-enolase of *Streptococcus pyogenes* was thought to comprise the two C-terminal lysine residues (Derbise *et al.*, 2004). However, the recently published crystal structure of *S. pneumoniae* α-enolase reveals that the enolase is present in an octamer in which the C-terminal lysines are shielded off from the molecular environment (Ehinger *et al.*, 2004). Instead, an internal motif of nine amino acids (FYDKERKVY) that has been identified by the same authors earlier to be important

for plasminogen-binding, is exposed to the surface of the octamer (Bergmann *et al.*, 2003). Plasminogen-binding has been shown *in vivo* to be required for the efficient transmission and invasion of *Borrelia burgdorferi*, the causative agent of Lyme disease (Coleman *et al.*, 1997). Others have identified a plasminogen-binding protein on the cell surface of *B. burgdorferi* (Hu *et al.*, 1997). This protein also contains two C-terminal lysine residues but not the FYDKERKVY motif.

Human plasminogen is a glycoprotein zymogen that is abundant in plasma (circa 2 μM). Its polypeptide is composed of a heavy chain (65 kDa), containing an N-terminal peptide and five triple-disulfide bonded kringle (K) domains, and a light chain (25 kDa) containing the protease domain (Pollanen *et al.*, 1991). The crystal structures of the individual K1, K4 and K5 domains reveal that the lysine binding site motifs are preformed and localized to the surfaces of the K domains (e.g. Chang *et al.*, 1998). The binding of plasminogen to lysine-exposing molecules induces marked conformational changes of plasminogen (Andronicos *et al.*, 2000; Lähteenmäki *et al.*, 2005), making it more accessible for plasminogen activators and at the same time protecting plasmin against inactivation by α_2-antiplasmin.

The role of plasminogen-binding by pathogens in bacterial peritonitis is so far not specifically investigated. In *B. fragilis* a protein of circa 60 kDa, now designated Pbp, has been found that may be responsible for plasminogen-binding to the bacterial cell surface (Otto *et al*., this laboratory). The α-enolase of *B. fragilis* has also been analyzed and it is not a plasminogen-binding molecule. The contribution of Pbp to the virulence of *B. fragilis* in peritonitis and the synergy with *E. coli* is currently under investigation.

Autotransporter proteins

The autotransporter secretion pathway

An important class of virulence factors in Gram-negative bacteria is the class of the autotransporter proteins (Henderson and Nataro, 2001). The name relates to the fact that autotransporters carry all signals necessary for their targeting to and translocation across the inner and outer membranes within one (pre) protein (Fig. 7). No accessory periplasmic or outer membrane proteins appear to be needed. However, this concept has been challenged by recent findings as discussed below. The prototype of autotransporter proteins is the immunoglobulin A1 (IgA1) protease of *Neisseria gonorrhoeae*, described by Pohlner *et al* (Pohlner *et al.*, 1987). The 169-kDa IgA1 precursor encodes three functional domains: an N-terminal signal peptide

that directs inner membrane targeting and translocation, the secreted IgA1 protease and a C-terminal domain that directs translocation across the outer membrane. The authors proposed that the C-terminal domain encodes a pore-forming structure in the outer membrane that facilitates the transport of the protease. Since that time, many more proteins with this type of design have been described in various species of Gram-negative bacteria, all containing the modular structure of signal peptide, passenger domain and translocation unit in one preprotein (Jose *et al.*,

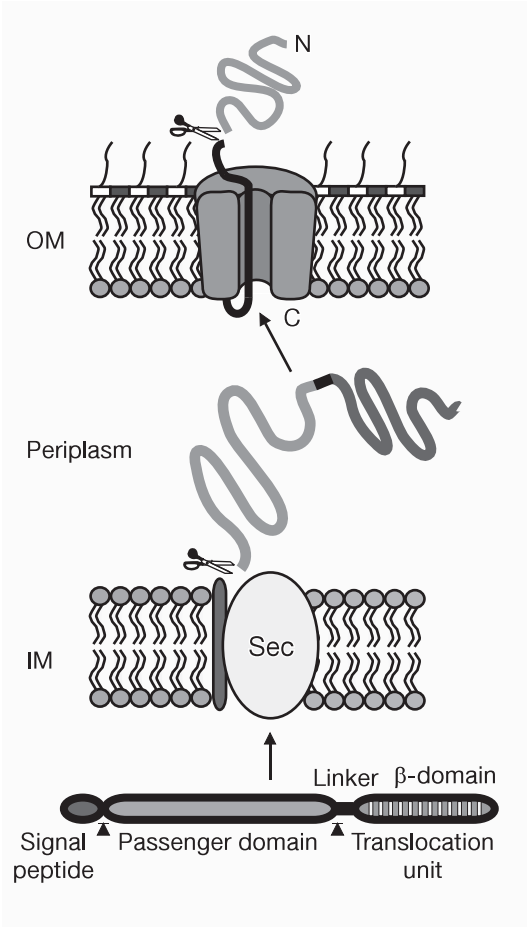

Fig. 7. Schematic overview of autotransporter secretion. The functional domains are the signal peptide, the passenger domain, the linker region and the β-domain. The latter two form the translocation unit. The complete pre-pro-protein is synthesized in the cytoplasm and translocated across the inner membrane through the Sec translocon. After cleavage of the signal peptide, the pro-protein travels through the periplasm and the β-domain inserts into the outer membrane as a pore. According to the classical model, the passenger domain is translocated through the β-barrel pore and cleaved off on the cell surface by either autoproteolysis or another protease. The arrowheads and scissors indicate the signal peptidase and protease cleavage sites.

1995; Henderson and Nataro, 2001). The secretion pathway followed by the autotransporters has been termed the type V or Va secretion pathway by Henderson *et al.* (Henderson *et al.*, 2000b). Nowadays, type V secretion also includes the

related two-passenger secretion (TPS) pathway (or type Vb) and the AT-2 or type Vc system (Jacob-Dubuisson *et al.*, 2001; Roggenkamp *et al.*, 2003; Cotter *et al.*, 2005). In the TPS pathway, the passenger domain (TpsA) and the translocation unit (TpsB) are produced by two different polypeptides instead of one. Therefore, this pathway needs a specific recognition event between the passenger and the translocator. Recognition is achieved by the addition of a conserved N-proximal module to the TpsA polypeptide, the TPS domain. The topology of the TpsB β-barrel appears to differ from that of the autotransporters by having 19 predicted amphipathic β-strands instead of 10 to 14 (see below). The AT-2 subfamily of autotransporters is defined by a short trimeric C-terminal translocation unit. After trimerization, a β-barrel pore consisting of 12 β-strands is formed in the outer membrane. In contrast to most conventional autotransporters, AT-2 proteins are not cleaved on the bacterial cell surface and they are generally involved in adhesion to extracellular matrix proteins or circulating host factors. A common property of all characterized type V proteins is that they are implicated to be bacterial virulence factors. Several reviews on type V and autotransporter secretion were published in 2004 (Desvaux *et al.*, 2004; Henderson *et al.*, 2004; Jacob-Dubuisson *et al.*, 2004; Newman and Stathopoulos, 2004).

The signal peptide of autotransporters

Analysis of the primary sequences of all known autotransporters reveals that they possess an N-terminal signal peptide that is typical for targeting of preproteins to the Sec translocon (Henderson *et al.*, 1998). The signal peptides, typically about 25 amino acids long, contain an N-domain with positively charged amino acids, an H-domain containing hydrophobic amino acids and a short C-domain with a signal peptidase recognition site (Martoglio and Dobberstein, 1998). Interestingly though, several autotransporters contain a conserved N-terminal extension to the classical signal peptide, making it about twice as long as a general signal peptide (Fig. 8) (Henderson *et al.*, 1998). Desvaux and Henderson describe the predicted presence of at least 80 proteins with extended signal peptides from completed genome sequences of Proteobacteria (Henderson *et al.*, 2004). Notably, the extended signal peptides appeared to be exclusively associated with proteins larger than 100 kDa. The N-terminal extensions also contain a N- and H-domain that are enriched in charged and in hydrophobic residues, respectively. Conserved aromatic residues characterize the extended N-domain and the H-domain typically contains a glutamate residue. The “classical” N-domain in these proteins contains an unusual number of charged residues (Brunder *et al.*, 1997). The biological function of the N-terminal

extension is not fully elucidated. Szabady *et al.* suggest a role in the transit of the passenger through the periplasm, based on their results with an N-terminally truncated construct (Szabady *et al.*, 2005). In their experiments, a construct lacking the N-terminal extension was dissociated from the inner membrane faster than the wild type protein. They suggest that the extension might function as an inner membrane retention signal, allowing the translocation unit to insert into the outer membrane and preventing premature folding of the passenger in the periplasm.

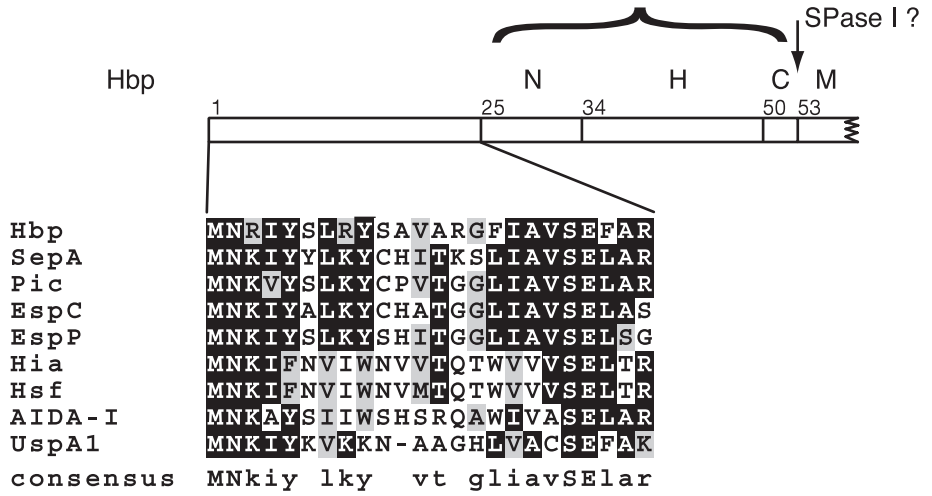

Fig. 8. The conserved N-terminal extension of a subset of autotransporters. Several autotransporters have a conserved extension of about 25 amino acids in front of the regular SecB-type signal sequence (bracket). The consensus sequence of the N-terminal extension is shown in the last line. Identical residues are depicted in black, similar residues in grey. N = N-terminal part, H = hydrophobic part and C = C-terminal part of the SecB-type signal sequence. M = mature protein. The putative signal peptidase I cleavage site is indicated by the arrow.

Inner membrane targeting of autotransporters

Targeting to the Sec translocon in the inner membrane of *E. coli* (among others) can involve either a post-translational or a cotranslational route. The posttranslational route often involves the cytoplasmic chaperone SecB that targets the complete preprotein to translocon-associated SecA (Randall and Hardy, 2002). The cotranslational route involves recognition of the signal peptide by the Signal

Recognition Particle (SRP) that directs the ribosome-nascent chain complex directly to the translocon via the SRP receptor FtsY (Herskovits *et al.*, 2000). A recently discovered pathway independent of the Sec translocon is the Twin-Arginine Translocation (Tat) pathway. This pathway is involved in the translocation of folded proteins across the inner membrane and recognizes signal peptides containing a typical twin-arginine motif. Twin-arginine motifs have not been found in autotransporters, therefore a role of the Tat pathway in the inner membrane translocation of autotransporters is unlikely. The work described in this thesis investigates the inner membrane targeting and translocation of the *E. coli* autotransporter Hbp, and it was found that Hbp is likely targeted to the membrane cotranslationally via SRP and translocated through the Sec translocon. The *Shigella flexneri* autotransporter IcsA also depends on the Sec translocon when expressed in *E. coli*, but under steady state conditions apparently not on SRP (Brandon *et al.*, 2003). Interestingly, Szabady *et al.* recently described the targeting of the *E. coli* autotransporter Pet and found targeting by SecB to the Sec translocon. Only when the N-terminal extension of the signal peptide was removed, the protein was rerouted into the cotranslational pathway (Szabady *et al.*, 2005).

Periplasmic transit of autotransporters

Signal Peptidase I (LepB) cleaves the signal peptide from the autotransporter precursor during or after inner membrane translocation. A few exceptional autotransporters, like NalP (AspA) (Turner *et al.*, 2002; van Ulsen *et al.*, 2003), carry a lipoprotein signal peptide and are subsequently cleaved by Signal Peptidase II. Between the translocation events at the inner and outer membranes, the autotransporter precursor molecule has to travel through the periplasm. Alternatively, secretion of the molecule may occur without the formation of periplasmic intermediates in one coupled inner/outer membrane translocation process. Periplasmic intermediates of autotransporters are generally not detected and most likely short-lived (Jacob-Dubuisson *et al.*, 2004). Several controversial reports exist about the folding status of the autotransporters during the periplasmic transit and outer membrane translocation. Oliver *et al.* showed that the *Bordetella pertussis* autotransporter BrkA contains an internal chaperone sequence that is conserved in many autotransporters. They suggest that the passenger protein remains in an unfolded, translocation competent state during the periplasmic transit and that folding of the protein occurs at the bacterial surface (Oliver *et al.*, 2003b). In contrast, Veiga *et al.* demonstrated the outer membrane translocation of a folded passenger domain, using a single-chain antibody as a heterologous passenger

molecule. Because of the dimensions of the (partially) folded passenger domain, they suggest that the passenger is not translocated through the small pore formed by the translocation unit, but through a central channel formed by a multimer of translocation units in the outer membrane (Fig. 9) (Veiga *et al.*, 1999; Veiga *et al.*, 2002). The only genuine autotransporter passenger domain demonstrated to form disulfide bonds in the periplasm is that of *Shigella flexneri* IcsA (Brandon and Goldberg, 2001).

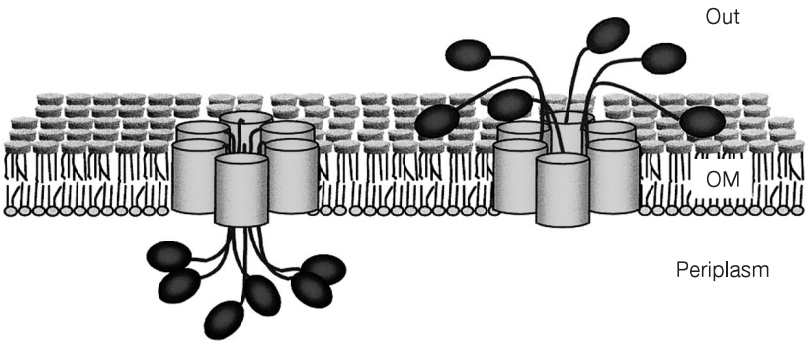

Fig. 9. Oligomer model for autotransporter secretion. Multiple autotransporter translocation units (cylinders) insert as a ring-shaped complex in the outer membrane (OM). The passenger domains (dark ovals) are translocated from the periplasm (left) to the extracellular environment (right) through the central hydrophilic pore formed by the oligomeric complex. Figure taken from (Veiga *et al.*, 2002).

Translocation of autotransporters across the outer membrane

The translocation unit of autotransporters consists of a short but essential linker region with a predicted α-helical structure and a β-core that presumably forms a β-barrel pore upon insertion in the outer membrane (Maurer *et al.*, 1999; Oliver *et al.*, 2003a). The pores are predicted to consist of 10 to 14 amphipathic β-strands connected by hairpin turns and loops (Jacob-Dubuisson *et al.*, 2004). This original model was supported by the publication of the first crystal structure of an autotransporter translocation unit by Oomen *et al.* (Oomen *et al.*, 2004). The translocation unit of the *Neisseria meningitidis* autotransporter NalP (AspA) has been isolated, refolded *in vitro*, crystallized and the structure was refined to 2.6 Å

resolution. The structure consists of a β-barrel formed by 12 antiparallel β-strands around a central cavity of circa 10 by 12.5 Å (Fig. 10). The pore was found to be occupied by an α-helix formed by the linker region as predicted. The cavity was shown to be hydrophylic with stretches of charged amino acids along the internal barrel wall. The dimensions of the pore and the presence of the α-helix in the β-barrel point towards a translocation mechanism in which the passenger is translocated through the β-barrel pore. The size of the pore is just wide enough to accommodate two extended polypeptide chains, allowing passing the protein only in an unfolded state. After translocation and cleavage of the passenger domain, the linker region accommodates an α-helix conformation and remains in the pore. Alternatively, the α-helix inserts into the β-barrel pore only after translocation of the passenger through a larger oligomeric β-barrel channel. Taken together, more data is needed to elucidate the mechanism of periplasmic transit and outer membrane translocation of autotransporter passenger domains and to address the possibility of partial folding before translocation.

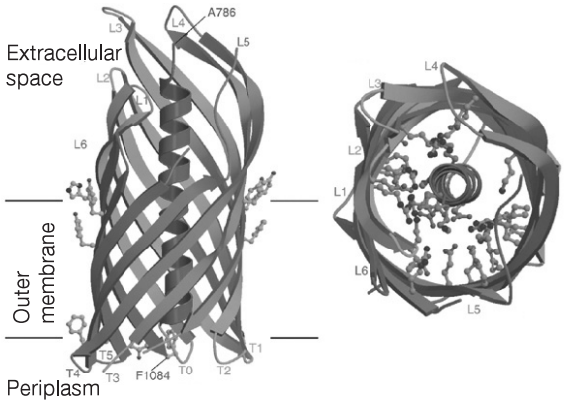

Fig. 10. Crystal structure of the translocation unit of the *N. meningitides* autotransporter NalP. In the side view, aromatic residues flanking the membrane-embedded region are shown as ball-and-stick. In the top view, charged amino acids are shown as ball-and-stick to indicate the hydrophylic nature of the barrel interior. Figure adapted from (Oomen *et al.*, 2004).

Folding of autotransporters

The recent discovery of an autochaperone domain in the BrkA autotransporter suggests that the final folding of passenger molecules occur on the outside of the cell (Oliver *et al.*, 2003b). This conserved C-terminal domain is present in several, but not all, autotransporters. The domain is important for folding of the

BrkA passenger, possibly by functioning as a chaperone, scaffolding the folding of the protein linked to it. *In silico* analysis of autotransporter passenger domains predicts that many possess a high degree of β-helical structure (Kajava *et al.*, 2001; Yen *et al.*, 2002). This might indicate that autotransporters generally adopt a conformation resembling that of pertactin, the first passenger domain of an autotransporter that was crystallized, although not completely (Emsley *et al.*, 1996). In this thesis, the first complete crystal structure of an autotransporter passenger, Hbp, is described. This protein also has a β-helical backbone structure with several domains extruding from it. The process of folding of the mainly β-helical structured passenger domain on the cell surface might actually be the driving force for the outer membrane translocation (Klauser *et al.*, 1992). According to Oliver *et al.*, the correct folding of the passenger domain is supposed to depend on the autochaperone domain (Oliver *et al.*, 2003b). A sequence homologous to the BrkA-like autochaperone domain is also found in Hbp. This C-terminal region has a remarkably high degree of structural homology to a similar domain in the pertactin crystal structure (Emsley *et al.*, 1996) (J. Tame, personal communication). Interestingly though, the domain in Hbp contains only 4 out of the 9 highly conserved residues present in BrkA (Oliver *et al.*, 2003b). Similar to this putative autochaperone function, a "junction region" at the C terminus of the *Serratia marcescens* PrtS passenger domain was identified that was necessary for correct folding of its passenger on the cell surface (Ohnishi *et al.*, 1994). The sequence of this junction region is not homologous to that of the BrkA autochaperone domain but it is present in several PrtS homologues. Jacob-Dubuisson *et al.* propose that these subtilase-like autotransporters belong to a different structural group of autotransporters than the β-helix passenger proteins such as Hbp (Jacob-Dubuisson *et al.*, 2004).

Outer membrane insertion of the β-barrel

The outer membrane insertion of the β-barrel itself is still subject to debate. All autotransporters contain a conserved amino acid motif at the extreme C terminus that is specific for outer membrane proteins (e.g. Struyvé *et al.*, 1991). The terminal amino acid is always phenylalanine or tryptophan, preceded by alternating hydrophylic and hydrophobic residues (Jose *et al.*, 1995; Loveless and Saier, 1997). Deletion of the final three residues of the *Haemophilus influenzae* autotransporter Hap abolishes outer membrane insertion of the protein (Hendrixson *et al.*, 1997). The traditional model proposes that the β-barrel structure spontaneously inserts itself in the outer membrane, without the assistence of accessory factors (hence the name autotransporter). The hydrophobic residues of the β-sheets will face the lipid bilayer,

while the alternating hydrophylic residues will face inwards and form the lining of the pore. This insertion process may be similar to the formation of porins in the outer membrane (Tamm *et al.*, 2001). Additionally, other β-barrel forming outer membrane proteins, like OmpA and PhoE, have been shown to require lipopolysaccharide (LPS) and the periplasmic chaperone Skp for efficient outer membrane insertion (de Cock *et al.*, 1999; Bulieris *et al.*, 2003). Deletion of the *skp* gene does not fully prevent outer membrane insertion, indicating that other mechanisms of membrane insertion exist (Bulieris *et al.*, 2003). Recently, Voulhoux *et al.* demonstrated the involvement of the highly conserved Omp85 protein in outer membrane insertion in *Neisseria meningitidis* (Voulhoux *et al.*, 2003). Depletion of this protein resulted in the accumulation of unassembled forms of outer membrane proteins, including autotransporters. On the other hand, Genevrois *et al.* showed an involvement of Omp85 in lipid export to the outer membrane (Genevrois *et al.*, 2003). Besides, the localization of several outer membrane proteins was not impaired upon Omp85 depletion. The exact role of Omp85 in outer membrane protein insertion and the molecular mechanism involved remain to be investigated. Interestingly though, Oomen *et al.* even speculated about the possible direct involvement of Omp85 in the outer membrane translocation of passenger domains (Oomen *et al.*, 2004). The passage of the passenger domain would then occur through a pore formed by Omp85 rather than by the translocation unit. Recently, Wu *et al.* identified a multiprotein complex required for the assembly of proteins in the OM of *E. coli* (Wu *et al.*, 2005). A homologue of Omp85, YaeT, is part of this multiprotein complex. It is likely that this multiprotein complex is also required for the insertion of the β-barrels of autotransporters into the OM.

Final processing of the autotransporter

Once the passenger domain of the autotransporter is folded on the outside of the cell, several alternative processing steps have been demonstrated. The passenger domain may be cleaved from the translocation unit and released into the extracellular environment, as shown for *E. coli* Hbp, Pet and EspP (Brunder *et al.*, 1997; Eslava *et al.*, 1998; Otto *et al.*, 1998). Alternatively, the passenger may not be cleaved but remains attached to the β-barrel and extends into the environment, like Hia or Hsr (O'Toole *et al.*, 1994; St Geme and Cutter, 2000). An intermediate form is also possible, in which the passenger domain is cleaved but remains non-covalently attached with the translocation unit, as is the case with AIDA-I and pertactin (Leininger *et al.*, 1991; Benz and Schmidt, 1992). Interestingly, the cleavage between passenger and translocation unit can occur at various positions depending on the

autotransporter, ranging from well upstream of the linker region to within the predicted α-helix (Oliver *et al.*, 2003a). This has important implications for the mechanism and cellular location of the cleavage. For several autotransporters, autoproteolytic cleavage involving the serine protease active site from the passenger has been demonstrated (Pohlner *et al.*, 1987; Hendrixson *et al.*, 1997; Serruto *et al.*, 2003). This event will likely only occur on the cell surface after folding of the passenger into its native conformation. Other autotransporters have been shown to be cleaved by the action of alternative proteases, like the *Shigella flexneri* autotransporter IcsA that is cleaved by the membrane protease IcsP (Egile *et al.*, 1997; Shere *et al.*, 1997). When the cleavage site is located within the α-helical linker region, as for Hbp, the protease recognition site might not become available at the cell surface for surface proteases or autoproteolytic cleavage. In this case, a role for periplasmic proteases might also be invisaged, but this has not been investigated so far. The fate of the translocation unit after cleavage of the passenger is unclear. Studies on the translocation unit of pertactin P.69 from *Bordetella pertussis* indicate that the β-barrel structure is rather stable (Charles *et al.*, 1994). On the other hand, studies in our lab on *E. coli* Hbp demonstrate that in a wild type Hbp-secreting *E. coli* strain EB1 hardly any translocation unit can be detected in the membrane (B.R. Otto, unpublished data). One might envisage that the accumulation of pore-forming outer membrane proteins without a plug domain could be detrimental for the cell because of potential massive leakage of ions through these open pores. The mechanism of regulation of the expression and degradation of translocation units requires further investigation.

Functions of autotransporters

As mentioned, autotransporters are virulence factors that are found in many Gram-negative pathogens (Yen *et al.*, 2002). Although the overall structure of autotransporters is similar and they basically use the same secretion mechanism, individual passenger domains are very diverse in sequence and function (Henderson *et al.*, 1998; Henderson and Nataro, 2001). The functions of autotransporters range from adhesin to protease and from lipase or esterase to mediator of intracellular motility. Phylogenetic relationships have been worked out and demonstrate the occurrence of horizontal gene transfer among evolutionarily separated species (Davis *et al.*, 2001; Henderson and Nataro, 2001; Dutta *et al.*, 2002; Henderson *et al.*, 2004). A distinct class of autotransporters is formed by the serine protease autotransporters of the *Enterobacteriaceae* (SPATEs). Even though these proteins show significant homology (40-100% identity) and all contain a trypsin-type serine

protease motif, the proteins have specific and distinct functions which are adaptive for the particular niche occupied by the pathogen (Dutta *et al.*, 2002). For example, EspC from enteropathogenic *E. coli* and Pet from enteroaggregative *E. coli* act as a toxin (Eslava *et al.*, 1998; Mellies *et al.*, 2001), EspP from enterohemorrhagic *E. coli* cleaves pepsin and human coagulation factor V (Brunder *et al.*, 1997), and SepA from *Shigella* plays a role in tissue invasion (Benjelloun-Touimi *et al.*, 1995). In our lab, Otto *et al.* have shown that enteropathogenic *E. coli* secretes Hbp that functions as a hemoglobinase and heme-binding protein (Otto *et al.*, 1998). An essentially identical protein has been identified as a temperature-sensitive hemagglutinin (Tsh) in avian pathogenic *E. coli* (Provence and Curtiss, 1994). Recent results question the hemagglutinin activity of Tsh and demonstrate just like Hbp a proteolytic activity of this molecule (Kostakioti and Stathopoulos, 2004). Otto *et al.* also demonstrated that Hbp contributes to the synergism with *B. fragilis* in peritoneal infections by delivering heme to *B. fragilis* (Otto *et al.*, 2002). No other autotransporters have been identified that contribute to synergy and abscess formation in intra-abdominal infections to date.

Outline of this thesis

The studies presented in this thesis describe the characterization of several proteins that are or may be involved in the pathogenic synergy between *E. coli* and *B. fragilis* in bacterial peritonitis. The protein Hbp is produced by the *E. coli* strain EB1 (O8-K43) and the proteins α-enolase P46 and Pbp are produced by the *B. fragilis* strain BE1. Both these strains have been isolated from a peritoneal abscess of a patient with a wound infection at the Academic Hospital of the Vrije Universiteit in Amsterdam (Verweij-van Vught *et al.*, 1985).

In 1998, Otto *et al.* described the discovery and initial characterization of the autotransporter protein Hbp from *E. coli* (Otto *et al.*, 1998). The *hbp* gene has been cloned and further analysis showed that the purified protein degrades hemoglobin and subsequently binds the released heme (Otto *et al.*, 1998; Tame *et al.*, 2002). Later it has been demonstrated that Hbp is a true virulence factor, involved in the synergistic abscess formation and heme-dependent growth of *B. fragilis* (Otto *et al.*, 2002). In this thesis, the molecular properties of Hbp are characterized in more detail.

In chapter 2, the targeting of the Hbp precursor to the inner membrane and its translocation across the inner membrane of *E. coli* is investigated. It is demonstrated that optimal processing of the precursor requires a functional SRP

pathway and Sec-translocon. SecB is not required for targeting of Hbp *in vivo*, but can compensate to some extent for the absence of SRP. These results give more insight into the mechanism of inner membrane targeting and translocation of autotransporters.

In chapter 3 the crystal structure of the complete passenger domain of Hbp, refined to 2.2 Å resolution is presented. This is the first complete structure of an autotransporter passenger domain and the largest parallel β-helical structure solved to date. Based on the prediction that an overall β-helical architecture is common for autotransporters (e.g. Kajava *et al.*, 2001), this structure may function as a homology model in the characterization of other autotransporters.

In chapter 4, the translocation unit of Hbp is further characterized. In 2004, the crystal structure of the translocation unit of the *Neisseria meningitidis* autotransporter NalP has been published (Oomen *et al.*, 2004). This was the first paper describing the structure of an autotransporter translocation unit. The translocation unit of Hbp has several similarities as well as differences with the NalP translocation unit. Besides a discussion of these differences and similarities, the chapter describes the first steps towards crystallization of the Hbp translocation unit.

The following chapters describe the identification and characterization of two putative virulence factors from *B. fragilis*: P46 and Pbp. In chapter 5 the identification, cloning and partial characterization of the α-enolase P46 of *B. fragilis* is described. This functional α-enolase protein is upregulated under conditions of iron- or heme-starvation. P46 is normally located mainly in the cytoplasm, but upon iron-depleted conditions it mainly localizes to the inner membrane.

Finally, in chapter 6 the cloning and characterization of the plasminogen-binding protein Pbp of *B. fragilis* is described. Pbp is a 60-kDa lipoprotein that is partially located on the cell surface where it can bind host plasminogen. This is the first study describing the functional characterization of a lipoprotein of *B. fragilis*, which may function as a plasminogen receptor on *B. fragilis* cells.

Chapter 2

Signal Recognition Particle (SRP)-mediated targeting and Sec-dependent translocation of an extracellular *Escherichia coli* protein

Robert Sijbrandi, Malene L. Urbanus, Corinne M. ten Hagen-Jongman, Harris D. Bernstein[1], Bauke Oudega, Ben R. Otto, and Joen Luirink

[1] Genetics and Biochemistry Branch, NIDDK, National Institutes of Health, Bethesda, Maryland, United States of America

Published in The Journal of Biological Chemistry 278 (2003): 4654-4659

Abstract

Hemoglobin protease (Hbp) is a hemoglobin-degrading protein that is secreted by a human pathogenic *Escherichia coli* strain via the autotransporter mechanism. Little is known about the earliest steps in autotransporter secretion, *i.e.* the targeting to and translocation across the inner membrane. Here, we present evidence that Hbp interacts with the signal recognition particle (SRP) and the Sec-translocon early during biogenesis. Furthermore, Hbp requires a functional SRP targeting pathway and Sec-translocon for optimal translocation across the inner membrane. SecB is not required for targeting of Hbp but can compensate to some extent for the lack of SRP. Hbp is synthesized with an unusually long signal peptide that is remarkably conserved among a subset of autotransporters. We propose that these autotransporters preferentially use the co-translational SRP/Sec route to avoid adverse effects of the exposure of their mature domains in the cytoplasm.

Introduction

Hemoglobin protease (Hbp) is secreted by a human pathogenic *Escherichia coli* strain (Otto *et al.*, 1998) and contributes to the pathogenic synergy between *E. coli* and *Bacteroides fragilis* in intra-abdominal infections (Otto *et al.*, 2002). It represents the first described member of the serine protease autotransporters of Enterobacteriaceae (SPATE) group of autotransporter proteins (Henderson *et al.*, 1998).

The key feature of an autotransporter is that it contains all the information for secretion in the precursor of the secreted protein itself (Henderson *et al.*, 1998). Autotransporters comprise three functional domains: 1) an N-terminal targeting domain; 2) a C-terminal translocation domain; and, in between these two, 3) the passenger domain that is the actual secreted moiety. The C-terminal domain is supposed to form a β-barrel structure in the outer membrane that may form an oligomeric channel around a cavity to allow the passage of the passenger domain (Veiga *et al.*, 2002). The N-terminal domain is thought to function as a signal peptide to mediate targeting to and translocation across the inner membrane.

Compared with other signal peptides in *E. coli*, the putative signal peptide of Hbp is unusually long (Otto *et al.*, 1998) (Fig. 1). Analogously, several other autotransporters are predicted to have long signal peptides (Henderson *et al.*, 1998; Henderson *et al.*, 2000a). All these signal peptides display a conserved domain

structure. The C terminus resembles a normal signal peptide with a basic N-terminal region, a hydrophobic core region, and a C-terminal consensus signal peptidase cleavage site. The N terminus forms a conserved extension, the function of which is not known (Fig. 1).

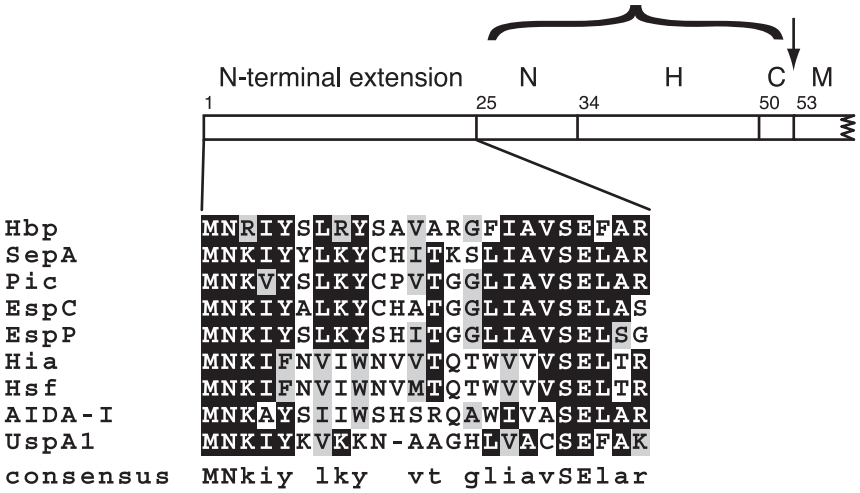

Fig. 1. The signal peptide of Hbp has a conserved N-terminal extension. A schematic representation of the 52 amino acid-long signal peptide of Hbp is shown, indicating the probable signal peptidase cleavage site (arrow). The basic N-terminal (N), hydrophobic (H), and C-terminal (C) domains characteristic of typical signal peptides are indicated. M indicates the beginning of the mature region of Hbp. A comparison of the N-terminal extensions of several autotransporters possessing extended signal peptides is given together with a consensus sequence of the conserved domain.

Most periplasmic and outer membrane proteins synthesized with a cleavable signal peptide are translocated through the Sec-translocon. The core translocase consists of the integral inner membrane proteins (IMPs) SecY, SecE, and SecG, which constitute an oligomeric complex homologous to the Sec61 channel complex in the endoplasmic reticulum (Manting and Driessen, 2000). The peripheral membrane ATPase SecA is unique to bacteria and catalyzes the actual polypeptide transfer through the translocase. Targeting to the Sec-translocon may occur after translation and often requires the cytosolic chaperone SecB.

The Sec-translocon is also used for the membrane insertion of most IMPs that are synthesized with uncleaved, relatively hydrophobic signal peptides (de Gier

and Luirink, 2001). Targeting of IMPs to the Sec-translocon is not mediated by SecB but by the signal recognition particle (SRP) and its receptor, FtsY, in a co-translational mechanism that resembles targeting to the Sec61 complex in the endoplasmic reticulum (Herskovits *et al.*, 2000).

Here we provide evidence that the long signal peptide of Hbp mediates targeting to the inner membrane via the SRP pathway. When the SRP pathway is compromised, SecB can prevent, to a certain extent, the mislocalization of pre-pro-Hbp. Subsequent translocation across the inner membrane involves the Sec-translocon. This is the first demonstration of the use of the co-translational SRP pathway for inner membrane targeting of an extracellular protein.

Experimental procedures

Bacterial Strains, Plasmids, and Media

E. coli K12-strains and the plasmids used are listed in Table 1. *E. coli* strains were routinely grown in Luria-Bertani (LB) medium (Miller, 1992). Strains MM152 and HDB52 were grown in M9 medium (Miller, 1992). If required, antibiotics were added to the culture medium.

Table 1. Bacterial strains and plasmids used in this study

Strain / plasmid	Relevant genotype	Reference
MC4100	F⁻ *araD139* Δ(*argF-lac*)U169 *rpsL150 relA1 flb5301 ptsF25 rbsR*	(Casadaban, 1976)
TOP10F'	F'{*lacI*^{q} Tn*10*(Tc^R)} *mcrA* Δ(*mrr-hsdRMS-mcrBC*) Φ*80lacZ*Δ*M15* Δ*lacX74 deoR recA1 araD139* Δ(*ara-leu*)*7697 galU galK rpsL*(Str^R) *endA1 nupG*	Invitrogen
BL21 (DE3)	F⁻ *ompT hsdS*$_B$ (r$_B$⁻ m$_B$⁻) *gal dcm* Δ(*srl-recA*)*306*::Tn*10*(Tc^R) (DE3)	(Studier *et al.*, 1990)
HDB51	MC4100 *ara*$^+$ *secB*$^+$ *zic-4901*::Tn*10 ffh*::*kan-1* λ(P$_{ara}$-*ffh* Ap^r)	(Lee and Bernstein, 2001)
HDB52	MC4100 *ara*$^+$ *secB*::Tn*5 zic-4901*::Tn*10 ffh*::*kan-1* λ(P$_{ara}$-*ffh* Ap^r)	(Lee and Bernstein, 2001)
HDB97	MC4100 *malP*::*lacI* Δ*ara714 cps*::*lacZ mal*$^+$	(Lee and Bernstein, 2001)
HDB107	MC4100 *malP*::*lacI* Δ*ara714 cps*::*lacZ mal*$^+$ Δ*lon510* Δ*clpYQ1172*::*tet*	(Lee and Bernstein, 2001)
IQ85	*secY24*(ts) Tn*10 thiA* Δ*lac araD rspL rspE relA*	(Shiba *et al.*, 1984)
IQ86	Tn*10 thiA* Δ*lac araD rspL rspE relA*	(Shiba *et al.*, 1984)
MM152	MC4100 *zhe*::Tn*10 malT^C secB*::Tn*5*	(Kumamoto and Beckwith, 1985)
JARV16	MC4100 Δ*tatA* Δ*tatE*	(Sargent *et al.*, 1999)
pET9-FtsY-A449	pET9, *ftsY-A449*	(Kusters *et al.*, 1995)
pACYC-Hbp	pACYC184 (Ori$_{p15A}$), *hbp*	(van Dooren *et al.*, 2001)
pC4MethssHbp	pC4Meth, *ss-Hbp*	this study
pHB6.4-Hbp	pBR322 (Ori$_{ColE1}$), *hbp*	this study
pHB6.4-HbpΔss	pBR322 (Ori$_{ColE1}$), *hbp*Δ*ss*	this study
pHE12.6	pBR322 (Ori$_{ColE1}$), *hbp*	(Otto *et al.*, 1998)

Reagents and Sera

Restriction enzymes, the Expand long template PCR system and the Lumi-light Western blotting substrate were obtained from Roche Molecular Biochemicals. All other chemicals were supplied by Sigma. Antiserum J40 raised against purified Hbp has been described previously (Otto *et al.*, 2002). Antisera against β-lactamase, OmpA/OmpC, trigger factor (TF)/SecA, and SufI were gifts from J.-M. van Dijl, J.-W. de Gier, W. Wickner, and T. Palmer, respectively.

Plasmid Construction

For cross-linking of nascent Hbp, we constructed pC4MethssHbp, which encodes the 110 N-terminal amino acid residues of Hbp fused to a C-terminal 4× methionine tag and a three amino acid linker sequence to improve labeling efficiency. The construct was obtained by PCR using pHE12.6 as a template and the primers Hbp-*Eco*RI-for (5'-GCCGGAATTCTAATATGAACAGAATTTATTCTCTTC-3' with the *Eco*RI restriction site in boldface) and Hbp-*Bam*HI-rev (5'-GCGGGATCCACCGATTT-CCGAATCCACA-3' with the *Bam*HI restriction site in boldface). The PCR fragment was cloned *Eco*RI/ *Bam*HI into pC4Meth (Valent, 1997). To construct plasmid pHB6.4-Hbp∆ss, the signal peptide coding region of *hbp* was removed from plasmid pHB6.4-Hbp using the Exsite PCR-based, site-directed mutagenesis kit (Stratagene). The plasmid pHB6.4-Hbp is derived from pHE12.6 (Otto *et al.*, 1998). The primers used were Hbp-*Nhe*I-for (5'-CTTGCTAGCGTCAATAATGAACTCGGGTATC-3' with the *Nhe*I restriction site in boldface) and Hbp-*Bgl*II-rev (5'-CTGATTTTATTTTTCTCA-GGAGTAATTAAAAATGAAGAGATCTAAG-3' with the *Bgl*II restriction site in boldface). Upon ligation of the linear DNA, the last three bases from each end constitute a *Hin*dIII restriction site. The resulting plasmid encodes the Hbp protein without its signal peptide but with six extra N-terminal amino acids (MKRSKL) and two altered amino acids (GT → AS) at the start of the mature Hbp region.

In Vitro Transcription, Translation, Targeting, and Cross-linking

Truncated mRNA was prepared as described previously (Scotti *et al.*, 2000) from *Hin*dIII linearized pC4MethssHbp. *In vitro* translation, targeting to inverted membrane vesicles (IMVs), cross-linking with DSS, and carbonate extraction of nascent Hbp were carried out as described (Scotti *et al.*, 2000). The samples were either analyzed directly by 15% SDS-PAGE or immunoprecipitated first using 4-fold the amount used for direct analysis.

Pulse-Chase Experiments

For Ffh depletion studies, strains HDB51 and HDB52 were grown overnight in M9 containing 0.1% casaminoacids (Difco), 0.2% fructose, and 0.2% L-arabinose, washed in the same medium lacking L-arabinose, and diluted to an OD_{660} of 0.004 in M9 containing fructose (0.2%) and either L-arabinose (0.2%) or glucose (0.2%). Cells were grown to an OD_{660} of ~0.3 before labeling. Depletion of Ffh was verified by Western blotting. The temperature-sensitive SecY mutant strains IQ85 and its isogenic wild type strain IQ86 were grown overnight at 30 °C in LB medium, diluted into fresh medium to an OD_{660} of 0.02, and grown to an OD_{660} of 0.3. Growth was then continued at 30 or 42 °C for 3 h. For overexpression of a dominant lethal *ftsY* allele, strain BL21(DE3) harboring pET9-FtsY-A449 was grown overnight at 37 °C in M9 medium with 0.2% glycerol as a carbon source and diluted into fresh medium to an OD_{660} of 0.03. When cells reached an OD_{660} of 0.2, 40 µM isopropyl-1-thio-β-D-galactopyranoside (IPTG) was added to induce FtsY-A449 expression, and growth was continued for 15 min. To inhibit SecA functioning in MC4100, 3 mM NaN_3 was added 3 min prior to labeling. In all experiments, 2.4 OD_{660} units of cells were washed and diluted into 3 ml of M9 medium containing appropriate sugars and a mixture of 18 amino acids except methionine and cysteine. After recovery for 15-45 min at 30, 37, or 42 °C as indicated, cells were pulse labeled for 1 min by the addition of 10 µCi/ml [^{35}S]methionine and chased for various times by adding cold methionine (2 mM). To stop the chase, cells were rapidly cooled in ice water and centrifuged at 4 °C for 2 min at 8,000 × *g*. Supernatants were precipitated with trichloroacetic acid and subjected directly to 8-15% SDS-PAGE. Cell pellets were first lysed and subjected to immunoprecipitation using anti-Hbp and anti-OmpA serum essentially as described (Luirink *et al.*, 1992).

Western Blotting

For analysis of steady-state levels of Hbp, *E. coli* strains harboring an *hbp* expression plasmid were grown to an OD_{660} of 0.5. Aliquots were removed from the cultures and centrifuged (1 min at 16,000 × *g*). The culture supernatants were trichloroacetic acid precipitated. Equivalent amounts of cells and supernatant were analyzed by Western blotting. Blots were developed by enhanced chemiluminescence using Lumi-light Western blotting substrate.

Sample Analysis

Radiolabeled proteins were visualized by phosphorimaging using a Amersham Biosciences PhosphorImager 473 and quantified using the ImageQuant quantification software from Amersham Biosciences. Chemiluminescent Western blots were analyzed using the Fluor-S MultiImager and Multianalyst software (Bio-Rad).

Results

Hbp That Lacks Its Signal Peptide Is Not Secreted and Degraded in the Cytosol

Hbp is synthesized in a pre-pro form (148 kDa) (Otto *et al.*, 1998). The N-terminal signal peptide is cleaved during passage of the pre-pro-Hbp through the inner membrane, leaving the pro-Hbp (142 kDa) in the periplasm. The C-terminal β-barrel domain is cleaved from the pro-Hbp at the outer membrane and mediates the transfer of the mature Hbp (111 kDa) into the culture medium. To analyze the role of the Hbp signal peptide, it was deleted from the pre-pro-Hbp, and the consequences for maturation and secretion were analyzed by Western blotting of cell samples and culture supernatants using Hbp-specific antibodies (Fig. 2A). As expected, deletion of the signal peptide (Δss) prevented secretion of mature Hbp into the medium. Only a small amount of pro-HbpΔss was detected in the cells. In contrast, most wild-type pre-pro-Hbp was processed to mature Hbp, which was either secreted or remained cell-associated as observed previously (Otto *et al.*, 1998). In addition, some pre-pro- or pro-Hbp accumulated in the cells.

We next investigated the reason for the low expression level of pro-HbpΔss. It has been observed previously that secreted proteins and IMPs that fail to be translocated across or inserted into the inner membrane are prone to proteolytic degradation (Bernstein and Hyndman, 2001). To investigate this possibility, HbpΔss was expressed in strain HDB107, which lacks the major cytoplasmic proteases Lon and ClpYQ (Bernstein and Hyndman, 2001). Pulse-chase labeling was employed to compare the stability of HbpΔss species in strain HDB107 and its isogenic parental strain HDB97 (Fig. 2B). HbpΔss remained almost completely stable for at least 10 min in HDB107, whereas only limited amounts were detected in HDB97 after a 10-min chase. In fact, relatively little HbpΔss was detected in HDB97 even when samples were analyzed directly after pulse labeling.

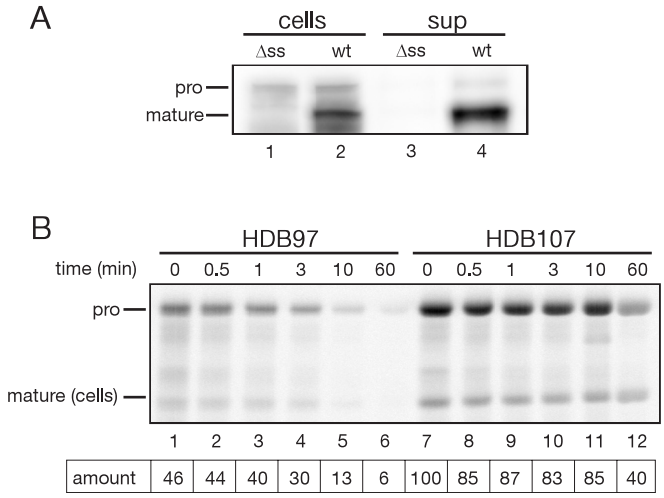

Fig. 2. A, the signal sequence of Hbp is required for secretion. Strain Top10F', harboring pHB6.4-Hbp (wt, wild-type) or pHB6.4-HbpΔss, was grown to an OD_{660} of 0.5 and split in cells and supernatant (sup). Samples corresponding to 0.1 OD_{660} unit were subjected to 8% SDS-PAGE and Western blotting using anti-Hbp serum. B, the proteases Lon and/or ClpYQ are involved in degradation of precursor Hbp in the cytosol. HDB97 (wild-type) and HDB107 *(lon⁻, clpYQ⁻),* harboring pHB6.4-HbpΔss, were grown to mid-log growth phase, radiolabeled with [^{35}S]methionine for 1 min, and chased for the times indicated. The cell samples were immunoprecipitated using anti-Hbp serum and subjected to SDS-PAGE. The numbers below the lanes show the relative quantified amount of pro-Hbp. Lanes 1-6, HDB97 cells; lanes 7-12, HDB107 cells. pro, pro-Hbp (142 kDa); mature, mature Hbp (111 kDa).

These data indicated that Hbp requires its signal peptide for targeting to the inner membrane and, consequently, for secretion of mature Hbp. Mislocalized pro-Hbp is rapidly degraded by the cytoplasmic proteases Lon and/or ClpYQ.

Nascent Hbp Interacts with SRP, Trigger Factor, SecA, and SecY in Vitro

To investigate the molecular interactions of the atypical Hbp signal peptide in the cytoplasm and the membrane, we used an *in vitro* cross-linking assay. A radiolabeled Hbp translation intermediate of 117 amino acid residues was generated by *in vitro* translation of truncated mRNA in a homologous cell-free translation system developed previously in our laboratory (Scotti *et al.*, 2000). Because the truncated RNA does not contain a stop codon, the nascent chain remains associated with the ribosome, and the signal peptide is exposed outside the ribosome that covers ~35 C-terminal amino acids. Translation was carried out in the presence of purified IMVs to allow targeting and membrane insertion. Subsequently, interactions of the nascent

Hbp were fixed by using the membrane-permeable, lysine-specific cross-linking reagent DSS. Finally, the samples were extracted with sodium carbonate to separate membrane integrated from the soluble and peripheral membrane proteins.

Approximately 30% of the synthesized nascent Hbp was detected in the carbonate pellet (Fig. 3, quantification data not shown). Given the relatively low intrinsic efficiency of the *E. coli in vitro* translocation system, this result indicated that nascent Hbp is properly targeted and inserted into the membrane and remains anchored via its signal peptide that is not cleaved at this nascent chain length. In the untargeted (carbonate soluble) fraction, a cross-linking product of ~60 kDa appeared

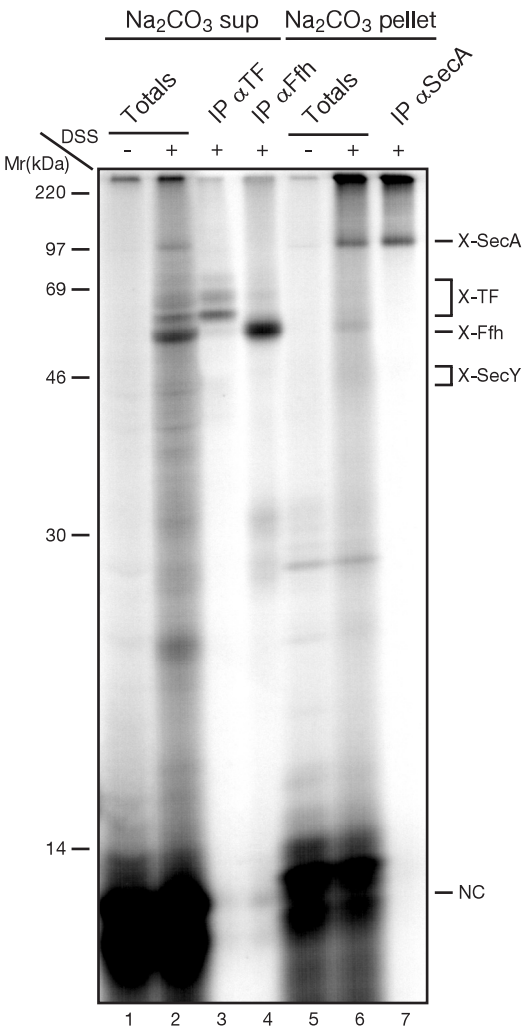

Fig. 3. Nascent Hbp interacts with TF, SRP and SecA. The 117-mer Hbp was synthesized in the presence of IMVs. After translation, samples were either treated with DSS (lanes 2-4 and 6 and 7) or mock treated (lanes 1 and 5) and subsequently extracted with carbonate (supernatant (sup), lanes 1-4; pellet, lanes 5-7). DSS-treated fractions were immunoprecipitated using antiserum against TF, Ffh, and SecA (lanes 3, 4, and 7). The translation products at 30 kDa present in lanes 5 and 6 represent the peptidyl-tRNA form of nascent Hbp. Cross-linked products and nascent chains (NC) are indicated.

that could be immunoprecipitated using serum directed against Ffh, the protein component of the SRP (Fig. 3, lane 4). The molecular mass of this product is consistent with the combined molecular mass of Ffh (50 kDa) and the Hbp 117-mer (13 kDa). The cross-linking to Ffh is remarkably strong considering the low abundance of the SRP in the translation lysate, suggesting that it represents a functional interaction. Weaker cross-linking products of slightly higher molecular mass were immunoprecipitated using anti-TF serum (Fig. 3, lane 3). TF (54 kDa) cross-linked to nascent chains often migrates at varying positions (Valent, 1997). The membrane-integrated nascent Hbp was primarily cross-linked to SecA (102kDa) (Fig. 3, lane 7). In addition, a very faint cross-linking smear was observed at ~46 kDa that contained SecY, as evident from long exposures of immunoprecipitated samples (not shown).

Together, the cross-link patterns are reminiscent of those found with the nascent IMPs FtsQ and leader peptidase I (Lep) (Valent, 1997; Houben *et al.*, 2000; Scotti *et al.*, 2000). Both FtsQ and leader peptidase I are targeted by the SRP to the Sec-translocon (de Gier *et al.*, 1996; Urbanus *et al.*, 2001). Apparently, nascent Hbp can be targeted to the inner membrane and inserts close to the Sec-translocon. The unprecedented strong cross-linking to Ffh, considering the extremely low abundance of Ffh in the translation lysate, suggests a high affinity of the Hbp signal peptide for the SRP and, consequently, a role for the SRP in the targeting of Hbp.

Hbp Requires the SRP for Optimal Processing and Secretion in Vivo

We investigated whether the interaction of nascent Hbp with the SRP observed *in vitro* reflects a dependence on the SRP targeting pathway for processing and secretion of the full-length protein *in vivo*. Strains that are conditional for the expression of targeting factors were used in pulse-chase experiments to analyze the effects on the kinetics of processing as described above. Furthermore, spent medium of the pulse-chase samples was analyzed to monitor the secretion of mature Hbp in time.

Under normal conditions, N-terminal processing appeared to be very fast, and pre-pro-Hbp could only be detected in the pulsed sample (Fig. 4A, lane 7) as has been observed for many pre-secretory proteins such as OmpA (see also Fig. 4C, lane 4). However, C-terminal processing of Hbp is much slower. Under the expression conditions used, not all pro-Hbp was converted into mature Hbp even after 1 h of chase (Fig. 4A, lane 12). The actual release of mature Hbp into the culture medium is even slower, appearing prominently only after 1 h of chase (Fig. 4B, lane 12). Depletion of Ffh resulted in an accumulation of pre-pro-Hbp in the cells (Fig. 4A,

left panel). The amount of secreted mature Hbp after 60 min of chase, but not the kinetics of the secretion of mature Hbp, appeared affected upon depletion of Ffh (Fig. 4B, left panel). As a control, the processing of OmpA was hardly influenced (Fig. 4C, left panel), which is in agreement with its requirement for SecB rather than SRP for targeting (Kumamoto and Beckwith, 1985). In an alternative approach to analyzing the role of the SRP-targeting pathway in Hbp secretion, the effect of overexpression of FtsY-A449 was investigated. This mutant SRP receptor has a reduced GTP-binding capacity as a result of an amino acid substitution in the fourth GTP-binding consensus element (Kusters *et al.*, 1995). Moderate overexpression of FtsY-A449 has been shown to compromise SRP-mediated protein targeting (Kusters *et al.*, 1995). Hbp processing and, consequently, also secretion appeared to be impaired upon moderate overexpression of FtsY-A449 as opposed to the non-induced expression level (Fig. 4, D and E). OmpA processing was not affected under these conditions (Fig. 4F).

To examine whether the other major targeting factor, SecB, is also involved in Hbp targeting, Hbp was expressed in strain MM152, which lacks SecB, and in its isogenic wild-type strain, MC4100. Pre-pro-Hbp did not accumulate in the SecB minus strain, nor was the secretion of mature Hbp affected (Fig. 4, G and H). As a control, pre-OmpA accumulated at early chase times in strain MM152. Apparently, SecB is not necessary for efficient targeting of Hbp *per se*.

We next considered the possibility that the residual processing and secretion of Hbp under Ffh-deficient conditions is due to alternative targeting via SecB. Consistent with this explanation, the expression of Hbp in a double mutant strain (SecB knockout, Ffh conditional) showed a much stronger secretion phenotype upon Ffh depletion than the single (Ffh conditional) mutant (Fig. 4, J and K, left panels). The secretion defect was greatly reduced in cells that express Ffh (Fig. 4, J and K, right panels), again suggesting that SecB is not required for the targeting of Hbp under normal conditions. The accumulation of pre-pro Hbp under these conditions at early chase times remains unexplained but may be related to adverse effects of the unnatural control of Ffh expression from the arabinose promoter. Interestingly, a similar but opposite additive effect is observed for OmpA. When the preferred targeting factor, SecB, is absent, processing is impaired (Fig. 4L, right panel). Additional depletion of Ffh completely blocks residual OmpA processing (Fig. 4L, left panel).

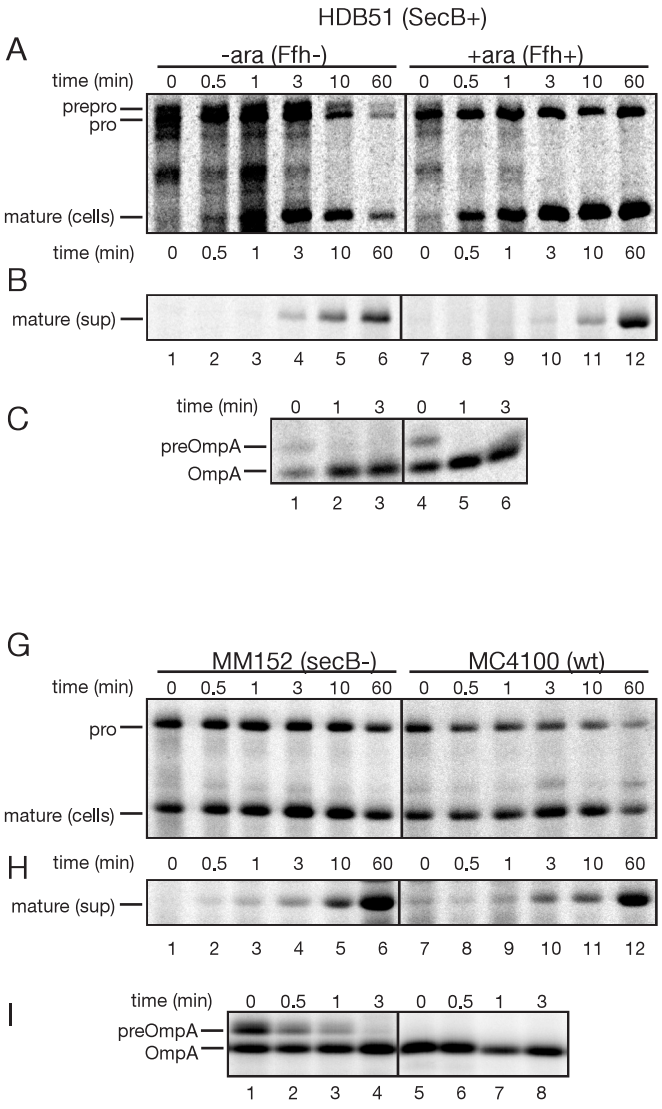

Fig. 4. The SRP-pathway is required for efficient targeting of Hbp. A-C, depletion of Ffh inhibits processing and secretion of Hbp. HDB51 (P_{ara}-*ffh secB*$^+$) harboring pACYC-Hbp was grown in M9 medium without (-ara) or with L-arabinose (+ara). Cells were radiolabeled with [^{35}S]methionine for 1 min and chased for the times indicated. Panel A shows Hbp immunoprecipitated from cell samples. Panel B shows trichloroacetic acid-precipitated proteins from the supernatant (sup), and panel C shows OmpA immunoprecipitated from cell samples. D-F, overexpression of mutant FtsY inhibits the processing and secretion of Hbp. BL21(DE3) harboring pET9-FtsY-A449 and pACYC-Hbp was grown in M9 medium. At an OD_{660} of 0.2, the expression of FtsY-A449 was induced with 40 µM isopropyl-1-thio-β-D-galactopyranoside for

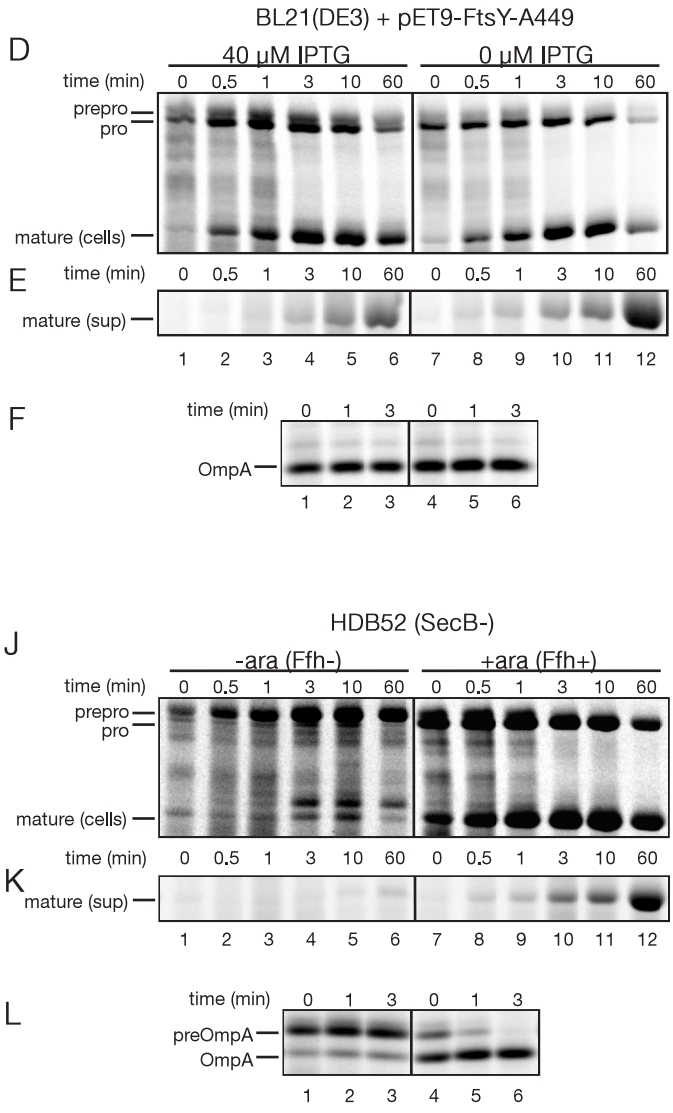

15 min or left uninduced as indicated. Samples were processed and displayed as described above. G-I, inactivation of SecB does not affect processing and secretion of Hbp. MM152 (*secB*$^-$), and MC4100 (wt) harboring pHE12.6 were grown in M9 medium. Samples were processed and displayed as described above. J-L, inactivation of SecB aggravates the effects of depletion of Ffh on the processing and secretion of Hbp. HDB52 (P_{ara}-*ffh secB*$^-$) harboring pACYC-Hbp was grown in M9 medium without (-ara) or with L-arabinose (+ara). Samples were processed and displayed as described above. Prepro, pre-pro-Hbp (148 kDa); pro, pro-Hbp (142 kDa); mature, mature Hbp (111 kDa).

Together, these results suggested that Hbp requires the SRP pathway for optimal targeting to the inner membrane. Although SecB is not essential for targeting *per se*, it can apparently compensate to a certain extent for depletion of the SRP.

Hbp Requires SecA and SecY for Efficient Processing and Secretion in Vivo

Two main types of translocons mediate the transfer of proteins across the inner membrane, namely the Sec-translocon (Manting and Driessen, 2000) and the Tat-translocon (Berks *et al.*, 2000). We investigated the role of these translocons in the secretion of Hbp *in vivo* using the pulse-chase approach described above.

A temperature-dependent conditional *secY* mutant strain was used to deplete the cells for functional Sec-translocons. At the non-permissive temperature, processing of the control Sec substrate OmpA was severely impaired in this strain as compared with its parental wild-type strain (Fig. 5C). Likewise, pre-pro-Hbp accumulated in the *secY* Ts cells (Fig. 5A, left panel), indicating that translocation of Hbp across the inner membrane proceeds through the Sec-translocon.

To study the role of SecA, its ATPase activity was perturbed with azide. Under the conditions used, processing of OmpA was almost completely inhibited (Fig. 5F, left panel). Again, pre-pro-Hbp accumulated in the cells, indicating that translocation of Hbp is dependent on SecA (Fig. 5D, left panel). A similar dependence on functional SecA was observed when a temperature-dependent conditional *secA* mutant strain was used (data not shown).

The Tat-translocon is used by a subset of preproteins that are folded prior to translocation (Berks *et al.*, 2000). Tat substrates carry an essential twin arginine motif in their signal peptide just upstream of the hydrophobic domain. Although the Hbp signal peptide does not fully comply with this motif, it does contain two consecutive arginine residues upstream of the hydrophobic core region. This feature prompted us to investigate a possible role of the Tat-translocon using a strain that lacks TatA and TatE, rendering it completely unable to translocate Tat substrates. This double mutant strain showed normal kinetics of processing and secretion of Hbp whereas processing of the known Tat substrate SufI was completely blocked, arguing that the Tat-translocon is not involved in secretion of Hbp (data not shown).

Together, the data suggest that Hbp uses the Sec-translocon for transfer across the inner membrane consistent with the *in vitro* cross-link data (Fig. 3). SecA appears to be required to drive the translocation process.

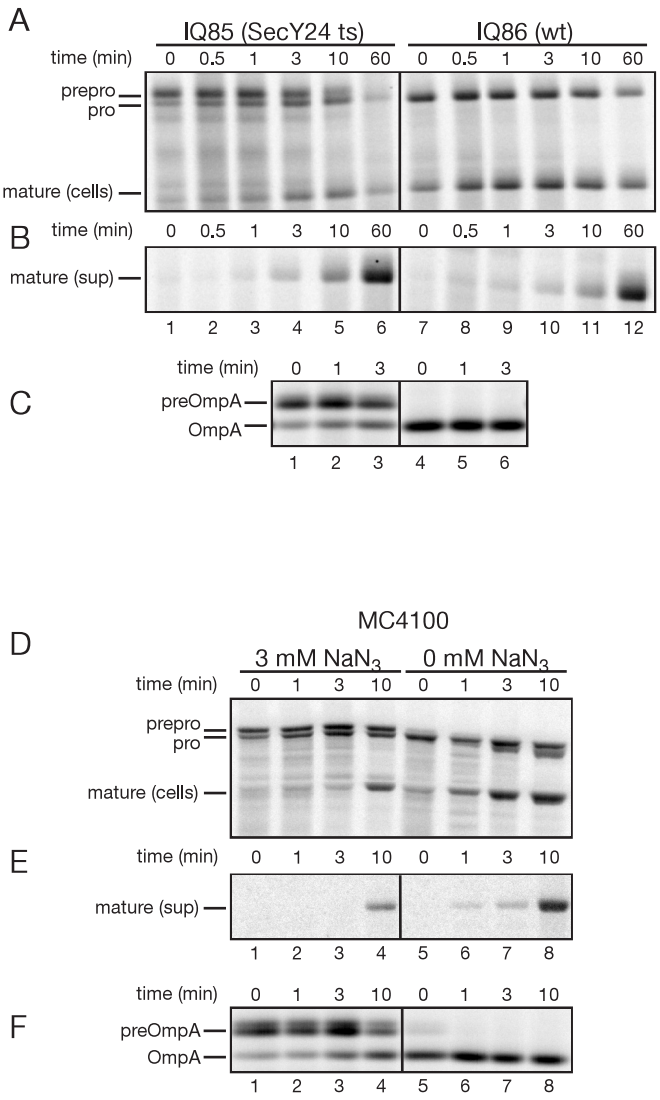

Fig. 5. The Sec-translocon is required for efficient translocation of Hbp. A, inactivation of SecY inhibits processing and secretion of Hbp. IQ85 (*secY24* ts) and IQ86 (wt, wild-type), harboring pHE12.6, were grown at 30 °C to an OD_{660} of 0.3 and shifted to 42 °C for 3 h. Samples were processed and displayed as described in the legend to Fig. 4. B, inhibition of SecA functioning with azide inhibits processing and secretion of Hbp. MC4100 (wild-type), harboring pHE12.6, was grown at 37 °C in M9 medium. Three minutes prior to labeling, 3 mM NaN_3 was added to inhibit the ATPase activity of SecA as indicated. Samples were processed and displayed as described in the legend to Fig. 4.

Discussion

In the present work, we have addressed the question how the autotransporter Hbp is targeted to and translocated across the inner membrane. Both *in vitro* cross-linking and *in vivo* pulse-chase labeling experiments point to the use of a co-translational targeting and translocation mechanism involving the targeting factor SRP and the Sec translocation machinery. This is the first example of an extracellular protein that can be targeted by the SRP. Interestingly, in the absence of a functional SRP pathway, part of the mistargeted Hbp is rescued by SecB, underscoring the inherent flexibility of protein targeting in *E. coli* (Kim *et al.*, 2001).

What are the features in the Hbp signal peptide that determine SRP binding? Previous work in our group has demonstrated that the SRP preferentially interacts with relatively hydrophobic signal peptides such as those that are present in IMPs (Valent, 1997). However, the hydrophobic core region at the C terminus of the Hbp signal peptide is not particularly hydrophobic. Interestingly, the Hbp signal peptide is relatively long (52 amino acids) and appears to contain an N-terminal extension that precedes a "classical" signal peptide (Fig. 1). It is attractive to speculate that the N-terminal extension plays a role in the recognition by the SRP either directly or indirectly by presenting the hydrophobic core in a favorable conformation or by recruiting other factors that increase the affinity of the Hbp signal peptide for the SRP. It is worth mentioning that the only other known example of a secreted protein that makes use of the SRP for targeting, SecM, is also synthesized with a long signal peptide that comprises an N-terminal extension and a moderately hydrophobic core region (Sarker *et al.*, 2000). SecM is a regulatory protein that functions in the secretion-responsive control of SecA expression. In wild-type cells, SecM is translocated to the periplasm where it is rapidly degraded (Nakatogawa and Ito, 2001).

Alternatively, the N-region (KCVHKSVRR) between the hydrophobic core and the N-terminal extension might be important for SRP recognition of the Hbp signal peptide. Compared with other signal peptides in Gram-negative bacteria, this region is more basic. Interestingly, the crystal structure of the SRP has revealed an unusual RNA-protein interface that is thought to constitute the signal peptide binding groove (Batey *et al.*, 2000). It has been suggested that the protein moiety of the interface interacts with the hydrophobic core of the signal peptide, whereas the RNA is responsible for recognizing the basic N-domain. Following this reasoning, a more basic N-domain might compensate for a less hydrophobic core region in SRP binding. These possibilities are currently being investigated.

Translocation of autotransporters across the inner membrane has been proposed to involve the N-terminal signal peptide and occur via the Sec-pathway, which is also used by periplasmic and outer membrane proteins (Henderson *et al.*, 1998). Consistent with this proposal, our data suggest that the Sec-translocon receives and translocates the nascent Hbp. In this respect, Hbp resembles IMPs like leader peptidase I, FtsQ, and MtlA (de Gier and Luirink, 2001). An accessory translocon component, YidC, is specifically involved in membrane integration of these IMPs but not in the translocation of secretory proteins (Samuelson *et al.*, 2000; Scotti *et al.*, 2000)[1]. We have not observed any cross-linking of nascent Hbp with YidC. Moreover, depletion of YidC did not affect processing and secretion of Hbp (data not shown). Apparently, YidC is dispensable for the reception of Hbp at, as well as the translocation of Hbp across, the inner membrane-embedded Sec-translocon.

It is not unlikely that other members of the autotransporter family follow the same pathway of targeting and translocation across the bacterial inner membrane. Many autotransporters carry signal peptides of similar length and domain structure (Henderson *et al.*, 1998). The N-terminal extension in these signal peptides is remarkably conserved, as is the basic character of the N-domain. In addition, substrates of an analogous secretion system, the "two-partner secretion" (TPS) pathway in which the β-barrel domain is present in a separate protein, also possess signal peptides that are conserved with members of the classical autotransporter family (Henderson *et al.*, 2000a). One of these substrates, the HMW1 adhesin from *Haemophilus influenzae* that carries a 68 amino acid-long signal peptide was shown to require SecA and SecE for maturation and secretion (Grass and St Geme, 2000).

What would be the benefit of co-translational translocation for autotransporters? For Hbp, it might prevent degradation or premature folding of Hbp in the cytoplasm. Hbp that lacks its signal peptide appeared to be vulnerable to degradation by cytoplasmic proteases. It should be noted that both the autotransporter and two-partner secretion families comprise many virulence factors such as hemagglutinins, hemolysins, cytolysins, and proteases (Henderson *et al.*, 2000a) that may be harmful when expressed in the cytoplasm of the pathogenic bacterium. Furthermore, the autotransporters are relatively large molecules with a typical domain structure. The passenger domain that is expressed in the cytoplasm may fold into a conformation that is incompatible with translocation through the Sec-translocon, even when the β-barrel domain is still being synthesized.

[1] E. N. G. Houben, personal communication.

Abbreviations

The abbreviations used are: Hbp, Hemoglobin protease; IMP, inner membrane protein; IMV, inverted membrane vesicle; SRP, signal recognition particle; DSS, 2,2-dimethyl-2-silapentanesulfonic acid; TF, trigger factor; TPS, two-partner secretion.

Chapter 3

Crystal structure of Hemoglobin protease, a heme binding autotransporter protein from pathogenic *Escherichia coli*

Ben R. Otto, Robert Sijbrandi, Joen Luirink, Bauke Oudega, Jonathan G. Heddle[1], Kenji Mizutani[1], Sam-Yong Park[1], and Jeremy R. H. Tame[1]

[1] Protein Design Laboratory,Yokohama City University, Tsurumi, Yokohama, Japan

Published in The Journal of Biological Chemistry 280 (2005): 17339-17345

Abstract

The acquisition of iron is essential for the survival of pathogenic bacteria, which have consequently evolved a wide variety of uptake systems to extract iron and heme from host proteins such as hemoglobin. Hemoglobin protease (Hbp) was discovered as a factor involved in the symbiosis of pathogenic *Escherichia coli* and *Bacteroides fragilis*, which cause intra-abdominal abscesses. Released from *E. coli*, this serine protease autotransporter degrades hemoglobin and delivers heme to both bacterial species. The crystal structure of the complete passenger domain of Hbp (110 kDa) is presented, which is the first structure from this class of serine proteases and the largest parallel β-helical structure yet solved.

Introduction

Autotransporters (ATs) are virulence proteins produced by a variety of pathogenic bacteria, including several types of *Escherichia coli* associated with severe, even fatal, diarrhea and urinary tract infections. An increasing number of these proteins have been discovered over the last decade, and a large body of research is now devoted to these proteins and their different roles in various diseases. ATs have evolved a unique export mechanism, the type V pathway (Henderson *et al.*, 2000b; Henderson *et al.*, 2004). Initially the protein is synthesized with an N-terminal leader peptide directing the protein to the periplasm via the signal recognition particle (SRP) (Sijbrandi *et al.*, 2003). Once across the inner membrane, the C-terminal domain forms a β-barrel structure within the outer membrane, allowing the passenger domain to escape to the external medium, where it is released proteolytically from the cell (Pohlner *et al.*, 1987; Klauser *et al.*, 1993; Jose *et al.*, 1995). Recently the crystal structure of a translocator (membrane) domain of an AT has been solved (Oomen *et al.*, 2004). AT passenger domains are generally more than 100 kDa in size and vary widely in sequence and function but include a group of closely related serine proteases, the SPATE family (serine protease autotransporters of the Enterobacteriaceae). These proteins are found only in pathogenic bacteria, but their precise roles remain unknown (Henderson and Nataro, 2001; Dutta *et al.*, 2002). The SPATE family includes EspC from enteropathogenic *E. coli* (Stein *et al.*, 1996), EspP from enterohemorrhagic *E. coli* (Brunder *et al.*, 1997), plasmid-encoded toxin (Pet) from enteroaggregative *E. coli* (Eslava *et al.*, 1998), Sat from uropathogenic *E. coli* (Guyer *et al.*, 2000), Tsh and Vat from avian pathogenic *E. coli* (Provence and

Curtiss, 1994; Parreira and Gyles, 2003), and Pic and SepA from *Shigella flexneri* (Benjelloun-Touimi *et al.*, 1995; Henderson *et al.*, 1999). These AT proteins are associated with a number of serious, possibly life-threatening diseases affecting millions world-wide. Tsh and Vat are essential virulence factors in avian diseases that cost the poultry industry millions of dollars annually. SPATE proteins do not appear to have conserved or even related functions (Henderson and Nataro, 2001; Dutta *et al.*, 2002). Vat has vacuolating activity, and Pet enters eukaryotic cells to disturb the cytoskeletal system. As essential proteins in pathogenesis, SPATE proteins are key drug targets and potential routes to vaccines. Knowledge of the molecular structure is a first step toward understanding their mechanisms and hopefully how they may be inactivated. We have solved the crystal structure of the passenger domain of Hemoglobin protease (Hbp), an AT involved in bacterial synergy in the development of peritonitis.

Peritonitis is an inflammation of the peritoneal cavity and may develop into a life-threatening condition through the formation of persistent abscesses, which leak pathogenic bacteria into the general circulation (Aldridge, 1995; Farthmann and Schöffel, 1998). This common complication of invasive surgery then results in septic shock and multiorgan failure with mortality rates well in excess of 50%. These abscesses are difficult to treat with antimicrobial therapy, and usually require surgical intervention. It is frequently found that pathogenic *E. coli* and the strictly anaerobic *Bacteroides fragilis* occur together in intra-abdominal abscesses, the combination surviving better than either species alone (Rotstein *et al.*, 1989a; Otto *et al.*, 2002). *B. fragilis* is a common member of the normal human gut flora, but it is also a significant opportunistic pathogen (Aldridge, 1995; Farthmann and Schöffel, 1998). It promotes fibrin deposition by the host, which localizes the bacteria and prevents systemic spread, but also provides an environment where the bacteria can escape attack by the immune system. In return, *E. coli* helps to supply both species with heme scavenged from hemoglobin (Hb). Hbp was discovered as the protease secreted by *E. coli*, which degrades Hb and binds heme (Otto *et al.*, 1998; Otto *et al.*, 2002). The *hbp* gene is located on a large episome, pColV-K30, which also encodes an aerobactin-dependent iron uptake system (Williams, 1979). Hbp is highly expressed by *E. coli* during peritonitis and plays a key role in bacterial synergy with *B. fragilis*. Adding Hbp and heme to cultures of *B. fragilis* was shown to stimulate growth, and mice immunized with Hbp showed no abscess formation when subsequently challenged with mixed *E. coli*/*B. fragilis* cultures. Hbp therefore appears to be a useful target in the treatment and prevention of peritonitis. We have determined the crystal structure of Hbp with the longer term view of producing inhibitors, vaccines, or other

treatments for peritonitis and other diseases caused by SPATE proteins. From this first molecular model of an AT, we have constructed homology models of other ATs to observe both common and unique features of these proteins.

Materials and Methods

Protein Purification and Crystallization

The cloning of Hbp has been described previously (Otto *et al.*, 1998). *E. coli* strain DH5α harboring plasmid pACYC-Hbp was grown to an A_{600} of 0.6 in MA medium, and the supernatant was collected and concentrated. Following 1000-fold concentration by ultrafiltration, the protein was purified by gel filtration in 10 mM Tris-HCl, pH 8.0, 300 mM sodium chloride. Apo-Hbp was crystallized by the published method (Tame *et al.*, 2002). 4 mg/ml protein was crystallized using the hanging drop method using 0.1 M sodium acetate, pH 4.6, 200 mM ammonium sulfate, 10% glycerol, and 15–20% polyethylene glycol 6000.

Data Collection and Processing

Multi-wavelength x-ray data were collected at beam line 45XU-PX, SPring8, Harima, Japan. Native data were collected at beam line BL5 of the Photon Factory, Tsukuba, to a resolution of 2.2 Å. All data were indexed and integrated using HKL2000 and scaled with the program SCALEPACK (Otwinowski and Minor, 1997). The crystals are in space group $P6_122$ with unit cell dimensions of $a = b = 114.86$ Å, $c = 437.05$ Å, with one molecule per asymmetric unit and a solvent content of 65%.

Structure Determination and Refinement

The structure of Hbp was solved by MAD (multiple-wavelength anomalous dispersion) using selenomethionine-containing protein. Phase determination and refinement were performed using the programs SOLVE and RESOLVE (Terwilliger and Berendzen, 1999; Terwilliger, 2003). 12 Se sites were located out of 14 expected. The 3.0-Å resolution electron density map obtained from RESOLVE was of sufficient quality to permit unambiguous chain tracing without further refinement of the heavy atom sites. After model building using the programs O (Jones *et al.*, 1991) and Turbo (Roussel and Cambillau, 1989), initial refinement was carried out with XPLOR (Brunger, 1996) and final refinement with REFMAC (Collaborative Computational Project, 1994; Murshudov *et al.*, 1999) using the 2.2-Å resolution native data. Solvent molecules were placed at positions where spherical electron-

density peaks were found above 1.5 σ in the $2F_o - F_c$ map and above 3.0 σ in the $F_o - F_c$ map and where stereochemically reasonable hydrogen bonds were allowed. The final model extends from the N terminus (residue 1 of the mature protein) to residue 1048, the C-terminal residue of the passenger domain. The Ramachandran plot has 86% of the residues in the most favorable regions and none in disallowed regions. A summary of the data collection and refinement statistics is given in Table 1. The final model and structure factors have been deposited in the Protein Data Bank (PDB, 1WXR).

Table 1. Data collection and refinement statistics

Space group, unit cell dimensions (Å)	$P6_122$, $a = b = 114.86$, $c = 437.05$		
Wavelength (Å)	peak	inflection	remote
Resolution range (Å)	50.0-3.0	50.0-3.0	50.0-3.0
Reflections (measured/unique)	214,532/33,539	242,451/34,130	232,344/33,910
Completeness (overall/outer shell, %)[a]	95.4/88.5	98.8/92.6	96.0/87.7
R_{merge} (overall/outer shell, %)[a]	10.2/21.2	8.3/18.3	8.5/18.8
Redundancy (overall)	6.4	7.1	6.9
Mean <I/σ(I)> (overall)	7.8	8.9	8.3
Phasing (20.0-3.0 Å)			
Mean FOM[c] after SOLVE phasing	0.33		
Refinement statistics			
Refinement resolution (Å)	30.0-2.20		
Reflections (measured/unique)	525,426/81,279		
Completeness (overall/outer shell, %)[a]	92.3/70.8		
R_{merge} (overall/outer shell, %)[a,b]	5.8/31.8		
Redundancy (overall)	6.5		
Mean <I/σ(I)> (overall)	11.0		
σ cut-off/reflections used	0.0/81,279		
R-factor[d]/free R-factor (%)[b]	20.3/24.3		
R.m.s.d. bond lengths/bond angles (Å)	0.016/1.7		
Water molecules	399		
Average B-factor (protein/water, Å^2)	35/33		
Ramachandran plot			
Residues in most favorable regions (%)	86.1		
Residues in additionally allowed regions (%)	12.9		
Residues in generously allowed regions (%)	1.0		

[a] Completeness and R_{merge}, are given for overall data and for the highest resolution shell (overall/the highest resolution shell).The highest resolution shells for the MAD data and native data are 3.11-3.0 Å and 2.28-2.20 Å, respectively.

[b] $R_{merge} = \Sigma\, I_i - \langle I \rangle / \Sigma\, I_i$; where I_i is intensity of observation and $\langle I \rangle$ is the mean value for that reflection.

[c] Figure of merit (FOM) = F_{best}/F.

[d] R factor = $\Sigma||F_o(h) - F_c(h)||/\Sigma hF_o(h)$; where F_o and F_c are the observed and calculated structure factor amplitudes, respectively. The free R-factor was calculated with 5% of the data excluded from the refinement.

Results

The overall structure of the protein is shown in Fig. 1. The most striking feature is the right-handed β-helical C-terminal tail which extends from residue 260 onwards, forming three parallel β-sheets. This is highly similar to pertactin (PDB 1DAB) (Emsley *et al.*, 1996) and the N terminus of filamentous hemagglutinin (PDB 1RWR) (Clantin *et al.*, 2004), both adhesins from *Bordetella pertussis*. Pertactin is the only AT structure refined to date, one of only a dozen or so right-handed parallel β-helix protein structures so far solved. The first was the pectate lyase PelC (PDB 1AIR), and a number of different pectate lyase structures are now known (Jenkins and Pickersgill, 2001). The pectate lyase superfamily members are a functionally eclectic mix including P22 tailspike protein (PDB 1TYU), chondroitinase B (PDB 1DGB) and insect cysteine-rich antifreeze protein (PDB 1EZG). All share a similar pattern of repeats of about 25 amino acid residues which form one turn of the right-handed helix. Each turn creates three β-strands which form extended β-sheets with neighboring turns. The core of this region is generally but not exclusively hydrophobic. The leucine-rich repeat family is another group of protein structures formed from repeated sequence motifs, but these include an α-helix in each turn and are found to be highly curved into horseshoe shapes. The pectate lyase superfamily forms a much straighter superhelix. The shape of Hbp was previously determined to low resolution using a combination of small-angle x-ray scattering and analytical ultracentrifugation (Scott *et al.*, 2002). The crystal structure shows a slightly straighter structure than the model from small-angle x-ray scattering, possibly due to greater flexibility in solution.

The Hbp model includes 24 turns of right-handed β-helix, compared with 16 in pertactin, the longest parallel β-helix known to date. Hbp is highly reminiscent of pertactin, but less regular and slightly kinked in the centre. It also has a large N-terminal globular domain, and a smaller domain of 75 residues (481-556) about half-way long the β-helix, as well as decorative loops where the polypeptide chain departs from the helical stem. The extra surface features make the length of Hbp (1048 residues) almost twice that of pertactin (539 residues). The extended hydrophobic core is largely but not exclusively filled with aliphatic side chains (Fig. 2, A and B). The N-terminal region close to the serine protease domain has a higher proportion of buried aromatic residues. Very few polar residues point into the hydrophobic core, but Ser^{780} is one exception (Fig. 2, B). Other SPATE proteins generally have threonine at this position. Unlike the pectate lyases there are no regular “stacks” of

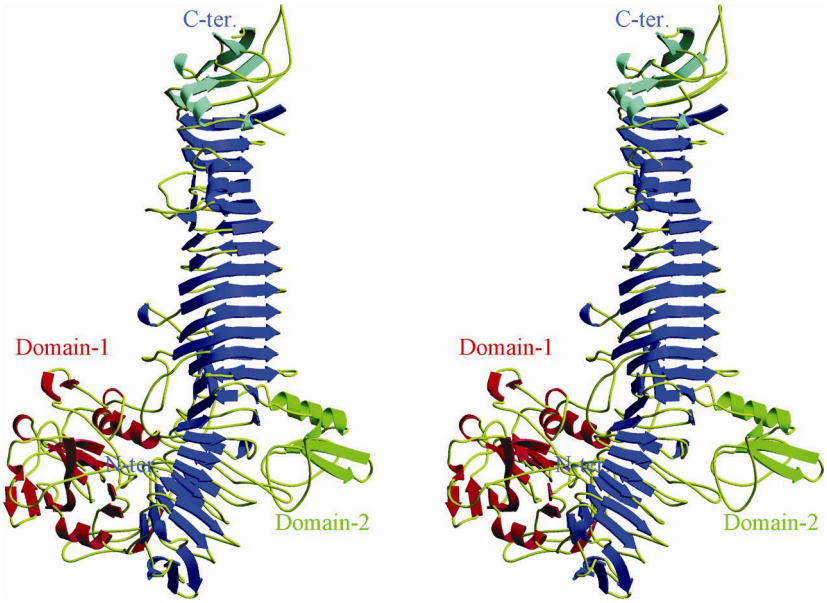

Fig. 1. A stereo ribbon diagram showing the overall structure of the entire passenger region of Hbp. Helices and strands are colored *red* for the protease domain (domain 1, residues 1-256) and *green* for the chitinase b-like domain (domain 2, residues 481-556). The β-strands in the parallel β-helix are colored *dark blue*. Residues 950-1048 (the C terminus of the mature protein) are colored *light blue*. This region is required for transport of the passenger domain through the membrane pore created by the C-terminal region of the complete protein.

identical residues packed in layers within the core, but a row of asparagine residues is found forming an extended hydrogen bonding chain on the surface of the β-helix (Fig. 3). Overall the electron density for the model is very clear, but model building became increasingly difficult towards the C terminus. LAFIRE, a model fitting and rebuilding program using local correlation of electron density,[1] was essential in assembling the last 100 residues of the model. Details of the program may be found at: http://altair.sci.hokudai.ac.jp/g6/Research/Lafire_English.html. There are several breaks in the final electron density maps in this region where short loops cannot be modeled. The C-terminal region from residue 950 to the end is a conserved domain found among AT proteins believed to assist folding after passage through the C-terminal pore domain (Oliver *et al.*, 2003b).

Residues 1-256 of the model form a clearly separate domain (*domain 1* in

[1] M. Yao, unpublished program.

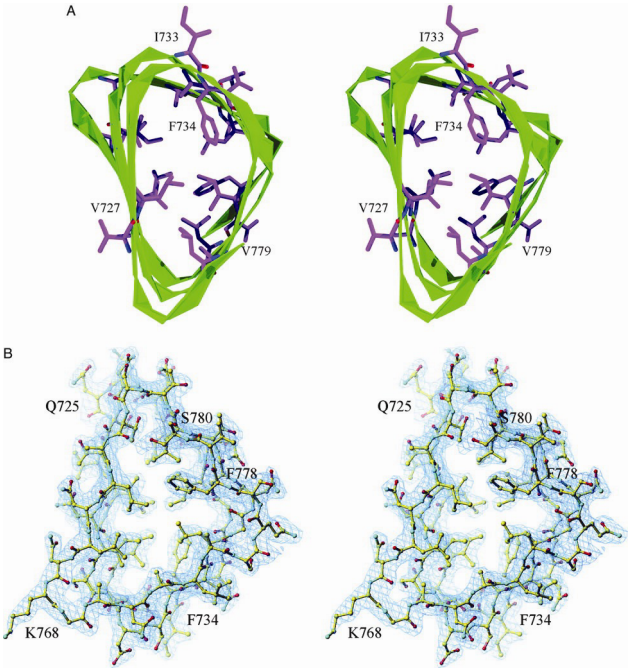

Fig. 2. A, a slice through the β-helix showing the hydrophobic core. The backbone is shown as a *green* ribbon, and hydrophobic side chains are shown in *pink*. B, the $2mF_o$ - DF_c electron density map, shown in stereo and contoured at 1.3σ, showing a cross-section through the β-helix.

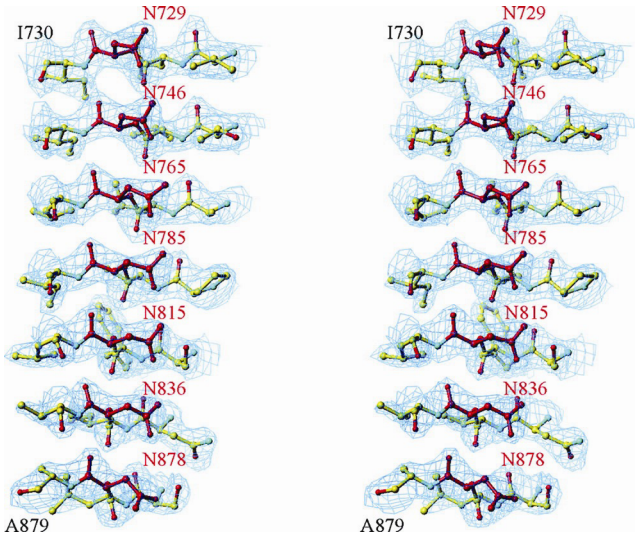

Fig. 3. An orthogonal view to Figure 2B of the final $2mF_o$ - DF_c electron density map, at the same contour level, showing a stack of asparagine residues on the surface of the β-helix (colored *red*), which are hydrogen bonding through their side chains. These asparagines are not conserved among AT sequences, which have a variety of hydrophilic side chains at equivalent positions.

Fig. 1), including six β-strands rolled into a barrel-like structure, with several long β-hairpins over its surface. The N-terminal glycine residue is deep within the structure, close to the bottom of the barrel. Folding of the domain can clearly only occur after the signal peptide has been removed. The glycine N atom hydrogen bonds to Asp^{206}, which also interacts with Arg^{140} and the main-chain of Gly^{144}. An α-helix (Leu^{245}-Asp^{255}) connects this domain to the β-helical stem. Searching the PDB for structural homologues with DALI (Holm and Sander, 1993, 1995) revealed that the N-terminal domain is highly similar to bovine trypsin (PDB 5PTP), which gave a Z-score of 17.5 (scores above 2.0 are considered significant). The 162 residues matched showed 20% sequence identity to Hbp, and could be fitted with rmsd 2.5 Å over the main chain. The Cα traces are overlaid in Fig. 4A. Other proteases gave rather poorer scores. Overlaying trypsin on the model of Hbp gave an excellent match of the catalytic triad (Ser^{195}, His^{57} and Asp^{102}) of trypsin with Ser^{207}, His^{73} and Asp^{101} of Hbp (Fig. 4B). Comparing the active sites, Hbp misses a loop (Ser^{93} to Asp^{101} in trypsin) just prior to the essential aspartate. In trypsin this loop includes Leu^{99}, which contacts Trp^{215}, one of the residues that forms antiparallel β-sheet interactions with the substrate polypeptide. Trp^{215} in trypsin is changed to alanine (Ala^{229}) in Hbp, making the active site of Hbp much more open. At the bottom of the specificity pocket, which accommodates the residue preceding the scissile bond, trypsin has an aspartate (Asp^{189}), which leads to the preference for Lys and Arg residues at the S1 position. Chymotrypsin and elastase have serine in this position, but Hbp has tyrosine (Tyr^{201}). Among the trypsin/chymotrypsin family, Pro^{225} is very highly conserved from bacteria to man, but Hbp misses a loop just before this residue and the nearest equivalent is Gly^{237}. Hbp is also unusual in having an asparagine residue at the position equivalent to glycine 226 in trypsin. Thus, although the fold of the N-terminal domain is close to trypsin, it also has unique features not seen in other serine proteases. The active site suggests broad substrate specificity with a preference for hydrophobic side chains in the specificity pocket. The very open active site presumably helps Hbp to attack folded globular proteins such as Hb, but more work is required to determine its functional properties as a protease. Low resolution electron density maps calculated using data collected with crystals soaked with two serine protease inhibitors, tosyl phenylalanine chloromethyl ketone (TPCK) and tosyl lysine chloromethyl ketone (TLCK), show peaks of density close to the active site serine, suggesting the protease is still active at pH 4.6 (data not shown).

Sequence alignments of SPATE family members shows the sequence GDSGSPL to be highly conserved between Gly^{205} and Leu^{211} (Fig. 5). *vat*, an AT gene found in a pathogenicity island of avian pathogenic *E. coli* Ec222, has a slightly

altered sequence, ATSGSPL, which may be related to its vacuolating activity (Parreira and Gyles, 2003), but it maintains both the active site serine (Ser^{207}) and Ser^{209}, which hydrogen bonds to the carbonyl oxygen of Asp^{206} to make the turn carrying Ser^{207}. The N-terminal Gly^{1} lies close to the active site serine and hydrogen bonds to the side chain of Asp^{206}. This strongly suggests the enzyme can only become active after the leader peptide is removed. All SPATE proteins tested show proteolytic activity, but with different substrate specificities, suggesting different functions (Dutta *et al.*, 2002). Replacement of the active site serine of Pet (a SPATE from enteroaggregative *E. coli*) with isoleucine did not prevent release of the passenger domain from the C-terminal pore, but did eliminate all cytotoxic effects (Navarro-Garcia *et al.*, 2001). Comparing the sequences of various ATs shows that Tyr^{201} in the specificity pocket of Hbp is preserved in Pic and SepA, whereas Pet and Sap have leucine (Fig. 5). The sequence alignment also suggests that EspC has glutamate at this position, which presumably would affect substrate preference strongly. Using the N domain structure of Hbp, a homology model of Pet protease domain was built using SwissModel (Schwede *et al.*, 2003). From this a second homology model of Sat protease domain was also constructed. The weaker sequence conservation between Hbp and Sat prevented a model of the latter being built more directly. These homology models show no unexpectedly loose packing or unfavorable geometry, indicating that each protein has identical connectivity, with minor differences in loop regions, in the N-terminal protease domain.

The N-terminal domain makes extensive contact with the β-helical stem of Hbp, but given its globular shape the contact region with the roughly cylindrical β-helix is long and narrow. Many N domain contacts are found between Asp^{108} and Val^{114}. For example, Arg^{106} makes buried hydrogen bonds to the carbonyl oxygen atoms of Asn^{301} and Gly^{303}. The main hydrophobic contact is provided by Leu^{110}, which is buried at the interface. Arg^{106} and Lys^{109} are very strongly conserved among ATs, the latter forming a salt bridge with Asp^{367}. Arg^{441} and Asp^{49}, both well conserved, make another bond between the N-terminal protease domain and the β-helix. These contacts, and the preservation of key glycines in the sequences of ATs, suggest that these proteins share a very similar structure over the first half of the protein.

Residues 481-556 of Hbp make a small separate domain (domain 2 in Fig. 1), the main-chain returning to the β-stem close to the point of departure. DALI found only one notable match, to the chitin binding domain (ChBD) of chitinase b (PDB 1E15). This domain consists of only 49 residues folded into three antiparallel β-

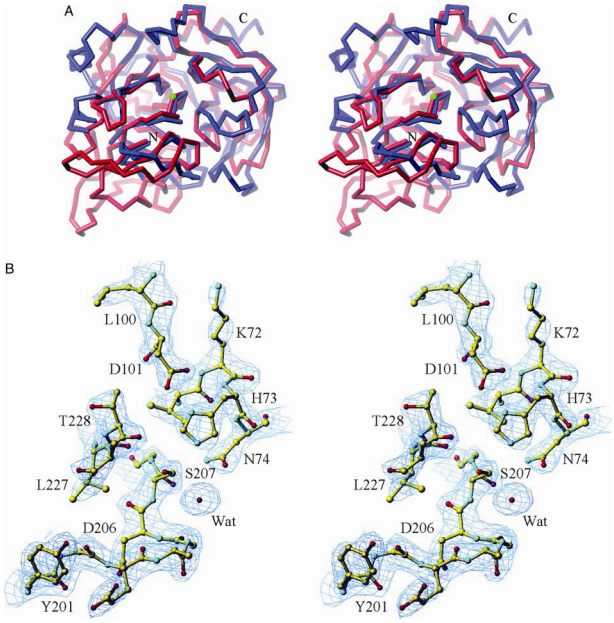

Fig. 4. A, a stereo overlay of the Cα trace of bovine trypsin (*blue*) and the serine protease domain of Hbp (*red*). The Cα of the catalytic serine (Ser^{207}) is shown as a *green* sphere. Trypsin (PDB 5PTP) was matched to Hbp by least-squares fitting residues 16-19 (1-4), 21-24 (15-18), 26-32 (49-55), 42-60 (58-76), 63-69 (78-84), 79-93 (85-99), 101-114 (100-113), 118-127 (114-123), 129-132 (128-131), 134-146 (136-148), 147-152 (156-161), 153-165 (163-175), 176-183 (177-184), 184-187 (186-189), 188-202 (200-214), 224-231 (236-243), 234-245 (244-255). These 648 main-chain atoms selected by DALI have a root mean square deviation of 2.5 Å, and a maximum deviation of 8.2 Å. B, the $2mF_o$ - DF_c electron density map contoured at 1.3σ over the catalytic site of the serine protease domain, showing the catalytic serine (Ser^{207}) and a water molecule hydrogen bonded to it. Tyr^{201}, the residue in the specificity pocket, is seen on the lower left.

strands connected by long loops. ChBD fitted the 481-556 loop of Hbp with a Z score of 3.6 over 44 residues, with 16% sequence identity. Not surprisingly, the surface aromatic groups of ChBD presumed to bind chitin are altered in Hbp, but the 481-556 loop has a different cluster of aromatic residues which appear to form a binding pocket of some sort. Tyr^{510} and Tyr^{526} point into solvent and are highly exposed (and make crystal contacts with a neighboring molecule). The nearby Trp^{492}, Tyr^{506} and Phe^{527} make a hydrophobic pocket open to solvent. The 481-556 domain is quite different to any known heme-binding site, and a mutant in which this domain is deleted shows identical heme binding to the wild-type protein (Fig. 6). Possibly its function is docking to the bacterial receptor proteins, but these have yet to be identified. Using residues 250-615 from the Hbp model, a homology model of the

same region could be built (again using SwissModel) for Pic. Key residues such as Glu[538] and Arg[554], which hold domain 2 against the β-helix by a salt bridge, are preserved in Pic. Sequence alignment of ATs shows that Pet, Sat and EspC among others do not have this domain.

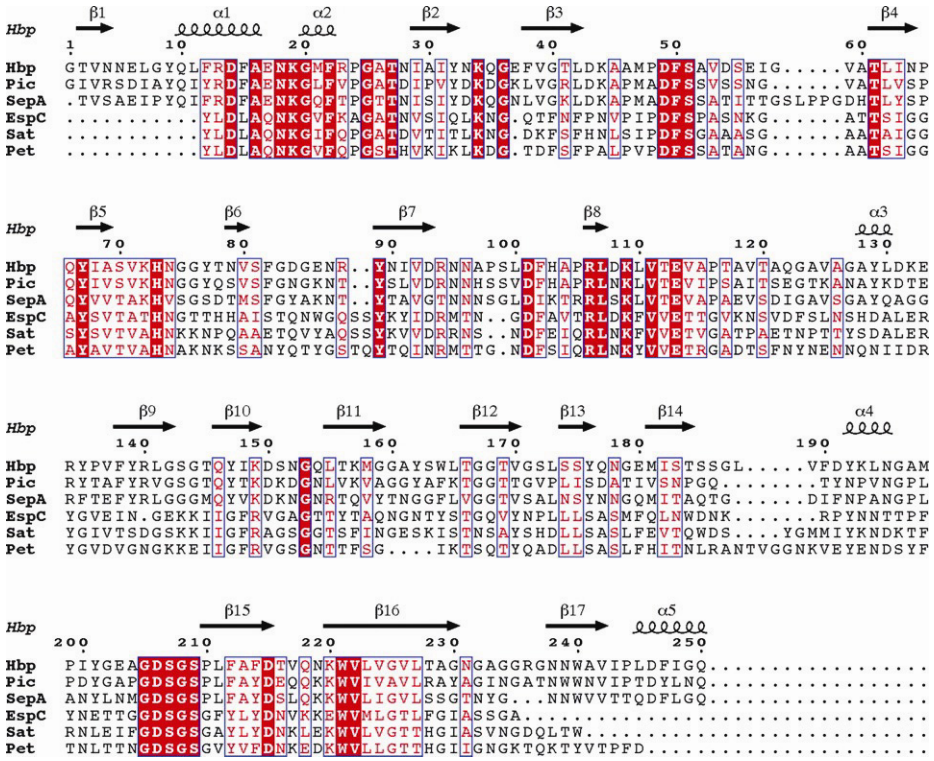

Fig. 5. A sequence alignment of Hbp with other members of the SPATE family, covering the N-terminal protease domain. Conservative mutations are shown in *red*, and residues common to all of the six compared sequences are shown in *white* on *red*. The UNIPROT reference numbers for the sequences are O88093 (Hbp), Q8CWC7 (Pic), Q8VSL2 (SepA), P77070 (EspC), Q6KD43 (Sat), and O68900 (Pet). Secondary structure elements of Hbp are shown over the alignment. The conserved regions show strong correlation to these structural elements, with the exception of the catalytic region GDSGS. The side-chain four residues upstream from this sequence sits in the specificity pocket (Tyr[201] in the case of Hbp).

Residues 608-644 of Hbp form a long discursive loop projecting from the β-helix, which also forms close contacts with the N domain. Thr[616]-Ala[626] form an α-helix, but this probably requires hydrophobic contact with the N domain residues Tyr[9]

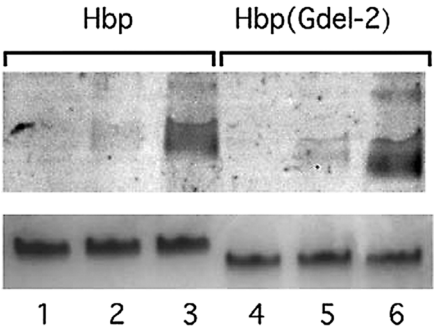

Fig. 6. Heme binding by Hbp. PCR was used to create an Hbp mutant (called "Gdel-2") missing domain 2 by linking Ala^{481} to Asn^{556} with a glycine residue. Purified native Hbp and Hbp(Gdel-2) (20 pmol) were incubated with different concentrations of heme and subsequently subjected to nondenaturing gel electrophoresis as described previously (Otto *et al.*, 1998). Heme containing proteins were visualized by tetramethyl benzidine staining. The upper panel shows the tetramethyl benzidine stained gel; lanes 1 to 3, Hbp incubated with 0, 50 or 100 pmol of heme, respectively. Heme binding, shown by the dark band, is unchanged in the mutant. Lanes 4 to 6, Hbp(Gdel-2) incubated with the different amounts of heme. The lower panel shows the Coomassie-stained gel of Hbp and Hbp(Gdel-2). The lower molecular weight of the mutant is apparent.

and Met^{158} in order to form. The 608-644 loop has no hydrophobic core of its own to suggest it is a stable independent fold. Because other ATs show no homology to Hbp in this region, it may be the heme binding site. Residue 629 is histidine, which is the most common residue bonding to heme groups, but the structure does not readily suggest how heme might bind. Repeated attempts to co-crystallize Hbp with heme or soak the crystals were unsuccessful, and mutagenesis is now underway to test the function of this region. The charge distribution over the molecular surface shows a concentration of negative charge on one face of the molecule, centered around the interface between the β-helix and domain 1 (Fig. 7). Further mutagenesis is required to determine whether this negatively charged patch is involved in heme transport.

Sequence similarity among ATs shows an increase again towards the C-terminal region of the passenger proteins. Glycines 868 and 875 in turns of Hbp are completely preserved, as are Met^{886} and Trp^{891}. The β-helix structure is broken at the conserved Ala^{979}/Pro^{980}, which mark a change in the direction of the polypeptide chain. Breaks in the electron density prevented modeling residues 913-918, 937-941 and 1024-1031. Despite the sequence conservation over the last 140 residues, these gaps in the Hbp model prevented making homology models of this region. The pattern of preserved residues matches very well interactions seen in the Hbp

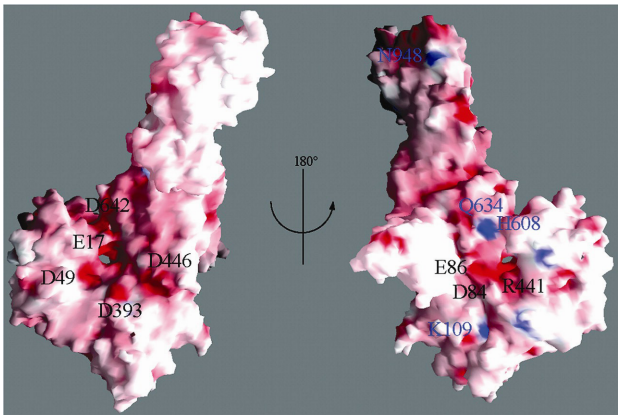

Fig. 7. Surface charge of Hbp. The molecular surface of the protein, colored by electrostatic charge (*red*, negative; *blue*, positive). Color saturation corresponds to an electron energy of ±20 k_BT.

structure however, and the C-terminal region of other ATs presumably show a very similar fold. Key residues include Trp^{1015}, which is buried and forms a hydrogen bond through its indole side chain to make a turn in the protein backbone.

Hbp has been shown to cross the inner membrane by the signal recognition particle (SRP)-dependent pathway (Sijbrandi *et al.*, 2003), but the precise mechanism of transport across the outer membrane of the cell remains unclear. Several different proposals have been made, including the suggestion that autotransporters form a multimeric pore in the outer membrane (Veiga *et al.*, 2002). Recently the structure of the pore-forming domain of NalP has been solved, showing that it is in fact a monomer, a 12-stranded β-barrel blocked by an N-terminal α-helix (Oomen *et al.*, 2004). The pore diameter, roughly 10–12 Å, is insufficient to allow passage of folded proteins and suggests that only extended polypeptides can pass through. This appears incompatible with the idea that the passenger domain is threaded through from its C-terminal end (the hairpin model), because the pore would then have to accommodate two stretches of polypeptide simultaneously. An alternative model is that the N terminus of the passenger domain is threaded through the pore, but, because other protein domains fused to the pore domain are also transported, there is no evidence of sequence-specific interactions that target the N terminus to the pore. Oomen and colleagues have suggested that the passenger domain may instead pass though the pore of the Omp85 complex, and that the name “autotransporter” is in fact a misnomer (Oomen *et al.*, 2004). From the crystal structure of Hbp described here, it is clear that the C-terminal domain (residues 950-1048) of the mature protein is more flexible and mobile than the N-terminal protease domain. This is consistent with the prediction that the C-terminal domain plays a key

role in passage across the outer membrane. On the other hand, because the N-terminal glycine of the mature protein is buried within the structure, the protease domain cannot fold properly until the signal peptide is removed, and this may provide a mechanism for keeping the protein in a readily transported form.

Tsh (temperature-sensitive hemagglutination), a SPATE found in avian pathogenic *E. coli*, has only two amino acid changes compared to Hbp (Provence and Curtiss, 1994; Stathopoulos *et al.*, 1999; Dozois *et al.*, 2000), but Hbp showed no hemagglutination activity in tests (Otto *et al.*, 1998). Recently this result has been confirmed for Tsh. The two mutations, Lys^{157} → Gln and Thr^{790} → Ala, are both on the protein surface. Lys^{157} is roughly 18 Å from the active site, but replacement with glutamine seems unlikely to alter the functional behavior of the protein greatly. Hbp and Tsh are therefore essentially identical, suggesting that Tsh too is a hemoglobin protease. If so, then the name "Tsh" seems redundant, and we suggest the name "Hbp" be used exclusively in future. Tsh has been shown to bind red blood cells, hemoglobin, fibronectin, and collagen IV (Kostakioti and Stathopoulos, 2004). It remains to be tested which of these are bound by domain 2.

Discussion

Hbp was first purified from *E. coli* EB1, a strain isolated from an intra-abdominal wound infection (Otto *et al.*, 1998). Without Hbp, *E. coli* and *B. fragilis* are unable to form abscesses and are more readily cleared from the site of infection by the immune system, presumably due to iron limitation. Although a great deal is known about iron uptake by pathogens through siderophores, very few bacterial heme uptake systems have been characterized in molecular detail. The best understood is the HasA protein of *Serratia marcescens* for which a crystal structure has been refined to 1.9 Å (Arnoux *et al.*, 1999). Hbp has a quite different fold, and is over five times larger. Much of the biology involving Hbp remains to be elucidated. No surface protein from either *E. coli* or *B. fragilis* has yet been identified which can interact with Hbp and receive heme from it, yet these must presumably exist given the known effects of the protein on these bacteria under conditions of iron limitation. *B. fragilis* up-regulates expression of a number of proteins under iron-limiting conditions (Otto *et al.*, 1998), and these are currently being examined as possible receptors for Hbp.

One functional role of Hbp is to remove heme from Hb and supply it to bacteria growing within the body. The crystal structure shows a novel trypsin-like

serine protease domain that is well conserved among the SPATE family. The overall β-helix architecture is also common to the ATs, but different loops and domains carried by this stable fold appear to give the proteins distinctive functional properties. Hbp does not have a sequence motif or structural domain which resembles a known heme binding site. Further heme binding studies with mutants of Hbp and other ATs are currently underway to determine how heme interacts with Hbp.

Homology models of other ATs based on the Hbp structure described here will hopefully be useful in designing new experiments to test their functional roles and find ways to block their activity. Hbp may be a convenient vehicle for presenting peptides for antibody and vaccine production, by inserting them in place of domain 2. Domain 2 itself may well allow us to produce a clinically useful vaccine to reduce substantially the occurrence of severe peritonitis.

Acknowledgments

We thank Drs. N. Kamiya, Y. Kawano, and H. Nakajima of SPring8 and Prof. S. Wakatsuki and Drs. M. Suzuki, N. Matsunaga, and N. Igarashi of the Photon Factory for help with data collection.

Abbreviations

The abbreviations used are: AT, autotransporter; Hb, Hemoglobin; Hbp, Hemoglobin protease.

Chapter 4

Purification, folding and preliminary structure of the translocator domain of the *Escherichia coli* autotransporter Hbp

In collaboration with Lucy Rutten[1] and Peter van Ulsen[2]

[1] Department of Crystal and Structural Chemistry and [2] Department of Molecular Microbiology, Universiteit Utrecht, Utrecht, The Netherlands

Abstract

Hemoglobin protease (Hbp) is an autotransporter protein produced by some pathogenic *Escherichia coli* species. Autotransporters are found in a variety of Gram-negative bacteria and have a common mechanism of secretion: a N-terminal signal sequence for translocation across the inner membrane and a C-terminal translocation unit necessary for translocation across the outer membrane. The translocation unit is composed of a predicted α-helical linker region and a β-core believed to form a β-barrel pore in the outer membrane to allow export of the passenger domain. A DNA construct was made encoding a full length Hbp in which a thrombin cleavage site for controlled cleavage replaced the natural cleavage site in the linker region. A histidine-tag was added to the linker region to facilitate purification of the protein. The complete recombinant Hbp pro-protein was expressed in *E. coli* and recovered from the outer membrane fraction. The histidine-tag and the thrombin cleavage site were found to be inaccessible for binding to a Ni^{2+}-charged chelating column and thrombin, respectively, which points to a localization of the linker region within the β-barrel pore. The translocation unit of Hbp was also expressed in *E. coli* without a signal peptide, resulting in the accumulation of the protein in the cytoplasm in the form of inclusion bodies. After solubilization of the inclusion bodies in urea, the protein was refolded *in vitro* by dilution in the presence of detergent. Refolding resulted in pure protein that was heat-modifiable. Circular dichroism spectroscopy revealed a high content of β-strand in agreement with the prediction of a β-barrel structure. A β-barrel topology model for the Hbp translocation unit is proposed.

Introduction

Outer membrane proteins (OMPs) are integral membrane proteins found in the outer membranes of Gram-negative bacteria, chloroplasts and mitochondria. All bacterial OMPs of which the structure has been determined have β-barrel transmembrane domains composed of an even number of β-strands (Schulz, 2003). Most bacterial OMPs are involved in transport processes for (bio-) molecules into and/or out of the cell. Other OMPs have diverse functions like adhesins, proteases, phospholipases or structural proteins (Mogensen *et al.*, 2005).

Bacterial OMPs that are involved in the secretion of proteins into the extracellular environment can be part of various types of secretion pathways (Lee

and Schneewind, 2001; Henderson *et al.*, 2004). These secretion pathways differ markedly in their composition and complexity. In some pathways (for instance type I and type III), proteins are translocated in one step across the inner and outer membrane, without a periplasmic intermediate. The type I system is quite simple, consisting of only three proteins (Gentschev *et al.*, 2002), while the type III system consists of more than 20 proteins (Cheng and Schneewind, 2000). Other pathways first translocate the secretory protein across the inner membrane and subsequently translocate the periplasmic intermediate in a second step across the outer membrane. Here too, simple systems exist, like the type V secretion system, as well as more complex systems like type II, which consists of at least 12 proteins (Sandkvist, 2001). The type V secretion system comprises type Va, the autotransporter pathway, type Vb, the two-partner secretion system, and type Vc, the trimeric autotransporter (AT-2) pathway (Cotter *et al.*, 2005). Several extensive reviews on type V and autotransporter secretion have been published recently (Desvaux *et al.*, 2004; Henderson *et al.*, 2004; Jacob-Dubuisson *et al.*, 2004; Newman and Stathopoulos, 2004).

The type Va or the autotransporter pathway can probably be considered as the most simple secretion mechanism, because the autotransporter protein itself contains most of the elements that are necessary for its secretion. The secreted functional protein, termed the passenger domain, is preceded by an N-terminal signal sequence that mediates targeting to and translocation across the inner membrane through the Sec translocon (Sijbrandi *et al.*, 2003). Following the passenger is a C-terminal translocator domain that is necessary for translocation across the outer membrane (Pohlner *et al.*, 1987). This translocator domain consists of a predicted outer membrane β-barrel forming structure preceded by a linker domain (Konieczny *et al.*, 2001; Oliver *et al.*, 2003a). The current models for outer membrane translocation predict that the passenger is translocated to the cell surface either in an unfolded state through a pore formed by the β-barrel translocation domain (Oliver *et al.*, 2003b), or (partially) folded through an oligomeric ring formed by multiple barrels (Veiga *et al.*, 2002). The autotransporter β-barrels are predicted to consist of 10 to 14 amphipathic transmembrane β-strands connected by hairpin turns and loops (Jacob-Dubuisson *et al.*, 2004). Recently, the first crystal structure of an autotransporter translocator domain was published (Oomen *et al.*, 2004). The translocation unit of the *Neisseria meningitidis* autotransporter NalP (AspA) was shown to consist of a β-barrel formed by 12 antiparallel β-strands around a central cavity. This pore was occupied by an α-helix that was formed by the linker region. The dimensions of the pore, circa 10 by 12.5 Å, and the presence of the helix in the barrel point towards a

translocation mechanism by which the passenger is translocated through the β-barrel pore.

Also quite recently, the first complete crystal structure of an autotransporter passenger domain, of the *Escherichia coli* Hemoglobin protease (Hbp), was published (Otto *et al.*, 2005). Hbp is a serine protease autotransporter that is involved in the pathogenic synergy between *E. coli* and *Bacteroides fragilis* in human intra-abdominal infections (Otto *et al.*, 1998; Otto *et al.*, 2002). The secreted passenger degrades hemoglobin and binds heme, which is probably delivered to both bacterial species. The structure of the passenger domain of Hbp was resolved to 2.2-Å resolution and shows a somewhat globular N-terminal protease domain followed by a very large right-handed β-helical structure with several smaller domains or loops protruding from this backbone.

In this chapter, the translocator domain of Hbp is studied in more detail. The final goal is to resolve the crystal structure of the Hbp translocator to gain more insight in the mechanism of passenger translocation and to be able to compare the similarities and differences between several autotransporter translocator domains. The purification process, as well as the *in vitro* folding of the Hbp translocator domain is described, and a model for the predicted topology of the translocation unit is presented.

Materials and methods

Bacterial strains, plasmids and media

The *Escherichia coli* strain Top10F' (Invitrogen) and the plasmid pACYC184 (Chang and Cohen, 1978) were routinely used in cloning procedures. The *E. coli* strain BL21AI (Invitrogen) and the plasmid pET11a (Novagen) were used for subcloning and controlled expression of β-barrel inclusion body constructs. The *E. coli* strain BL21(DE3)omp8 (a gift from R. Koebnik) (Prilipov *et al.*, 1998) was used for expression and purification of the construct pACYC-HbpThromHisBarrel. The *E. coli* strains were routinely grown in Luria-Bertani (LB) medium (Miller, 1992). Appropriate antibiotics were added to the culture medium. For culturing of the strain BL21(DE3)omp8, the chemically defined MA medium was used (Miller, 1992).

Table 1. Plasmids used in this study

pACYC-Hbp	(Otto *et al*., 2002)
pACYC-HbpHisBarrel	(this study)
pACYC-HbpThromHisBarrel	(this study)
pET11a	(Novagen)
pET11a-βHbp encodes residues 1102 to 1377, starts at amino acid +2 after natural cleavage site, introducing mutation $Leu^{1102}Met$	(this study)
pET11a-β13Hbp encodes residues 1088 to 1377, starts 13 amino acids upstream of natural cleavage site at Met^{1088}	(this study)
pET11a-β25Hbp encodes residues 1076 to 1377, starts 25 amino acids upstream of natural cleavage site, introducing mutation $Arg^{1076}Met$	(this study)

General methods

Recombinant DNA techniques were carried out as described (Sambrook *et al.*, 1989). DNA sequencing was carried out using the Big Dye Terminator Cycle sequencing kit on an ABI Prism 310 automated sequencer (Perkin Elmer). Bound antibodies were visualized on immunoblots by chemiluminescence. The (relative) intensity of protein bands from both chemoluminescent blots and Coomassie-stained gels were quantified using a FluorS MultiImager with the Multi-Analyst software package (BioRad).

Polyclonal antibodies and reagents

Goat anti-rabbit HRP-conjugated antibodies used for immunodetection were obtained from BioRad. For Western blotting, anti-β-barrel antiserum raised against purified β-barrel was used. Restriction enzymes, the Expand long template PCR system, Complete EDTA-free protease inhibitors and the Lumi-light western blotting substrate were obtained from Roche Molecular Biochemicals. IPTG was purchased from Anatrace. The zwitterionic detergent SB3-12 was obtained from Fluka. Acidic impurities from SB3-12 were removed as described (Kramer *et al.*, 2000). Sigma Chemicals supplied all other chemicals.

Construction of plasmids

The T7 expression system was used for IPTG-arabinose inducible expression of β-barrel inclusion bodies (Studier *et al.*, 1990). The β-barrel from the *hbp* gene was amplified by PCR using the plasmid pACYC-Hbp as template DNA.

Primers used were the Bar*Nde*I primer (5'-CATTG**CATATG**AACAAACGCATGGGC-GATTTG-3', with the *Nde*I restriction site in boldface letters) and the *Bam*HI primer (5'-TATAA**CCTAGG**TCTCTACACAAGTCCTCAATC-3', with the *Bam*HI restriction site in boldface letters). Constructs encoding 13 or 25 extra amino acids in front of the β-barrel were also constructed using the primers Bar13*Nde*I (5'-CCTGTG-**CATATG**CACATCAGCTATAACAACTTCCATC-3' with the *Nde*I restriction site in boldface letters) or Bar25*Nde*I (5'-CTTCC**CATATG**AACGACGGCCAGGGTAAG-GTG-3' with the *Nde*I restriction site in boldface letters) in combination with the *Bam*HI primer. The three fragments were cloned into pET11a using the created *Nde*I and *Bam*HI restriction sites, resulting in the plasmids pET11a-βHbp, pET11a-β13Hbp and pET11a-β25Hbp.

A histidine tag was introduced at the N-terminal side of the Hbp β-barrel in the full-length construct by nested PCR using pACYC-Hbp as template DNA. In the first amplification rounds, the primers used were the gap4,10for primer (5'-GAACTCAACACTGACCAGTAC-3') which anneals just upstream of the natural *Kpn*I restriction site in the Hbp passenger domain and the HisβBarRev primer (5'-**ATGGTGGTGATGGTGATG**GCGTTTGTTCAGGTTGTTAACTTCAGTGATGAAGTT-GTTATAGC-3' with the His-tag in boldface letters) for the first fragment and the HisβBarFor primer (5'-**CATCACCATCACCACCAT**ATGGGCGATTTGAGGGATAT-TAATGGCGAAGCCGGTACGTGGG-3' with the His-tag in boldface letters) and the *Bam*HI primer for the second fragment. Both fragments were used together as template DNA in the second amplification round using the gap4,10for primer and the *Bam*HI primer. Using the *Kpn*I and *Bam*HI restriction sites, the fragment was inserted into the corresponding sites of pACYC-Hbp, resulting in the plasmid pACYC-HbpHisBarrel.

This plasmid was then used to make a construct encoding Hbp, in which a thrombin cleavage site for controlled cleavage replaced the natural cleavage site between passenger domain and translocation unit. This thrombin-cleavable His-tagged construct was also made by nested PCR. In the first amplification rounds, the primers used were the gap4,10for primer and the ThromBbarRev primer (5'-**ACTACCGCGTGGCACCAG**GTTGTTATAGCTGATGTGCATGAATGTGGCGGCA-GCCTTACCCTG-3' with the thrombin cleavage site in boldface letters) for the first fragment and the ThromBbarFor (5'-**CTGGTGCCACGCGGTAGT**AACCTGAAC-AAACGCCATCACCATCACCACCATATGGGCGATTTG-3' with the thrombin cleavage site in boldface letters) primer and the *Bam*HI primer for the second fragment. Both fragments were used together as template DNA in the second amplification round using the gap4,10for primer and the *Bam*HI primer. Using the

*Kpn*I and *Bam*HI restriction sites, the fragment was inserted into the corresponding sites of pACYC-HbpHisBarrel, resulting in the plasmid pACYC-HbpThromHisBarrel.

All constructed plasmids were sequenced to check for second site mutations.

Purification of native translocator domain from the outer membrane

Native Hbp translocator domain was purified from the outer membrane of *E. coli* BL21(DE3)omp8 (pACYC-HbpThromHisBarrel) over-expressing full length Hbp with a thrombin cleavage site between the passenger domain and the β-barrel to cleave off the β-barrel *in vitro*. Cells were cultivated in 4 L MA medium at 37 °C to an OD_{660} of circa 0.6. Cells were harvested, washed and resuspended in 40 ml buffer K (50 mM triethanolamine-HAc, 250 mM sucrose and 1 mM EDTA, pH 7.5). The whole procedure was carried out on ice or at 4 °C. Complete EDTA-free protease inhibitors, 1 mM EDTA, DNase and RNase were added and the cells were lysed using a French pressure cell. The cellular debris was removed by centrifugation at 11.000 rpm in a Sorvall SS34 rotor for 5 min (twice). A total membrane preparation was obtained by ultracentrifugation of the lysate at 165.000 × *g* for 90 min. The membrane pellet was washed in 50 mM Tris-HCl, pH 8.0. Inner membrane proteins were selectively removed by dissolving the membranes in 10 ml 50 mM Tris-HCl, pH 8.0 with 0.2% sodium-sarkosyl for 1 h. An outer membrane enriched protein fraction was obtained by ultracentrifugation at 300.000 × *g* for 20 min. Outer membrane proteins were extracted from the membranes by incubation for 1 h at room temperature in 4 ml 50 mM Tris-HCl, pH 8.0 with 1% Triton X-100. Undissolved material was removed by ultracentrifugation at 300.000 × *g* for 20 min at room temperature. The buffer for the dissolved proteins was exchanged into T_{omp} buffer (20 mM Tris-HCl, 125 mM NaCl, 2.5 mM $CaCl_2$ and 0.5% SB3-12, pH 8.0) using a HiTrap desalting column (Amersham Biosciences). The β-barrel was cleaved from the full length Hbp protein using the introduced thrombin cleavage site. The 8 ml sample was incubated overnight with circa 90 µg of human α-thrombin (Haematologic Technologies). The protein sample was diluted 2.5 times in 20 mM Tris-HCl, pH 8.0 and loaded on a HiTrap DEAE column (Amersham Biosciences) equilibrated in 20 mM Tris-HCl, 50 mM NaCl, pH 8.0 with 0.2% SB3-12. Bound proteins were eluted from the column using a linear gradient to 500 mM NaCl. Samples taken during the procedure were analysed by SDS-PAGE and Coomassie staining.

Isolation of inclusion bodies

For production of inclusion bodies, *E. coli* BL21AI cells harboring plasmids pET11a-βHbp, pET11a-β13Hbp or pET11a-β25Hbp, encoding three versions of the Hbp translocator domain, were grown in 4 L LB medium at 37 °C. At OD_{660} = 0.4, expression was induced with 0.2% arabinose and 1 mM IPTG for 2 h. Cells were harvested and resuspended in 60 ml 50 mM Tris-HCl and 2 mM EDTA, pH 8.0. DNase was added and the suspension was lysed using a French pressure cell. Then 1/10 volume 1% Triton X-100 was added and the suspension was incubated at 30 °C for 20 min. The sample was centrifuged at 20.000 × *g* for 10 min at 4 °C. Repeated washing and centrifugation steps purified the pellet fraction containing the inclusion bodies. The pellet was first washed in ice-cold 50 mM Tris-HCl (pH 8.0) containing 100 mM NaCl, 1 mM EDTA and 1% NP-40. Then the pellet was washed in ice-cold 50 mM Tris-HCl (pH 8.0) containing 100 mM NaCl and 1 mM EDTA. Subsequently, the pellet was washed in ice-cold 50 mM Tris-HCl (pH 7.0) containing 1 M urea. Finally, the pellet was resuspended in 4 ml ice-cold 20 mM Tris-HCl (pH 7.0) containing 0.1 M glycine. The purity and concentration of the translocator domain containing inclusion bodies was analyzed by SDS-PAGE and Coomassie staining.

In vitro refolding of translocator domain inclusion bodies

For small scale refolding experiments, 1 mg of translocator domain containing inclusion bodies was centrifuged at 20.000 × *g* for 15 min. The supernatant was removed and the inclusion bodies were unfolded in 100 µl buffer A (20 mM sodium phosphate (NaH_2PO_4 / Na_2HPO_4), 100 mM glycine, pH 7 to which solid urea was added to 8 M). The sample was incubated O/N on a shaker at room temperature. The non-dissolved material was pelleted by ultracentrifugation at 300.000 × *g* for 1 h. Unfolded protein was refolded by rapid dilution at room temperature in 900 µl buffer B (20 mM sodium phosphate (NaH_2PO_4 / Na_2HPO_4), 1 M NaCl, 0.5% SB3-12, pH 7.0). Refolding was allowed to occur over a period of 3 days at 37 °C while the sample was standing still. Aggregates were removed by centrifugation at 20.000 × *g* for 15 min. To be able to record CD spectra, the refolded protein samples were dialyzed against buffer C (20 mM sodium phosphate (NaH_2PO_4 / Na_2HPO_4), 100 mM NaCl, 0.2% SB3-12, 80 mM urea, 1 mM glycine, pH 7.0) for 3 h. Subsequently, the samples were centrifuged at 20.000 × *g* for 15 min and concentrated 2-3 times using a Microsep microconcentrator (Pall Life Sciences). CD spectra were recorded at room temperature on a Jasco J-600 spectropolarimeter.

Results

For a fast and easy purification procedure of the Hbp translocator domain under native conditions, a construct was prepared containing two modifications in the predicted α-helical linker region (Fig. 1). The natural cleavage site of Hbp (between Asn^{1100} and Asn^{1101}) was replaced by a thrombin cleavage site for controlled cleavage of the passenger from the translocator domain. Also, a histidine tag was introduced near the N-terminal end of the translocator domain sequence to facilitate the purification of the translocator domain.

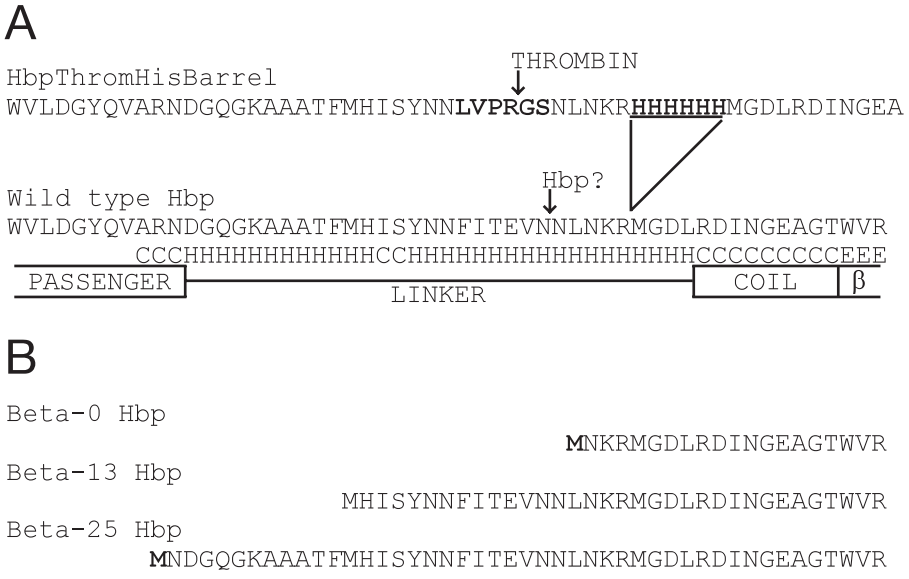

Fig. 1. A, Partial amino acid sequence of wild type Hbp (bottom) and the HbpThromHisBarrel construct (top), indicating the transition between the passenger and the translocation unit, consisting of the linker region and the predicted β-barrel. At the bottom, the C-terminal end of the passenger domain (passenger), the α-helical linker region (linker) and the N-terminal end of the predicted β-barrel (random coil, followed by a β-strand) are indicated schematically for the wild type protein. C = random coil, H = α-helix, E = β-strand, as predicted by the PSIPRED algorithm (http://bioinf.cs.ucl.ac.uk/psipred/). In the wild type sequence, the natural cleavage site is indicated by the arrow marked Hbp? since Hbp is presumed to be responsible for the cleavage reaction. In the HbpThromHisBarrel construct, the introduced thrombin cleavage site (boldface letters) is indicated by the arrow marked Thrombin. The introduced histidine tag in this construct is also indicated (boldface letters). B, Partial amino acid sequence of the inclusion body constructs β-0, β-13 and β-25 Hbp. All sequences start at their respective N-termini. Mutated amino acids with respect to the wild type Hbp sequence are shown in boldface letters.

This construct (pACYC184-HbpThromHisBarrel) was introduced into *E. coli* BL21(DE3)omp8 cells for high expression of the modified Hbp. This strain is lacking eight major outer membrane proteins, thereby creating more available space in the outer membrane for accumulation of Hbp translocator domain molecules. Cells expressing this construct were collected and after cell lysis, a total membrane pellet was obtained by ultracentrifugation. Inner membrane proteins were selectively removed by incubation of the membranes in 0.2% sodium sarkosyl and recentrifugation. In this way, a crude outer membrane pellet was obtained, that was dissolved in 1% Triton X-100 to extract the outer membrane proteins from the membranes (Fig. 2, lanes 1-8). Subsequently, thrombin was added to the outer membrane proteins in order to cleave the translocator domain from the Hbp protein using the introduced thrombin cleavage site. The buffer in which the outer membrane proteins were dissolved was changed into a thrombin cleavage buffer, and thrombin cleavage was allowed to take place overnight. As shown in Fig. 2 (lane 9), the pro-Hbp (translocator domain plus passenger domain) form of 142 kDa was still present in the thrombin treated sample and no accumulation of translocator domain (ca. 32 kDa) was detectable. Only when the concentration of the detergent SB3-12 was increased to at least 1%, the translocator domain was cleaved off. However, this was probably due to (partial) unfolding of the protein, as the CD spectrum that was recorded for this sample did not show a β-fold conformation (data not shown).

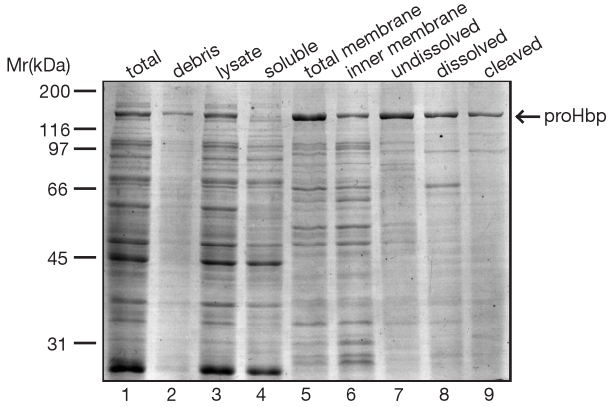

Fig. 2. Purification and thrombin cleavage of the HbpThromHisBarrel construct. Samples taken at different steps during the purification and thrombin cleavage procedures were resolved on an 11% SDS-PAGE gel and stained with Coomassie. Relative molecular weight markers are indicated on the left of the figure, and the position of pro-Hbp in the gel is indicated on the right. The contents of the lanes are indicated above the figure and further explained in the text.

In another approach, the pro-Hbp was first purified using the histidine tag and then cleaved with thrombin. However, despite several attempts, the pro-Hbp did not bind to a Ni^{2+}-charged chelating column (data not shown). These results suggest that both the thrombin cleavage site and the histidine tag are not accessible in the isolated and native protein possibly due to a localization of these sites halfway inside the channel.

In an alternative approach, the translocator domain was expressed inside the *E. coli* cytoplasm in the form of inclusion bodies. Three different constructs for translocator domain proteins of various lengths were made. The β-0 construct encodes a translocator domain that starts just one amino acid after the natural cleavage site of Hbp. The β-13 construct starts 13 amino acids upstream of the natural cleavage site and the β-25 construct starts 25 amino acids upstream the natural cleavage site. The latter two variants contain a larger part (β-13) or even the complete (β-25) predicted α-helical linker (Fig. 1). The constructs were introduced into *E. coli* BL21AI cells for the production of inclusion bodies. After culturing and induction for 2 h, the cells were harvested and analyzed. Analysis of cells under a phase contrast light microscope clearly showed the inclusion bodies in the β-0 and β-13 expressing cells, but hardly any inclusion bodies in the cells with expression the β-25 construct. The inclusion bodies were isolated and purified. The purity and concentration of the translocator domain containing inclusion bodies were analysed by SDS-PAGE and Coomassie staining (Fig. 3A). In accordance with the observations under the light microscope, only small amounts of β-25 protein were detected in the inclusion body preparations.

Equal amounts of protein from all three inclusion body preparations were unfolded overnight in 8 M urea. After removal of non-dissolved material by centrifugation, the unfolded proteins were allowed to refold by rapid ten-fold dilution in refolding buffer containing 1 M NaCl and 0.5% SB3-12. The β-25 protein did not dissolve well in 8 M urea, but it was found in the pellet material after the centrifugation step. It appeared that the β-25 protein was mainly present in the membranous material that still contaminated the inclusion bodies. Because of the lack of proper inclusion body formation the β-25 construct was not further used.

Samples from the refolded β-0 and β-13 proteins were analyzed on an 11% native PAGE gel. The samples were applied either in a non-denaturing loading buffer or in SDS loading buffer after boiling them (Fig. 3B). For both proteins, folded as well as unfolded forms are visible in the native condition (lanes 1 and 2). Intriguingly, the folded forms of both proteins run at a similar position in the gel, below the 31-kDa

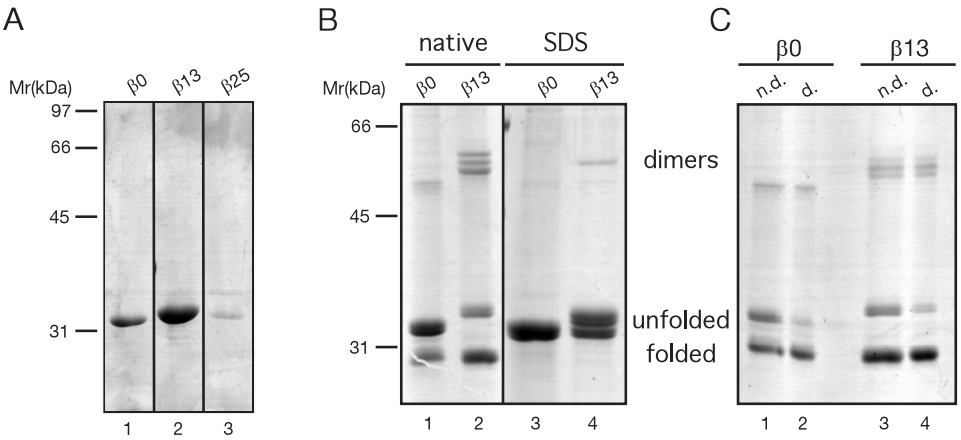

Fig. 3. Purification and *in vitro* folding of translocator domain inclusion bodies. A. Equal amounts of purified inclusion bodies from the β-0, β-13 and β-25 inclusion body constructs were boiled in SDS-solubilization buffer and resolved on an 11% SDS-PAGE gel. B. Analysis of the refolding of the β-0 and β-13 proteins. Equal amounts of protein were dissolved and unfolded in buffer containing 8 M urea and subsequently refolded by rapid 10-fold dilution in buffer without urea containing 1 M NaCl and 0.5% SB3-12. Samples were taken in native sample buffer and resolved on an 11% native PAGE gel, or in SDS-solubilization buffer, boiled at 95°C and resolved on the same native gel. C. Effect of dialysis on the refolded proteins. The refolded material was dialyzed against a low-salt buffer. Samples before and after dialysis were resolved on an 11% native PAGE gel. n.d. = not dialyzed. d. = dialyzed. The positions of folded and unfolded proteins and of possible dimers are indicated between panels B and C. Relative molecular weight markers are indicated on the left of panels A and B. All gels were stained with Coomassie.

protein marker. Besides monomeric forms around 30 kDa, some possible protein dimers were visible. The proteins were confirmed to be translocator domain proteins by western blotting using anti-translocator domain antibodies. When the refolded samples were boiled in SDS, the folded forms completely disappeared (lanes 3 and 4). For the β-13 protein an extra band appeared at the position of the β-0 protein, which is probably partially or incorrectly folded protein.

To be able to record circular dichroism (CD) spectra of the refolded proteins, the protein samples were dialyzed to lower the salt concentration. Some precipitation occurred during the dialysis, and the samples were centrifuged to remove all precipitated protein. When protein samples before and after dialysis were compared on native PAGE, it appeared that the unfolded proteins were quite specifically removed upon dialysis, while the folded proteins remained in solution (Fig. 3C). This step increased the folding efficiency to above 80 or 90% as quantified from the

Coomassie stained gels. CD spectra were recorded for the refolded, dialyzed protein samples to determine if the refolded proteins had a β-folded conformation as expected. Although impurities or buffer components disturbed the measurements below 200 nm, the minimum of the ellipticity around 218 nm clearly indicated a β-folded content for both proteins (Fig. 4).

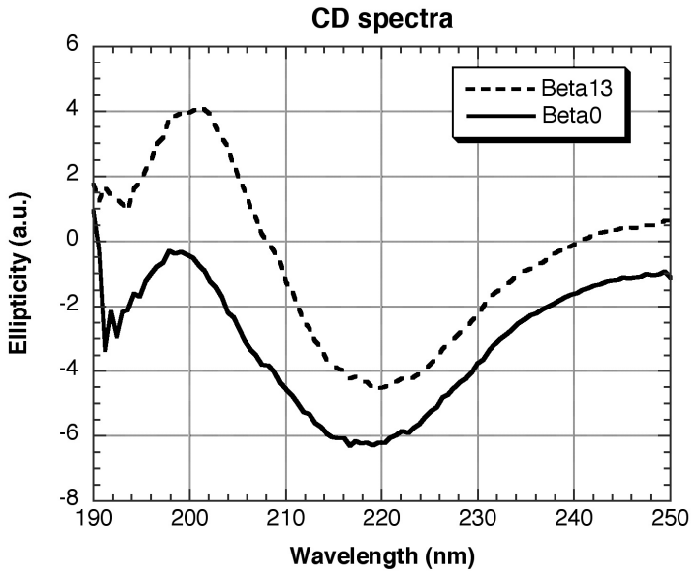

Fig. 4. CD spectra of refolded Hbp translocation units. Spectra were recorded for the refolded and dialyzed β-0 (solid line) and β-13 (broken line) constructs. The ellipticity (θ) on the vertical axis is in arbitrary units.

Discussion

This study describes the purification, *in vitro* folding and preliminary characterization of the translocation unit of the *E. coli* autotransporter Hbp. The Hbp translocation unit is predicted to consist of a short α-helical linker region of circa 32 amino acids, followed by a β-barrel structure forming a pore in the outer membrane. First an attempt was made to purify the translocation unit by using a mutant construct in which the naturally occurring cleavage site of Hbp was replaced by a thrombin cleavage site. In this way, complete 142 kDa pro-Hbp molecules were expected to accumulate in the outer membranes of *E. coli* cells expressing this construct. The

idea was then to cleave off the passenger domain from the predicted β-barrel structure by the addition of purified thrombin to the reaction mixture. Pro-Hbp did accumulate in the outer membranes and did have its passenger domain exposed at the cell surface (data not shown), but it was not possible to cleave off the passenger domain with thrombin under native conditions. Only when a high concentration of detergent was present, cleavage was observed. Similarly, a histidine tag that was introduced close to the thrombin cleavage site appeared to be unavailable for binding to a Ni^{2+}-charged affinity column under native conditions. These observations led to the conclusion that both the thrombin cleavage site and the histidine tag are not exposed to the buffer/solvent in the pro-Hbp molecule. This might be related to the positioning of both sites within the predicted α-helical linker region or shielding by LPS or other membrane proteins. When an α-helix is indeed formed in Hbp, which is analogous to the α-helix in the NalP crystal structure and is positioned in the β-barrel pore, then the thrombin cleavage site and the histidine tag are predicted to be located inside the pore structure.

In another attempt to obtain intracellular inclusion bodies a translocator domain without a signal sequence was constructed. Constructs encoding the Hbp translocation unit of three different lengths were used. The shortest construct starts just one amino acid C-terminal to the natural cleavage site of Hbp. The longest version starts 25 amino acids upstream of the natural cleavage site and encompasses the complete predicted α-helical linker region. The middle construct (β-13) starts in between the former two and encodes about two-third of the predicted α-helix. Hardly any inclusion bodies were formed in cells producing the β-25 construct. When 8 M urea was added to preparations containing the β-25 construct, the protein did not dissolve and was recovered in a membranous pellet after centrifugation. Possibly, the β-25 translocation unit may partly insert into or stick to the inner membranes of the cells. Experiments testing the heat-modifiability of this β-25 protein on native PAGE gels indicated that this mutant protein was quite stable, although it probably did not acquire its native conformation (data not shown).

High amounts of proteins were easily obtained from the β-0 and β-13 constructs. These proteins unfolded well and solubilized easily in 8 M urea. A high percentage of refolding was observed after dilution. Interestingly, upon dialysis against a low salt buffer, unfolded protein precipitated, thereby increasing the overall refolding efficiency. When CD spectra were recorded for these samples, the minimum at 218 nm clearly indicated a high β-strand content. Taken together, these results point towards a native β-barrel conformation for the refolded proteins encoded by the β-0 and β-13 constructs.

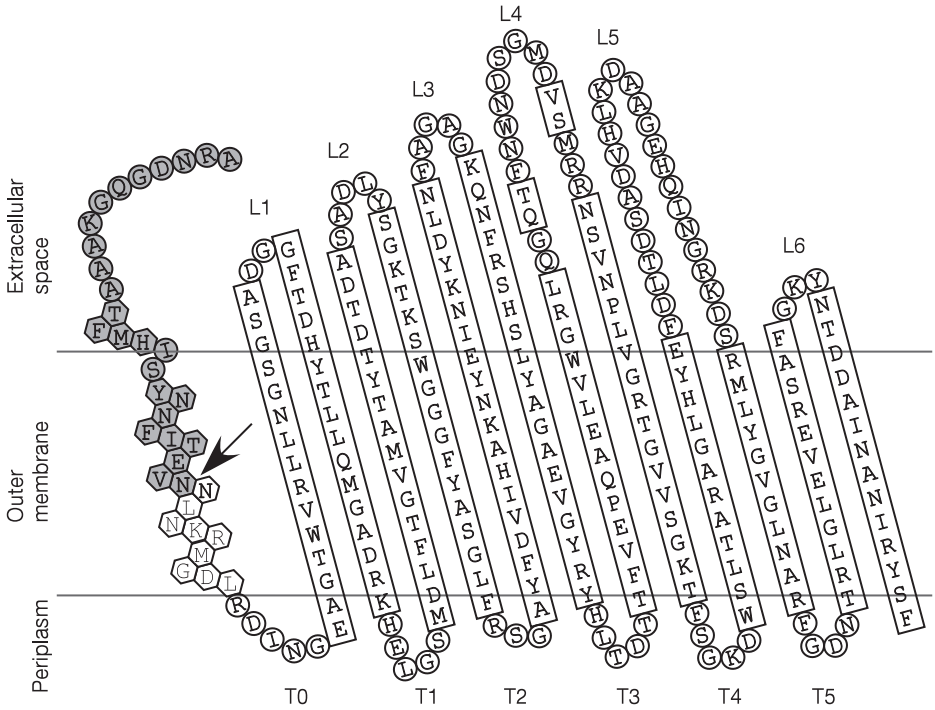

Fig. 5. Topology model for the Hbp translocation unit. Amino acids in β-strands are indicated in long rectangles, in α-helix as hexagonals and in loops or random coils as circles. The periplasmic turns and extracellular loops of the barrel are assigned as T and L, respectively. The natural cleavage site between passenger and translocator is indicated by the arrow, the C-terminal residues of the passenger are indicated in grey. The model is based on the crystal structures of NalP and the Hbp passenger domain and on predictions by the PSIPRED and PRED-TMBB (http://bioinformatics.biol.uoa.gr/PRED-TMBB/) algorithms.

The purified and refolded Hbp translocation units will be used for crystallization studies to resolve the crystal structure of the Hbp translocation unit. Because the crystal structure of the passenger domain of Hbp is already known (Otto *et al.*, 2005), the complete Hbp structure would then be known, crystallized as two separate entities. Furthermore, the crystal structure of the Hbp translocation unit can be compared with that of NalP, so far the only known structure of an autotransporter translocation unit (Oomen *et al.*, 2004). Based on the crystal structure of the NalP translocation unit and secondary structure predictions by the PSIPRED (McGuffin *et al.*, 2000) and PRED-TMBB (Bagos *et al.*, 2004) algorithms, a topology model for the translocation unit of Hbp has been developed (Fig. 5). Like NalP, in the model, Hbp contains 12 antiparallel β-strands forming a pore and an α-helical linker spanning the

membrane. Using the program Deep View / Swiss-Pdb Viewer (Guex and Peitsch, 1997), a homology model for the three-dimensional structure of the Hbp translocation unit was devised, based on the crystal structure of the NalP translocation unit (Fig. 6). The crystal structure itself will have to reveal whether the α-helix occupies the pore, like in NalP, or whether it is located outside the barrel. In contrast to NalP, the major part of the helix in Hbp remains connected to the passenger domain after cleavage from the translocation unit (depicted in Fig. 1A and 5). In case the α-helix will be found within the barrel, a model can be developed in which passenger domain translocation proceeds through the β-barrel pore. This translocation process could be either N terminus first (the threading model) (Oomen *et al.*, 2004) or C terminus first (the hairpin model) (Pohlner *et al.*, 1987; Henderson *et al.*, 1998). The major unresolved issue for the threading model is the mechanism of targeting of the N terminus of the passenger domain to the pore. The hairpin model has the problem that the pore diameter appears not to be large enough to accommodate two

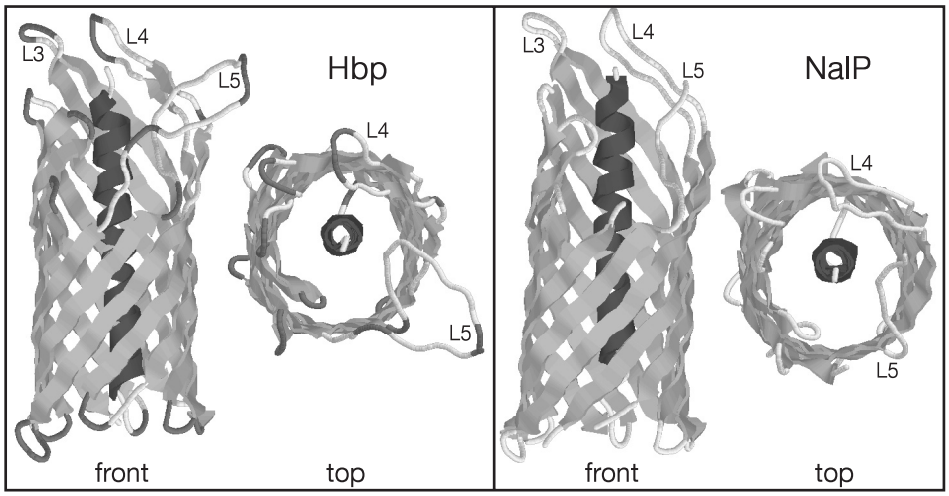

Fig. 6. Homology model for the three-dimensional structure of the Hbp translocation unit in comparison with the NalP translocation unit (PDB indentifier 1UYN shown here). Homology modelling was carried out using the Deep View / Swiss-Pdb Viewer program (http://www.expasy.org/spdbv/), in which the primary sequence of Hbp was manually aligned with the NalP primary sequence. The three-dimensional structure of the Hbp translocation unit was subsequently treaded unto the two NalP crystal structures (PDB identifiers 1UYN and 1UYO). Note that loop 5 (L5) is not completely resolved in the NalP crystal structure, but the loop is present in the Hbp model. Front and top views are shown for both proteins.

stretches of extended polypeptide simultaneously (Oomen *et al.*, 2004; Otto *et al.*, 2005). Alternatively, in case the α-helix does not occupy the pore, the multimer model for passenger domain translocation as proposed by Veiga *et al*. (Veiga *et al.*, 2002), will be the most probable model. However, because the membrane interface of the NalP translocation unit is hydrophobic, the central pore of a multimer is likely to be filled with outer membrane lipids. To date, translocation through a multimeric pore has only been observed for non-native passenger molecules. As an alternative to the multimer model or the models in which translocation takes place through the pore, Oomen *et al.* postulated a model involving the conserved Omp85 protein (Oomen *et al.*, 2004). Autotransporter secretion has been shown to (partially) depend on Omp85 (Voulhoux *et al.*, 2003), but more experiments are needed to elucidate the role of this protein in autotransporter secretion, as Omp85 might also facilitate the outer membrane insertion of the translocation unit itself. In this respect it is noteworthy that a homologue of Omp85, YaeT, was recently found to be present in a multiprotein complex required for the assembly of outer membrane proteins in *E. coli* (Wu *et al.*, 2005). Another component of this complex, the lipoprotein YfgL, is involved in a homeostatic control mechanism that coordinates the overall assembly process of the outer membrane (Wu *et al.*, 2005). This complex may very well be required for the insertion of autotransporter translocation units in the outer membrane. It is expected that the crystal structure of the Hbp translocation unit will contribute to the knowledge about the mechanism of autotransporter passenger domain translocation across the outer membrane.

Acknowledgments

We would like to thank Jessica Sipkens, Edwin van Bloois and Hugo Groot for their scientific contribution to this project.

Chapter 5

Characterization of an iron-regulated α-enolase of *Bacteroides fragilis*

Robert Sijbrandi, Tanneke Den Blaauwen[1], Jeremy R.H. Tame[2], Bauke Oudega, Joen Luirink and Ben R. Otto

[1] Department of Molecular Cytology, Swammerdam Institute for Life Sciences, University of Amsterdam, Amsterdam, The Netherlands
[2] Protein Design Laboratory, Yokohama City University, Tsurumi, Yokohama, Japan

Published in Microbes and Infection 7 (2005): 9-18

Abstract

This study describes the identification, cloning and molecular characterization of the α-enolase P46 of *Bacteroides fragilis*. The Gram-negative anaerobic bacterium *B. fragilis* is a member of the commensal flora of the human intestine but is also frequently found in severe intra-abdominal infections. Several virulence factors have been described that may be involved in the development of these infections. Many of these virulence factors are upregulated under conditions of iron- or heme-starvation. We found a major protein of 46 kDa (P46) that is upregulated under iron-depleted conditions. This protein was identified as an α-enolase. α-Enolases in several Gram-positive bacteria and eukaryotic cells are located at the cell surface and function as plasminogen-binding proteins. Localization studies demonstrated that P46 is mainly located in the cytoplasm and partly associated with the inner membrane (IM). Under iron-restricted conditions, however, P46 is localized primarily in the IM fraction. Plasminogen-binding to *B. fragilis* cells did occur but was not P46 dependent. A 60-kDa protein was identified as a putative plasminogen-binding protein in *B. fragilis*.

Introduction

Bacteroides fragilis is a Gram-negative obligate anaerobic bacterium of the colon and a common member of the normal human gut flora, but it is also a significant opportunistic pathogen. This bacterium is the most frequently isolated anaerobic species from human intraperitoneal and intra-abdominal infections (Aldridge, 1995; Farthmann and Schöffel, 1998). These types of infection due to an abdominal trauma or surgery are a serious clinical problem, especially when abscesses are formed (Aldridge, 1995; Farthmann and Schöffel, 1998; Hall *et al.*, 1998). Intra-abdominal infections are polymicrobial in nature and especially, *B. fragilis* and *Escherichia coli* are often isolated from the abscesses (Farthmann and Schöffel, 1998; Hall *et al.*, 1998). The molecular mechanism of the pathogenesis in these infections is poorly understood. Bacterial factors include the capsular polysaccharide of *B. fragilis*, which promotes the formation of abscesses to shelter the microorganisms from circulating host defense mechanisms (Tzianabos *et al.*, 1993), the secretion by *B. fragilis* of short-chain fatty acids that inhibit the killing of *E. coli* by neutrophils (Rotstein *et al.*, 1989b) and the secretion of the heme-scavenger protein Hbp by *E. coli*, which makes heme accessible for bacterial growth to both *E.*

coli and *B. fragilis* (Otto *et al.*, 1998; Otto *et al.*, 2002). Nearly all bacterial virulence factors are tightly regulated with their expression linked to various environmental signals. Some parameters that affect virulence factor regulation include temperature, pH, osmolarity, carbon source availability and iron levels (Finlay and Falkow, 1997). In this study, we searched for virulence factors of *B. fragilis* regulated by iron. An iron-regulated α-enolase was found and characterized.

α-Enolase is a cytosolic enzyme that catalyses the conversion of 2-phosphoglycerate into phosphoenolpyruvate. It is therefore essential for the degradation of carbohydrates via glycolysis and other catabolic pathways as well as for glucose synthesis via gluconeogenesis. A remarkable feature of α-enolase is that this enzyme is also part of RNA-degradosomes, multienzyme complexes in the inner membrane (IM) involved in the processing of mRNAs (Carpousis *et al.*, 1994). These degradosomes enable the bacterium to respond efficiently on the dynamic fluctuation of environmental signals.

Interestingly, several α-enolases have been shown to possess plasminogen-binding activity. For plasminogen-binding, α-enolase has to be cell-surface exposed. This unexpected feature has recently been described for several bacterial, fungal, nematode and human α-enolases (Redlitz *et al.*, 1995; Pancholi and Fischetti, 1998; Bergmann *et al.*, 2001; Jolodar *et al.*, 2003; Jong *et al.*, 2003). Conversion of surface-bound plasminogen into plasmin by bacterial or host plasminogen activators changes the bacterium into a proteolytic and invasive organism (Parry *et al.*, 2000; Lähteenmäki *et al.*, 2001). Thus, α-enolase might carry out different functions, depending on its subcellular localization.

Here we report the identification and characterization of the α-enolase P46 of *B. fragilis*. The expression of this protein appeared to be iron-regulated, subcellular redistribution of P46 occurred under iron limitation, and the enzyme did not show plasminogen-binding activity. A 60-kDa outer membrane (OM) protein appeared to be a plasminogen-binding protein in this microorganism.

Materials and methods

Bacterial strains, plasmids and media

The clinical isolate *B. fragilis* BE1 (Verweij-van Vught *et al.*, 1986) was used as a source of chromosomal DNA for cloning and PCR experiments and for functional studies on the P46 α-enolase. *E. coli* TOP10F' (Invitrogen) and the plasmid pACYC184 (Chang and Cohen, 1978) were used in routine cloning

procedures (Sambrook *et al.*, 1989). *E. coli* BL21AI (Invitrogen) and the plasmid pET16b (Studier *et al.*, 1990) were used for subcloning and controlled expression of p46. The *E. coli* strains were routinely grown in Luria–Bertani (LB) medium (Miller, 1992). Appropriate antibiotics were added to the culture medium. *B. fragilis* BE1 was maintained on 5% horse blood agar plates (no. 2 agar; Oxoid) and cultured anaerobically in BM medium (Verweij-van Vught *et al.*, 1986) in the presence of 50 µg/ml kanamycin and 20 µg/ml nalidixic acid (Sigma Chemicals) as the standard medium. Anaerobiosis was achieved using the Anaerogen system from Oxoid. Where indicated, 15 µM hemin, 125 µM 2,2′-bipyridyl or 150 µM Fe(II)SO_4 was added to the culture medium.

General methods

Recombinant DNA techniques were carried out as described (Sambrook *et al.*, 1989). DNA sequencing was carried out using the Big Dye Terminator Cycle sequencing kit on an ABI Prism 310 automated sequencer (Perkin–Elmer). The N-terminal amino acid sequence of proteins was determined by a gas phase sequencer (model 470A; Applied Biosystems), which was coupled to an on-line high-performance chromatograph. Bound antibodies were visualized on immunoblots by chemiluminescence (Roche Molecular Biochemicals). The (relative) intensity of protein bands from both chemoluminescent blots and Coomassie-stained gels were quantified using a FluorS MultiImager with the Multi-Analyst software package (BioRad).

Polyclonal antibodies and reagents

Goat anti-human plasminogen antibodies and human plasminogen used in plasminogen-binding assays were purchased from Haematologic Technologies. Rabbit anti-goat HRP-conjugated antibodies and goat anti-rabbit HRP-conjugated antibodies used for immunodetection were obtained from Santa Cruz Biotechnology and BioRad, respectively. For Western blotting, anti-P46 antiserum raised against purified histidine-tagged P46 (His-P46) was used. Rabbits were injected with a mixture of 50% of native and 50% of denatured His-P46 protein (Agrisera, Sweden). IgG fractions were purified from the anti-P46 antiserum and anti-Hbp antiserum (Otto *et al.*, 2002) by protein A affinity chromatography (Amersham Biosciences). The IgG fractions were conjugated to FluoReporter Oregon Green 488 (Molecular Probes) and used for immunofluorescence microscopy. Anti-P44 antiserum was used to identify a 44-kDa iron-repressible OM protein of *B. fragilis* (Otto *et al.*, 1990). Restriction enzymes, the Expand long template PCR system, Complete EDTA-free

protease inhibitors and the Lumi-light Western blotting substrate were obtained from Roche Molecular Biochemicals. Sigma Chemicals supplied all other chemicals.

Cloning of the α-enolase gene

The coding sequence of p46 was amplified by PCR using chromosomal DNA from *B. fragilis* BE1 as template. The primers used were the Frag46kDa-forward primer 5′-CTAAC**AAGCTT**ATTAATAGTGATTCTTCCGCTTCC-3′, introducing a *Hin*dIII site (boldface letters) 40 bp upstream of the putative promoter of p46 (see Fig. 1) and the Frag46kDa-reverse primer 5′-CGCGC**GGATCC**TAACCTTTTATCA-TGCTATGCTATCATG-3′, introducing a *Bam*HI site (boldface letters). The complete gene, including its own promoter, was cloned into pACYC184 using the created *Hin*dIII and *Bam*HI sites. The plasmid pACYC-46kDa was introduced into *E. coli* TOP10F'.

The T7 expression system was used for IPTG-arabinose-inducible expression of p46 (Studier *et al.*, 1990). The p46 gene was amplified by PCR using the plasmid pACYC-46kDa as template DNA. Primers used were the Bf46kDa-forward primer 5′-ACAAGAGAAA**CATATG**AAAATAGAA-3′, with the *Nde*I restriction site in boldface letters and the Frag46kDa-reverse primer. The p46 gene was cloned into the expression vector pET16b using the created *Nde*I and *Bam*HI sites. This vector allows N-terminal fusion to a cleavable histidine-tagged sequence. Plasmid pET16b-46kDa was introduced into *E. coli* BL21AI for an IPTG- and arabinose-inducible expression of p46. Both plasmids pACYC-46kDa and pET16b-46kDa were sequenced to check for second site mutations.

Purification of the P46 α-enolase

Strain BL21AI(pET16b-46kDa) over-expressing the N-terminal 10His-tagged P46, was cultivated in 4 L of LB-medium for the isolation of P46. Cells were induced with 1 mM IPTG and 0.2% arabinose for 1 h at an OD_{660} of 0.3. The cells were harvested, resuspended in a phosphate-buffered saline solution (PBS), containing 500 mM NaCl, 50 mM imidazole and protease inhibitors and lyzed using a French pressure cell. The obtained cell lysate was loaded on a Ni^{2+}-charged HiTrap chelating column (Amersham Biosciences), washed at 100 mM imidazole and eluted in reverse flow using a gradient to 250 mM imidazole. Peak fractions were pooled and concentrated to 3.5 mg/ml with a centrifugal concentrator. Glycerol was added to 8% (v/v) before storage at minus 80 °C.

Subcellular localization of α-enolase in B. fragilis

To determine the location of P46 in *B. fragilis*, cells were fractionated into their subcellular compartments by using sucrose density centrifugation techniques (Kotarski and Salyers, 1984; Otto *et al.*, 1988). The advantages of this separation procedure are the high yields and purity of the different fractions and the absence of detergents. Cell lysates were obtained from iron-restricted and iron-unrestricted cultures (1200 OD_{660} units) by passing the cells through a 23-gauge needle and a French pressure cell. The cell lysate was loaded onto two-step gradients of 70% and 37% of sucrose and centrifuged at 140,000 × *g* for 1 h. The upper fraction including the 10–37% interface was collected and run on a 37% sucrose cushion. The fraction above the cushion contains an enrichment of IM and soluble proteins. Membranes and soluble proteins were separated from each other by ultracentrifugation at 270,000 × *g* for 5 h. The IM-enrichment fraction was then loaded onto a 30–60% sucrose step gradient and centrifuged at 140,000 × *g* for 16 h to purify the IM. The buoyant densities of the fractions were calculated from the refractive index by refractometry. IM were found at a buoyant density of 1.14 g/cm^3. Material in the 37% and 70% fraction of the first two-step gradients was pelleted into a 57% sucrose cushion to obtain an enrichment of OM. The OM-enrichment fraction was loaded on a 40–70% sucrose step gradient and centrifuged at 140,000 × *g* for 16 h to purify the OM. OM proteins fractionated at a buoyant density of 1.22 g/cm^3. Fractions of interest were pooled, diluted 1:1 with PBS and centrifuged at 270,000 × *g* for 5 h. The membrane pellets were resuspended in 40% sucrose in PBS and stored at –80 °C. To separate integral IM proteins from peripheral ones, purified IM vesicles were treated with 0.18 M Na_2CO_3 (pH 11.3) for 15 min on ice. The membrane fractions containing integral membrane proteins were collected by ultracentrifugation (10 min, 115,000 × *g*). The pellet and supernatant fractions contained the integral and peripheral IM proteins, respectively.

α-Enolase activity

For the measurement of α-enolase activity, a direct enzyme assay was used, as described (Pancholi and Fischetti, 1998). The assay was carried out at 37 °C in 1 ml reaction buffer, 5 µg of purified His-P46 or P46, from which the histidine tag had been cleaved off, and concentrations of 2-PGE from 0 to 6.0 mM were used. The absorbance at 240 nm was recorded at 11-s intervals for 198 s. The initial rates of conversion were calculated from the resulting curves, using the extinction coefficient for phosphoenolpyruvate (PEP) as calculated by Pancholi and Fischetti (ε_m = 1164 per M (Pancholi and Fischetti, 1998)). The kinetic determinants K_M and V_{max} were

estimated from the curve obtained by fitting the datapoints to the equation $V = V_{max}S/(S + K_M)$ using the program KaleidaGraph (Synergy Software).

Immunofluorescence microscopy

Experiments were carried out essentially as described (den Blaauwen *et al.*, 2003), with the following modifications. IgG fractions from anti-P46 and control anti-Hbp antisera were conjugated to FluoReporter Oregon Green 488 (Molecular Probes). The intracellular pool of P46 was visualized by permeabilization of the cells prior to antibody incubation. The cells were permeabilized by treatment with 0.1% Triton X-100 in PBS for 45 min at room temperature, washing three times with PBS and subsequent treatment with 400 µg/ml lysozyme and 5 mM EDTA in PBS for 45 min at room temperature. Untreated cells were used to detect P46 localized at the cell surface. Incubation with the conjugated antibodies was overnight instead of 60 min. After washing, the cells were resuspended in PBS for microscopic analysis.

Identification of plasminogen-binding proteins

A blot overlay assay (Bergmann *et al.*, 2001) and an enzyme-linked immunosorbant assay (ELISA) (Konieczny *et al.*, 2000) were used to identify plasminogen-binding proteins of *B. fragilis*. For the blot overlay assay, equal amounts of protein from several subcellular fractions were separated on an 11% SDS-polyacrylamide gel and blotted electrophoretically onto PVDF membrane (Immobilon-P, Millipore). The membranes were blocked with 4% skimmed milk powder in PBS for 30 min before the binding reaction. The blots were incubated with human plasminogen (1 µg/ml) for 2 h, washed with PBS and then incubated with anti-human plasminogen for 2 h. After washing, the blots were probed with rabbit anti-goat HRP-conjugated antibody (Santa Cruz Biotechnology) for 1 h. The probed blots were washed two times with PBS, incubated with Lumilight substrate and exposed to Kodak X-Omat AR film. Afterwards, the blot was stained with Coomassie Brilliant Blue to identify the bands visualized on film. An ELISA was carried out to detect surface-exposed plasminogen-binding proteins of *B. fragilis*. Serial dilutions of iron-restricted and iron-unrestricted BE1 cells (initial OD_{660}-units of 0.088) were coated to the wells of a microtiter plate. After coating of the cells, 4% skimmed milk powder in PBS containing 0.07% Tween 80 was applied to block unbound places. Plasminogen (1 µg/ml) was added to the wells, the cells were washed after 2 h of incubation, and the amount of cell-bound plasminogen was measured using an anti-plasminogen antibody. Absorbance at 450 nm was measured in a FLUOstar Galaxy (BMG Labtechnologies) plate reader and plotted in a graph.

Genbank accession numbers

The obtained sequences of *p46* and *p60* were deposited in the EMBL/GenBank nucleotide database under accession number AJ495857 and AJ786264, respectively.

Results

The P46 protein is iron-regulated

B. fragilis upregulates the production of several proteins in the cell in response to the iron-restricted conditions imposed by the host (Otto *et al.*, 1990). These iron-regulated proteins may be involved in the pathogenesis of an intra-abdominal infection by *B. fragilis*. SDS-PAGE protein profiles from cells grown under iron-depleted and normal conditions were compared. A prominent protein band with an approximate molecular mass of 46,000 was discovered under iron-depleted conditions.

The iron-regulated expression of P46 was assayed with *B. fragilis* BE1 cells cultured under different iron-restricted conditions. Hemin or iron(II)sulfate were added to standard BM2-medium as additional sources of heme and excess of iron, while the iron-chelator 2,2′-bipyridyl was used to achieve iron-depleted conditions (Otto *et al.*, 1988; Otto *et al.*, 1994). Total cell lysates were subjected to SDS-PAGE, and the expression levels of P46 were visualized by Coomassie staining and immunoblotting with specific anti-P46 antiserum (Fig. 1). As shown in lane 3 of Fig. 1, depletion of iron from the medium increased the levels of P46 by two- to threefold. Addition of iron(II)sulfate to the iron-depleted medium completely reversed this effect (Fig. 1; lane 4), which was not the case with the addition of equal concentrations of Cu-, Mg-, Mn- or $ZnSO_4$ (data not shown). Addition of extra hemin or iron to the iron-unrestricted medium did not completely abolish the expression of the P46 protein (Fig. 1, lane 2 and 5). Depletion of heme from the standard medium also resulted in two- to threefold increased levels of P46 (data not shown).

Similar growth and expression experiments were carried out with *E. coli* TOP10F'(pACYC-46kDa) harboring cloned p46 under control of its own promoter (see below). Although expression levels were low compared to *B. fragilis*, the same upregulation of P46 expression was observed under iron-depleted conditions (data not shown).

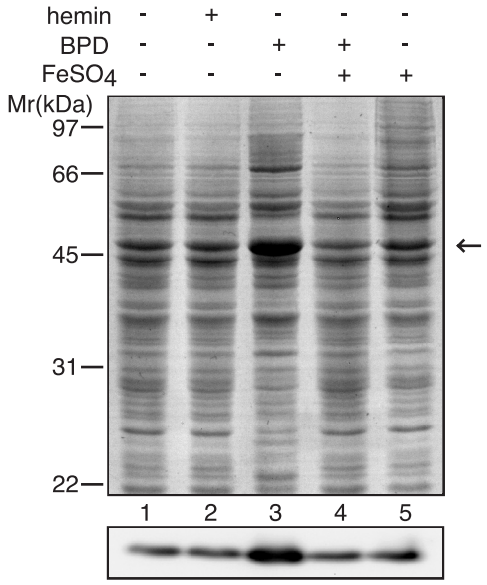

Fig. 1. Iron-regulated expression of P46. SDS-PAGE profile (top) and Western blot analysis (bottom) of cell lysates from *B. fragilis* BE1 cells. Cells were grown in the presence or absence of 15 μM hemin, 125 μM bipyridyl (BPD) and/or 150 μM $FeSO_4$, as indicated. The arrow indicates the position of P46 in the Coomassie-stained gel. Anti-P46 antibodies were used for the detection P46.

In previous studies (Otto *et al.*, 1988), we characterized a 44-kDa iron-repressible OM protein. This molecule is probably part of a heme-binding protein complex in the OM of *B. fragilis* (Otto *et al.*, 1990; Otto *et al.*, 1994). Immunoblot experiments with P46 and P44 antisera (Otto *et al.*, 1990) showed that these two iron-repressible proteins co-migrate more or less at the same position in SDS-PAGE and can only be distinguished from each other using specific antisera. P46 is present in both iron-depleted and control cells, while P44 is exclusively expressed under iron-restricted conditions (data not shown). Surprisingly, P44 appears to have a slightly higher molecular weight than P46 in the immunoblot assay. Another important difference between the two molecules is that P44 is an OM protein (Otto *et al.*, 1988), whereas P46 is not (see below).

The molecular characterization of P46

Analysis of the P46 protein revealed the NH_2-terminal amino acid sequence MKIEKITGGEILD. A protein versus translated DNA BLAST in the *B. fragilis* shotgun reads database (http://www.sanger.ac.uk/Projects/B_fragilis/) resulted in a 92% confidentiality hit (MKIEKITGREILD). The open reading frame (ORF) found encodes a putative 426-amino acid protein with a deduced monomer molecular weight of 46.4 kDa. A protein BLAST search with the putative protein sequence in the NCBI

sequence database (http://www.ncbi.nlm.nih.gov/BLAST/) revealed a significant homology to bacterial α-enolases, a family of proteins involved in carbohydrate transport and metabolism. The identity between the putative *B. fragilis* protein and the α-enolase from the closely related *Bacteroides thetaiotaomicron* was 93% and with the Gram-positive *Staphylococcus aureus* α-enolase 72%. An NCBI Conserved Domain Search revealed a 97% alignment with α-enolase conserved domains. These results indicated that P46 is most likely an α-enolase.

The nucleotide sequence up- and downstream of the p46 gene was further analyzed (Fig. 2). In total, five ORFs were detected, which encode putative proteins larger than 100 amino acids, all in the same direction as the α-enolase gene. The predicted products of these ORFs were subjected to a protein BLAST search. An ORF located directly upstream of the α-enolase gene encodes a putative 221-amino

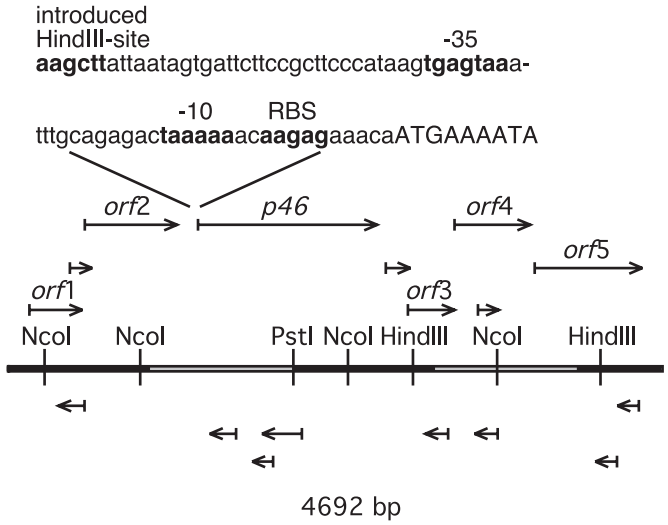

Fig. 2. Organization of ORFs of the 4692-bp contig. Part of the *B. fragilis* chromosome is indicated in a linear fashion. The positions of several *Hin*dIII, *Nco*I and *Pst*I sites are indicated. Arrows in all six frames indicate the ORFs. The *p46* gene encodes an α-enolase. The putative promoter and Shine-Dalgarno sequences and start codon of *p46* are depicted above the diagram. The ORFs in the same direction as *p46* and longer than 200 bp are numbered. The *orf1* gene encodes a CrcB-like protein, the *orf2* product belongs to the pentapeptide repeat protein and/or acetyltransferase family, and *orf5* encodes a putative glycosyltransferase. No homologues were found for ORF 3 and 4. The sequence data of this contig can be found in the database of The Welcome Trust Sanger Institute (http://www.sanger.ac.uk).

acid protein with significant homology to the quinolone-resistance protein, Qnr (Tran and Jacoby, 2002). This putative protein belongs to the pentapeptide repeat protein family and/or acetyltransferase family. Further upstream, an ORF was found encoding a putative 127-amino acid protein with homology to an integral membrane protein that belongs to the CrcB protein family. This protein, which has been reported to be involved in chromosome condensation and overexpression in *E. coli*, leads to camphor resistance (Hu *et al.*, 1996). Downstream of the p46 gene, are situated two ORFs which encode putative proteins without significant homology to known proteins. Further downstream is an ORF possibly encoding a 258-amino acid glycosyltransferase with significant homology to ArnC. This protein has also been shown to be necessary for polymyxin resistance in *Salmonella typhimurium* (Gunn *et al.*, 1998).

Analysis of the DNA sequence directly in front of the α-enolase gene revealed a putative promoter sequence and Shine–Dalgarno sequence that could potentially function as transcription and translation signals (Fig. 2). The p46 gene was cloned and expressed in *E. coli* for further investigations, and the cloned gene was sequenced to check for second site mutations. Minor differences found between the nucleotide sequences of p46 and the α-enolase of *B. fragilis* NCTC9343 (http://www.sanger.ac.uk/Projects/B_fragilis/) did not result in amino acid differences.

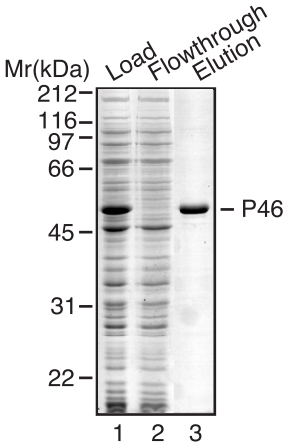

Fig. 3. Purification of His-tagged P46. *E. coli* BL21AI(pET16b-46kDa) was used to overexpress the histidine-tagged α-enolase. His-P46 was purified from the lysate of these cells by affinity chromatography using a Ni^{2+}-charged chelating column. Samples from the total cell lysate (lane 1), flow through fraction (lane 2) and eluted fractions (lane 3) were subjected to SDS-PAGE and Coomassie staining. The position of His-tagged P46 in the gel is indicated on the right. The amount of purified protein obtained from 1 L culture was circa 6.5 mg.

α-Enolase activity of P46

The sequence of the P46 protein reveals similarity with known α-enolases. A direct enzyme assay was used to analyze the expected activity (Pancholi and Fischetti, 1998). P46 was purified to homogeneity by affinity chromatography (Fig. 3). For this purpose a histidine tag was introduced at the N terminus of the molecule. Due to the introduction of the histidine tag, P46 migrated at an apparent molecular weight of ±49 instead of ±46 kDa in SDS-PAGE. The results of the enzyme reaction rates were analyzed in Michaelis–Menten plots and fitted to the equation $V = V_{max}S/(S + K_M)$ (Fig. 4). A Michaelis–Menten coefficient (K_M) of 2.1 × 10^{-4} M and a V_{max} of 42 mM/min per mg were calculated. Similar results were obtained with P46 without a His-tag. The obtained values are in agreement with those found for other α-enolases (Kitamura *et al.*, 2004).

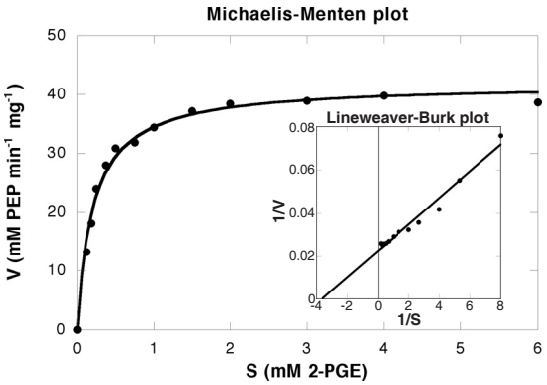

Fig. 4. α-Enolase activity of P46. Enzyme kinetics of purified His-P46. Activity was determined according to the direct enzyme assay (Pancholi and Fischetti, 1998). The conversion-rate (*V*) of 2-PGE (*S*) to PEP was measured at 240 nm using 5 µg of P46 and various concentrations of 2-PGE (0–6.0 mM). Measurements were performed for 3 min, but only the initial reaction rates were used for calculation. Data from two independent experiments were plotted by the method of Michaelis–Menten and fitted to the equation $V = V_{max} \cdot S/(S + K_M)$. This fit yielded the kinetic parameters K_M = 2.1 × 10^{-4} M and V_{max} = 4.2 × 10^{-2} M/min per·mg.

P46 is not cell-surface exposed

α-Enolases are generally known as cytosolic enzymes. However, several studies have indicated a cell-surface localization for α-enolases of both prokaryotic and eukaryotic origin despite the lack of a cleavable signal sequence (Redlitz *et al.*, 1995; Bergman *et al.*, 1997; Pancholi and Fischetti, 1998; Bergmann *et al.*, 2001).

P46 also lacks a cleavable signal sequence. Immunodetection of P46 on intact cells of *B. fragilis* by immunofluorescence microscopy was carried out to assess the possible surface localization of P46.

IgG fractions from anti-P46 antiserum were covalently linked to a fluorescent label and used as a probe for the detection of putative cell-surface-localized P46. Permeabilization of cells with the detergent Triton X-100 made the intracellular pool of α-enolase accessible to the fluorescently labeled antibody (Fig. 5). The iron-depleted cells that were not permeabilized showed a very weak fluorescence signal in the immunofluorescence microscopy experiments. The fluorescence signal of the iron-depleted cells was slightly higher than in control cells. Notably, the extent of the

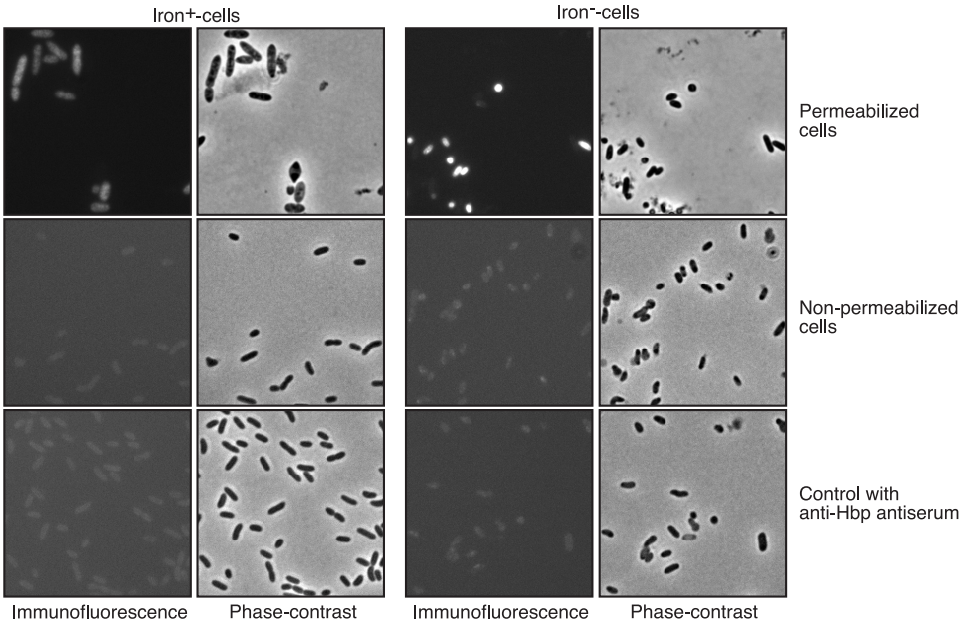

Fig. 5. Immunofluorescence microscopy of *B. fragilis* cells. Iron-restricted and iron-unrestricted BE1 cells were fixed with formaldehyde and glutaraldehyde immediately after culturing. To visualize intracellular P46, cells were permeabilized with Triton X-100, lysozyme and EDTA prior to immunolabeling (top panels). Non-permeabilized cells were used to detect P46 on the cell surface (middle panels). To measure background binding of fluorescent antibody to the cells, a non-related antiserum (anti-Hbp) was used in an equal concentration and degree of labeling of the fluorescent probe (lower panels). The brightness of the immunofluorescence pictures of non-permeabilized cells was enhanced with respect to the permeabilized cells.

fluorescence signal did not exceed the background signal elicited by a non-related fluorescently labeled antibody. In contrast, the permeabilized cells showed high levels of fluorescence over the entire cross-section of the cells, suggesting P46 is located intracellularly and can only be accessed upon permeabilization. The amount of internal P46 was significantly higher in the iron-depleted cells than in the control cells (Fig. 5), confirming the iron-repressible expression of P46. In conclusion, these results, plus the finding that P46 is not present in the OM of *B. fragilis* (see below), indicated that P46 is not cell-surface localized in *B. fragilis*.

Redistribution of the subcellular localization of P46 under iron-restricted conditions

To determine where P46 is localized in the cell, the subcellular distribution of this protein in *B. fragilis* was analyzed using cells that were grown under conditions of excess hemin or iron limitation. IM and OM were separated by sucrose gradient centrifugation. The cytoplasmic marker enzymes lactate dehydrogenase (LDH) and glucose-6-phosphate dehydrogenase (G6PDH) were used to measure the possible contamination of the membrane fractions with cytoplasmic proteins. The purified IM and OM fractions were hardly contaminated by cytoplasmic proteins (6% and 2.5%, respectively). All fractions were analyzed by SDS-PAGE followed by protein staining or Western blotting using P46 antiserum. The P46 protein was clearly present in the IM fractions and in the cytoplasm of iron-depleted and iron-unrestricted cells and is almost absent in the OM fractions of these cells (Fig. 6A; lanes 3, 4, 7 and 8). The trace amount of P46 found in the OM is most likely due to contamination of the purified membranes with cytosolic P46, as it does not exceed this contamination (Fig. 6A; lanes 4 and 8). Together, these results strongly suggested that P46 is located in the cytoplasm and IM but not in the OM. The iron-depleted cells contained twice the amount of P46 detected in control cells (Fig. 6A; lanes 1 and 5). Furthermore, the P44 iron-regulated OM protein is clearly visible in the OM fraction from iron-depleted cells in the Coomassie-stained gel (Fig. 6A, lane 8). Strikingly, under iron-limited conditions, a redistribution of P46 to the IM fraction occurred (Fig. 6B). A comparable ratio of P46 (±40%) is detected in the soluble and IM fractions of control cells. In contrast, iron-depleted cells contained proportionally more P46 in the IM (64%) than in the soluble fraction (26%). To determine whether P46 is an integral or peripheral IM protein, IM vesicles were subjected to Na_2CO_3 extraction. Peripheral IM proteins are removed from the membrane by Na_2CO_3

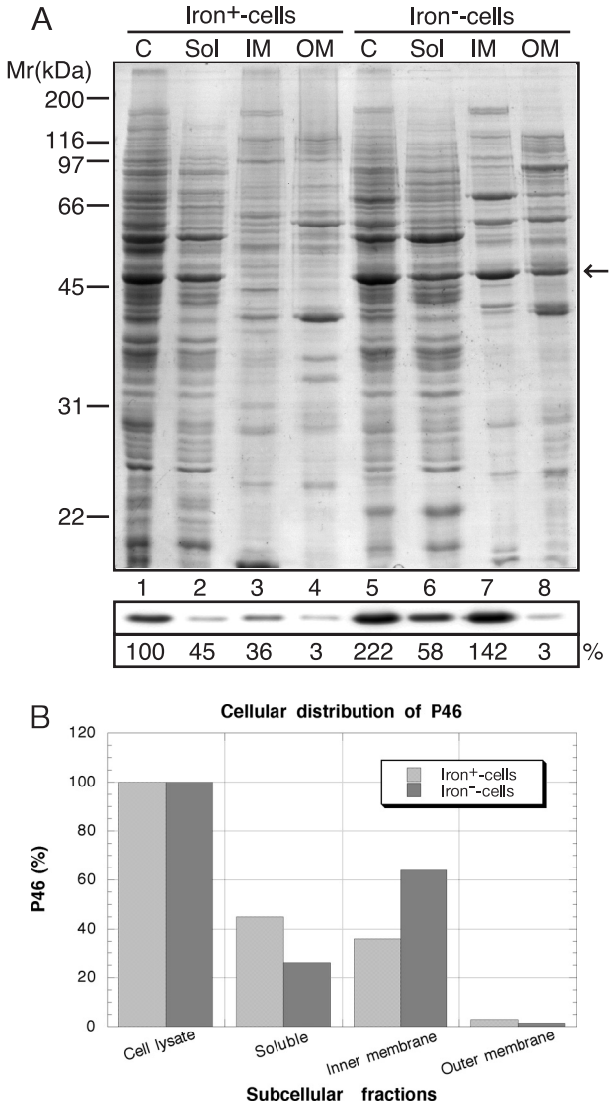

Fig. 6. Subcellular localization of P46. A, SDS-PAGE profile (top) and Western blot analysis (bottom) of the different cellular fractions of strain BE1. Cells were grown in the presence of 15 μM hemin ($Iron^+$ cells) or 125 μM bipyridyl ($Iron^-$ cells). Membrane fractions were isolated using sucrose gradients as described in Section 2. Equal amounts of protein were loaded in each lane. C: cell lysate, S: soluble protein, IM: inner membrane fraction, OM: outer membrane fraction. Anti-P46 antibodies were used as probe in the blotting experiments. The arrow indicates the position of P46 in the Coomassie-stained gel. For the quantification of the relative amounts of P46 in the different cellular compartments, the detected amount of P46 in cell lysate from iron-unrestricted cells was set at 100%. B, the cellular distribution of P46 in iron-restricted and -unrestricted cells. The distribution of P46 in the cell was quantified by setting both the amounts of P46 in the lysates from iron-restricted and -unrestricted cells at 100%.

treatment, in contrast to integral IM proteins. Ultracentrifugation of the Na_2CO_3-treated membrane vesicles separate the released proteins from the pelleted membranes. P46 was only found back in the supernatant, indicating that P46 is not an integral IM protein (data not shown).

Plasminogen-binding to intact B. fragilis cells and OM proteins

Recent studies have suggested that α-enolases from eukaryotic and prokaryotic cells possess plasminogen-binding activity (Redlitz *et al.*, 1995; Bergman *et al.*, 1997; Pancholi and Fischetti, 1998; Bergmann *et al.*, 2001). Plasminogen binds to surface-exposed α-enolase and is subsequently activated to plasmin by host or bacterial activators. Specific plasminogen-binding motifs have been characterized in α-enolases (Pancholi and Fischetti, 1998; Bergmann *et al.*, 2001; Bergmann *et al.*, 2003; Derbise *et al.*, 2004). The P46 α-enolase of *B. fragilis* is very likely not cell-surface localized (see above), and analysis of the primary structure of this molecule did not reveal any plasminogen-binding motif. In particular, P46 does not possess a C-terminal lysine residue. Thus, P46 is probably not a plasminogen-binding protein. Regardless of this fact, *B. fragilis* cells were tested for their ability to bind plasminogen.

B. fragilis cells were grown under iron-restricted and iron-unrestricted conditions. Serial dilutions of the cells were coated onto a microtiter plate. After incubation with human plasminogen (1 µg/ml), the amount of bound plasminogen was measured using an anti-plasminogen antibody. The *B. fragilis* cells showed a dose-dependent plasminogen-binding activity (Fig. 7A). The plasminogen-binding activity was similar for both normal and iron-depleted cells, indicating that the synthesis of the plasminogen receptor is not iron-regulated.

A blot overlay assay was used to identify possible candidates responsible for the interaction with human plasminogen. Subcellular fractions from *B. fragilis* cells grown under normal or iron-depleted conditions were subjected to SDS-PAGE, electroblotted to PVDF membranes, which were subsequently incubated with plasminogen (1 µg/ml), and probed with anti-plasminogen antibodies to identify bound plasminogen (Fig. 7B). Interaction of plasminogen with an OM protein of circa 60 kDa was observed (Fig. 7B; lanes 4 and 5). The expression of this 60-kDa protein is not iron-regulated. Weaker plasminogen-interacting OM protein bands of 50 kDa and a double protein band of circa 40 kDa were detected in this blot overlay assay. The expression of the 40-kDa protein seemed to be iron-regulated (Fig. 7B; lanes 4 and 5). Purified P46 protein did not show any interaction with plasminogen in this

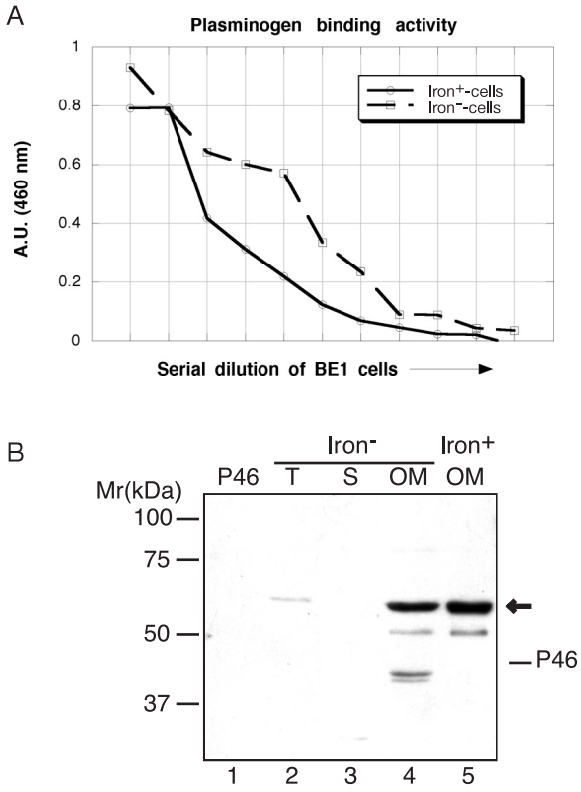

Fig. 7. Plasminogen-binding activity. A, plasminogen-binding by intact BE1 cells. Twofold serial dilutions of iron-restricted cells (dashed line) and of iron-unrestricted cells (solid line) were coated onto a microtiter plate and incubated with plasminogen (1 µg/ml). Cell-bound plasminogen was detected with anti-plasminogen antibodies. Each value is a mean of triplicates. B, immunodetection of plasminogen-binding activity by *B. fragilis* OM proteins. Plasminogen-binding to *B. fragilis* cellular fractions and purified P46 (1 µg) was assayed using a blot overlay assay. Total cell lysate (T), the soluble fraction (S) and outer membranes (OM) isolated from cells grown under different iron conditions were subjected to SDS-PAGE and electroblotted onto PVDF membrane. The membrane was incubated with plasminogen. Bound plasminogen was probed with anti-plasminogen antiserum and visualized by chemoluminescence. Afterwards the blot was stained with Coomassie to visualize the protein bands and the position of P46. The positions on the blot of P46 and the plasminogen-binding OM protein (arrow) are indicated.

assay. The prominent protein band of 60 kDa was treated with trypsin and analyzed by mass spectrometry. Analysis of the observed peptide masses revealed an OM protein with homology to proteins with unknown function in related organisms. In conclusion, *B. fragilis* cells are able to bind plasminogen. This plasminogen-binding activity is not P46 dependent but likely dependent on a 60-kDa OM protein.

Discussion

This study showed that the *B. fragilis* α-enolase P46 is upregulated and intracellularly redistributed under iron- and heme-limited conditions. The enzyme has a monomer molecular weight of 46 kDa, contains α-enolase-conserved domains and shows enzyme kinetics similar to those of other α-enolases (Kitamura *et al.*, 2004). The iron-regulated expression of the α-enolase is probably important under conditions of infection. Depending on its subcellular localization, α-enolase carries out different functions. It might be involved in cell-surface plasminogen-binding or in proper RNA processing and decay in the IM (Liou *et al.*, 2001), or in the cytoplasm, it might be necessary for sufficient ATP production under iron-restricted conditions (Heithoff *et al.*, 1997).

In Gram-positive bacteria and eukaryotic cells, α-enolase may act as a cell-surface receptor for plasminogen (Redlitz *et al.*, 1995; Pancholi and Fischetti, 1998; Bergmann *et al.*, 2001; Jolodar *et al.*, 2003; Jong *et al.*, 2003; Derbise *et al.*, 2004). Bound plasminogen is converted into the protease plasmin by host or bacterial plasminogen activators, allowing bacteria to acquire surface-associated proteolytic activity (Lähteenmäki *et al.*, 2001). To assess the possible surface exposure of P46, immunofluorescence microscopy and subcellular localization experiments were carried out. The results of these experiments clearly showed that P46 is not present in the OM or at the cell surface. In addition, P46 did not show any plasminogen-binding activity, which is consistent with the lack of plasminogen-binding motifs in this molecule. The consensus motif FYDKERKVYD and C-terminal lysine residues in α-enolases are crucial for plasminogen-binding activity (Pancholi and Fischetti, 1998; Bergmann *et al.*, 2001; Bergmann *et al.*, 2003; Derbise *et al.*, 2004). Screening of bacterial α-enolases on the presence of these motifs revealed that none of the known α-enolases from Gram-negative bacteria contains such motifs. Thus, it seems that the surface expression of plasminogen-binding α-enolase is restricted to Gram-positive bacteria.

In *E. coli*, α-enolase is part of RNA-degradosomes, multicomponent IM complexes involved in RNA processing and decay (Carpousis *et al.*, 1994). Degradosomes consist of α-enolase, a polyphosphate kinase, the endonuclease RNase E, a polynucleotide phosphorylase and helicase RhlB. The degradosomes are associated with the cytoplasmic membrane via the N-terminal region of RNase E (Liou *et al.*, 2001). α-Enolase binds to a specific region of the cytoplasmic membrane-bound RNase E molecule. However, significant amounts of α-enolase and other proteins of the multienzyme complex remain separated from the

membrane. We showed that P46 is not cell-surface exposed nor present in the OM. The next step in our study was to determine whether P46 might be located in the IM of *B. fragilis*. We found that P46 is located both in the cytoplasm and in the IM of *B. fragilis*. Remarkably, under iron-limited conditions, P46 is mainly present in the IM. This is the first evidence that the subcellular location of α-enolase varies, depending on the amount of available iron. The nature of the interaction between the IM and P46 is not known. It is tempting to speculate that the subcellular redistribution of P46 is due to an interaction between an IM-bound RNase E and P46 and that IM-associated P46 is part of RNA-degradosomes, especially under iron-limited conditions.

The higher expression of P46 under iron-limited conditions could also be necessary for sufficient ATP production. In *B. fragilis*, the maximum energy from glucose is obtained under heme-unrestricted conditions. At low concentrations of heme *in vivo*, glycolysis and the lactate and malate metabolism are the only sources of ATP (Macy *et al.*, 1978; Chen and Wolin, 1981). In an abscess, lactate may be the predominant carbon and energy source and glucose may be limiting. To compensate to some extent for the lower gain of energy from glucose, a higher expression of α-enolase could be a way to generate sufficient ATP.

We demonstrated that the expression of P46 is iron-regulated. Iron-regulated genes are often preceded by a Fur-box sequence to which the regulatory Fur protein can bind (Baichoo and Helmann, 2002). The Fur-binding site overlaps the promoters of iron-regulated genes. Iron acts as a corepressor with Fur at sufficient concentrations of iron. The active Fur-iron complex binds to the Fur-binding site and prevents transcription. No sequence related to a consensus Fur-box sequence was detected in the promoter region of *p46*. Additionally, the expression of P46 under its own promoter is iron-regulated in both *B. fragilis* and *E. coli*. However, a complete repression of P46 was not possible under high iron conditions, which is consistent with the essential role of α-enolase in glycolysis. These results suggest that the expression of P46 is Fur independent.

This study showed that *B. fragilis* cells bound plasminogen to their surface. An OM protein of 60 kDa (P60) binds plasminogen in a blot overlay assay and is likely responsible for the plasminogen-binding activity of the *B. fragilis* cells. Analysis of the primary structure of this molecule reveals a signal-peptide sequence containing a motif for lipid attachment. This suggests that P60 is likely a membrane lipoprotein. Furthermore, P60 does possess a C-terminal lysine residue. However, P60 lacks a plasminogen-binding consensus motif, as described for Gram-positive bacteria.

In summary, we have shown that the *B. fragilis* α-enolase P46 is upregulated and intracellularly redistributed under iron- and heme-limited conditions. This mechanism is probably essential to survive at the site of an infection, because it guarantees an efficient ATP production and a dynamic regulation of the processing and decay of mRNAs under stressful conditions. The plasminogen-binding activity by *B. fragilis* cells is not P46 dependent but highly likely depends on a 60-kDa OM protein. Further studies will be directed at the characterization of this 60-kDa protein and the nature of the interaction between the IM and P46.

Acknowledgments

The authors would like to thank M.E.G. Aarsman for technical assistance with the immunofluorescence microscopy experiments and R.C. van der Schors for the mass spectrometry analysis.

Abbreviations

The abbreviations used are: IM, inner membrane; OM, outer membrane; ORF, open reading frame.

Chapter 6

Cloning and preliminary characterization of Pbp, a putative plasminogen binding lipoprotein of *Bacteroides fragilis*

Abstract

The cloning and preliminary characterization of a possible plasminogen-binding protein (Pbp) of *Bacteriodes fragilis* is described. The Gram-negative anaerobic bacterium *B. fragilis* is a member of the commensal flora of the human intestine, but is also frequently found in severe intra-abdominal infections. Several *B. fragilis* virulence factors have been described that may be involved in the development of these infections. A *B. fragilis* protein of circa 60 kDa was identified as a putative plasminogen-binding protein. The corresponding gene was now cloned, its sequence was analyzed using various computer programs and the subcellular localization of the protein (Pbp) was investigated. Pbp was found in the outer membrane fraction of *B. fragilis* cells and also in outer membranes of *E. coli* cells expressing the protein. Protease accessibility studies gave the first indications for a cell-surface location of the protein. In overlay experiments Pbp was able to bind plasminogen, but C-terminally His-tagged Pbp did not. Primary sequence analysis suggested that Pbp is a lipoprotein. Pbp-like proteins were also found in various other *Bacteroides* strains and clinical isolates. The role of this potential *B. fragilis* virulence factor in pathogenicity is discussed.

Introduction

B. fragilis is a Gram-negative anaerobic bacterium that is a member of the commensal gut flora in humans. However, it can be an important opportunistic pathogen that is frequently isolated from human intra-abdominal infections (Aldridge, 1995; Farthmann and Schöffel, 1998). These infections are a common complication of invasive surgery or the result of abdominal trauma in which the gut microflora enters the abdominal cavity (Hall *et al.*, 1998). In these infections, persistent abscesses are often formed which leak pathogenic bacteria into the general circulation, resulting in septic shock and multi-organ failure. It is frequently found that pathogenic *E. coli* and *B. fragilis* occur together in these abscesses, the combination surviving better than either species alone. These polymicrobial abscesses are usually difficult to treat with antimicrobial therapy and pose a serious clinical problem. The molecular mechanism underlying the pathogenesis of these infections and the way in which formation of abscesses is initiated is only partially understood. Several putative virulence factors involved in peritonitis have been described. These include the capsular polysaccharide of *B. fragilis*, a secreted hemoglobin protease by *E. coli* and

secreted short-chain fatty acids and hemolysins of *B. fragilis*. The capsular polysaccharide of *B. fragilis* promotes the formation of fibrin clots by the host (Tzianabos *et al.*, 1993), providing an environment where the bacteria are protected against circulating factors from the immune system. *E. coli* cells involved in peritonitis often secrete a hemoglobin protease (Hbp) that is capable of degrading hemoglobin. This protein can also bind the released heme from hemoglobin, which is then delivered to both *E. coli* and *B. fragilis*, facilitating their growth (Otto *et al.*, 1998; Otto *et al.*, 2002). The secretion of short-chain fatty acids by *B. fragilis* inhibits killing by neutrophils (Rotstein *et al.*, 1989b). In *B. fragilis* as many as nine functional hemolysin homologues have been found (E.R. Rocha and C.J. Smith, unpublished observations). In addition, *B. fragilis* displays hemolytic activity in an iron-regulated manner (B.R. Otto, unpublished observations).

Plasminogen-binding to the bacterial cell surface may also contribute to the pathogenesis of peritonitis. Plasminogen-binding properties have recently been described for a range of bacterial species. Conversion of surface-bound plasminogen to plasmin changes the bacterium into a proteolytic organism capable of degrading fibrin and extracellular matrix proteins (Parry *et al.*, 2000; Lähteenmäki *et al.*, 2001). Binding of plasminogen to the cell surface could therefore be an important virulence factor involved in pathogenic synergy in intra-abdominal infections. Several bacterial cell-surface receptors for plasminogen have been identified. In Gram-positive bacteria, α-enolase is often present on the cell surface as a plasminogen-binding protein (Pancholi and Fischetti, 1998; Bergmann *et al.*, 2001). However, we have recently shown that in *B. fragilis* α-enolase is only present intracellularly and does not possess plasminogen-binding capability (Sijbrandi *et al.*, 2005). There are only a few reports describing plasminogen-binding proteins in Gram-negative bacteria. In *Borrelia burgdorferi*, a 70 kDa plasminogen-binding protein has been isolated (Hu *et al.*, 1997), and in *Helicobacter pylori*, two homologous cell-surface proteins were characterized that could bind plasminogen: PgbA (50 kDa) and PgbB (60 kDa) (Jonsson *et al.*, 2004).

It has been reported recently that *B. fragilis* cells possess plasminogen-binding activity. In an overlay assay, a 60 kDa protein was identified as a possible plasminogen-binding protein (Sijbrandi *et al.*, 2005). In this study, the 60 kDa protein, referred to as Pbp for Plasminogen-binding protein, was further investigated. The *pbp* gene was cloned and sequenced, the subcellular location of the *pbp* gene product was studied, and its plasminogen-binding property was confirmed in an overlay assay using (semi) denatured proteins. In addition, indications were obtained that in other *Bacteriodes* subspecies Pbp-like proteins are present.

Materials and methods

Bacterial strains, plasmids and media

Clinical isolates of 26 different strains of *Bacteroides* subspecies, all isolated from extra-intestinal infections, were used in this study. All strains, except *B. fragilis* ATCC23745, were isolated from hospitalized patients in The Netherlands and identified with a BBL Minitek Numerical Identification System (Becton Dickinson). The three *B. fragilis* strains were designated BE1, BE4 and BE12. The two *B. vulgatus* strains were designated BE18 and BE20. The nine *B. distasonis* strains were designated BE2, BE4, BE5, BE14, BE16, BE17, BE50, BE62 and BE66. The four *B. thetaiotaomicron* strains were designated BE22, BE33, BE34 and BE46. The seven *B. ovatus* strains were designated BE10, BE15, BE20, BE35, BE48, BE60 and BE74. The *B. fragilis* strain ATCC23745 was obtained from the American Type Culture Collection and has been isolated from a pleural infection.

The clinical isolate *B. fragilis* BE1 (Verweij-van Vught *et al.*, 1986) was used as a source of chromosomal DNA for cloning, PCR experiments and for functional studies on Pbp. The *Escherichia coli* strain TOP10F' (Invitrogen) and the plasmid pACYC184 (Chang and Cohen, 1978) were used in routine cloning procedures (Sambrook *et al.*, 1989). The *E. coli* strains BL21AI (Invitrogen) and BL21(DE3)omp8 (Prilipov *et al.*, 1998) and the plasmids pET17b and pET22b (Studier *et al.*, 1990) were used for subcloning and controlled expression of the *pbp* gene.

The *E. coli* strains were routinely grown in Luria-Bertani (LB) medium (Miller, 1992). Appropriate antibiotics were added to the culture medium. All *Bacteroides* strains were maintained on 5% horse blood agar plates (no. 2 agar; Oxoid) and cultured anaerobically in BM medium (Verweij-van Vught *et al.*, 1986) in the presence of 50 μg/ml kanamycin and 20 μg/ml nalidixic acid (Sigma Chemicals) as the standard medium. Anaerobiosis was achieved using the Anaerogen system from Oxoid.

General methods

Recombinant DNA techniques were carried out as described (Sambrook *et al.*, 1989). DNA sequencing was carried out using the Big Dye Terminator Cycle sequencing kit on an ABI Prism 310 automated sequencer (Perkin Elmer). Bound antibodies were visualized on immunoblots by chemiluminescence (Roche Molecular Biochemicals). The (relative) intensity of protein bands from both chemoluminescent

blots and Coomassie-stained gels were quantified using a FluorS Multi-Imager with the Multi-Analyst software package (BioRad).

Polyclonal antibodies and reagents

Goat anti-human plasminogen antibodies and human plasminogen used in plasminogen-binding assays were purchased from Haematologic Technologies. Rabbit anti-goat HRP-conjugated antibodies and goat anti-rabbit HRP-conjugated antibodies used for immunodetection were obtained from Santa Cruz Biotechnology and BioRad, respectively. For Western blotting, anti-Pbp antiserum raised against purified histidine-tagged Pbp (His-Pbp) was used. Rabbits were injected with a mixture of native and denatured His-Pbp protein (50%/50%; Agrisera, Sweden). Antiserum against *B. fragilis* P46 has been described (Sijbrandi *et al.*, 2005). Antisera against *E. coli* β-lactamase and OmpA were gifts from J.-M. van Dijl and J.-W. de Gier, respectively. Restriction enzymes, the Expand long template PCR system, Complete EDTA-free protease inhibitors and the Lumi-light western blotting substrate were obtained from Roche Molecular Biochemicals. Sigma Chemicals supplied all other chemicals.

Cloning of the pbp gene

The coding sequence of *pbp* was amplified by PCR using chromosomal DNA from *B. fragilis* BE1 as template. The primers used were the BfFor60 primer 5'-CGCGC**ATCGAT**CTTTGCGTGGCATTTATGGGCAATCC-3', introducing a *Cla*I restriction site (boldface letters) 85 bp upstream of the putative promoter of *pbp* and the BfRev60 primer 5'-GCGCC**GTCGAC**GTCCGTCATTTGTGTGACGGACAACTC-3', introducing a *Sal*I site (boldface letters). The complete gene, including its own promoter, was cloned into pACYC184 using the created *Cla*I and *Sal*I sites. The plasmid pACYC-60kDa was introduced into *E. coli* TOP10F'.

The T7 expression system was used for IPTG-arabinose inducible expression of *pbp* (Studier *et al.*, 1990). The *pbp* gene was amplified by PCR using the plasmid pACYC-60kDa as template DNA. Primers used were the BfpETFor60 forward primer 5'-GCGCC**CATATG**ATCAAGAAGTTGTATTTGCCTTTACTTATGG-3', introducing a *Nde*I restriction site (boldface letters) and the BfRev60 primer. The *pbp* gene was cloned into the expression vector pET17b using the *Nde*I and *Sal*I restriction sites of the insert and the compatible *Nde*I and *Xho*I restriction sites of the vector.

The *pbp* gene was also cloned with a histidine tag to facilitate purification of the protein. Therefore, the *pbp* gene was amplified by PCR using the plasmid

pACYC-60kDa as template DNA. Primers used were the BfpETFor60 forward primer and the BfpET22Rev60 reverse primer 5'-TCT**CTCGAG**TTTTACGATGCTCATGAA-ATCTGC-3', introducing a *Xho*I restriction site (boldface letters). The *pbp* gene was cloned into the expression vector pET22b using the created *Nde*I and *Xho*I sites. This vector creates a C-terminal fusion to a histidine-tagged sequence. Plasmid pET22b-Pbp was introduced into *E. coli* BL21Omp8 for an IPTG and arabinose inducible expression of *pbp*. The plasmids pACYC-60kD, pET17b-Pbp and pET22b-Pbp were sequenced to check for second site mutations.

Purification of Pbp

Strain BL21(DE3)omp8(pET22b-Pbp) over-expressing the C-terminal His-tagged Pbp, was cultivated in 3 L of LB-medium for the isolation of Pbp. Cells were induced with 1 mM IPTG and 0.2% arabinose for 1.5 h at an OD_{660} of 0.4. The cells were harvested, washed with a phosphate buffered saline solution (PBS), resuspended in 50 mM Tris-HCl, pH 8.0, containing 1 mM EDTA, protease inhibitors, DNase and RNase and lysed using a French pressure cell. After removal of the cellular debris, the obtained cell lysate was centrifuged at 270,000 × *g* for 90 min at 4 °C. The membrane pellet was resuspended in PBS containing 500 mM NaCl, 5 mM Imidazole and 1.0% Triton X-100 and rotated for 16 h. The sample was centrifuged at 270,000 × *g* for 90 min at 4 °C. The solubilized proteins were loaded on a Ni^{2+}-charged HiTrap Chelating column equilibrated in PBS containing 500 mM NaCl, 5 mM Imidazole and 0.5% Triton X-100, and eluted using a gradient to 250 mM imidazole. Peak fractions were pooled, desalted to PBS buffer containing 0.5% Triton X-100 using a HiTrap Desalting column and loaded on a HiTrap Heparin column (all HiTrap columns from Amersham Biosciences) equilibrated with the same buffer. The proteins were eluted from the column using a linear gradient to 2 M NaCl. Peak fractions were pooled and purified again on a Ni^{2+}-charged HiTrap Chelating column. The purest fractions, as determined by protein staining of an SDS-PAGE gel, were pooled and desalted to PBS buffer containing 0.1% Triton X-100. Finally the protein sample was concentrated from 4 to 2 ml using a Microsep centrifugal device (Pall Life Sciences). The final protein concentration of the purified His-tagged Pbp was 1.15 mg/ml.

Subcellular localization of Pbp in B. fragilis

To determine the location of Pbp in *B. fragilis* BE1, cells were fractionated and subcellular fractions (cytoplasm, inner membranes, and outer membranes) were

separated by using sucrose density gradient techniques (Kotarski and Salyers, 1984; Sijbrandi *et al.*, 2005). Fractions were stored at minus 80 °C.

Detection of plasminogen-binding proteins

A blot overlay assay (Bergmann *et al.*, 2001; Sijbrandi *et al.*, 2005) was used to detect plasminogen-binding proteins. Equal amounts of soluble protein fractions or outer membrane preparations of *B. fragilis* BE1 were separated on an 11% SDS-polyacrylamide gel and blotted electrophoretically onto PVDF membrane (Immobilon-P, Millipore). The membranes were then blocked with 4% skimmed milk powder in PBS for 30 min. Next, the blots were incubated with human plasminogen (1 μg/ml) in PBS for 2 h, washed with PBS and then incubated with anti-human plasminogen in Tris-buffered saline (TBS) containing 0.1% Tween 80 for 2 h. After washing, the blots were probed with rabbit anti-goat HRP conjugated antibody (Santa Cruz Biotechnology) for 1 h. The probed blots were washed four times with TBS containing 0.3% Tween 80, incubated with Lumilight substrate and exposed to Kodak X-Omat AR film. Afterwards, the blot was stained with Coomassie Brilliant Blue to identify the bands visualized on film. Where indicated in the text, blots were incubated with human plasminogen (1 μg/ml) in the presence of human serum that was diluted 1:5 in PBS.

Protease accessibility assay

A protease accessibility assay was used to confirm the cell-surface localization of Pbp (Jonsson *et al.*, 2004). Cells of *E. coli* BL21AI (pET22b-Pbp) overexpressing Pbp or of *B. fragilis* BE1 were washed with PBS and resuspended in PBS to an optical density at 660 nm of 20. The cell suspension (250 μl) was incubated with Proteinase K to a final concentration of 0.4 mg/ml for 1 h on ice. Other samples were incubated with both Proteinase K and 0.5% Triton X-100, 0.5% Triton X-100 and proteinase inhibitors, or left untreated. Protease inhibitor cocktail tablets were purchased from Roche. Following incubation, the reactions containing Triton X-100 were immediately boiled in SDS sample buffer. The other reactions were treated with PMSF for 45 min on ice and subsequently boiled in SDS sample buffer. Samples of 0.1 OD_{660} unit were taken and resolved by SDS-PAGE. After immunoblotting, the levels of Pbp and *E. coli* OmpA or *B. fragilis* P46 were analyzed using their respective antibodies.

Results

The molecular characterization of Pbp

Previously, the discovery was reported of a 60 kDa protein with plasminogen-binding properties in an overlay assay, and present in outer membrane protein extracts of *B. fragilis* BE1 (Sijbrandi *et al.*, 2005). To study this newly found protein in more detail, a mass spectrometry analysis of trypsin-digested fragments of this protein was carried out. A range of peptide masses were then used to search the Swiss-Prot and TrEMBL databases using PeptIdent. This search resulted in a match of six fragments with the hypothetical protein BT2844 from *B. thetaiotaomicron*. The complete genome sequence of *B. fragilis* was not available at the time of this analysis, and the search did not match with a protein from *B. fragilis*. Recently, using the predicted amino acid sequence of this protein, a highly homologous protein was identified in a protein versus translated DNA BLAST in the genome sequence of *B. fragilis* strain NCTC9343 at http://www.sanger.ac.uk/Projects/B_fragilis/. A virtual trypsin digestion was carried out on this protein sequence with the Peptide Mass program. Then a comparison was carried out between the predicted peptide masses and the masses from the mass spectrometry results on the Pbp protein of *B. fragilis* BE1; 31 of the 45 possible fragments were identical. This suggested that *B. fragilis* NCT9343 contains a gene encoding a protein that is highly comparable to the putative plasminogen-binding protein of *B. fragilis* strain BE1.

The *pbp* gene of *B. fragilis* BE1 was then cloned from the genome of this bacterium, using PCR as described in the Materials and Methods section. The entire open reading frame (ORF) found after sequencing, encodes a putative protein of 563 amino acids with a calculated relative molecular mass of 61.5 kDa. This mass is in accordance with the relative molecular mass found upon SDS-PAGE of circa 60 kDa (Sijbrandi *et al.*, 2005). A protein BLAST with this putative protein sequence in the NCBI sequence database (http://www.ncbi.nlm.nih.gov/BLAST/) revealed significant homology to proteins with unknown function in other organisms. A hypothetical protein designated BF4485 in the recently published genome sequence of *B. fragilis* YCH46 (Kuwahara *et al.*, 2004) is 100% identical to this protein, but the first 10 amino acids are not present in the ORF. An NCBI Conserved Domain Search revealed a 90% alignment of 100 amino acids with a tetratricopeptide repeat (TPR) domain. This domain is conserved among proteins from very different species and is proposed to be involved in a very broad range of activities including protein-protein interactions. Interestingly, the Pbp protein shows a high degree of conservation (55%

identity) with the TPR domain of the protein designated PG1028 of *Porphyromonas gingivalis*, an important pathogen of the human oral cavity (Nelson *et al.*, 2003).

Analysis of the nucleotide sequence upstream of the ORF showed sequences that closely resembled the consensus –35 and –10 promoter sequences and a Shine-Dalgarno sequence (EMBL Nucleotide Sequence Database accession number AJ786264). The ORF is located between two other ORFs in the same reading frame probably encoding a 317 amino acid tyrosine type site-specific recombinase (upstream) and a 356 amino acid hypothetical protein with homology to thiol:disulfide interchange proteins (downstream).

The recovery of the 60-kDa protein from the outer membrane fraction of *B. fragilis* BE1 makes it likely that newly synthesized Pbp polypeptides contain a signal peptide necessary for translocation across the inner membrane. Using the SignalP server (Bendtsen *et al.*, 2004), no indications were found for a signal peptidase I cleavage site. However, a cysteine residue was present in the N-terminal part of the protein sequence that could point to the existence of a lipoprotein signal peptide and a signal peptidase II cleavage site. Using the LipoP signal sequence prediction algorithm (Juncker *et al.*, 2003), a strong prediction for the presence of a signal peptidase II cleavage site between amino acid positions 19 and 20, was obtained. This suggests that the 60-kDa protein may be a lipoprotein that will be lipidated at the cysteine at position +1 of the mature protein. The amino acid at position +2 is a serine, and in accordance with the "+2 rule" the protein would be targeted to the outer membrane of gram-negative bacteria (Seydel *et al.*, 1999). When the preprotein is cleaved at the expected position, the calculated molecular mass of the mature protein (excluding lipids) is 59.4 kDa.

The *pbp* gene was then subcloned and expressed in *E. coli*, and the construct was sequenced to check for second site mutations. No base pair differences were found between the nucleotide sequence of *pbp* and ORF BF4485 from *B. fragilis* strain YCH46. Five base pair differences were found in comparison to the ORF from *B. fragilis* strain NCTC9343, but these did not result in any differences in amino acid sequence.

Purification of His-tagged Pbp

In order to purify Pbp and to raise specific antibodies for further analyses, the *pbp* gene was cloned in an *E. coli* expression vector with an inducible promoter. The cloned construct encoded Pbp with a C-terminal histidine tag. The His-tagged Pbp was then purified (Fig. 1), and specific antibodies were raised in rabbits.

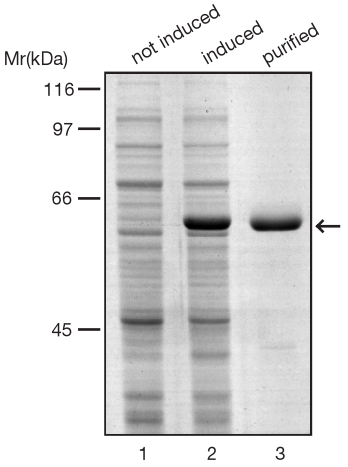

Fig. 1. Purification of His-tagged Pbp. *E. coli* BL21(DE3)omp8(pET22b-Pbp) was used to express histidine-tagged Pbp. His-Pbp was purified from the membranes to near homogeneity using detergent extraction of membrane(-associated) proteins followed by affinity chromatography using a Ni^{2+}-charged chelating column and a heparin column. Samples from the non-induced (lane 1) and induced cells (lane 2) and purified protein (lane 3) were subjected to SDS-PAGE and Coomassie staining. The arrow indicates the position of His-Pbp in the gel.

Subcellular localization of Pbp and possible cell-surface exposure

The subcellular distribution of Pbp in *B. fragilis* cells was analyzed. Preparations of soluble proteins, inner membrane proteins, as well as outer membrane protein fractions were isolated (Sijbrandi *et al.*, 2005). The presence of Pbp in these fractions was then analyzed by SDS-PAGE followed by Coomassie staining and/or Western blotting using anti-Pbp antiserum. The Pbp protein was mainly found in the outer membrane fraction (Fig. 2, lane 4) and to a lesser extent in the inner membrane fraction (lane 3). There was hardly any Pbp detectable in the soluble protein fraction that mainly consists of the cytoplasm (lane 2).

To assess a possible cell-surface localization of Pbp, a protease accessibility assay was carried out with cells of *B. fragilis* BE1. Upon incubation of intact cells with Proteinase K (Prot. K), Pbp was completely degraded (Fig. 3, lane 2). The α-enolase P46, localized in the cytoplasm and the inner membrane of *B. fragilis*, was used as an intracellular control protein (Sijbrandi *et al.*, 2005). As expected, P46 was not degraded by Prot. K in intact cells (panel C), but after disruption of the cell envelope by the addition of Triton X-100, P46 was also degraded (panel C, lane 4). Similar results were obtained using intact cells of *E. coli* BL21AI (pET22b-Pbp) expressing Pbp. Upon incubation with Prot. K, Pbp completely disappeared (panel D and E, lane 6). In intact cells, the periplasmic protein β-lactamase (Bla), that is inaccessible to externally added proteases, was not cleaved by Prot. K. However,

after treatment of the cells with Triton X-100, this “control” protein was completely degraded (panel F). Furthermore, the outer membrane protein OmpA was used as a control in *E. coli*. Although part of this protein is surface exposed, it cannot be cleaved by the external addition of Prot. K when present in intact membranes (panel G), as described before (Morona *et al.*, 1985). OmpA can only be degraded after solubilization of the membranes. Also in the presence of protease inhibitors, OmpA was degraded after solubilization. A possible explanation could be that only protease inhibitors effective against serine and cysteine proteases were used, which do not inhibit metallo or aspartic proteases. The proteolysis observed after disruption of cells with Triton X-100 and incubation for 45 min on ice in the presence of inhibitors (lane 3 and 7) could be the result of intracellular proteases not affected by the inhibitors added. Together, these results suggest that Pbp is exposed to the surface of *B. fragilis* cells, and that it is also cell-surface exposed when expressed in *E. coli*.

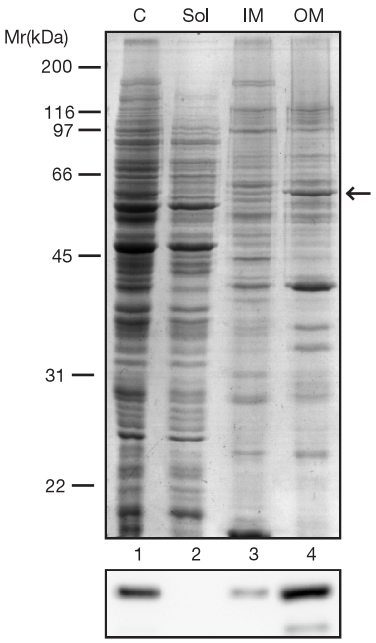

Fig. 2. Subcellular localization of Pbp. SDS-PAGE profile (top panel) and Western blot analysis (bottom panel) of the different cellular fractions of strain *B. fragilis* BE1. Pure membrane fractions were prepared using sucrose density gradients. Equal amounts of protein from the different subcellular fractions were loaded in each lane. C: Cell lysate, Sol: soluble protein, IM: inner membrane fraction, OM: outer membrane fraction. Anti-Pbp antibodies were used in the immunoblotting experiment. The arrow indicates the position of Pbp in the Coomassie-stained gel.

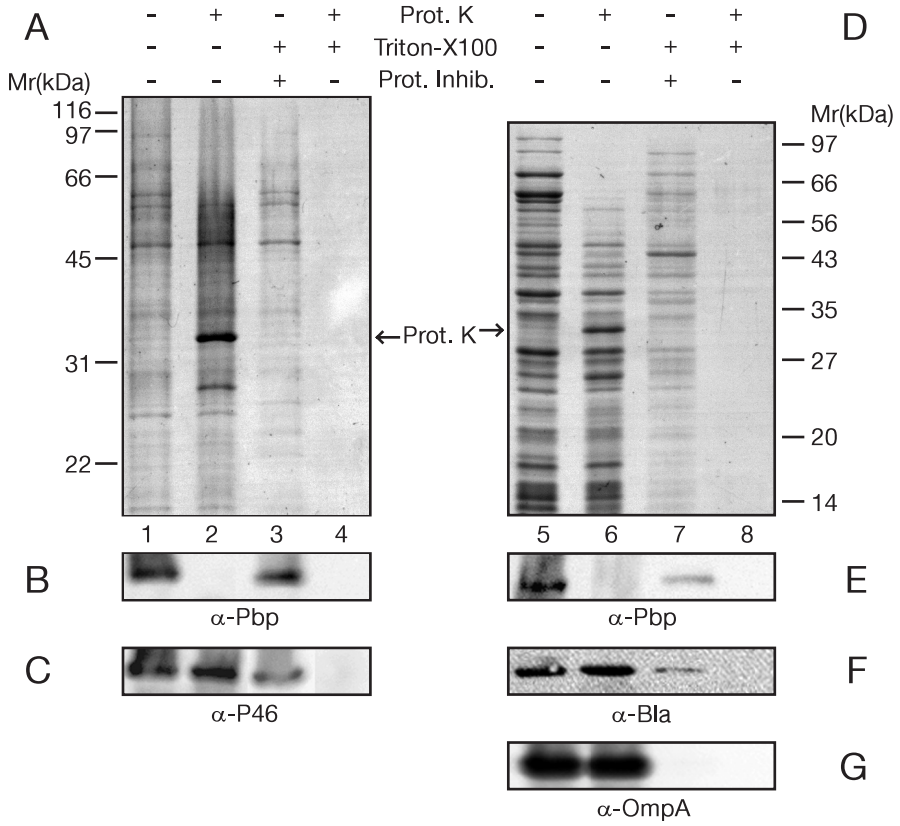

Fig. 3. Protease accessibility of Pbp in intact cells. A, intact cells of *B. fragilis* were incubated in the absence (lane 1) or presence (lane 2) of Proteinase K (Prot. K). As a control, cells were lysed using Triton-X100 in the presence of protease inhibitors (lane 3) or lysed and treated with Prot. K (lane 4). Samples were resolved by SDS-PAGE and stained with Coomassie. B, immunoblot of the samples from panel A, using anti-Pbp antiserum. C, immunoblot of the samples from panel A, using control anti-P46 antiserum. D, whole cells of *E. coli* BL21AI (pET22b-Pbp) overexpressing Pbp were incubated in the absence (lane 5) or presence (lane 6) of Proteinase K. As a control, cells were lysed using Triton-X100 in the presence of protease inhibitors (lane 7) or lysed and treated with Prot. K (lane 8). Samples were resolved by SDS-PAGE and stained with Coomassie. E, immunoblot of the samples from panel D, using anti-Pbp antiserum. F, immunoblot of the samples from panel D, using anti-Bla antiserum. G, immunoblot of the samples from panel D, using anti-OmpA antiserum. The arrows indicate the position of Prot. K in the stained gels.

Pbp binds plasminogen in an overlay assay

The Pbp protein was originally identified by mass spectrometry analysis of a protein band extracted from an SDS-PAGE gel. This band corresponded in apparent

molecular mass with the protein band that bound human plasminogen in a blot overlay assay (Sijbrandi *et al.*, 2005). To obtain more evidence that Pbp is indeed the putative plasminogen-binding protein, Pbp, as well as His-tagged Pbp, was expressed in *E. coli* , with or without induction, and the binding of plasminogen was assayed.

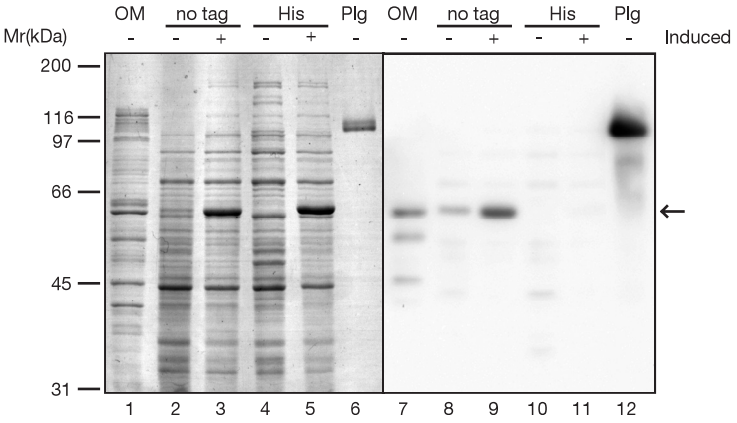

Fig. 4. Plasminogen binding of Pbp with or without a C-terminal histidine tag. Outer membrane fractions from *B. fragilis* BE1 (OM, lanes 1 and 7) and total cell samples from *E. coli* BL21AI(pET17b-Pbp) or BL21AI(pET22b-Pbp) cells expressing Pbp with or without a His-tag, respectively, were subjected to SDS-PAGE and stained with Coomassie (left panel) or to immunoblotting (right panel). Induction with IPTG and arabinose is indicated above the figure. As a control, purified human plasminogen was loaded (Plg, lanes 6 and 12). A blot overlay assay was carried out with the blot. The blot was incubated with human plasminogen and bound plasminogen was probed with anti-plasminogen antibodies and detected by chemiluminescence. The arrow indicates the position of Pbp in de gel and on the blot.

A blot overlay assay with human plasminogen was carried out using *E. coli* lysates in which expression of wild type or histidine-tagged Pbp was induced. In this assay, plasminogen bound to a 60-kDa protein that was strongly present in the induced lysate containing wild type Pbp (Fig. 4, lanes 3 and 9). This protein had the same apparent molecular mass as the 60-kDa plasminogen-binding protein in the outer membrane fraction of *B. fragilis* cells (lanes 1 and 7). The protein was less pronounced in non-induced samples and clearly less plasminogen bound. The His-tagged version of Pbp did not bind human plasminogen (lanes 5 and 11). Because the His-tag is added to the C terminus of Pbp, it might be that the C-terminal residues

of the Pbp protein are involved in the binding of human plasminogen. This is in good accordance with observations on other plasminogen-binding proteins (Redlitz *et al.*, 1995; Pancholi and Fischetti, 1998; Winram and Lottenberg, 1998; Bergmann *et al.*, 2001; Derbise *et al.*, 2004). The blot overlay experiment has also been carried out with human plasminogen in the presence of a complex protein mixture (diluted human serum). The results were comparable, indicating that the binding of plasminogen to Pbp in the overlay assay was specific (data not shown).

Detection of Pbp like protein in other Bacteropides species

Based on the high homology between the primary sequence of the Pbp protein of *B. fragilis* and a putative 60-kDa protein of *B. thetaiotaomicron*, it was expected that the anti-Pbp antiserum might cross-react. To investigate the presence of a Pbp like protein in *B. thetaiotaomicron*, as well as in other *Bacteroides* species like *B. vulgatus*, *B. ovatus* and *B. distasonis,* equal amounts of soluble (mainly cytoplasmic) protein fractions and outer membrane fractions of representatives of these five *Bacteroides* subspecies were analyzed by SDS-PAGE and immunoblotting. As shown in Fig. 5 (top panel), the Pbp protein of *B. fragilis* BE1 reacted as expected strongly and specifically with the Pbp antiserum. In the OM fractions of *B. vulgatus*, *B. distasonis*, *B. thetaiotaomicron* and *B. ovatus* a protein band of about 60 kDa was recognized by the Pbp antiserum. These results indicated that cross-reacting Pbp-like proteins are present in these *Bacteroides* subspecies. Analyses of other clinical isolates of *Bacteroides* gave comparable results (not shown). The binding of plasminogen to Pbp and Pbp-like proteins was also studied using an overlay assay (Fig. 5, lower panel). The results indicated that Pbp as well as the Pbp-like cross-reacting proteins found in *B. thetaiotaomicron* and *B. ovatus* bind plasminogen in this assay, albeit to a different extent. The binding of plasminogen to the Pbp-like proteins found in *B. vulgatus* and *B. distasonis* was less clear, but very weak signals were found after long staining and exposure (not shown).

Discussion

The *pbp* gene was cloned from the genome of *B. fragilis* BE1, and its sequence analysis predicted a 60-kDa protein that might be an outer membrane located lipoprotein. The experimental results presented in this study show that Pbp is indeed an outer membrane protein with plasminogen-binding activity in an overlay

assay, and probably exposed at the cell surface. Pbp can also be expressed in *E.*

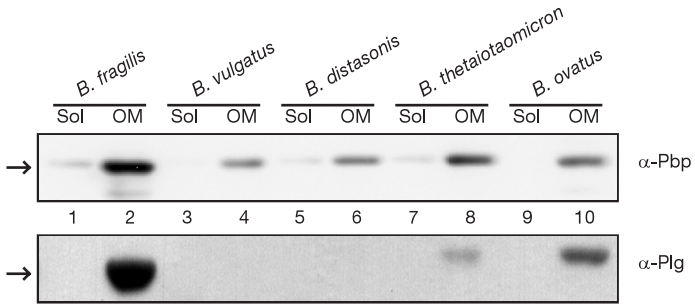

Fig. 5. Presence of Pbp-like proteins in *Bacteroides* subspecies. Representatives of each of the five available *Bacteroides* subspecies were used: *B. fragilis* BE1, *B. vulgatus* BE18, *B. distasonis* BE5, *B. thetaiotaomicron* BE33 and *B. ovatus* BE15. Soluble protein fractions were separated from membranes fractions by ultracentrifugation. Crude outer membrane protein fractions were prepared by selective extraction of inner membrane proteins from the pelleted membranes using sodium sarkosyl. Samples of the soluble protein (lanes 1, 3, 5, 7 and 9) and outer membrane protein (lanes 2, 4, 6, 8 and 10) fractions from all subspecies were subjected to SDS-PAGE and Western blotting in duplicate. For the top panel, anti-Pbp antibodies were used as a probe. The blot in the bottom panel was first incubated with 1 µg/ml human plasminogen and then bound plasminogen was detected using anti-plasminogen antibodies. The arrow on the left of both panels indicates the position of the *B. fragilis* Pbp protein.

coli and protease experiments also pointed to a cell-surface exposure in this bacterium. Because C-terminally His-tagged Pbp did not bind plasminogen anymore, the C-terminal lysine residue and probably other C-terminal residues might be crucial in plasminogen-binding.

A homologue of Pbp, BT2844, is present in the genome of *B. thetaiotaomicron* (Xu *et al.*, 2003). Antibody experiments showed cross-reactivity of the Pbp of *B. fragilis* and BT2844 of *B. thetaiotaomicron.* In a blot overlay assay it was shown that this homologue was also capable of binding plasminogen, although to a lesser extent than Pbp. Pbp-like proteins were also found in clinical isolates of *B. vulgatus*, *B. distasonis* and *B. ovatus*. It is tempting to speculate that the relatively high expression of Pbp contributes to the virulence of *B. fragilis*, the most pathogenic strain of the *Bacteroides* subspecies.

Cell-surface plasminogen-binding proteins have also been found in other bacteria. Especially, α-enolases in Gram-positive bacteria and eukaryotic cells are often found to possess plasminogen-binding properties (Redlitz *et al.*, 1995; Pancholi and Fischetti, 1998; Bergmann *et al.*, 2001; Jolodar *et al.*, 2003; Jong *et al.*, 2003). A

plasminogen-binding lipoprotein has been found in the spirochete *Borrelia burgdorferi*, the causative agent of Lyme disease. This protein is known as BPBP (*Borrelia* Plasminogen Binding Protein), OppA-1 or PlpA (Hu *et al.*, 1997; Kornacki and Oliver, 1998). In *Helicobacter pylori*, which causes gastric ulcers, the two proteins PgbA and PgbB were identified as plasminogen-binding proteins (Jonsson *et al.*, 2004). Nevertheless, there is no significant homology in the primary sequences between Pbp and BPBP, PgbA or PgbB. Pbp might represent a novel class of bacterial plasminogen-binding proteins with homologues in other pathogens like *B. thetaiotaomicron* and *P. gingivalis*.

The binding of host plasminogen on the bacterial surface might give the organism two advantages. First, the bound plasminogen may become more easily accessible to either bacterial of host-derived plasminogen activating proteins (Parry *et al.*, 2000; Lähteenmäki *et al.*, 2001). These proteins activate plasminogen to become plasmin, converting the cell into a proteolytic organism with the capability to function in fibrinolysis and to degrade extracellular matrix proteins. This may play a role in the spread of the infection as the cell can even penetrate the basal membrane. In fact, *B. fragilis* has been shown to be able to invade HeLa cells (Goldner *et al.*, 1991). Cell-surface bound plasmin has been shown to be protected against quick inactivation by inhibitors like α-2 antiplasmin (Lottenberg *et al.*, 1992). Bound plasminogen may also be protected against activation by plasminogen activators. This would in turn prevent dissolution of fibrin clots and shield off the organism against the immune system of the host, facilitating the establishment of the bacterial infection. Further experiments need to be carried out in order to elucidate the precise *in vivo* role of Pbp as a virulence factor of *B. fragilis*.

The computer analyses pointed to a possible lipoprotein nature of Pbp. Remarkably, Pbp could be purified using a Heparin Sepharose column (see Materials and Methods). Immobilized heparin is often used to purify proteins such as DNA binding proteins, coagulation factors and lipoproteins. The affinity of Pbp for Heparin is another indication for a possible lipoprotein nature of Pbp. Further experiments have to be carried out to show that Pbp is in fact a genuine lipoprotein. In the annotated genome of *B. fragilis* YCH46 six open reading frames are predicted to encode (putative) lipoproteins. Pbp is not one of these. On the other hand, one predicted lipoprotein is homologous to the lipoprotein ApbE from *Salmonella,* but is most likely not a lipoprotein in *B. fragilis* because there is no cysteine residue present in the N-terminal region of the molecule. Lipoproteins have a so called lipobox sequence around the signal sequence cleavage site with an invariant cysteine at position +1 from the cleavage site (Sankaran and Wu, 1995). In the genome of *B.*

fragilis, an ORF has been identified that encodes a prelipoprotein diacylglycerol transferase enzyme (Lgt) that attaches the lipid molecule to the cysteine at position +1, and another ORF has been found to encode a putative lipoprotein signal peptidase (LspA or SPaseII). In *E. coli*, both proteins mentioned above are essential for the processing of prelipoproteins at the periplasmic side of the inner membrane (Wu, 1996). If the mature lipoprotein does not contain a Lol-avoidance signal (usually an aspartate at position +2 (Seydel *et al.*, 1999)), the protein is targeted to the outer membrane by the Lol machinery. The Lol system is composed of five proteins (LolABCDE) which are all essential for the correct targeting of lipoproteins to the outer membrane and even essential for viability of *E. coli* (Narita *et al.*, 2004). However, analysis of the *B. fragilis* genome only clearly identifies a predicted LolD protein. It is not known whether *B. fragilis* contains proteins that can carry out the function of LolA, -B, -C and -E. It has been reported that certain cell-surface localized lipoproteins of Gram-negative bacteria are targeted by other mechanisms than the Lol system (Pugsley, 1993). In *Neisseria meningitidis*, LPS is required for the biogenesis of cell-surface exposed lipoproteins, but not for outer membrane localized lipoproteins facing the periplasm (Steeghs *et al.*, 2001).

The identification of the putative lipoprotein Pbp as a potentially important virulence factor of *B. fragilis* has interesting clinical implications. Because the processing of bacterial lipoproteins absolutely requires a functional Signal Peptidase II, inhibition of the SPaseII function by administration of globomycin-type antibiotics in patients could interfere with the establishment or further spread of infections (Dev *et al.*, 1985). This may be relevant not only to infections where *B. fragilis* is involved but also for other types of infection where lipoproteins play crucial roles in the viability or virulence of bacteria.

Chapter 7

Summarizing discussion

Introduction

Intra-abdominal infections (IAI) caused by secondary peritonitis are a common cause of death in humans (Farthmann and Schöffel, 1998; Bosscha *et al.*, 1999). These infections are usually the result of leakage of the intestinal contents into the peritoneal cavity due to surgery or other abdominal traumas. A common complication of these infections is the formation of abscesses, making the treatment of secondary peritonitis very complicated (Anaya and Nathens, 2003). Often, two Gram-negative bacterial species are isolated from the site of infection: the aerobic *Escherichia coli* and the anaerobic *Bacteroides fragilis* ((Farthmann and Schöffel, 1998) and references therein). The frequent co-occurrence of these two species has led to the concept of microbial synergy between *E. coli* and *B. fragilis*. The synergy between the two species has been demonstrated experimentally in mouse and rat infection models (e.g. Onderdonk *et al.*, 1976; Brook *et al.*, 1984). However, the molecular basis of this synergism is only partially understood. The known virulence factors of *E. coli* and *B. fragilis* that are involved either inhibit phagocytosis by polymorphonuclear neutrophyls (PMNs) or aid in the provision of essential growth factors to the bacteria. An example of the latter process is the acquisition of iron and heme from host proteins, because bacteria need much higher concentrations of iron to maintain growth than is freely available in the human body (Weinberg, 1974). A hemoglobin protease (Hbp) has been identified that contributes to the synergistic abscess formation and heme-dependent growth of *B. fragilis* in a murine infection model (Otto *et al.*, 1998; Otto *et al.*, 2002). It has been proposed that, after proteolysis of hemoglobin, heme-bound Hbp provides the heme as an iron or heme source to the bacteria at the site of infection. Another mechanism that has been implicated in the bacterial synergy between *E. coli* and *B. fragilis* is the secretion of proteases that cause tissue destruction in the host (Aldridge, 1995). Alternatively, bacteria might use host proteins to accomplish this task. Although this has not been demonstrated for *E. coli* or *B. fragilis* so far, other bacteria have been shown to be able to bind host plasminogen at their cell surface and to convert it to plasmin (Lähteenmäki *et al.*, 2005). This property gives the bacterium the opportunity to interfere in the finely tuned system of coagulation and fibrinolysis of the host (Norris, 2003).

The experiments presented in this thesis investigate three proteins that are or may be involved in the pathogenic synergy between *E. coli* and *B. fragilis* in human intra-abdominal infections. These three proteins are Hbp of *E. coli* and P46

and Pbp of *B. fragilis*. Hbp is a hemoglobin protease with heme-binding activity. It is a secreted protein belonging to the autotransporter family of proteins. P46 is the α-enolase of *B. fragilis* and was shown to reside intracellularly. Finally, Pbp was identified as a possible plasminogen-binding factor at the cell surface of *B. fragilis*.

Hemoglobin protease (Hbp)

Hemoglobin protease (Hbp) is a hemoglobin degrading and heme-binding protein secreted by human pathogenic *E. coli*. The protein is a member of the serine protease autotransporters of the Enterobacteriaceae (SPATE) group of autotransporter proteins. Autotransporters are large proteins carrying three functional domains: an N-terminal signal peptide for targeting to and translocation across the inner membrane, the passenger domain (the secreted effector molecule), and a C-terminal translocation unit that is necessary for translocation across the outer membrane. In chapter 2, experiments are described that deal with the targeting to and translocation across the inner membrane of the Hbp preprotein. In chapter 3, the crystal structure of the complete passenger domain of Hbp is described as well as its heme binding properties. In chapter 4, the purification, folding properties and proposed β-barrel structure of the translocator domain of Hbp are presented.

Inner membrane targeting and translocation

In chapter 2, the earliest steps in the secretion of Hbp are studied, especially the targeting to and translocation across the inner membrane (Fig. 1). Evidence is presented showing that Hbp interacts with the signal recognition particle (SRP), that Hbp is dependent on SRP for inner membrane targeting and that the Sec-translocon is required for its translocation across the inner membrane. SecB is not required for targeting of Hbp to the inner membrane, but it can compensate to some extent for the lack of a functional SRP pathway. This is the first example of an extracellular bacterial protein that follows the co-translational SRP targeting route instead of the post-translational SecB pathway that is commonly used by secretory proteins. Indications were obtained that pre-pro-Hbp in the cytoplasm is rapidly degraded by cytoplasmic proteases. This might be the reason for a faster, co-translational targeting pathway, because premature folding and degradation in the cytoplasm can be avoided. Following this study two articles from the group of J. Beckwith appeared in the literature (Schierle *et al.*, 2003; Huber *et al.*, 2005). These articles describe the

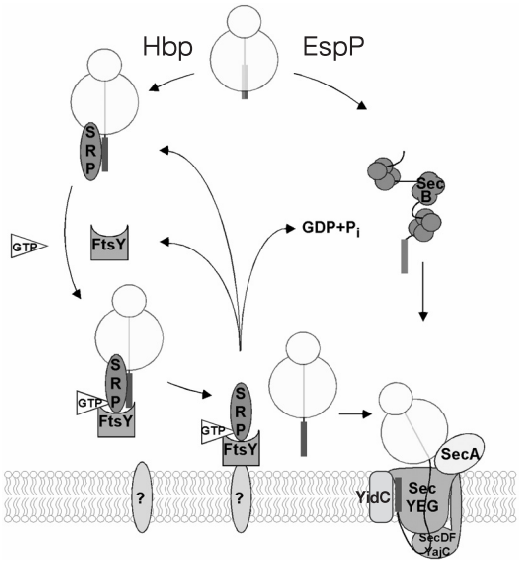

Fig. 1. Inner membrane targeting and translocation of autotransporter proteins. Model of the SRP and SecB targeting pathways in *E. coli*, specified for the targeting of the autotransporters Hbp (left) and EspP (right). Nascent chains with a particularly hydrophobic signal sequence, like Hbp (see text), are recognized by SRP at the ribosome. The ribosome-nascent chain complex is bound by FtsY and targeted to the inner membrane, possibly to a proteinaceous membrane component (question mark). The nascent polypeptide is then transferred to the Sec-translocon (SecYEGDF-YidC-YajC) in a GTP-dependent reaction. SecA energizes the (cotranslational) translocation of the preprotein through the translocon to the periplasmic space. During or after translocation, the signal peptide is cleaved off by Leader peptidase (Lep, not shown). Alternatively, less hydrophobic signal sequences, like that of another autotransporter EspP, are not bound by SRP. Instead, the cytosolic chaperone/targeting factor SecB binds to the mature region of the secretory protein. SecB posttranslationally targets the preprotein to the Sec-translocon, where both pathways converge.

inner membrane targeting of the *E. coli* DsbA protein and of other proteins using the DsbA signal sequence via the SRP pathway. Their results also suggest that proteins found to be targeted by SRP-dependent signal peptides may require this mode of export to prevent rapid folding and nonproductive accumulation in the cytoplasm.

To study the interaction of signal peptides and SRP in more detail, Huber *et al.* (2005) carried out an extensive screen of signal sequences with a range of hydrophobicities. From the numerous scales and window lengths tested, the Wertz-Scheraga scale (Wertz and Scheraga, 1978) and a window length of 12 amino acids gave the most optimal performance and a threshold hydrophobicity required for SRP recognition was defined. The hydrophobicity of the Hbp signal sequence was

calculated using the same optimal scale and window length, and a WS score of 0.715 was obtained, which was well above the defined threshold of 0.690. This score of hydrophobicity was found for the amino acids Cys35 to Phe46, roughly corresponding to the hydrophobic H domain of the signal peptides. Recently, Szabady *et al.* (2005) described that the signal peptide of the *E. coli* EspP autotransporter routes the pre-pro-protein into the posttranslational targeting pathway (unpublished data in Szabady *et al.*, 2005). FHA, a member of the related two-partner secretion (or type Vb) family of proteins, was shown to be dependent on SecB for its export through the Sec-translocon, but not on SRP (Chevalier *et al.*, 2004). By calculating the WS scores (also with window length 12) of the signal sequences of EspP and FHA, it was found that both signal sequences score below the defined 0.690 threshold that was necessary for SRP recognition (0.681 and 0.659, respectively).

Although signal sequence hydrophobicity is generally recognized as the main determinant for SRP recognition (Peterson *et al.*, 2003; Huber *et al.*, 2005), a role for basic residues in the N region of signal peptides has also been described (Peterson *et al.*, 2003). It has been suggested that basic residues promote the binding of SRP to a subset of signal peptides whose hydrophobicity falls slightly below a critical level (Peterson *et al.*, 2003). For the EspP signal peptide, whose hydrophobicity (WS score 0.681) falls just below the threshold of 0.690, this actually might play a role. Curiously, upon removal of the conserved N-terminal extension that is present in the EspP signal peptide, the truncated signal peptide acts as a cotranslational targeting signal (Peterson *et al.*, 2003; Szabady *et al.*, 2005). This truncated EspP signal peptide has a particularly high number of basic amino acids in the N region. It seems that the basic residues somehow have a larger effect when they are not preceded by the N-terminal extension. Upon removal of these charges, the mutated truncated signal peptide reroutes the protein into the posttranslational SecB pathway (Peterson *et al.*, 2003).

The function of the N-terminal extension that is found in a subset of proteins belonging to the autotransporter and two-partner secretion pathways is not known. In chapter 2, it has been proposed that the N-terminal extension of autotransporter signal peptides might actually be the signal for co-translational SRP-dependent targeting of these proteins. Based on the recent data described above, this might not be the case. Experiments with an N-terminally truncated version of the Hbp signal peptide are currently carried out. These experiments will ultimately prove whether or not there is rerouting into the SecB pathway upon deletion of the N-terminal

extension. However, recent findings of Szabady *et al.* (2005) indicate a role for the extended signal peptides that is completely unrelated to inner membrane targeting. The N-terminal extension of EspP was not required for efficient inner membrane targeting, but deletion of the extension led to misfolding of EspP in the periplasm and impaired later stages of autotransporter biogenesis. These data suggest that the translocation unit was not able to adopt its native conformation in the outer membrane upon removal of the N-terminal extension. It was suggested that the long signal peptide transiently anchors the passenger domain to the periplasmic side of the inner membrane and prevents it from folding into a conformation that would block translocation across the outer membrane. This tethering to the inner membrane is probably accomplished by slowing down the release of the preprotein from the Sec-translocon. Future research will further elucidate the role of the N-terminal extension of the autotransporters and will show whether the results presented for the Hbp protein will also be applicable to other autotransporters.

Structure of the passenger domain

In chapter 3, the three-dimensional structure of the complete passenger domain of Hbp is presented. This is the first crystal structure of a full-length autotransporter passenger domain, and it is the largest parallel β-helical structure solved so far. The protein contains a very long right-handed β-helical structure forming three parallel β-sheets. Three distinct domains can be recognized in the structure of Hbp (Fig. 2). The N-terminal domain is a large globular domain containing the trypsin-like serine protease domain. Folding of this domain and functional protease activity can only occur after removal of the signal peptide (i.e. after IM translocation). The relatively open active site presumably can attack globular proteins (like hemoglobin) and suggests broad substrate specificity. Current research on the function of the Hbp protein focusses on the proteolytic properties and substrate specificity of the serine protease domain. Besides some decorative loops, the β-helical stem contains a small “domain 2” that has homology to a chitin binding domain and appears to form a binding pocket of some kind. It was shown that this domain is not responsible for the heme binding of Hbp, but it might alternatively be involved in the binding to a cell-surface receptor of *B. fragilis* and/or *E. coli*. The heme-binding site of Hbp has not been identified yet, but studies involving deletion mutants are carried out. The third domain, the conserved C-terminal region of the protein, may be involved in the translocation of the passenger molecule across the outer membrane and in the folding of the mature protein.

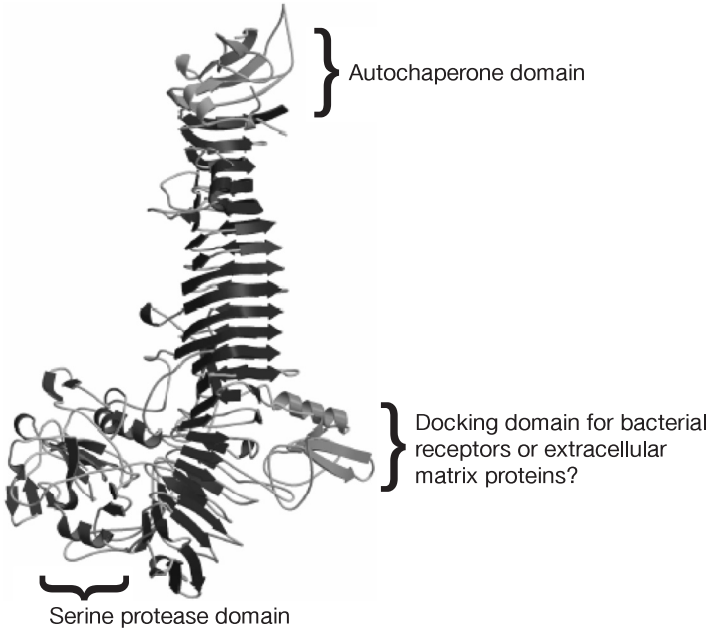

Fig. 2. A ribbon diagram of the overall structure of the passenger region of Hbp. The C-terminus of the mature protein contains the autochaperone domain necessary for a proper folding of the passenger domain. Halfway the molecule a small side domain is present. Possibly its function is docking to extracellular matrix proteins or the bacterial receptor proteins. The proteolytic domain of Hbp is N-terminally located in the molecule. This globular domain is responsible for the serine protease activity of Hbp.

Very little is known about the actual folding of the passenger domain of autotransporters. One idea is that autotransporter proteins adopt their final conformation during translocation across the outer membrane by virtue of their large β-helical content (Klauser *et al.*, 1992). Recently, an autochaperone domain important for folding of the passenger was described in the *B. pertussis* BrkA autotransporter (Oliver *et al.*, 2003b). This conserved C-terminal domain is present in a subset of autotransporters and was also identified in the C-terminal part of Hbp. Interestingly, this domain in Hbp has a remarkably high degree of structural homology to the corresponding domain in the crystal structure of P69 pertactin from *B. pertussis* (J. Tame, personal communication).

The translocation unit

The purification and preliminary characterization of the translocation unit of Hbp is described in chapter 4. The goal of that study is to resolve the crystal structure of the Hbp translocator to obtain more insight in the mechanism of autotransporter passenger translocation across the outer membrane. In Hbp, cleavage of the passenger domain from the β-barrel structure, takes place between two asparagine residues located in the middle of the linker region that is part of the translocation unit. Indications were obtained that the predicted α-helical linker region is localized in the β-barrel pore. This would imply that, *in vivo*, the passenger domain can not be cleaved off from the translocation unit when the α-helix is formed. In that case, cleavage should take place either on the periplasmic side of the outer membrane, before translocation is completed, or on the cell surface with an extended linker region structure, i.e. before the formation of the linker α-helix. It should be pointed out that mature Hbp has always been found in the cell pellets under conditions of overexpression (see chapter 2). This observation could mean either of two things: processing of pro-Hbp takes place in the periplasm and, as a consequence, mature Hbp is present in the periplasm before or during OM translocation, and thus in the cell pellet after centrifugation. Alternatively, processing could take place at the cell surface and mature Hbp might remain partially attached to the outside of the cell.

In chapter 4, a model is presented for the three-dimensional structure of the Hbp translocation unit. The model was based on the published crystal structure of the *Neisseria meningitidis* NalP translocation unit (Oomen *et al.*, 2004). In this structure, the α-helical linker region, which forms part of the translocation unit of NalP, was found to reside within the β-barrel pore. The cleavage site between passenger domain and translocation unit is located on the cell surface, where autoproteolytic cleavage of NalP takes place (Turner *et al.*, 2002). However, the cleavage site between passenger domain and translocation unit of Hbp is in the middle of the α-helical linker region. The consequences for the processing of pro-Hbp when the α-helix of Hbp is indeed localized in the β-barrel pore are discussed above.

Currently, several models for autotransporter translocation have been proposed, involving either translocation of the passenger through the β-barrel pore, translocation through the central channel of a multimeric pore, or translocation involving other outer membrane (translocator) proteins (Fig. 3).

The first and oldest model is the hairpin model, in which the passenger domain is pulled through the β-barrel pore structure with the C-terminal end first (Pohlner *et al.*, 1987). In this model, the proposed autochaperone domain is

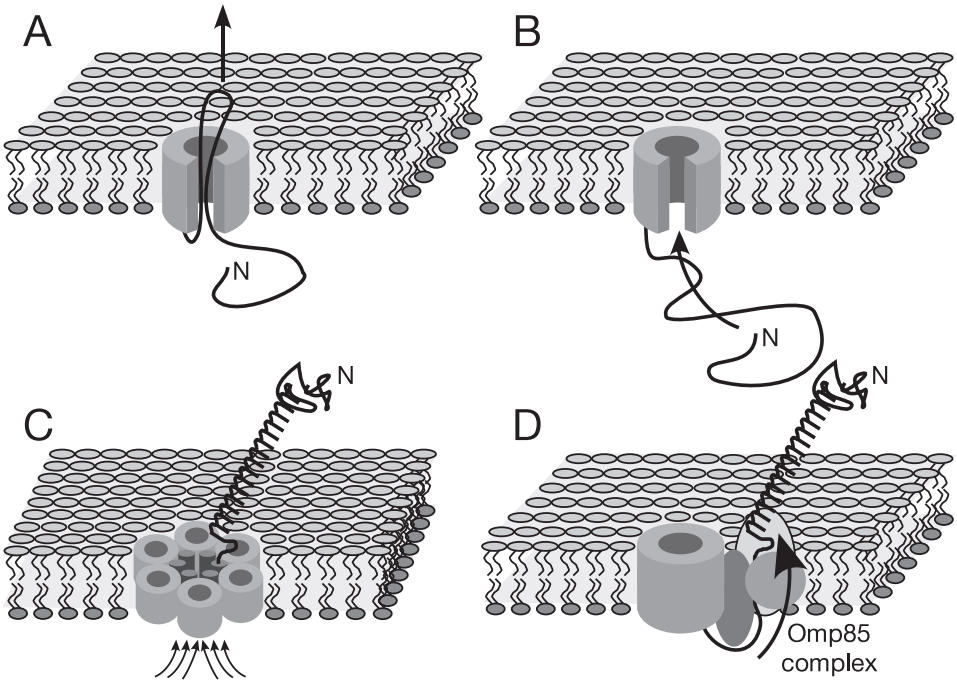

Fig. 3. Four models for outer membrane translocation of autotransporter proteins. Only one step in the translocation process is depicted for each model. In all models, the insertion of the β-barrel domain in the outer membrane occurs either spontaneously or with the help of accesory factors. A, hairpin model. The linker region of the translocation unit inserts into the β-barrel as a transient hairpin structure. The passenger domain is then pulled through the pore from the C-terminal to the N-terminal end, probably energized by the folding of the passenger domain on the cell surface, which is mediated, by the autochaperone domain. Following the translocation of the passenger domain, the linker region adopts an α-helical conformation (not shown). B, threading model. Here the passenger domain is also translocated through the β-barrel pore, but translocation occurs from the N-terminal to the C-terminal end of the molecule. The N-terminus of the passenger domain needs to be directed to the entrance of the pore (arrow). In A and B, the β-barrel is represented as an incomplete cylinder to visualize the targeting to and translocation through the pore. C, multimer model (drawn at smaller scale). The translocation of the passenger domain does not occur through the pore formed by the β-barrel monomer, but through a central channel formed by the multimerization of several (probably six) β-barrels into a ring-shaped structure. The endpoint of translocation is represented here, with the α-helical linker regions as dark cylinders in the central channel and the passenger domain folded at the cell surface (only one passenger domain is shown for clarity). D, Omp85 model. An outer membrane protein complex (represented as circles and ovals) containing the Omp85/YaeT protein is involved in the translocation of the autotransporter passenger domain. The passenger has been proposed to be translocated through the β-barrel pore formed by the Omp85/YaeT protein. The passenger domain is shown folded at the cell surface, but the linker region has not (yet) adopted an α-helical conformation.

translocated first and could facilitate the folding of the rest of the passenger domain when it reaches the cell surface (Oliver *et al.*, 2003b). This model dictates that the β-barrel pore should be able to accommodate two stretches of possibly extended polypeptide simultaneously. Based on the size of the β-barrel pore of the NalP translocation unit, the two stretches would almost or just fit (Oomen *et al.*, 2004; Otto *et al.*, 2005). Alternatively, the N-terminal end of the passenger domain could go first through the β-barrel pore. This second model is called the threading model (Oomen *et al.*, 2004). In this model, only one stretch of polypeptide has to be transported through the pore. The unknown and weak part of this model, is the targeting of the N terminus of the passenger domain to the entrance of the channel. A specific N-terminal signal seems not necessary, because it has been shown that heterologous passenger domains could be secreted using the autotransporter system (Jose *et al.*, 1996; Maurer *et al.*, 1997). Another drawback of this model is that the globular catalytic domain instead of the autochaperone domain would be translocated first in this model, and that should have implications the folding of the mature protein at the cell surface.

It is obvious from the diameter of the β-barrel pore of NalP that translocation of (partially) folded proteins through the pore would be impossible. Nevertheless, several authors describe the potential translocation of disulfide bridge-containing proteins across the outer membrane using the autotransporter system with heterologous proteins (Veiga *et al.*, 1999, 2004) or even natural substrates (Brandon and Goldberg, 2001). This, and the observation of ring-like structures of IgA protease translocation units under the electron microscope (Veiga *et al.*, 2002), led to the idea of the so called multimer model. Veiga *et al.* (2002) proposed that the translocation of autotransporter passengers occurs through the central channel of a multimeric assembly of translocation units in the outer membrane. However, because the membrane interface of the translocation units is quite hydrophobic, the central cavity of a multimer would likely be filled with outer membrane lipids (Oomen *et al.*, 2004). A large pore in the outer membrane would also be quite harmful for a bacterial cell. An extensive search for oligomeric structures of AIDA translocation units using a variety of techniques could not demonstrate higher-order structures other than a small percentage of dimers (Müller *et al.*, 2005). The multimeric rings observed by Veiga *et al.* might possibly be formed by alternating upward and downward oriented molecules, as was also observed in the crystals of the NalP translocation unit (Oomen *et al.*, 2004). Based on these later findings, it seems that oligomeric rings are most likely not functional moieties *in vivo*. Besides, the initial observations of the translocation of disulfide-bridge containing proteins across the outer membrane also

deserve more attention. For the *Shigella flexneri* autotransporter IcsA it was found that a DsbB-dependent disulfide-bridge could be formed, suggesting this had to take place in the periplasm (Brandon and Goldberg, 2001). However, the surface localization of IcsA was not dependent on the presence of DsbB.

Finally, a fourth model for the outer membrane translocation of autotransporter proteins was proposed by Oomen *et al.* (Oomen *et al.*, 2004). This model could be referred to as the Omp85 model. This model is based on the observation that autotransporter secretion depends on the presence of the conserved Omp85 protein in meningococci (Voulhoux *et al.*, 2003). It has been proposed that the autotransporter passenger is translocated through the Omp85 outer membrane pore instead of through the translocation unit pore. This hypothesis needs further investigations. It is likely that the Omp85 protein is involved in the assembly of outer membrane proteins in the membrane (Voulhoux *et al.*, 2003). This is supported by recent findings of an outer membrane protein complex in *E. coli*, containing a homologue of Omp85, YaeT (Wu *et al.*, 2005). However, not all outer membrane proteins are mislocalized after depletion of Omp85 (Genevrois *et al.*, 2003).

In conclusion, all four models for outer membrane translocation of autotransporters have their drawbacks or unresolved questions. Besides, it should be taken into consideration that not all autotransporters have to use exactly the same translocation mechanism. For instance, the modular organization of the AIDA translocation unit is different from that of NalP in having a surface-exposed β1-domain attached to the transmembrane pore (Konieczny *et al.*, 2001; Mogensen *et al.*, 2005). Also, the pore size of the PalA translocation unit appears to be circa 2 nm, significantly larger than that of NalP (Lee and Byun, 2003). It is clear that further research is necessary to elucidate the mechanism by which autotransporter passengers cross the outer membrane. In this respect it is noteworthy to point to the dimeric structures of refolded Hbp translocation units, as described in chapter 5. It would be highly interesting to know whether these dimers have a physiological function, also with respect to the observed dimers of the AIDA translocation units by Müller *et al.* (2005).

α-Enolase (P46)

In chapter 5, the identification, cloning and molecular characterization of the α-enolase P46 of *B. fragilis* is described. This 46-kDa protein was shown to be the functionalα-enolase of *B. fragilis*. Surprisingly, the protein was identified as an iron-

regulated protein, upregulated under conditions of iron- or heme-starvation. This property is often observed for bacterial virulence factors, because bacteria have to be able to grow under the conditions of low iron concentrations in the human body (Finlay and Falkow, 1997; Wandersman and Delepelaire, 2004). The iron-regulation of P46 could point to a role for the protein in the virulence of *B. fragilis* in intra-abdominal infections. Interestingly, several α-enolases of Gram-positive bacteria and eukaryotic cells were shown to function as plasminogen-binding molecules at the cell surface (Redlitz *et al.*, 1995; Pancholi and Fischetti, 1998; Bergmann *et al.*, 2001; Jolodar *et al.*, 2003; Jong *et al.*, 2003). However, subcellular localization experiments showed that P46 was not present at the cell surface, but it is mainly located in the cytoplasm and to a lesser extent in the inner membranes. Curiously, under iron-restricted conditions, moreof P46 is located in or at the inner membranes. The nature of the interaction of P46 with the membrane has to be studied in more detail, for instance using the blue native-PAGE technique (Stenberg *et al.*, 2005). It is possible that this interaction is related to the presence of α-enolase in the RNA degradosome complex at the inner membrane (Liou *et al.*, 2001). These multi-enzyme complexes are involved in the processing and degradation of mRNAs (Carpousis *et al.*, 1994). It is tempting to speculate that the subcellular redistribution of P46 is due to the presence of this protein in the degradosomes, especially under iron-limited conditions. It has been shown that α-enolase plays a crucial role in the processing of mRNA under conditions of cellular stress (Morita *et al.*, 2004), which could very well be the case under iron-limited conditions. Alternatively, the upregulation of P46 under iron- and heme-limited conditions could have an energetic background. At low concentrations of heme, *B. fragilis* cells depend on glycolysis and on lactate and malate as energy sources for ATP generation (Macy *et al.*, 1978; Chen and Wolin, 1981). In an intra-abdominal abscess, lactate may become the predominant carbon source instead of glucose. An increased expression of glycolytic enzymes, like α-enolase, might be a way to compensate for the lower energy yield from these alternative carbon sources.

The absence of P46 at the cell surface of *B. fragilis* makes it unlikely that P46 functions as a plasminogen-binding protein. Plasminogen-binding activity could not be detected for P46. This is consistent with the lack of known plasminogen-binding motifs in P46. This protein contains neither a C-terminal lysine, nor the consensus FYDKERKVY motif. These motifs were shown to be necessary for plasminogen-binding by Gram-positive α-enolases (Pancholi and Fischetti, 1998; Bergmann *et al.*, 2001; Bergmann *et al.*, 2003). However, the role for the C-terminal lysine in plasminogen-binding has become questionable by the recent publication of

the crystal structure of *S. pneumoniae* α-enolase (Ehinger *et al.*, 2004). In this structure, the α-enolase is present as an octamer in which the C-terminal lysines are shielded from the environment. In contrast, the internal motif FYDKERKVY is exposed to the surface of the octamer. It should be noted that the role for the C-terminal lysine in plasminogen-binding is commonly assayed by solid phase assays: the so called blot overlay assay (Miles *et al.*, 1991; Pancholi and Fischetti, 1998; Bergmann *et al.*, 2001). In this assay, the α-enolase is subjected to SDS-PAGE and Western blotting in the denatured form. Then, the blot is incubated with native plasminogen, and subsequently probed for bound plasminogen. One could envision binding of a freely available C-terminal lysine residue to the plasminogen Kringle domains, while this would not be possible with the α-enolase in its native conformation (Bergmann *et al.*, 2003). Therefore, results from these solid phase assays should always be supported by (*in vivo*) experiments using properly folded protein. The C-terminal lysine residues of *S. pyogenes* surface enolase (SEN) were shown to contribute significantly to the plasminogen-binding activity and penetration of the extracellular matrix (ECM) of intact Group A streptococci (Derbise *et al.*, 2004). However, recently, the internal plasminogen-binding motif in *S. pneumoniae* α-enolase (Eno) was shown to be the key cofactor for plasmin-mediated degradation of extracellular matrix proteins and transmigration through ECM by pneumococci (Bergmann *et al.*, 2005).

Plasminogen-binding protein (Pbp)

Instead of the α-enolase P46, another protein in *B. fragilis* was identified as a possible plasminogen-binding protein (Sijbrandi *et al.*, 2005). This 60-kDa protein is referred to as Pbp for Plasminogen-binding protein (chapter 5, chapter 6). It was found that Pbp-like proteins are present in other *Bacteroides* subspecies. Subcellular localization experiments showed that Pbp and Pbp-like proteins are located in or at the outer membrane. *B. fragilis* Pbp was found to be accessible to extracellular protease, suggesting a cell-surface localization for this protein. The plasminogen-binding properties of Pbp were studied in a solid phase assay. The lack of plasminogen-binding of a C-terminally His-tagged version of the protein in *E. coli* suggests that the C-terminal lysine residue is important for the plasminogen-binding activity. The blot overlay assay also demonstrated plasminogen-binding properties for Pbp-like proteins of other *Bacteriodes* subspecies. As discussed above, the results of these solid phase assays should be supported by experiments using

correctly folded protein. Additionally, the *in vivo* relevance of the plasminogen-binding activity of Pbp should be investigated.

Finally, analysis of the primary structure of Pbp showed that the protein is probably a lipoprotein. Although this prediction still has to be confirmed experimentally, the possibility of a surface localized lipoprotein in *B. fragilis* raises an interesting question regarding the targeting of *B. fragilis* lipoproteins. *In silico* analysis of the *B. fragilis* genome showed that the organism probably possesses genes encoding a specific lipoprotein signal peptidase and a diacylglycerol transferase. Both proteins are essential for the processing of prelipoproteins at the inner membrane, at least in *E. coli* (Wu, 1996). However, no homologs of *lolA*, *-B*, *-C* and *-E* were found in the *B. fragilis* genome, while these genes and their products are essential for the targeting of lipoproteins to the outer membrane in *E. coli* (Narita *et al.*, 2002; Narita *et al.*, 2004). It would be very interesting to identify the targeting factors that direct Pbp to the outer membrane, when Pbp is indeed a genuine lipoprotein.

Concluding remarks

In this thesis, three proteins were analyzed that could play a role as virulence factors in the bacterial synergy between *E. coli* and *B. fragilis* in human intra-abdominal infections: Hbp, P46 and Pbp (Fig. 4).

For Hbp, a role in the synergistic abscess formation in these infections has already been demonstrated using a murine infection model (Otto *et al.*, 2002). Hbp has shown to contribute to the heme-dependent growth of *B. fragilis*. It is very likely that *E. coli* itself can also benefit directly from the secretion of this hemoglobin protease in a similar fashion.

Based on the finding that Pbp might be a plasminogen-binding factor on the surface of *B. fragilis* cells, a role for this protein as a virulence factor can be envisioned. Binding of plasminogen and conversion to plasmin increases the proteolytic potential of the cell and creates to possibility to degrade the fibrin network that the host uses to trap the microorganisms, thereby preventing that bacteria emerge into the circulation. The contribution of both Hbp and Pbp to abscess formation in bacterial peritonitis will be further tested in a rat infection model (Bosscha *et al.*, 2000).

A potential role for P46 in the virulence of *B. fragilis* and in intra-abdominal infections is more difficult to envision.

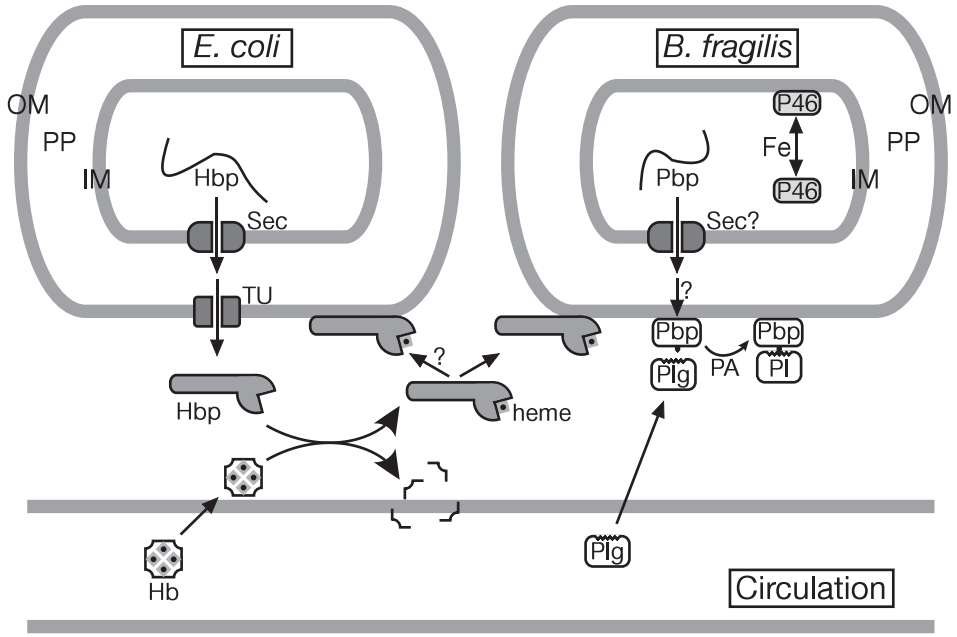

Fig. 4. Model for the synergy of *E. coli* and *B. fragilis* in intra-abdominal infections, including the proteins described in this thesis. In *E. coli*, the Hbp protein is synthesized and secreted through the Sec-translocon (Sec) and the Hbp translocation unit (TU). After folding and secretion, Hbp degrades hemoglobin (Hb) and binds the released heme moiety. The hemoglobin may have been released from circulating red blood cells by the action of hemolysins secreted by *B. fragilis* (not shown). The holo-Hbp molecule is probably recognized and bound by a proteinaceous outer membrane (OM) component of *B. fragilis* and very likely also *E. coli*, after which heme uptake takes place (not shown). The α-enolase P46 is localized intracellularly in *B. fragilis* where it functions in glycolysis. Under iron (Fe)-limited conditions, P46 is upregulated and redistributed to the inner membrane (IM) where it may form part of the RNA degradosome complex. *B. fragilis* also produces the plasminogen binding protein Pbp. Pbp is probably translocated across the IM through the Sec-translocon, after which cleavage of the signal peptide of this putative lipoprotein takes place by Signal peptidase II (SPaseII, not shown). After lipidation, the molecule is transferred to the OM, where translocation takes place through an unknown mechanism. Once localized at the cell surface, Pbp is able to bind circulating host plasminogen (Plg). By the action of plasminogen activators (PA), Plg is converted to the protease plasmin (Pl). This gives the bacterium the ability to degrade fibrin and extracellular matrix proteins at the site of infection.

The three-dimensional structures of the Hbp translocation unit, P46 and Pbp would be a very useful tool in the study of these proteins. Currently, attempts are being made to elucidate the crystal structures of all these proteins. It is expected that the research described in this thesis, upcoming results and suggested future studies on Hbp, P46 and Pbp will help in the understanding of the molecular mechanism of the bacterial synergy between *E. coli* and *B. fragilis* in human intra-abdominal infections. This knowledge in turn may help in the prevention and/or treatment of these life-threatening infections in the future.

References

Adhikari, P., Kirby, S.D., Nowalk, A.J., Veraldi, K.L., Schryvers, A.B., and Mietzner, T.A. (1995) Biochemical characterization of a *Haemophilus influenzae* periplasmic iron transport operon. *J Biol Chem* **270**: 25142-25149.

Aldridge, K.E., Gelfand, M., Reller, L.B., Ayers, L.W., Pierson, C.L., Schoenknecht, F., Tilton, R.C., Wilkins, J., Henderberg, A., Schiro, D.D., and et al. (1994) A five-year multicenter study of the susceptibility of the *Bacteroides fragilis* group isolates to cephalosporins, cephamins, penicillins, clindamycin, and metronidazole in the United States. *Diagn Microbiol Infect Dis* **18**: 235-241.

Aldridge, K.E. (1995) The occurrence, virulence, and antimicrobial resistance of anaerobes in polymicrobial infections. *Am J Surg* **169**: S2-S7.

Altemeier, W.A. (1942) The pathogenicity of the bacteria of appendicitis peritonitis. *Surgery* **11**: 374-378.

Anaya, D.A., and Nathens, A.B. (2003) Risk factors for severe sepsis in secondary peritonitis. *Surg Infect (Larchmt)* **4**: 355-362.

Andronicos, N.M., Baker, M.S., Lackmann, M., and Ranson, M. (2000) Deconstructing the interaction of glu-plasminogen with its receptor [alpha]-enolase. *Fibrinolysis and Proteolysis* **14**: 327-336.

Arnoux, P., Haser, R., Izadi, N., Lecroisey, A., Delepierre, M., Wandersman, C., and Czjzek, M. (1999) The crystral structure of HasA, a hemophore secreted by *Serratia marcescens*. *Nat Struct Biol* **6**: 516-520.

Bagos, P.G., Liakopoulos, T.D., Spyropoulos, I.C., and Hamodrakas, S.J. (2004) PRED-TMBB: a web server for predicting the topology of beta-barrel outer membrane proteins. *Nucleic Acids Res* **32**: W400-404.

Baichoo, N., and Helmann, J.D. (2002) Recognition of DNA by Fur: a reinterpretation of the Fur box consensus sequence. *J Bacteriol* **184**: 5826-5832.

Batey, R.T., Rambo, R.P., Lucast, L., Rha, B., and Doudna, J.A. (2000) Crystal structure of the ribonucleoprotein core of the signal recognition particle. *Science* **287**: 1232-1239.

Bendtsen, J.D., Nielsen, H., von Heijne, G., and Brunak, S. (2004) Improved prediction of signal peptides: SignalP 3.0. *J Mol Biol* **340**: 783-795.

Benjelloun-Touimi, Z., Sansonetti, P.J., and Parsot, C. (1995) SepA, the major extracellular protein of *Shigella flexneri*: Autonomous secretion and involvement in tissue invasion. *Mol Microbiol* **17**: 123-135.

Benz, I., and Schmidt, M.A. (1992) AIDA-I, the Adhesin Involved in Diffuse Adherence of the Diarrheogenic *Escherichia coli* Strain-2787 (O126-H27), Is Synthesized via a Precursor Molecule. *Mol Microbiol* **6**: 1539-1546.

Bergman, A.C., Linder, C., Sakaguchi, K., Sten-Linder, M., Alaiya, A.A., Franzen, B., Shoshan, M.C., Bergman, T., Wiman, B., Auer, G., Appella, E., Jornvall, H., and Linder, S. (1997) Increased expression of alpha-enolase in c-jun transformed rat fibroblasts without increased activation of plasminogen. *FEBS Lett* **417**: 17-20.

Bergmann, S., Rohde, M., Chhatwal, G.S., and Hammerschmidt, S. (2001) alpha-Enolase of *Streptococcus pneumoniae* is a plasmin(ogen)-binding protein displayed on the bacterial cell surface. *Mol Microbiol* **40**: 1273-1287.

Bergmann, S., Wild, D., Diekmann, O., Frank, R., Bracht, D., Chhatwal, G.S., and Hammerschmidt, S. (2003) Identification of a novel plasmin(ogen)-binding motif in surface displayed alpha-enolase of *Streptococcus pneumoniae*. *Mol Microbiol* **49**: 411-423.

Bergmann, S., Rohde, M., Preissner, K.T., and Hammerschmidt, S. (2005) The nine residue plasminogen-binding motif of the pneumococcal enolase is the major cofactor of plasmin-mediated degradation of extracellular matrix, dissolution of fibrin and transmigration. *Thromb Haemost* **94**: 304-311.

Berks, B.C., Sargent, F., and Palmer, T. (2000) The Tat protein export pathway. *Mol Microbiol* **35**: 260-274.

Bernstein, H.D., and Hyndman, J.B. (2001) Physiological Basis for Conservation of the Signal Recognition Particle Targeting Pathway in *Escherichia coli*. *J Bacteriol* **183**: 2187-2197.

Bosscha, K., van Vroonhoven, T.J., and van der Werken, C. (1999) Surgical management of severe secondary peritonitis. *Br J Surg* **86**: 1371-1377.

Bosscha, K., Nieuwenhuijs, V.B., Gooszen, A.W., van Duijvenbode-Beumer, H., Visser, M.R., Verweij, W.R., and Akkermans, L.M. (2000) A standardised and reproducible model of intraabdominal infection and abscess formation in rats. *Eur J Surg* **166**: 963-967.

Boulton, I.C., Gorringe, A.R., Shergill, J.K., Joannou, C.L., and Evans, R.W. (1999) A dynamic model of the meningococcal transferrin receptor. *J Theor Biol* **198**: 497-505.

Bracken, C.S., Baer, M.T., Abdur-Rashid, A., Helms, W., and Stojiljkovic, I. (1999) Use of heme-protein complexes by the *Yersinia enterocolitica* HemR receptor: histidine residues are essential for receptor function. *J Bacteriol* **181**: 6063-6072.

Brandon, L.D., and Goldberg, M.B. (2001) Periplasmic transit and disulfide bond formation of the autotransported *Shigella* protein IcsA. *J Bacteriol* **183**: 951-958.

Brandon, L.D., Goehring, N., Janakiraman, A., Yan, A.W., Wu, T., Beckwith, J., and Goldberg, M.B. (2003) IcsA, a polarly localized autotransporter with an atypical signal peptide, uses the Sec apparatus for secretion, although the Sec apparatus is circumferentially distributed. *Mol Microbiol* **50**: 45-60.

Braun, V. (2001) Iron uptake mechanisms and their regulation in pathogenic bacteria. *Int J Med Microbiol* **291**: 67-79.

Braun, V., and Braun, M. (2002a) Active transport of iron and siderophore antibiotics. *Curr Opin Microbiol* **5**: 194-201.

Braun, V., and Braun, M. (2002b) Iron transport and signaling in *Escherichia coli*. *FEBS Lett* **529**: 78-85.

Braun, V. (2003) Iron uptake by Escherichia coli. *Front Biosci* **8**: s1409-1421.

Brickman, T.J., and McIntosh, M.A. (1992) Overexpression and purification of ferric enterobactin esterase from *Escherichia coli*. Demonstration of enzymatic hydrolysis of enterobactin and its iron complex. *J Biol Chem* **267**: 12350-12355.

Brook, I., Hunter, V., and Walker, R.I. (1984) Synergistic effect of *Bacteroides*, *Clostridium*, *Fusobacterium*, anaerobic cocci, and aerobic bacteria on mortality and induction of subcutaneous abscesses in mice. *J Infect Dis* **149**: 924-928.

Brook, I. (1985) Enhancement of growth of aerobic and facultative bacteria in mixed infections with Bacteroides species. *Infect Immun* **50**: 929-931.

Brook, I. (1988) Recovery of anaerobic bacteria from clinical specimens in 12 years at two military hospitals. *J Clin Microbiol* **26**: 1181-1188.

Brook, I. (1989) Anaerobic bacterial bacteremia: 12-year experience in two military hospitals. *J Infect Dis* **160**: 1071-1075.

Brook, I., Myhal, L.A., and Dorsey, C.H. (1992) Encapsulation and pilus formation of *Bacteroides* spp. in normal flora abscesses and blood. *J Infect* **25**: 251-257.

Brook, I., and Gillmore, J.D. (1994) Increased resistance of encapsulated Bacteroides fragilis to clindamycin. *Chemotherapy* **40**: 16-20.

Broze, G.J., Jr. (1995) Tissue factor pathway inhibitor and the current concept of blood coagulation. *Blood Coagul Fibrinolysis* **6 Suppl 1**: S7-13.

Brummel, K.E., Paradis, S.G., Butenas, S., and Mann, K.G. (2002) Thrombin functions during tissue factor-induced blood coagulation. *Blood* **100**: 148-152.

Brunder, W., Schmidt, H., and Karch, H. (1997) EspP, a novel extracellular serine protease of enterohaemorrhagic *Escherichia coli* O157:H7 cleaves human coagulation factor V. *Mol Microbiol* **24**: 767-778.

Brunger, A.T. (1996) *X-PLOR version 3.85.* New Haven, CT.: Yale University Press.

Bryant, R.E., Rashad, A.L., Mazza, J.A., and Hammond, D. (1980) beta-Lactamase activity in human pus. *J Infect Dis* **142**: 594-601.

Buchanan, S.K., Smith, B.S., Venkatramani, L., Xia, D., Esser, L., Palnitkar, M., Chakraborty, R., van der Helm, D., and Deisenhofer, J. (1999) Crystal structure of the outer membrane active transporter FepA from *Escherichia coli*. *Nat Struct Biol* **6**: 56-63.

Bulieris, P.V., Behrens, S., Holst, O., and Kleinschmidt, J.H. (2003) Folding and insertion of the outer membrane protein OmpA is assisted by the chaperone Skp and by lipopolysaccharide. *J Biol Chem* **278**: 9092-9099.

Bullen, J.J., Rogers, H.J., Spalding, P.B., and Ward, C.G. (2005) Iron and infection: the heart of the matter. *FEMS Immunol Med Microbiol* **43**: 325-330.

Caldwell, M.T., and Watson, R.G. (1994) Peritoneal aspiration cytology as a diagnostic aid in acute appendicitis. *Br J Surg* **81**: 276-278.

Camiolo, S.M., Thorsen, S., and Astrup, T. (1971) Fibrinogenolysis and fibrinolysis with tissue plasminogen activator, urokinase, streptokinase-activated human globulin, and plasmin. *Proc Soc Exp Biol Med* **138**: 277-280.

Carpousis, A.J., Van Houwe, G., Ehretsmann, C., and Krisch, H.M. (1994) Copurification of *E. coli* RNAase E and PNPase: evidence for a specific association between two enzymes important in RNA processing and degradation. *Cell* **76**: 889-900.

Carrondo, M.A. (2003) Ferritins, iron uptake and storage from the bacterioferritin viewpoint. *EMBO J* **22**: 1959-1968.

Casadaban, M.J. (1976) Transposition and fusion of the lac genes to selected promoters in *Escherichia coli* using bacteriophage lambda and Mu. *J Mol Biol* **104**: 541-555.

Castellino, F.J. (1984) Biochemistry of human plasminogen. *Semin Thromb Hemost* **10**: 18-23.

Chandler, W.L., Trimble, S.L., Loo, S.C., and Mornin, D. (1990) Effect of PAI-1 levels on the molar concentrations of active tissue plasminogen activator (t-PA) and t-PA/PAI-1 complex in plasma. *Blood* **76**: 930-937.

Chang, A.C.Y., and Cohen, S.N. (1978) Construction and characterization of amplifiable multicopy DNA cloning vehicles derived from the p15A cryptic miniplasmid. *J Bacteriol* **134**: 1141-1156.

Chang, Y., Mochalkin, I., McCance, S.G., Cheng, B., Tulinsky, A., and Castellino, F.J. (1998) Structure and ligand binding determinants of the recombinant kringle 5 domain of human plasminogen. *Biochemistry* **37**: 3258-3271.

Charles, I., Fairweather, N., Pickard, D., Beesley, J., Anderson, R., Dougan, G., and Roberts, M. (1994) Expression of the *Bordetella pertussis* P.69 pertactin adhesin in *Escherichia coli*: fate of the carboxy-terminal domain. *Microbiology* **140 (Pt 12)**: 3301-3308.

Chen, M., and Wolin, M.J. (1981) Influence of heme and vitamin B12 on growth and fermentations of *Bacteroides* species. *J Bacteriol* **145**: 466-471.

Cheng, L.W., and Schneewind, O. (2000) Type III machines of Gram-negative bacteria: delivering the goods. *Trends Microbiol* **8**: 214-220.

Chevalier, N., Moser, M., Koch, H.G., Schimz, K.L., Willery, E., Locht, C., Jacob-Dubuisson, F., and Muller, M. (2004) Membrane targeting of a bacterial virulence factor harbouring an extended signal peptide. *J Mol Microbiol Biotechnol* **8**: 7-18.

Clantin, B., Hodak, H., Willery, E., Locht, C., Jacob-Dubuisson, F., and Villeret, V. (2004) The crystal structure of filamentous hemagglutinin secretion domain and its implications for the two-partner secretion pathway. *Proc Natl Acad Sci U S A* **101**: 6194-6199.

Clarke, T.E., Braun, V., Winkelmann, G., Tari, L.W., and Vogel, H.J. (2002) X-ray crystallographic structures of the *Escherichia coli* periplasmic protein FhuD bound to hydroxamate-type siderophores and the antibiotic albomycin. *J Biol Chem* **277**: 13966-13972.

Coleman, J.L., Gebbia, J.A., Piesman, J., Degen, J.L., Bugge, T.H., and Benach, J.L. (1997) Plasminogen is required for efficient dissemination of *B. burgdorferi* in ticks and for enhancement of spirochetemia in mice. *Cell* **89**: 1111-1119.

Collaborative Computational Project, N. (1994) The CCP4 suite: programs for protein crystallography. *Acta Crystallogr D Biol Crystallogr* **50**: 760-763.

Cope, L.D., Thomas, S.E., Latimer, J.T., Slaughter, C.A., Mullereberhard, U., and Hansen, E.J. (1994) The 100 kDa haem:haemopexin-binding protein of *Haemophilus influenzae*: Structure and localization. *Mol Microbiol* **13**: 863-873.

Cope, L.D., Yogev, R., Muller-Eberhard, U., and Hansen, E.J. (1995) A gene cluster involved in the utilization of both free heme and heme:hemopexin by *Haemophilus influenzae*. *J Bacteriol* **177**: 2644-2653.

Cornelissen, C.N. (2003) Transferrin-iron uptake by Gram-negative bacteria. *Front Biosci* **8**: d836-847.

Cotter, S.E., Surana, N.K., and St Geme, J.W., 3rd (2005) Trimeric autotransporters: a distinct subfamily of autotransporter proteins. *Trends Microbiol* **13**: 199-205.

Cuchural, G.J., Jr., and Tally, F.P. (1986) *Bacteroides fragilis*: current susceptibilities, mechanisms of drug resistance, and principles of antimicrobial therapy. *Drug Intell Clin Pharm* **20**: 567-573.

Darling, G.E., Duff, J.H., Mustard, R.A., and Finley, R.J. (1988) Multiorgan failure in critically ill patients. *Can J Surg* **31**: 172-176.

Davis, J., Smith, A.L., Hughes, W.R., and Golomb, M. (2001) Evolution of an Autotransporter: Domain Shuffling and Lateral Transfer from Pathogenic *Haemophilus* to *Neisseria*. *J Bacteriol* **183**: 4626-4635.

de Cock, H., Brandenburg, K., Wiese, A., Holst, O., and Seydel, U. (1999) Non-lamellar structure and negative charges of lipopolysaccharides required for efficient folding of outer membrane protein PhoE of *Escherichia coli*. *J Biol Chem* **274**: 5114-5119.

de Gier, J.W., Mansournia, P., Valent, Q.A., Phillips, G.J., Luirink, J., and von Heijne, G. (1996) Assembly of a cytoplasmic membrane protein in *Escherichia coli* is dependent on the signal recognition particle. *FEBS Lett* **399**: 307-309.

de Gier, J.W., and Luirink, J. (2001) Biogenesis of inner membrane proteins in *Escherichia coli*. *Mol Microbiol* **40**: 314-322.

Delepelaire, P., and Wandersman, C. (1998) The SecB chaperone is involved in the secretion of the *Serratia marcescens* HasA protein through an ABC transporter. *EMBO J* **17**: 936-944.

den Blaauwen, T., Aarsman, M.E., Vischer, N.O., and Nanninga, N. (2003) Penicillin-binding protein PBP2 of *Escherichia coli* localizes preferentially in the lateral wall and at mid-cell in comparison with the old cell pole. *Mol Microbiol* **47**: 539-547.

Derbise, A., Song, Y.P., Parikh, S., Fischetti, V.A., and Pancholi, V. (2004) Role of the C-terminal lysine residues of streptococcal surface enolase in glu- and lys-plasminogen-binding activities of group a streptococci. *Infect Immun* **72**: 94-105.

Desvaux, M., Parham, N.J., and Henderson, I.R. (2004) The autotransporter secretion system. *Res Microbiol* **155**: 53-60.

Dev, I.K., Harvey, R.J., and Ray, P.H. (1985) Inhibition of prolipoprotein signal peptidase by globomycin. *J Biol Chem* **260**: 5891-5894.

Dhungana, S., Taboy, C.H., Anderson, D.S., Vaughan, K.G., Aisen, P., Mietzner, T.A., and Crumbliss, A.L. (2003) The influence of the synergistic anion on iron chelation by ferric binding protein, a bacterial transferrin. *Proc Natl Acad Sci U S A* **100**: 3659-3664.

Dozois, C.M., Dho-Moulin, M., Bree, A., Fairbrother, J.M., Desautels, C., and Curtiss, R., 3rd (2000) Relationship between the Tsh autotransporter and pathogenicity of avian

Escherichia coli and localization and analysis of the Tsh genetic region. *Infect Immun* **68**: 4145-4154.

Drechsel, H., and Jung, G. (1998) Peptide siderophores. *J Pept Sci* **4**: 147-181.

Dunn, D.L., Rotstein, O.D., and Simmons, R.L. (1984) Fibrin in peritonitis. IV. Synergistic intraperitoneal infection caused by *Escherichia coli* and *Bacteroides fragilis* within fibrin clots. *Arch Surg* **119**: 139-144.

Dutta, P.R., Cappello, R., Navarro-Garcia, F., and Nataro, J.P. (2002) Functional Comparison of Serine Protease Autotransporters of *Enterobacteriaceae*. *Infect Immun* **70**: 7105-7113.

Egile, C., d'Hauteville, H., Parsot, C., and Sansonetti, P.J. (1997) SopA, the outer membrane protease responsible for polar localization of IcsA in *Shigella flexneri*. *Mol Microbiol* **23**: 1063-1073.

Ehinger, S., Schubert, W.D., Bergmann, S., Hammerschmidt, S., and Heinz, D.W. (2004) Plasmin(ogen)-binding alpha-Enolase from *Streptococcus pneumoniae*: Crystal Structure and Evaluation of Plasmin(ogen)-binding Sites. *J Mol Biol* **343**: 997-1005.

Emsley, P., Charles, I.G., Fairweather, N.F., and Isaacs, N.W. (1996) Structure of *Bordetella pertussis* virulence factor P.69 pertactin. *Nature* **381**: 90-92.

Eslava, C., NavarroGarcia, F., Czeczulin, J.R., Henderson, I.R., Cravioto, A., and Nataro, J.P. (1998) Pet, an autotransporter enterotoxin from enteroaggregative *Escherichia coli*. *Infect Immun* **66**: 3155-3163.

Evans, R.W., Crawley, J.B., Joannou, C.L., and Sharma, N. (1999) Iron proteins. In *Iron Infection*. Bullen, J.J. and Griffiths, E. (eds). Chichester: John Wiley & Sons.

Faraldo-Gomez, J.D., and Sansom, M.S. (2003) Acquisition of siderophores in gram-negative bacteria. *Nat Rev Mol Cell Biol* **4**: 105-116.

Farthmann, E.H., and Schöffel, U. (1998) Epidemiology and pathophysiology of intraabdominal infections (IAI). *Infection* **26**: 329-334.

Ferguson, A.D., Hofmann, E., Coulton, J.W., Diederichs, K., and Welte, W. (1998) Siderophore-mediated iron transport: crystal structure of FhuA with bound lipopolysaccharide. *Science* **282**: 2215-2220.

Ferguson, A.D., and Deisenhofer, J. (2004) Metal import through microbial membranes. *Cell* **116**: 15-24.

Finlay, B.B., and Falkow, S. (1997) Common themes in microbial pathogenicity revisited. *Microbiol Mol Biol Rev* **61**: 136-169.

Frost, G.E., and Rosenberg, H. (1975) Relationship between the tonB locus and iron transport in Escherichia coli. *J Bacteriol* **124**: 704-712.

Fuchs, H.E., Shifman, M.A., and Pizzo, S.V. (1982) In vivo catabolism of alpha 1-proteinase inhibitor-trypsin, antithrombin III-thrombin and alpha 2-macroglobulin-methylamine. *Biochim Biophys Acta* **716**: 151-157.

Furrer, J.L., Sanders, D.N., Hook-Barnard, I.G., and McIntosh, M.A. (2002) Export of the siderophore enterobactin in *Escherichia coli*: involvement of a 43 kDa membrane exporter. *Mol Microbiol* **44**: 1225-1234.

Genevrois, S., Steeghs, L., Roholl, P., Letesson, J.J., and van der Ley, P. (2003) The Omp85 protein of *Neisseria meningitidis* is required for lipid export to the outer membrane. *EMBO J* **22**: 1780-1789.

Gentschev, I., Dietrich, G., and Goebel, W. (2002) The E. coli alpha-hemolysin secretion system and its use in vaccine development. *Trends Microbiol* **10**: 39-45.

Ghigo, J.M., Létoffé, S., and Wandersman, C. (1997) A new type of hemophore-dependent heme acquisition system of *Serratia marcescens* reconstituted in *Escherichia coli*. *J Bacteriol* **179**: 3572-3579.

Goldner, M., Coquis-Rondon, M., and Carlier, J.P. (1991) Demonstration by confocal laserscanning microscopy of invasive potential with *Bacteroides fragilis*. *Microbiologica* **14**: 71-75.

Goldstein, E.J., and Citron, D.M. (1988) Annual incidence, epidemiology, and comparative in vitro susceptibilities to cefoxitin, cefotetan, cefmetazole, and ceftizoxime of recent community-acquired isolates of the *Bacteroides fragilis* group. *J Clin Microbiol* **26**: 2361-2366.

Gomez, J.A., Criado, M.T., and Ferreiros, C.M. (1998) Cooperation between the components of the meningococcal transferrin receptor, TbpA and TbpB, in the uptake of transferrin iron by the 37-kDa ferric-binding protein (FbpA). *Res Microbiol* **149**: 381-387.

Grass, S., and St Geme, J.W., 3rd (2000) Maturation and secretion of the non-typable *Haemophilus influenzae* HMW1 adhesin: roles of the N-terminal and C-terminal domains. *Mol Microbiol* **36**: 55-67.

Guex, N., and Peitsch, M.C. (1997) SWISS-MODEL and the Swiss-PdbViewer: an environment for comparative protein modeling. *Electrophoresis* **18**: 2714-2723.

Gunn, J.S., Lim, K.B., Krueger, J., Kim, K., Guo, L., Hackett, M., and Miller, S.I. (1998) PmrA-PmrB-regulated genes necessary for 4-aminoarabinose lipid A modification and polymyxin resistance. *Mol Microbiol* **27**: 1171-1182.

Guyer, D.M., Henderson, I.R., Nataro, J.P., and Mobley, H.L. (2000) Identification of sat, an autotransporter toxin produced by uropathogenic *Escherichia coli*. *Mol Microbiol* **38**: 53-66.

Hall, J.C., Heel, K.A., Papadimitriou, J.M., and Platell, C. (1998) The pathobiology of peritonitis. *Gastroenterology* **114**: 185-196.

Hantke, K. (1981) Regulation of ferric iron transport in *Escherichia coli* K12: isolation of a constitutive mutant. *Mol Gen Genet* **182**: 288-292.

Hart, P.H., Spencer, L.K., Nulsen, M.F., McDonald, P.J., and Finlay-Jones, J.J. (1986) Neutrophil activity in abscess-bearing mice: comparative studies with neutrophils isolated from peripheral blood, elicited peritoneal exudates, and abscesses. *Infect Immun* **51**: 936-941.

Hau, T., Ahrenholz, D.H., and Simmons, R.L. (1979) Secondary bacterial peritonitis: the biologic basis of treatment. *Curr Probl Surg* **16**: 1-65.

Heithoff, D.M., Conner, C.P., Hanna, P.C., Julio, S.M., Hentschel, U., and Mahan, M.J. (1997) Bacterial infection as assessed by in vivo gene expression. *Proc Natl Acad Sci U S A* **94**: 934-939.

Henderson, I.R., Navarro-Garcia, F., and Nataro, J.P. (1998) The great escape: structure and function of the autotransporter proteins. *Trends Microbiol* **6**: 370-378.

Henderson, I.R., Czeczulin, J., Eslava, C., Noriega, F., and Nataro, J.P. (1999) Characterization of pic, a secreted protease of *Shigella flexneri* and enteroaggregative *Escherichia coli*. *Infect Immun* **67**: 5587-5596.

Henderson, I.R., Cappello, R., and Nataro, J.P. (2000a) Autotransporter proteins, evolution and redefining protein secretion. *Trends Microbiol* **8**: 529-532.

Henderson, I.R., Nataro, J.P., Kaper, J.B., Meyer, T.F., Farrand, S.K., Burns, D.L., Finlay, B.B., and St Geme, J.W., 3rd (2000b) Renaming protein secretion in the Gram-negative bacteria. *Trends Microbiol* **8**: 352.

Henderson, I.R., and Nataro, J.P. (2001) Virulence Functions of Autotransporter Proteins. *Infect Immun* **69**: 1231-1243.

Henderson, I.R., Navarro-Garcia, F., Desvaux, M., Fernandez, R.C., and Ala'aldeen, D. (2004) Type V protein secretion pathway: the autotransporter story. *Microbiol Mol Biol Rev* **68**: 692-744.

Hendrixson, D.R., de la Morena, M.L., Stathopoulos, C., and St Geme, J.W., 3rd (1997) Structural determinants of processing and secretion of the *Haemophilus influenzae* Hap protein. *Mol Microbiol* **26**: 505-518.

Herskovits, A.A., Bochkareva, E.S., and Bibi, E. (2000) New prospects in studying the bacterial signal recognition particle pathway. *Mol Microbiol* **38**: 927-939.

Higgs, P.I., Larsen, R.A., and Postle, K. (2002) Quantification of known components of the *Escherichia coli* TonB energy transduction system: TonB, ExbB, ExbD and FepA. *Mol Microbiol* **44**: 271-281.

Hoffman, M. (2003) Remodeling the blood coagulation cascade. *J Thromb Thrombolysis* **16**: 17-20.

Holm, L., and Sander, C. (1993) Protein structure comparison by alignment of distance matrices. *J Mol Biol* **233**: 123-138.

Holm, L., and Sander, C. (1995) Dali: a network tool for protein structure comparison. *Trends Biochem Sci* **20**: 478-480.

Houben, E.N., Scotti, P.A., Valent, Q.A., Brunner, J., de Gier, J.L., Oudega, B., and Luirink, J. (2000) Nascent Lep inserts into the *Escherichia coli* inner membrane in the vicinity of YidC, SecY and SecA. *FEBS Lett* **476**: 229-233.

Hu, K.H., Liu, E., Dean, K., Gingras, M., DeGraff, W., and Trun, N.J. (1996) Overproduction of three genes leads to camphor resistance and chromosome condensation in *Escherichia coli*. *Genetics* **143**: 1521-1532.

Hu, L.T., Pratt, S.D., Perides, G., Katz, L., Rogers, R.A., and Klempner, M.S. (1997) Isolation, cloning, and expression of a 70-kilodalton plasminogen binding protein of *Borrelia burgdorferi*. *Infect Immun* **65**: 4989-4995.

Huber, D., Boyd, D., Xia, Y., Olma, M.H., Gerstein, M., and Beckwith, J. (2005) Use of thioredoxin as a reporter to identify a subset of *Escherichia coli* signal sequences that promote signal recognition particle-dependent translocation. *J Bacteriol* **187**: 2983-2991.

Ingham, H.R., Sisson, P.R., Tharagonnet, D., Selkon, J.B., and Codd, A.A. (1977) Inhibition of phagocytosis in vitro by obligate anaerobes. *Lancet* **2**: 1252-1254.

Izadi, N., Henry, Y., Haladjian, J., Goldberg, M.E., Wandersman, C., Delepierre, M., and Lecroisey, A. (1997) Purification and characterization of an extracellular heme-binding protein, HasA, involved in heme iron acquisition. *Biochemistry* **36**: 7050-7057.

Jacob-Dubuisson, F., Locht, C., and Antoine, R. (2001) Two-partner secretion in Gram-negative bacteria: a thrifty, specific pathway for large virulence proteins. *Mol Microbiol* **40**: 306-313.

Jacob-Dubuisson, F., Fernandez, R., and Coutte, L. (2004) Protein secretion through autotransporter and two-partner pathways. *Biochim Biophys Acta* **1694**: 235-257.

Jenkins, J., and Pickersgill, R. (2001) The architecture of parallel beta-helices and related folds. *Prog Biophys Mol Biol* **77**: 111-175.

Jolodar, A., Fischer, P., Bergmann, S., Buttner, D.W., Hammerschmidt, S., and Brattig, N.W. (2003) Molecular cloning of an alpha-enolase from the human filarial parasite *Onchocerca volvulus* that binds human plasminogen. *Biochim Biophys Acta* **1627**: 111-120.

Jones, T.A., Zou, J.Y., Cowan, S.W., and Kjeldgaard (1991) Improved methods for building protein models in electron density maps and the location of errors in these models. *Acta Crystallogr A* **47 (Pt 2)**: 110-119.

Jong, A.Y., Chen, S.H., Stins, M.F., Kim, K.S., Tuan, T.L., and Huang, S.H. (2003) Binding of *Candida albicans* enolase to plasmin(ogen) results in enhanced invasion of human brain microvascular endothelial cells. *J Med Microbiol* **52**: 615-622.

Jonsson, K., Guo, B.P., Monstein, H.J., Mekalanos, J.J., and Kronvall, G. (2004) Molecular cloning and characterization of two *Helicobacter pylori* genes coding for plasminogen-binding proteins. *Proc Natl Acad Sci U S A* **101**: 1852-1857.

Jose, J., Jahnig, F., and Meyer, T.F. (1995) Common structural features of IgA1 protease-like outer membrane protein autotransporters. *Mol Microbiol* **18**: 378-380.

Jose, J., Krämer, J., Klauser, T., Pohlner, J., and Meyer, T.F. (1996) Absence of periplasmic DsbA oxidoreductase facilitates export of cysteine-containing passenger proteins to the *Escherichia coli* cell surface via the Iga_{β} autotransporter pathway. *Gene* **178**: 107-110.

Juncker, A.S., Willenbrock, H., Von Heijne, G., Brunak, S., Nielsen, H., and Krogh, A. (2003) Prediction of lipoprotein signal peptides in Gram-negative bacteria. *Protein Sci* **12**: 1652-1662.

Kajava, A.V., Cheng, N., Cleaver, R., Kessel, M., Simon, M.N., Willery, E., Jacob-Dubuisson, F., Locht, C., and Steven, A.C. (2001) Beta-helix model for the filamentous haemagglutinin adhesin of *Bordetella pertussis* and related bacterial secretory proteins. *Mol Microbiol* **42**: 279-292.

Kammler, M., Schon, C., and Hantke, K. (1993) Characterization of the ferrous iron uptake system of *Escherichia coli*. *J Bacteriol* **175**: 6212-6219.

Kim, J., Rusch, S., Luirink, J., and Kendall, D.A. (2001) Is Ffh required for export of secretory proteins? *FEBS Lett* **505**: 245-248.

Kisiel, W. (1979) Human plasma protein C: isolation, characterization, and mechanism of activation by alpha-thrombin. *J Clin Invest* **64**: 761-769.

Kitamura, M., Takayama, Y., Kojima, S., Kohno, K., Ogata, H., Higuchi, Y., and Inoue, H. (2004) Cloning and expression of the enolase gene from *Desulfovibrio vulgaris* (Miyazaki F). *Biochim Biophys Acta* **1676**: 172-181.

Klauser, T., Pohlner, J., and Meyer, T.F. (1992) Selective extracellular release of cholera toxin B subunit by *Escherichia coli*: dissection of *Neisseria* IgA beta-mediated outer membrane transport. *EMBO J* **11**: 2327-2335.

Klauser, T., Pohlner, J., and Meyer, T.F. (1993) The secretion pathway of IgA protease-type proteins in gram-negative bacteria. *BioAssays* **15**: 799-805.

Konieczny, M.P., Suhr, M., Noll, A., Autenrieth, I.B., and Alexander Schmidt, M. (2000) Cell surface presentation of recombinant (poly-) peptides including functional T-cell epitopes by the AIDA autotransporter system. *FEMS Immunol Med Microbiol* **27**: 321-332.

Konieczny, M.P.J., Benz, I., Hollinderbaumer, B., Beinke, C., Niederweis, M., and Schmidt, M.A. (2001) Modular organization of the AIDA autotransporter translocator: the N-terminal beta1-domain is surface-exposed and stabilizes the transmembrane beta2-domain. *Antonie Van Leeuwenhoek* **80**: 19-34.

Kornacki, J.A., and Oliver, D.B. (1998) Lyme disease-causing *Borrelia* species encode multiple lipoproteins homologous to peptide-binding proteins of ABC-type transporters. *Infect Immun* **66**: 4115-4122.

Koronakis, V., Sharff, A., Koronakis, E., Luisi, B., and Hughes, C. (2000) Crystal structure of the bacterial membrane protein TolC central to multidrug efflux and protein export. *Nature* **405**: 914-919.

Kostakioti, M., and Stathopoulos, C. (2004) Functional Analysis of the Tsh Autotransporter from an Avian Pathogenic *Escherichia coli Strain*. *Infect Immun* **72**: 5548-5554.

Koster, W. (2001) ABC transporter-mediated uptake of iron, siderophores, heme and vitamin B12. *Res Microbiol* **152**: 291-301.

Kotarski, S.F., and Salyers, A.A. (1984) Isolation and characterization of outer membranes of *Bacteroides thetaiotaomicron* grown on different carbohydrates. *J Bacteriol* **158**: 102-109.

Kramer, R.A., Zandwijken, D., Egmond, M.R., and Dekker, N. (2000) In vitro folding, purification and characterization of *Escherichia coli* outer membrane protease OmpT. *Eur J Biochem* **267**: 885-893.

Kumamoto, C.A., and Beckwith, J. (1985) Evidence for specificity at an early step in protein export in *Escherichia coli*. *J Bacteriol* **163**: 267-274.

Kusters, R., Lentzen, G., Eppens, E., van Geel, A., van der Weijden, C.C., Wintermeyer, W., and Luirink, J. (1995) The functioning of the SRP receptor FtsY in protein-targeting in *E. coli* is correlated with its ability to bind and hydrolyse GTP. *FEBS Lett* **372**: 253-258.

Kuwahara, T., Yamashita, A., Hirakawa, H., Nakayama, H., Toh, H., Okada, N., Kuhara, S., Hattori, M., Hayashi, T., and Ohnishi, Y. (2004) Genomic analysis of *Bacteroides fragilis* reveals extensive DNA inversions regulating cell surface adaptation. *Proc Natl Acad Sci U S A* **101**: 14919-14924.

Lähteenmäki, K., Kuusela, P., and Korhonen, T.K. (2001) Bacterial plasminogen activators and receptors. *FEMS Microbiol Rev* **25**: 531-552.

Lähteenmäki, K., Edelman, S., and Korhonen, T.K. (2005) Bacterial metastasis: the host plasminogen system in bacterial invasion. *Trends Microbiol* **13**: 79-85.

Lee, H.C., and Bernstein, H.D. (2001) The targeting pathway of *Escherichia coli* presecretory and integral membrane proteins is specified by the hydrophobicity of the targeting signal. *Proc Natl Acad Sci U S A*: 051484198.

Lee, H.W., and Byun, S.M. (2003) The pore size of the autotransporter domain is critical for the active translocation of the passenger domain. *Biochem Biophys Res Commun* **307**: 820-825.

Lee, V.T., and Schneewind, O. (2001) Protein secretion and the pathogenesis of bacterial infections. *Genes Dev* **15**: 1725-1752.

Leininger, E., Roberts, M., Kenimer, J.G., Charles, I.G., Fairweather, N., Novotny, P., and Brennan, M.J. (1991) Pertactin, an Arg-Gly-Asp-containing *Bordetella pertussis* surface protein that promotes adherence of mammalian cells. *Proc Natl Acad Sci U S A* **88**: 345-349.

Létoffé, S., Ghigo, M., and Wandersman, C. (1994) Secretion of the *Serratia marcencens* HasA protein by an ABC transporter. *J Bacteriol* **176**: 5372-5377.

Létoffé, S., Nato, F., Goldberg, M.E., and Wandersman, C. (1999) Interactions of HasA, a bacterial haemophore, with haemoglobin and with its outer membrane receptor HasR. *Mol Microbiol* **33**: 546-555.

Lewis, L.A., Gray, E., Wang, Y.P., Roe, B.A., and Dyer, D.W. (1997) Molecular characterization of hpuAB, the haemoglobin-haptoglobin-utilization operon of *Neisseria meningitidis*. *Mol Microbiol* **23**: 737-749.

Lijnen, H.R., and Collen, D. (1995) Mechanisms of physiological fibrinolysis. *Baillieres Clin Haematol* **8**: 277-290.

Liou, G.G., Jane, W.N., Cohen, S.N., Lin, N.S., and Lin-Chao, S. (2001) RNA degradosomes exist in vivo in *Escherichia coli* as multicomponent complexes associated with the cytoplasmic membrane via the N-terminal region of ribonuclease E. *Proc Natl Acad Sci U S A* **98**: 63-68.

Locher, K.P., Rees, B., Koebnik, R., Mitschler, A., Moulinier, L., Rosenbusch, J.P., and Moras, D. (1998) Transmembrane signaling across the ligand-gated FhuA receptor: crystal structures of free and ferrichrome-bound states reveal allosteric changes. *Cell* **95**: 771-778.

Lottenberg, R., DesJardin, L.E., Wang, H., and Boyle, M.D. (1992) Streptokinase-producing streptococci grown in human plasma acquire unregulated cell-associated plasmin activity. *J Infect Dis* **166**: 436-440.

Loveless, B.J., and Saier, M.H., Jr. (1997) A novel family of channel-forming, autotransporting, bacterial virulence factors. *Mol Membr Biol* **14**: 113-123.

Luirink, J., High, S., Wood, H., Giner, A., Tollervey, D., and Dobberstein, B. (1992) Signal-sequence recognition by an *Escherichia coli* ribonucleoprotein complex. *Nature* **359**: 741-743.

MacLaren, D.M., Namavar, F., Verweij-van Vught, A.M.J.J., Vel, W.A.C., and Kaan, J.A. (1984) Pathogenic synergy: mixed intra-abdominal infections. *Anthonie Van Leeuwenhoek* **50**: 775-787.

Macy, J.M., Ljungdahl, L.G., and Gottschalk, G. (1978) Pathway of succinate and propionate formation in *Bacteroides fragilis*. *J Bacteriol* **134**: 84-91.

Manting, E.H., and Driessen, A.J. (2000) Escherichia coli translocase: the unravelling of a molecular machine. *Mol Microbiol* **37**: 226-238.

Marshall, J.C. (2004) Intra-abdominal infections. *Microbes Infect* **6**: 1015-1025.

Martoglio, B., and Dobberstein, B. (1998) Signal sequences: more than just greasy peptides. *Trends Cell Biol* **8**: 410-415.

Maurer, J., Jose, J., and Meyer, T.F. (1997) Autodisplay: one-component system for efficient surface display and release of soluble recombinant proteins from *Escherichia coli*. *J Bacteriol* **179**: 794-804.

Maurer, J., Jose, J., and Meyer, T.F. (1999) Characterization of the essential transport function of the AIDA-I autotransporter and evidence supporting structural predictions. *J Bacteriol* **181**: 7014-7020.

McGuffin, L.J., Bryson, K., and Jones, D.T. (2000) The PSIPRED protein structure prediction server. *Bioinformatics* **16**: 404-405.

McHugh, J.P., Rodriguez-Quinones, F., Abdul-Tehrani, H., Svistunenko, D.A., Poole, R.K., Cooper, C.E., and Andrews, S.C. (2003) Global iron-dependent gene regulation in *Escherichia coli*. A new mechanism for iron homeostasis. *J Biol Chem* **278**: 29478-29486.

Meleney, F., Olpp, J., Harvey, H.D., and Zaysteff-Jern, H. (1932) Peritonitis. II. Synergism of bacteria commonly found in peritoneal exudates. *Arch Surg* **25**: 709-721.

Mellies, J.L., Navarro-Garcia, F., Okeke, I., Frederickson, J., Nataro, J.P., and Kaper, J.B. (2001) espC pathogenicity island of enteropathogenic *Escherichia coli* encodes an enterotoxin. *Infect Immun* **69**: 315-324.

Miles, L.A., Dahlberg, C.M., Plescia, J., Felez, J., Kato, K., and Plow, E.F. (1991) Role of cell-surface lysines in plasminogen binding to cells: identification of alpha-enolase as a candidate plasminogen receptor. *Biochemistry* **30**: 1682-1691.

Miller, J.H. (1992) *A short course in bacterial genetics; A laboratory manual and handbook for* Escherichia coli *and related bacteria.* New York: Cold Spring Harbor Laboratory Press.

Mogensen, J.E., Tapadar, D., Schmidt, M.A., and Otzen, D.E. (2005) Barriers to folding of the transmembrane domain of the *Escherichia coli* autotransporter adhesin involved in diffuse adherence. *Biochemistry* **44**: 4533-4545.

Morita, T., Kawamoto, H., Mizota, T., Inada, T., and Aiba, H. (2004) Enolase in the RNA degradosome plays a crucial role in the rapid decay of glucose transporter mRNA in the response to phosphosugar stress in *Escherichia coli*. *Mol Microbiol* **54**: 1063-1075.

Morona, R., Tommassen, J., and Henning, U. (1985) Demonstration of a bacteriophage receptor site on the *Escherichia coli* K12 outer-membrane protein OmpC by the use of a protease. *Eur J Biochem* **150**: 161-169.

Morrisey, J.H. (2001) Tissue factor: an enzyme cofactor and a true receptor. *Thromb Haemost* **86**: 66-74.

Müller, D., Benz, I., Tapadar, D., Buddenborg, C., Greune, L., and Schmidt, M.A. (2005) Arrangement of the translocator of the autotransporter adhesin involved in diffuse adherence on the bacterial surface. *Infect Immun* **73**: 3851-3859.

Müller, K., Matzanke, B.F., Schünemann, V., Trautwein, A.X., and Hantke, K. (1998) FhuF, an iron-regulated protein of *Escherichia coli* with a new type of [2Fe-2S] center. *Eur J Biochem* **258**: 1001-1008.

Murshudov, G.N., Vagin, A.A., Lebedev, A., Wilson, K.S., and Dodson, E.J. (1999) Efficient anisotropic refinement of macromolecular structures using FFT. *Acta Crystallogr D Biol Crystallogr* **55 (Pt 1)**: 247-255.

Nakatani, T., Ohtani, O., and Tanaka, S. (1996) Lymphatic stomata in the murine diaphragmatic peritoneum: the timing of their appearance and a map of their distribution. *Anat Rec* **244**: 529-539.

Nakatogawa, H., and Ito, K. (2001) Secretion monitor, SecM, undergoes self-translation arrest in the cytosol. *Mol Cell* **7**: 185-192.

Narita, S., Tanaka, K., Matsuyama, S., and Tokuda, H. (2002) Disruption of lolCDE, encoding an ATP-binding cassette transporter, is lethal for *Escherichia coli* and prevents release of lipoproteins from the inner membrane. *J Bacteriol* **184**: 1417-1422.

Narita, S., Matsuyama, S., and Tokuda, H. (2004) Lipoprotein trafficking in *Escherichia coli*. *Arch Microbiol* **182**: 1-6.

Navarro-Garcia, F., Canizalez-Roman, A., Luna, J., Sears, C., and Nataro, J.P. (2001) Plasmid-encoded toxin of enteroaggregative *Escherichia coli* is internalized by epithelial cells. *Infect Immun* **69**: 1053-1060.

Nelson, K.E., Fleischmann, R.D., DeBoy, R.T., Paulsen, I.T., Fouts, D.E., Eisen, J.A., Daugherty, S.C., Dodson, R.J., Durkin, A.S., Gwinn, M., Haft, D.H., Kolonay, J.F., Nelson, W.C., Mason, T., Tallon, L., Gray, J., Granger, D., Tettelin, H., Dong, H., Galvin, J.L., Duncan, M.J., Dewhirst, F.E., and Fraser, C.M. (2003) Complete genome sequence of the oral pathogenic bacterium *Porphyromonas gingivalis* strain W83. *J Bacteriol* **185**: 5591-5601.

Nesheim, M.E., Taswell, J.B., and Mann, K.G. (1979) The contribution of bovine Factor V and Factor Va to the activity of prothrombinase. *J Biol Chem* **254**: 10952-10962.

Newman, C.L., and Stathopoulos, C. (2004) Autotransporter and two-partner secretion: delivery of large-size virulence factors by gram-negative bacterial pathogens. *Crit Rev Microbiol* **30**: 275-286.

Norris, L.A. (2003) Blood coagulation. *Best Pract Res Clin Obstet Gynaecol* **17**: 369-383.

O'Toole, P.W., Austin, J.W., and Trust, T.J. (1994) Identification and molecular characterization of a major ring-forming surface protein from the gastric pathogen *Helicobacter mustelae*. *Mol Microbiol* **11**: 349-361.

Ohnishi, Y., Nishiyama, M., Horinouchi, S., and Beppu, T. (1994) Involvement of the COOH-terminal pro-sequence of Serratia marcescens serine protease in the folding of the mature enzyme. *J Biol Chem* **269**: 32800-32806.

Oliver, D.C., Huang, G., and Fernandez, R.C. (2003a) Identification of secretion determinants of the *Bordetella pertussis* BrkA autotransporter. *J Bacteriol* **185**: 489-495.

Oliver, D.C., Huang, G., Nodel, E., Pleasance, S., and Fernandez, R.C. (2003b) A conserved region within the *Bordetella pertussis* autotransporter BrkA is necessary for folding of its passenger domain. *Mol Microbiol* **47**: 1367-1383.

Onderdonk, A.B., Weinstein, W.M., Sullivan, N.M., Bartlett, J.G., and Gorbach, S.L. (1974) Experimental intra-abdominal abscesses in rats: quantitative bacteriology of infected animals. *Infect Immun* **10**: 1256-1259.

Onderdonk, A.B., Bartlett, J.G., Louie, T., Sullivan-Seigler, N., and Gorbach, S.L. (1976) Microbial synergy in experimental intra-abdominal abscess. *Infect Immun* **13**: 22-26.

Onderdonk, A.B., Cisneros, R.L., Finberg, R., Crabb, J.H., and Kasper, D.L. (1990) Animal model system for studying virulence of and host response to *Bacteroides fragilis*. *Rev Infect Dis* **12 Suppl 2**: S169-177.

Oomen, C.J., Van Ulsen, P., Van Gelder, P., Feijen, M., Tommassen, J., and Gros, P. (2004) Structure of the translocator domain of a bacterial autotransporter. *EMBO J* **23**: 1257-1266.

Otto, B.R., Verweij-van Vught, A.M., van Doorn, J., and Maclaren, D.M. (1988) Outer membrane proteins of *Bacteroides fragilis* and *Bacteroides vulgatus* in relation to iron uptake and virulence. *Microb Pathog* **4**: 279-287.

Otto, B.R., Sparrius, M., Verweij-van Vught, A.M., and MacLaren, D.M. (1990) Iron-regulated outer membrane protein of *Bacteroides fragilis* involved in heme uptake. *Infect Immun* **58**: 3954-3958.

Otto, B.R., Sparrius, M., Worst, D.J., deGraaf, F.K., and Maclaren, D.M. (1994) Utilization of haem from the haptoglobin-haemoglobin complex by *Bacteroides fragilis*. *Microb Pathog* **17**: 137-147.

Otto, B.R., van Dooren, S.J., Nuijens, J.H., Luirink, J., and Oudega, B. (1998) Characterization of a hemoglobin protease secreted by the pathogenic *Escherichia coli* strain EB1. *J Exp Med* **188**: 1091-1103.

Otto, B.R., van Dooren, S.J.M., Dozois, C.M., Luirink, J., and Oudega, B. (2002) *Escherichia coli* hemoglobin protease autotransporter contributes to synergistic abscess formation and heme-dependent growth of *Bacteroides fragilis*. *Infect Immun* **70**: 5-10.

Otto, B.R., Sijbrandi, R., Luirink, J., Oudega, B., Heddle, J.G., Mizutani, K., Park, S.-Y., and Tame, J.R.H. (2005) Crystal Structure of Hemoglobin Protease, a Heme Binding Autotransporter Protein from Pathogenic *Escherichia coli*. *J Biol Chem* **280**: 17339-17345.

Otwinowski, Z., and Minor, W. (1997) Processing of X-ray diffraction data collected in oscillation mode. *Meth Enzymol* **276**: 307-326.

Pancholi, V., and Fischetti, V.A. (1998) alpha-enolase, a novel strong plasmin(ogen) binding protein on the surface of pathogenic streptococci. *J Biol Chem* **273**: 14503-14515.

Paoli, M., Anderson, B.F., Baker, H.M., Morgan, W.T., Smith, A., and Baker, E.N. (1999) Crystal structure of hemopexin reveals a novel high-affinity heme site formed between two beta-propeller domains. *Nat Struct Biol* **6**: 926-931.

Parreira, V.R., and Gyles, C.L. (2003) A novel pathogenicity island integrated adjacent to the thrW tRNA gene of avian pathogenic *Escherichia coli* encodes a vacuolating autotransporter toxin. *Infect Immun* **71**: 5087-5096.

Parry, M.A., Zhang, X.C., and Bode, I. (2000) Molecular mechanisms of plasminogen activation: bacterial cofactors provide clues. *Trends Biochem Sci* **25**: 53-59.

Pascual, M., and French, L.E. (1995) Complement in human diseases: looking towards the 21st century. *Immunol Today* **16**: 58-61.

Patrick, S., Reid, J.H., and Larkin, M.J. (1984) The growth and survival of capsulate and non-capsulate *Bacteroides fragilis in vivo* and *in vitro*. *J Med Microbiol* **17**: 237-246.

Perutz, M.F., Rossman, M.G., Cullis, A.F., Muirhead, H., and North, A.C.T. (1960) Structure of haemoglobin. A three-dimensional Fourier synthesis at 5.5 A resolution obtained by X-ray analysis. *Nature* **185**: 416-422.

Peterson, J.H., Woolhead, C.A., and Bernstein, H.D. (2003) Basic amino acids in a distinct subset of signal peptides promote interaction with the signal recognition particle. *J Biol Chem*.

Pettersson, A., Prinz, T., Umar, A., van der Biezen, J., and Tommassen, J. (1998) Molecular characterization of LbpB, the second lactoferrin-binding protein of *Neisseria meningitidis*. *Mol Microbiol* **27**: 599-610.

Pixley, R.A., Schapira, M., and Colman, R.W. (1985) The regulation of human factor XIIa by plasma proteinase inhibitors. *J Biol Chem* **260**: 1723-1729.

Plow, E.F., Ploplis, V.A., Carmeliet, P., and Collen, D. (1999) Plasminogen and cell migration *in vivo*. *Fibrinolysis* **13**: 49-53.

Pohlner, J., Halter, R., Beyreuther, K., and Meyer, T.F. (1987) Gene structure and extracellular secretion of *Neisseria gonorrhoeae* IgA protease. *Nature* **325**: 458-462.

Pollanen, J., Stephens, R.W., and Vaheri, A. (1991) Directed plasminogen activation at the surface of normal and malignant cells. *Adv Cancer Res* **57**: 273-328.

Prilipov, A., Phale, P.S., Van Gelder, P., Rosenbusch, J.P., and Koebnik, R. (1998) Coupling site-directed mutagenesis with high-level expression: large scale production of mutant porins from *E. coli*. *FEMS Microbiol Lett* **163**: 65-72.

Provence, D.L., and Curtiss, R., 3rd (1994) Isolation and characterization of a gene involved in hemagglutination by an avian pathogenic *Escherichia coli* strain. *Infect Immun* **62**: 1369-1380.

Pugsley, A.P. (1993) The complete general secretory pathway in Gram-negative bacteria. *Microbiol Rev* **57**: 50-108.

Randall, L.L., and Hardy, S.J. (2002) SecB, one small chaperone in the complex milieu of the cell. *Cell Mol Life Sci* **59**: 1617-1623.

Ratledge, C., and Dover, L.G. (2000) Iron metabolism in pathogenic bacteria. *Annu Rev Microbiol* **54**: 881-941.

Redlitz, A., Fowler, B.J., Plow, E.F., and Miles, L.A. (1995) The role of an enolase-related molecule in plasminogen binding to cells. *Eur J Biochem* **227**: 407-415.

Reijnen, M.M., Bleichrodt, R.P., and van Goor, H. (2003) Pathophysiology of intra-abdominal adhesion and abscess formation, and the effect of hyaluronan. *Br J Surg* **90**: 533-541.

Richardson, A.R., and Stojiljkovic, I. (1999) HmbR, a hemoglobin-binding outer membrane protein of *Neisseria meningitidis*, undergoes phase variation. *J Bacteriol* **181**: 2067-2074.

Robinson, S.C. (1962) Observations on the peritoneum as an absorbing surface. *Am J Obstet Gynecol* **83**: 446-452.

Roggenkamp, A., Ackermann, N., Jacobi, C.A., Truelzsch, K., Hoffmann, H., and Heesemann, J. (2003) Molecular analysis of transport and oligomerization of the *Yersinia enterocolitica* adhesin YadA. *J Bacteriol* **185**: 3735-3744.

Rotstein, O.D., Pruett, T.L., and Simmons, R.L. (1985a) Lethal microbial synergism in intra-abdominal infections. *Escherichia coli* and *Bacteroides fragilis*. *Arch Surg* **120**: 146-151.

Rotstein, O.D., Pruett, T.L., and Simmons, R.L. (1985b) Mechanisms of microbial synergy in polymicrobial surgical infections. *Rev Infect Dis* **7**: 151-170.

Rotstein, O.D., Kao, J., and Houston, K. (1989a) Reciprocal synergy between *Escherichia coli* and *Bacteroides fragilis* in an intra-abdominal infection model. *J Med Microbiol* **29**: 269-276.

Rotstein, O.D., Vittorini, T., Kao, J., McBurney, M.I., Nasmith, P.E., and Grinstein, S. (1989b) A soluble *Bacteroides* by-product impairs phagocytic killing of *Escherichia coli* by neutrophils. *Infect Immun* **57**: 745-753.

Rotstein, O.D. (1992) Role of fibrin deposition in the pathogenesis of intraabdominal infection. *Eur J Clin Microbiol Infect Dis* **11**: 1064-1068.

Roussel, A., and Cambillau, C. (1989) Silicon Graphics Geometry Partners Directory. Mountain View, CA.: Silicon Graphics.

Sambrook, J., Fritsch, E.F., and Maniatis, T. (1989) *Molecular cloning: a laboratory manual.* New York: Cold Spring Harbor Laboratory Press.

Samuelson, J.C., Chen, M., Jiang, F., Moller, I., Wiedmann, M., Kuhn, A., Phillips, G.J., and Dalbey, R.E. (2000) YidC mediates membrane protein insertion in bacteria. *Nature* **406**: 637-641.

Sandkvist, M. (2001) Biology of type II secretion. *Mol Microbiol* **40**: 271-283.

Sankaran, K., and Wu, H.C. (1995) Bacterial prolipoprotein signal peptidase. *Methods Enzymol* **248**: 169-180.

Sargent, F., Stanley, N.R., Berks, B.C., and Palmer, T. (1999) Sec-independent Protein Translocation in *Escherichia coli*. A DISTINCT AND PIVOTAL ROLE FOR THE TatB PROTEIN. *J Biol Chem* **274**: 36073-36082.

Sarker, S., Rudd, K.E., and Oliver, D. (2000) Revised translation start site for *secM* defines an atypical signal peptide that regulates *Escherichia coli secA* expression. *J Bacteriol* **182**: 5592-5595.

Savage, D.C. (1977) Microbial ecology of the gastrointestinal tract. *Annu Rev Microbiol* **31**: 107-133.

Schierle, C.F., Berkmen, M., Huber, D., Kumamoto, C., Boyd, D., and Beckwith, J. (2003) The DsbA signal sequence directs efficient, cotranslational export of passenger proteins to the *Escherichia coli* periplasm via the signal recognition particle pathway. *J Bacteriol* **185**: 5706-5713.

Schryvers, A.B., Bonnah, R., Yu, R.H., Wong, H., and Retzer, M. (1998) Bacterial lactoferrin receptors. *Adv Exp Med Biol* **443**: 123-133.

Schulz, G.E. (2003) Transmembrane beta-barrel proteins. *Adv Protein Chem* **63**: 47-70.

Schwede, T., Kopp, J., Guex, N., and Peitsch, M.C. (2003) SWISS-MODEL: an automated protein homology-modeling server. *Nucleic Acids Research* **31**: 3381-3385.

Scott, D.J., Grossmann, J.G., Tame, J.R., Byron, O., Wilson, K.S., and Otto, B.R. (2002) Low Resolution Solution Structure of the Apo form of *Escherichia coli* Haemoglobin Protease Hbp. *J Mol Biol* **315**: 1179-1187.

Scotti, P.A., Urbanus, M.L., Brunner, J., de Gier, J.W., von Heijne, G., van der Does, C., Driessen, A.J., Oudega, B., and Luirink, J. (2000) YidC, the *Escherichia coli* homologue of mitochondrial Oxa1p, is a component of the Sec translocase. *Embo J* **19**: 542-549.

Sebulsky, M.T., Shilton, B.H., Speziali, C.D., and Heinrichs, D.E. (2003) The role of FhuD2 in iron(III)-hydroxamate transport in *Staphylococcus aureus*. Demonstration that FhuD2 binds iron(III)-hydroxamates but with minimal conformational change and implication of mutations on transport. *J Biol Chem* **278**: 49890-49900.

Serruto, D., Adu-Bobie, J., Scarselli, M., Veggi, D., Pizza, M., Rappuoli, R., and Arico, B. (2003) Neisseria meningitidis App, a new adhesin with autocatalytic serine protease activity. *Mol Microbiol* **48**: 323-334.

Seydel, A., Gounon, P., and Pugsley, A.P. (1999) Testing the '+2 rule' for lipoprotein sorting in the *Escherichia coli* cell envelope with a new genetic selection. *Mol Microbiol* **34**: 810-821.

Shere, K.D., Sallustio, S., Manessis, A., D'Aversa, T.G., and Goldberg, M.B. (1997) Disruption of IcsP, the major *Shigella* protease that cleaves IcsA, accelerates actin-based motility. *Mol Microbiol* **25**: 451-462.

Shiba, K., Ito, K., Yura, T., and Cerretti, D.P. (1984) A defined mutation in the protein export gene within the spc ribosomal protein operon of *Escherichia coli*: isolation and characterization of a new temperature-sensitive *secY* mutant. *EMBO J* **3**: 631-635.

Sijbrandi, R., Urbanus, M.L., ten Hagen-Jongman, C.M., Bernstein, H.D., Oudega, B., Otto, B.R., and Luirink, J. (2003) Signal Recognition Particle (SRP)-mediated Targeting and Sec-dependent Translocation of an Extracellular *Escherichia coli* Protein. *J Biol Chem* **278**: 4654-4659.

Sijbrandi, R., Den Blaauwen, T., Tame, J.R.H., Oudega, B., Luirink, J., and Otto, B.R. (2005) Characterization of an iron-regulated alpha-enolase of *Bacteroides fragilis*. *Microbes Infect* **7**: 9-18.

Sprencel, C., Cao, Z., Qi, Z., Scott, D.C., Montague, M.A., Ivanoff, N., Xu, J., Raymond, K.M., Newton, S.M., and Klebba, P.E. (2000) Binding of ferric enterobactin by the *Escherichia coli* periplasmic protein FepB. *J Bacteriol* **182**: 5359-5364.

St Geme, J.W., 3rd, and Cutter, D. (2000) The haemophilus influenzae hia adhesin is an autotransporter protein that remains uncleaved at the C terminus and fully cell associated. *J Bacteriol* **182**: 6005-6013.

Stassen, J.M., Arnout, J., and Deckmyn, H. (2004) The hemostatic system. *Curr Med Chem* **11**: 2245-2260.

Stathopoulos, C., Provence, D.L., and Curtiss, R., 3rd (1999) Characterization of the avian pathogenic *Escherichia coli* hemagglutinin Tsh, a member of the immunoglobulin A protease-type family of autotransporters. *Infect Immun* **67**: 772-781.

Steeghs, L., de Cock, H., Evers, E., Zomer, B., Tommassen, J., and van der Ley, P. (2001) Outer membrane composition of a lipopolysaccharide-deficient *Neisseria meningitidis* mutant. *EMBO J* **20**: 6937-6945.

Stein, M., Kenny, B., Stein, M.A., and Finlay, B.B. (1996) Characterization of EspC, a 110-kilodalton protein secreted by enteropathogenic *Escherichia coli* which is homologous to members of the immunoglobulin A protease-like family of secreted proteins. *J Bacteriol* **178**: 6546-6554.

Stenberg, F., Chovanec, P., Maslen, S.L., Robinson, C.V., Ilag, L.L., von Heijne, G., and Daley, D.O. (2005) Protein Complexes of the *Escherichia coli* Cell Envelope. *J. Biol. Chem.* **280**: 34409-34419.

Struyvé, M., Moons, M., and Tommassen, J. (1991) Carboxy-terminal Phenylalanine is Essential for the Correct Assembly of a Bacterial Outer Membrane Protein. *J Mol Biol* **218**: 141-148.

Studier, F.W., Rosenberg, A.H., Dunn, J.J., and Dubendorff, J.W. (1990) Use of T7 RNA polymerase to direct expression of cloned genes. *Methods Enzymol* **185**: 60-89.

Szabady, R.L., Peterson, J.H., Skillman, K.M., and Bernstein, H.D. (2005) An unusual signal peptide facilitates late steps in the biogenesis of a bacterial autotransporter. *Proc Natl Acad Sci U S A* **102**: 221-226.

Tame, J.R., Van Dooren, S.J., Oudega, B., and Otto, B.R. (2002) Characterization and crystallization of a novel haemoglobinase from pathogenic *Escherichia coli*. *Acta Crystallogr D Biol Crystallogr* **58**: 843-845.

Tamm, L.K., Arora, A., and Kleinschmidt, J.H. (2001) Structure and assembly of beta-barrel membrane proteins. *J Biol Chem* **276**: 32399-32402.

Terwilliger, T.C., and Berendzen, J. (1999) Automated MAD and MIR structure solution. *Acta Crystallogr D Biol Crystallogr* **55 (Pt 4)**: 849-861.

Terwilliger, T.C. (2003) SOLVE and RESOLVE: automated structure solution and density modification. *Methods Enzymol* **374**: 22-37.

Tran, J.H., and Jacoby, G.A. (2002) Mechanism of plasmid-mediated quinolone resistance. *Proc Natl Acad Sci U S A* **99**: 5638-5642.

Tsilibary, E.C., and Wissig, S.L. (1983) Lymphatic absorption from the peritoneal cavity: regulation of patency of mesothelial stomata. *Microvasc Res* **25**: 22-39.

Turner, D.P., Wooldridge, K.G., and Ala'Aldeen, D.A. (2002) Autotransported serine protease A of *Neisseria meningitidis*: an immunogenic, surface-exposed outer membrane, and secreted protein. *Infect Immun* **70**: 4447-4461.

Tzianabos, A.O., Onderdonk, A.B., Rosner, B., Cisneros, R.L., and Kasper, D.L. (1993) Structural features of polysaccharides that induce intra-abdominal abscesses. *Science* **262**: 416-419.

Urbanus, M.L., Scotti, P.A., Froderberg, L., Saaf, A., de Gier, J.W., Brunner, J., Samuelson, J.C., Dalbey, R.E., Oudega, B., and Luirink, J. (2001) Sec-dependent membrane protein insertion: sequential interaction of nascent FtsQ with SecY and YidC. *EMBO Rep* **2**: 524-529.

Valent, Q.A., de Gier, J.W.L., von Heijne, G., Kendall, D.A., ten Hagen-Jongman, C.M., Oudega, B., Luirink, J. (1997) Nascent membrane and presecretory proteins synthesized in *Escherichia coli* associate with signal recognition particle and trigger factor. *Mol Microbiol* **25**: 53-64.

van Dooren, S.J., Tame, J.R., Luirink, J., Oudega, B., and Otto, B.R. (2001) Purification of the autotransporter protein Hbp of *Escherichia coli*. *FEMS Microbiol Lett* **205**: 147-150.

van Goor, H., de Graaf, J.S., Grond, J., Sluiter, W.J., van der Meer, J., Bom, V.J., and Bleichrodt, R.P. (1994) Fibrinolytic activity in the abdominal cavity of rats with faecal peritonitis. *Br J Surg* **81**: 1046-1049.

van Ulsen, P., van Alphen, L., ten Hove, J., Fransen, F., van der Ley, P., and Tommassen, J. (2003) A Neisserial autotransporter NalP modulating the processing of other autotransporters. *Mol Microbiol* **50**: 1017-1030.

Veiga, E., de Lorenzo, V., and Fernandez, L.A. (1999) Probing secretion and translocation of a beta-autotransporter using a reporter single-chain Fv as a cognate passenger domain. *Mol Microbiol* **33**: 1232-1243.

Veiga, E., Sugawara, E., Nikaido, H., de Lorenzo, V., and Fernandez, L.A. (2002) Export of autotransported proteins proceeds through an oligomeric ring shaped by C-terminal domains. *EMBO J* **21**: 2122-2131.

Veiga, E., de Lorenzo, V., and Fernandez, L.A. (2004) Structural tolerance of bacterial autotransporters for folded passenger protein domains. *Mol Microbiol* **52**: 1069-1080.

Verweij-van Vught, A.M.J.J., Namavar, F., Sparrius, M., Vel, W.A.C., and MacLaren, D.M. (1985) Pathogenic synergy between *Escherichia coli* and *Bacteroides fragilis:* studies in an experimental mouse model. *J Med Microbiol* **19**: 325-331.

Verweij-van Vught, A.M.J.J., Namavar, F., Vel, W.A.C., Sparrius, M., and MacLaren, D.M. (1986) Pathogenic synergy between *Escherichia coli* and *Bacteroides fragilis* or *B. vulgatus* in experimental infections: a non-specific phenomenon. *J Med Microbiol* **21**: 43-47.

Verweij, W.R., Namavar, F., Schouten, W.F., and MacLaren, D.M. (1991) Early events after intra-abdominal infection with *Bacteroides fragilis* and *Escherichia coli*. *J Med Microbiol* **35**: 18-22.

Vipond, M.N., Whawell, S.A., Thompson, J.N., and Dudley, H.A. (1994) Effect of experimental peritonitis and ischaemia on peritoneal fibrinolytic activity. *Eur J Surg* **160**: 471-477.

Voulhoux, R., Bos, M.P., Geurtsen, J., Mols, M., and Tommassen, J. (2003) Role of a highly conserved bacterial protein in outer membrane protein assembly. *Science* **299**: 262-265.

Wandersman, C., and Delepelaire, P. (2004) Bacterial iron sources: from siderophores to hemophores. *Annu Rev Microbiol* **58**: 611-647.

Wee, S., Neilands, J.B., Bittner, M.L., Hemming, B.C., Haymore, B.L., and Seetharam, R. (1988) Expression, isolation and properties of Fur (ferric uptake regulation) protein of *Escherichia coli* K 12. *Biol Met* **1**: 62-68.

Weinberg, E.D. (1974) Iron and susceptibility to infectious disease. *Science* **184**: 952-956.

Weisel, J.W. (1986) Fibrin assembly. Lateral aggregation and the role of the two pairs of fibrinopeptides. *Biophys J* **50**: 1079-1093.

Wertz, D.H., and Scheraga, H.A. (1978) Influence of water on protein structure. An analysis of the preferences of amino acid residues for the inside or outside and for specific conformations in a protein molecule. *Macromolecules* **11**: 9-15.

Wilks, A. (2001) The ShuS protein of *Shigella dysenteriae* is a heme-sequestering protein that also binds DNA. *Arch Biochem Biophys* **387**: 137-142.

Williams, P.H. (1979) Novel iron uptake system specified by ColV plasmids: an important component in the virulence of invasive strains of *Escherichia coli*. *Infect Immun* **26**: 925-932.

Wiman, B., and Collen, D. (1978) On the kinetics of the reaction between human antiplasmin and plasmin. *Eur J Biochem* **84**: 573-578.

Winram, S.B., and Lottenberg, R. (1998) Site-directed mutagenesis of streptococcal plasmin receptor protein (Plr) identifies the C-terminal Lys334 as essential for plasmin binding, but mutation of the plr gene does not reduce plasmin binding to group A streptococci. *Microbiology* **144 (Pt 8)**: 2025-2035.

Wittmann, D.H., Schein, M., and Condon, R.E. (1996) Management of secondary peritonitis. *Ann Surg* **224**: 10-18.

Wu, H.C. (1996) Biosynthesis of lipoproteins. In *Escherichia coli and Salmonella*. Neidhardt, F.C. (ed). Washington, DC: American Society of Microbiology Press, pp. 1005-1014.

Wu, T., Malinverni, J., Ruiz, N., Kim, S., Silhavy, T.J., and Kahne, D. (2005) Identification of a multicomponent complex required for outer membrane biogenesis in *Escherichia coli*. *Cell* **121**: 235-245.

Xu, J., Bjursell, M.K., Himrod, J., Deng, S., Carmichael, L.K., Chiang, H.C., Hooper, L.V., and Gordon, J.I. (2003) A genomic view of the human-*Bacteroides thetaiotaomicron* symbiosis. *Science* **299**: 2074-2076.

Yen, M.-R., Peabody, C.R., Partovi, S.M., Zhai, Y., Tseng, Y.-H., and Saier, J., Milton H. (2002) Protein-translocating outer membrane porins of Gram-negative bacteria. *Biochim Biophys Acta* **1562**: 6-31.

Yull, A.B., Abrams, J.S., and Davis, J.H. (1962) The peritoneal fluid in strangulation obstruction. The role of the red blood cell and *E. coli* bacteria in producing toxicity. *J Surg Res* **2**: 223-232.

Zaleznik, D.F., and Kasper, D.L. (1982) The role of anaerobic bacteria in abscess formation. *Annu Rev Med* **33**: 217-229.

Zhu, W., Wilks, A., and Stojiljkovic, I. (2000) Degradation of heme in gram-negative bacteria: the product of the *hemO* gene of *Neisseriae* is a heme oxygenase. *J Bacteriol* **182**: 6783-6790.

Zinsser, H.H., and Pryde, A.W. (1952) Experimental study of physical factors, including fibrin formation, influencing the spread of fluids and small particles within and from the peritoneal cavity of the dog. *Ann Surg* **136**: 818-827.

Nederlandse samenvatting

Moleculair inzicht in de pathogene synergie tussen *E. coli* en *B. fragilis* in secundaire peritonitis

Intra-abdominale infecties (IAI) die door secundaire peritonitis worden veroorzaakt zijn een veel voorkomende doodsoorzaak in mensen. Deze infecties zijn gewoonlijk het resultaat van lekkage van de darminhoud in de buikholte, veroorzaakt door chirurgie of andere buiktrauma's. Een veel voorkomende complicatie van deze infecties is de vorming van abcessen, die de behandeling van secundaire peritonitis zeer ingewikkeld maken. Vaak worden twee Gram-negatieve bacteriesoorten geïsoleerd van de plaats van infectie: de aërobe *Escherichia coli* en anaërobe *Bacteroides fragilis*. Het frequente samen-voorkomen van deze twee soorten heeft geleid tot het concept van microbieel synergisme tussen *E. coli* en *B. fragilis*. Het synergisme tussen de twee soorten is experimenteel aangetoond in muis- en ratteninfectiemodellen. Op dit moment wordt de moleculaire basis van dit synergisme slechts gedeeltelijk begrepen. Bekende virulentiefactoren van *E. coli* en *B. fragilis* die hierbij betrokken zijn, remmen fagocytose door polymorfonucleaire neutrofielen (PMNs) of helpen in de levering van essentiële groeifactoren aan de bacteriën. Een voorbeeld van het laatstgenoemde proces is de voorziening van ijzer en heem afkomstig van gastheereiwitten, omdat de bacteriën veel hogere concentraties ijzer nodig hebben om de groei te handhaven dan vrij beschikbaar is in het menselijk lichaam. Een hemoglobine protease (Hbp) is geïdentificeerd dat bijdraagt tot de synergistische abcesvorming en de heem-afhankelijke groei van *B. fragilis* in een ratteninfectiemodel. Het wordt gedacht dat, na afbraak van hemoglobine, Hbp het gebonden heem als ijzer- of heembron aan de bacteriën op de plaats van infectie verstrekt. Een ander mechanisme dat betrokken is bij het bacteriële synergisme tussen *E. coli* en *B. fragilis* is de uitscheiding van proteasen die weefselafbraak in de gastheer veroorzaken. Ook zouden de bacteriën gastheereiwitten kunnen gebruiken om deze taak uit te voeren. Hoewel dit tot dusver niet voor *E. coli* of *B. fragilis* is aangetoond, is bij andere bacteriën gevonden dat ze plasminogeen van de gastheer op hun celoppervlak kunnen binden, waarna het wordt omgezet in plasmine. Deze eigenschap biedt de bacterie de mogelijkheid om zich te mengen in het fijn afgestemde systeem van coagulatie en fibrinolyse van de gastheer.

De experimenten die in dit proefschrift worden beschreven behandelen drie eiwitten die (mogelijk) betrokken zijn bij het pathogene synergisme tussen *E. coli* en *B. fragilis* bij menselijke intra-abdominale infecties. Deze drie eiwitten zijn Hbp van *E. coli* en P46 en Pbp van *B. fragilis*. Hbp is een hemoglobine protease met heem-

bindende activiteit. Het is een uitgescheiden (gesecreteerd) eiwit dat tot de autotransporter familie van eiwitten behoort. P46 is het α-enolase van *B. fragilis* en dit eiwit bevindt zich intracellulair. Tot slot werd Pbp geïdentificeerd als mogelijk plasminogeen-bindend eitwit aan het celoppervlak van *B. fragilis*.

Hemoglobine protease (Hbp)

Het hemoglobine protease (Hbp) is een hemoglobine afbrekend en heem-bindend eiwit dat door ziekteverwekkende *E. coli* bacteriën wordt gesecreteerd. Het eiwit maakt deel uit van de groep van serine protease autotransporters van de *Enterobacteriaceae* (SPATE). Autotransporters zijn grote eiwitten die drie functionele domeinen bevatten: een N-terminaal signaalpeptide voor het sturen (targeting) naar en de translocatie over het binnenmembraan, het passagiersdomein (het uitgescheiden effector-molecuul), en een C-terminaal translocatiedomein dat voor translocatie over het buitenmembraan noodzakelijk is.

In hoofdstuk 2 worden de vroegste stappen in de secretie van Hbp bestudeerd, met name het sturen naar en de translocatie over het binnenmembraan. Het wordt aangetoond dat Hbp interactie heeft met het Signal Recognition Particle (SRP, vertaald: Signaal Herkennings Deeltje), dat Hbp om naar het binnenmembraan gestuurd te worden afhankelijk is van SRP en dat het Sec-translocon nodig is voor de translocatie over het binnenmembraan. SecB is niet noodzakelijk om Hbp naar het binnenmembraan te sturen, maar het kan tot op zekere hoogte het gebrek aan een functionele SRP-route compenseren. Dit is het eerste voorbeeld van een extracellulair bacterieel eiwit dat de zogenaamde co-translationele SRP-route in plaats van de post-translationele SecB-route volgt, die normaalgesproken door gesecreteerde eiwitten wordt gebruikt. Aanwijzingen werden verkregen dat pre-pro-Hbp in het cytoplasma snel door cytoplasmatische proteasen wordt afgebroken. Dit zou de reden kunnen zijn voor het gebruik van de snellere, co-translationele SRP-route, aangezien hierdoor voortijdige vouwing en afbraak in het cytoplasma kunnen worden vermeden.

In hoofdstuk 3 wordt de driedimensionale structuur van het volledige passagiersdomein van Hbp gepresenteerd. Dit is de eerste volledige kristalstructuur van een passagiersdomein van een autotransporter eiwit en het toont de grootste parallelle β-spiraalvorm (β-helix) tot dusver opgelost. Het eiwit bevat een zeer lange rechtshandige β-helix structuur die drie parallelle β-bladen (β-sheets) vormt. Drie verschillende domeinen kunnen in de structuur van Hbp worden herkend. Het N-terminale domein is een groot bolvormig domein dat het trypsine-achtige serine proteasedomein bevat. Vouwing van dit domein en proteaseactiviteit kan slechts

optreden na verwijdering van het signaalpeptide (d.w.z. na binnenmembraan-translocatie). De vrij open actieve plaats (active site) kan vermoedelijk bolvormige eiwitten (zoals hemoglobine) aanvallen en suggereert brede substraatspecificiteit. Naast sommige “decoratieve” uitstekende delen, bevat de β-helix stam een klein "domein 2" dat homologie met een chitine-bindend domein heeft en een soort bindingsplaats lijkt te vormen. Het werd aangetoond dat dit domein niet voor de heem-binding van Hbp verantwoordelijk is, maar het zou betrokken kunnen zijn bij het binden aan een receptor op het celoppervlak van *B. fragilis* en/of *E. coli*. Het derde domein, het geconserveerde C-terminale domein van het eiwit, is vermoedelijk betrokken bij de translocatie van het passagiersdomein over het buitenmembraan en het vouwen van het volwassen eiwit.

De zuivering en de voorlopige karakterisering van het translocatiedomein van Hbp worden beschreven in hoofdstuk 4. Het doel van die studie is de kristalstructuur van het translocatiedomein van Hbp op te lossen om meer inzicht te verkrijgen in het mechanisme van de translocatie van het passagiersdomein van autotransporters over het buitenmembraan. Bij Hbp vindt de splitsing tussen het passagiersdomein en het translocatiedomein plaats tussen twee asparagineresiduen die zich bevinden in het midden van het linkerdomein dat deel uitmaakt van de translocatie-eenheid. Aanwijzingen werden verkregen dat het voorspelde spiraalvormige (α-helix vormige) linkergebied in de porie van het translocatiedomein gelokaliseerd is. Dit impliceert dat in de bacterie het passagiersdomein niet van de translocatie-eenheid kan worden afgesplitst wanneer de α-helix reeds is gevormd. In dat geval zou het splitsen of aan de periplasmatische kant van het buitenmembraan moeten plaatsvinden, dus vóór de translocatie, of op het celoppervlak met een uitgestrekt linkerdomein, d.w.z. voordat de vorming van de α-helix van het linkerdomein wordt voltooid. In hoofdstuk 4 wordt een model voorgesteld voor de driedimensionale structuur van het Hbp translocatiedomein.

α-Enolase (P46)

In hoofdstuk 5 worden de identificatie, het kloneren en de moleculaire karakterisering van het α-enolase P46 van *B. fragilis* beschreven. Van dit eiwit werd aangetoond dat het het functionele enolase van *B. fragilis* is. Verrassend genoeg werd gevonden dat het eiwit een ijzer-gereguleerd eiwit is dat onder ijzer- of heem-beperkte omstandigheden wordt opgereguleerd. Deze eigenschap wordt vaak waargenomen bij bacteriële virulentiefactoren, omdat de bacteriën onder de omstandigheden van lage ijzerconcentraties in het menselijk lichaam moeten kunnen

groeien. De ijzer-reguleerbaarheid van P46 kan een rol spelen in de virulentie van *B. fragilis* in intra-abdominale infecties.

De afwezigheid van P46 aan het celoppervlak van *B. fragilis* maakt het onwaarschijnlijk dat P46 als plasminogeen-bindend eiwit functioneert. Een plasminogeen-bindende activiteit kon niet voor P46 worden ontdekt.

Plasminogeen bindend eiwit (Pbp)

In plaats van het P46 eiwit werd een ander eiwit in *B. fragilis* geïdentificeerd als mogelijk plasminogeen bindend eiwit. Dit eiwit wordt Pbp genoemd, voor Plasminogeen bindend proteïne (hoofdstuk 6). Het werd aangetoond dat eiwitten die sterk lijken op Pbp in andere *Bacteroides* ondersoorten aanwezig zijn. Subcellulaire localisatie-experimenten toonden aan dat Pbp zich in of aan het buitenmembraan bevindt. *B. fragilis* Pbp bleek toegankelijk voor extracellulair protease te zijn, wat een localisatie aan het celoppervlak voor dit eiwit suggereert. De plasminogeen-bindende eigenschappen van Pbp werden bestudeerd en het eindstandige aminozuur lysine lijkt bij de plasminogeen-binding betrokken te zijn. Tot slot toonde de analyse van de primaire structuur van Pbp aan dat het eiwit waarschijnlijk een lipoproteïne is, hoewel deze voorspelling nog experimenteel moet worden bevestigd. Wanneer Pbp inderdaad een echt lipoproteïne is, zou het zeer interessant zijn om de factoren te identificeren die Pbp naar het buitenmembraan sturen.

In dit proefschrift werden drie eiwitten geanalyseerd die een rol als virulentiefactoren in het bacteriële synergisme tussen *E. coli* en *B. fragilis* kunnen spelen in menselijke intra-abdominale infecties: Hbp, P46 en Pbp. Voor Hbp is een rol in de synergistische abcesvorming in deze infecties reeds aangetoond met behulp van een ratteninfectiemodel. Van Hbp is reeds aangetoond dat het tot de heem-afhankelijke groei van *B. fragilis* bijdraagt. Het is zeer waarschijnlijk dat *E. coli* zelf ook direct van de uitscheiding van dit eiwit kan profiteren op een soortgelijke manier. Omdat Pbp een plasminogeen-bindend eiwit op het oppervlak van *B. fragilis* cellen zou kunnen zijn, is een rol voor dit eiwit als virulentiefactor zeer wel denkbaar. De mogelijkheid om plasminogeen te binden en om te zetten in plasmine verhoogt het proteolytische potentieel van de cel en geeft de mogelijkheid om het fibrine netwerk te degraderen dat de gastheer gebruikt om de micro-organismen in te sluiten, daardoor verhinderend dat de bacteriën in de circulatie terechtkomen. De bijdrage van zowel Hbp als Pbp tot abcesvorming in bacteriële peritonitis zal verder getest worden in een ratteninfectiemodel. Een potentiële rol voor P46 in de virulentie van *B. fragilis* en in intra-abdominale infecties is moeilijker voor te stellen.

De driedimensionale structuren van het Hbp translocatiedomein, P46 en Pbp zouden een zeer nuttig hulpmiddel in de studie van deze eiwitten zijn. Momenteel worden pogingen gedaan om de kristalstructuren van al deze eiwitten op te lossen. Het valt te verwachten dat het onderzoek dat in dit proefschrift wordt beschreven, nog te verwachten resultaten en voorgestelde toekomstige studies naar Hbp, P46 en Pbp zullen bijdragen aan het begrip van het moleculaire mechanisme van het bacteriële synergisme tussen *E. coli* en *B. fragilis* in menselijke intra-abdominale infecties. Deze kennis kan op haar beurt helpen bij de preventie en/of de behandeling van deze levensgevaarlijke infecties in de toekomst.

Dankwoord

Tenslotte wil ik graag een aantal mensen bedanken die zo belangrijk zijn geweest voor de totstandkoming van dit proefschrift.

Ben (Mac-Ben), als primaire begeleider en copromotor kom jij voor mij bovenaan in dit lijstje. Ik heb in de afgelopen jaren veel aan je ideeën, kennis en hulp gehad. Met ons wat meer medisch gerichte onderzoek voelden we ons binnen MolMic misschien wel eens wat minder begrepen, maar dit proefschrift toont volgens mij aan dat het allemaal wel ergens toe geleid heeft. Veel succes met de grote hoeveelheid plannen die je nog hebt met Hbp en al die nog te karakteriseren *fragilis* eiwitten. En blijf tegenstand bieden aan Bill Gates!

Bauke (voor mij blijft het Bob), bedankt voor je inzet als promotor, niet in de laatste plaats de aandacht voor de voortgang in het afgelopen jaar toen ik al niet meer op de VU rondliep. Ondanks alle bestuurlijke bezigheden kwam je altijd weer met enthousiaste en goede input tijdens de werkbesprekingen op maandagmorgen en had je goed in de gaten hoe de proeven vorderden.

Joen (waar staat die S. toch voor?), met jou als tweede copromotor had ik iets minder direct te maken, zeker nadat het SRP-verhaal af was. Maar je positief-kritische blik op mijn resultaten gaven altijd weer stof tot nadenken en verder onderzoek, en hebben daarmee een belangrijke bijdrage geleverd aan het uiteindelijke resultaat.

Nellie (soms ook Snellie genoemd), jij maakt de staf letterlijk en figuurlijk compleet. Bedankt voor je interesse in mijn onderzoek. Je had vaak net een andere invalshoek om naar de data te kijken, waardoor er regelmatig weer nieuwe ideeën ontstonden om mee verder te gaan.

Ronald (Roon), nooit meer zal ik jarig zijn en nooit meer kan ik Herman van Veen horen zonder aan jou te moeten denken. Het op en neer reizen tussen Utrecht en Amsterdam was met jou altijd weer een goed begin of einde van de dag, vooral als er weer iets raars werd omgeroepen (Heren, …). Maak er wat moois van in Genève en natuurlijk ook daarna.

Wouter (Wout), jij bent de volgende! Succes met de laatste loodjes en bedankt voor alle goede gesprekken over autotransporters en aanverwante zaken. Jouw parate kennis van de literatuur is me regelmatig goed van pas gekomen. En ik

wens je toe dat je nooit van je leven meer een PowerPoint hoeft te maken voor een promotiestukje, want dat heeft je inmiddels al genoeg jaren van je leven gekost.

Edwin (de hooligan), je was een fijne kamer- en labgenoot. Al ben ik geloof ik wel blij dat je je favoriete muziek alleen luisterde met oordopjes in. Ach, smaken verschillen. Maar dat zei ze vast gisteravond ook… Als je nou niet te vaak en te lang werkt, zien we elkaar vast nog wel eens in Utrecht.

Edith (de kleine), ik vraag me af hoe vaak MolMic na jouw vertrek nog in de Stelling is geweest. Met jou was het in elk geval altijd lachen op het lab, en vooral in de legendarische combinatie met Ronald in het RNC. Veel succes nog in Basel en natuurlijk bedankt dat je in de leescommissie wilde zitten.

Malene (de rooie), al wat langer weg bij MolMic, maar in dit lijstje mag je zeker niet ontbreken. Ook jij bedankt voor je bijdrage aan de goede tijd die ik als AIO heb gehad. Het beste met je werk en je gezin.

Erica, we hebben elkaar helaas niet lang genoeg meegemaakt voor een bijnaam. Toch ben je wel degelijk belangrijk geweest voor dit proefschrift en ik wil je dan ook bedanken voor wat je allemaal na mijn vertrek nog hebt gedaan aan het Pbp eiwit.

Gregory en Corinne (Greg en Co), eens te meer mag weer gezegd worden hoe onmisbaar jullie zijn voor het lab. Ik geloof echt dat zonder jullie het lab allang eens ontruimd had moeten worden van de inspectie. Als ik nog eens een restaurantje in Amsterdam zoek, weet ik jullie te vinden voor advies. Maar graag iets minder pittig dan jullie het zelf graag hebben.

Gert Jan en Dirk-Jan (GJ en DJ), fijn om jullie als postdocs op het lab gehad te hebben. En leuk dat we elkaar bij sociale gebeurtenissen nog altijd tegenkomen. Ook de collega's van al wat langer geleden: Rob, Maho en Aafke, bedankt voor jullie aanwezigheid en gezelligheid.

Inge en Jessica, "mijn" studenten, bedankt voor jullie goede en enthousiaste bijdrage aan mijn project. Zoals jullie aan dit proefschrift al kunnen zien, moet die receptor voor Hbp nog altijd gevonden worden. Maar nu mag iemand anders dat doen. Ook de andere studenten "van Ben" bedankt voor jullie inzet in ons clubje.

I would like to thank the people from other research groups with whom I collaborated during my PhD studies, especially Jeremy Tame and Atsushi Izumi in Japan, Peter van Ulsen and Lucy Rutten in Utrecht, Tanneke den Blaauwen at the UvA, Jeff Smith and Harris Bernstein in the USA. As far as not mentioned personally before, I would like to thank the members of the reading committee for reviewing my thesis.

Hoewel misschien niet direct betrokken bij dit proefschrift, wil ik toch ook Marc Timmers en FCH bedanken voor de goede tijd die ik in het Stratenum gehad heb, en Eefjan Breukink en BvM voor mijn opname in de groep als nog niet-gepromoveerde postdoc. Trouwens wel een *contradictio in termini*…

Mirjam en Sjaak, bedankt dat jullie mijn paranimfen willen zijn om mij terzijde te staan op die grote dag. Bedankt ook voor jullie vriendschap en interesse in mijn werk de afgelopen jaren. Dat laatste geldt natuurlijk ook voor alle vrienden en bekenden die ik hier niet met name heb genoemd.

Marieke, je kwam pas kijken toen de vier jaar van onderzoek net om waren. Toch wil ik je enorm bedanken voor je steun in het afgelopen jaar, waarin we elkaar soms jammer genoeg niet zagen omdat ik dan druk was met tikken. Hopelijk breken er wat dat betreft betere tijden aan, en zal dat ook nog heel lang duren. Ook je familie wil ik bedanken voor hun interesse in de vorderingen van mijn werk en het schrijven.

Papa en mama, heel erg bedankt voor alle mogelijkheden die ik heb gekregen voor school en studie, die er uiteindelijk in hebben geresulteerd dat ik AIO werd. Het blijft natuurlijk een vrij onbegrijpelijke baan, met vrij onbegrijpelijk onderzoek (zelfs in zo'n Nederlandse samenvatting), maar evengoed bleven jullie altijd belangstellend en enthousiast.

Mijn grootste dank ben ik echter verschuldigd aan Hem die hemel en aarde geschapen heeft. Ik wil daarom graag afsluiten met de woorden waarmee elke promotie aan de VU wordt afgesloten: De naam des HEREN zij geprezen van nu aan tot in eeuwigheid. (Psalm 113, vers 2)